ASPECTS OF SUSPENSION AND EMULSION POLYMERISATION

A dissertation submitted to the Council for National Academic Awards in fulfilment of the Degree of Doctor of Philosophy.

The research was conducted at:-

The Department of Chemical Engineering, The Polytechnic of Wales.

The Development Laboratory, Cray Valley Products Limited, Machen, Newport, Gwent.

R.Topping, M.Phil., MPRI., C.Chem., MRSC.
Cray Valley Products Limited,
Waterloo Works,
Machen,
Newport
GWENT.
NP1 8 YN

Submitted November 1983

PREFACE

The work described in this dissertation was carried out in the Department of Chemical Engineering at the Polytechnic of Wales and the Development Laboratory of Cray Valley Products Limited, Machen, between December 1977 and May 1983, and is the original and independent work of the author except where specifically acknowledged in the text. No part of this dissertation has been submitted to any other body.

I would like to express my gratitude to my supervisors Dr C Morgan and Mr K R Smith, particularly the former for his continual advice and encouragement throughout the course of this research study. Further, I would like to thank Mr L C Baker for many helpful discussions. I am also indebted to the technical staff at the Department of Chemical Engineering at the Polytechnic of Wales for their ready help and assistance at all times.

Finally I would like to acknowledge the support of my employers, Cray Valley Products Limited, and especially Mr A G North for the confidence he has placed in me by allowing me to pursue this research programme.

CONTENTS

ABSTRACT

Suspension polymerisation involves a dynamic equilibrium between monomer break up and coalescence.

A water soluble polymer (the suspending agent) is added to the aqueous phase to stabilise the monomer drop form during its conversion to a solid reaction product. Depending on the type and molecular weight of the suspending agent the aqueous phase can behave in a Newtonian or non Newtonian manner.

In a Newtonian system the final particle size is a function of the Weber and Reynold s number:

$$Re < 9000 \quad \frac{d}{L\emptyset} = K_1 \, (We)^a \, e^{b/Re}$$

$$Re > 9000 \quad \frac{d}{L\emptyset} = K_2 \, (We)^c$$

This dissertation is concerned with the properties of the suspension system and, in particular, those factors which influence the equilibrium drop size under non Newtonian conditions.

The process variables (stirrer size and speed, volume fraction of monomer and interfacial tension) are studied using a laboratory scale suspension system.

The results obtained are incorporated into an experimental model involving monomer polarity, interfacial tension and Reynold s number. The equations used to correlate the data are of the form:

$$d = K_3(\phi)^{7.56} \qquad (\phi' = 0.2)$$

$$d = K_4(Re)^{0.64} \qquad (\phi = 0.2)$$

It was found possible to relate the observed particle size directly with the polymer polarity.

In section 2, factors which cause sub micron/ polystyrene particle to agglomerate or disperse in a water/polyvinyl alcohol system are investigated.

It was shown that both monomer and monomer soluble initiator pass into the aqueous phase from the monomer phase by mass transfer where homogeneous particle nucleation of the monomer occurs. Particle destabilisation then occurs which is followed by the coalescence and agglomeration of the polymer particles.

The size of the spherical agglomerates produced is shown to be a function of the protective colloid concentration.

The bonding energy between the particles in the agglomerate is independent of the protective colloid concentration and is of the order 0.30×10^{10} dynes per particle pair.

It was shown that under high shear conditions the agglomeration process is reversible.

In the presence of difunctional monomers, fibrous agglomerates are produced. The bonding energy between these particles is lower than that found in spherical agglomerates and is of the order 0.20×10^{-12} dynes per particle pair.

The agglomeration process in the presence of the protective colloid is explained in terms of particle stabilisation theory.

CHAPTER 1

1.1 STRUCTURE AND PROPERTIES OF POLYMERS

A polymer is a large molecule built up by the repetition of small chemical units into a chain. In some cases the polymer chain is linear, but in may other cases it may be branched or interconnected to form three dimensional networks. The length of the polymer chain is specified in terms of the number of repeating units and this is called the degree of polymerisation.

The molecular weight is the product of the molecular weight of the repeat unit and the degree of polymerisation. Most high polymers useful for plastics: rubbers, or fibres have a molecular weight between 10,000 and 1,000,000.

1.1.1 POLYMERISATION PROCESSES

The processes of polymerisation were divided by Carothers into groups known as condensation and addition polymerisation.

In polymer formation, condensation takes place with the elimination of a small molecule such as water to produce a larger polyfunctional unit. The reaction is normally carried out at temperatures of 180 - 240^{o}C and continues until all of one of the reagents is used up.

The reaction product molecular weight can be controlled by changes in the reactant ratio.

Addition polymerisations involve chain reactions in which the chain carrier is a reactive substance with one unpaired electron called a free radical.

The free radical can be produced by different methods but is usually formed by the decomposition of a material called an initiator.

The free radical can react with and open the double bond of a monomer and add on regenerating the free radical.

In a very short time many more monomers add successively to the growing chain. Finally two free radicals combine to stop the growth.

1.1.2 MOLECULAR WEIGHT

In both condensation and addition polymerisation the length of the polymer chain is determined by purely random reactions.

In condensation reactions, the chain length depends on the local availablility of the reactive groups at the end of the growing chain. In addition polymerisation, the chain length is determined by the length of time during which the chain grows before a second free radical is encountered which then stops the reaction.

In both cases the product will consist of polymer chains having many different chain lengths, and this distribution of molecular weights can be calculated statistically.

Any experimental determination of molecular weight will give only an average value.

The method of measurement is important since it is possible to obtain the number average molecular $\bar{M}n$ weight or the weight average molecular weight $\bar{M}w$ depending on the method employed.

The ratio $\bar{M}w/\bar{M}n$ is a measure of the breadth of the molecular weight distribution (values of $\bar{M}w/\bar{M}n$ for typical polymers may range between 1.5-2 and 20-50).

The formation of crosslinked structures is possible if reactants containing more than two reactive groups are used in a condensation polymerisation, while the presence of two double bonds in a monomer molecule will give a crosslinked product during an addition polymerisation. Polymers which are crosslinked are stable to heat (thermosetting) while linear polymers are thermoplastic

1.1.3 POLYMERS IN THE SOLID STATE

The forces of attraction in polymeric material may be high enough to cause the polymer molecules to become aligned in an orderly fashion in a small crystalline region. This effect is reduced by thermal agitation and, if the intermolecular forces are low or the temperature high, there will be little ordering of the molecules.

The ordered domains are called crystallites, and are usually identified using X-ray diffraction techniques. IF no regions are found then the polymer is said to be amorphous.

The symmetry of the monomeric repeat unit plays an important part in determining whether a particular polymer will be crystalline or not. Unsymmetrical vinyl monomers usually polymerise in a stereically random structure in which crystallinity cannot develop. Hence, ordinary polystyrene is non crystalline, polyethylene is partially crystalline, and unstretched natural rubber is partially crystalline below room temperature. The extent of crystallinity and molecular weight may be used to classify polymers on the basis of their expected properties at a given temperature and this is shown in Fig 1.

Many polymers are partially but never completely crystalline. The close relationship between regularity of molecular structure and crystallizability is well known and typical crystalline polymers are those which are chemically and geometrically regular in structure.

Typical non crystalline polymers include those in which an irregularity in structure occurs - copolymers with significant amounts of two or more different monomer constituents or homopolymers with unsymmetrical repeating units in which the d and L configurations can occur at random along the chain.

The preparation of highly crystalline polymers from monomers including propylene and styrene in which the groups are isotactic confirms this.

Another factor which influences crystallite formation is the association in the molten state acting through highly polar groups present.

The tendency of polymers to crystallise varies over a wide range. Some can be cooled rapidly from above their crystalline melting point through temperature regions of rapid crystallisation to form stable amorphous products.

1.1.4 GLASS TRANSITIONS

Polymer properties may change markedly with a small change in temperature as a result of two different mechanisms.

The first of these is the mechanism of crystalline melting. The disappearance of a polymer crystalline phase is accompanied by large changes in physical properties. Measurement of density, refractive index etc, can be used to detect the crystalline melting point Tm which is a first order transition.

The second mechanism is a second order transition called the glass transition (Tg) and refers to the change from a hard brittle state to a more flexible rubbery state.

Since glass transitions are associated with the amorphous phase of polymers, the effect is greatest for completely amorphous polymers and becomes smaller in partially crystalline materials.

The glass transition is usually interpreted in terms of the ability of groups of chain atoms to undergo cooperative localised motion. Below the glass transition, thermal energy is not available to allow segments of

chain to move as a whole, and the structure is stiff and brittle. As the glass transition temperature (Tg) is approached the increased thermal energy allows larger molecular motions.

It has been found that Tm and Tg are simply related for many polymers - this is because the same energy factors and entropy factors must exist in both the crystalline and amorphous regions and influence the respective transition point in similar ways. This is shown in a plot of Tm - Tg (Fig 2).

The effect of molecular weight, transitions and polymer properties is shown in Fig 3. It can be seen that both Tm and Tg level off as the molecular weight increases above 100,000.

1.2 POLYMERISATION IN SUSPENSION

Suspension polymerisation, a method of polymerising a monomer in macro-sized beads which do not coalesce during the polymerisation, has been developed industrially mainly by empirical means.

During the period in which the process has been in commercial operation (~30 years) almost all the possible suspending agents have been employed either alone or in combination.

An examination of the literature shows that two monomers, styrene and vinyl chloride, especially the latter, occupy the major development interest. The principal difference between these monomers is that

polystyrene is soluble in its own monomer whilst PVC is substantially insoluble in vinyl chloride, although the polymer is swollen considerably by liquid monomer. These differences are also mainly true of copolymers in which these monomers occupy the major proportion. In the present work the principal monomer considered is styrene and the other monomers used have similar solubility characteristics, eg methacrylate esters.

1.2.1 ADDITION POLYMERISATION

This type of polymerisation is characterised by monomers of the type $CH_2 = CHX$, and suspension polymerisation is a specific method of addition polymerisation, which generally includes solution polymerisation, emulsion and bulk methods.

Three steps in the process can be identified:

(1) Initiation - activation of the monomers.
(2) Propagation - polymer chain grows.
(3) Termination - the polymer chain stops growing.

1.2.2 INITIATION

The most common source of free radicals for polymerisation initiation are the organic peroxides and azo compounds.

Benzoyl peroxide decomposes on heating to give free radicals.

$$C_6H_5 - \overset{O}{\overset{\|}{C}} - O - O - \overset{O}{\overset{\|}{C}} - C_6H_5 \xrightarrow{\text{heat}} 2\ C_6H_5 - \overset{O}{\overset{\|}{C}} - O$$

These radicals react with the monomer molecules to initiate the polymer chain.

1.2.3 PROPAGATION

A monomer $CH_2 = CHX$ adds to the free radical produced by the initiation process to form a larger free radicals ($R - CH_2 - CHX$) and this process is then repeated in rapid succession to produce the growing polymer chain.

1.2.4 TERMINATION

Two growing polymer chains can collide together and mutually destroy their free radical activity in the termination step. This can occur in two ways:

(1) Combination termination - two radicals combine together (head to head).

(2) Disproportionation termination - in this process two radicals stabilise themselves by the transfer of an hydrogen atom from one to another.

1.2.5 CHAIN TRANSFER

For some simple kinetic expressions such as the overall rate of polymerisation the simple reaction scheme, initiation, propagation and termination leads to theoretical expressions which are in accord with experimental results. However several other aspects have to be introduced to fully explain all experimental results.

For example it is necessary to introduce reactions in which a particular radical ceases growing without simultaneous termination of the radical chain. For this to occur the free radical activity must be transferred to some other molecule.

$$R - X + \sim\sim\dot{C}H_2 \longrightarrow \dot{R} + \sim\sim CH_2X$$

The compound R-X is termed a transfer agent and it is sometimes added to a particular reaction to control the molecular weight of the polymer produced.

1.2.6 KINETIC OF ADDITION POLYMERISATION

To simplify the presentation, chain transfer is ignored in the present treatment.

The three principal processes may then be represented as follows:

(1) INITIATION

$$I \xrightarrow{Kd} 2R^{\bullet} \qquad (1)$$

$$R^{\bullet} + M \xrightarrow{Ka} M^{\bullet}_1 \qquad (2)$$

(2) PROPAGATION

$$M^{\bullet}_1 + M \xrightarrow{Kp} M^{\bullet}_2 \qquad (3)$$

$$M^{\bullet}_2 + M \xrightarrow{Kp} M^{\bullet}_3 \qquad (4)$$

$$M^{\bullet}_3 + M \xrightarrow{Kp} M^{\bullet}_4 \qquad (5)$$

$$M^{\bullet}_n + M \xrightarrow{Kp} M^{\bullet}_{n+1} \qquad (6)$$

(3) TERMINATION

(combination) $$M^{\bullet}_x + M^{\bullet}y \xrightarrow{Ktc} Mx + y \qquad (7)$$

(disproportionation) $$M^{\bullet}x + M^{\bullet}y \xrightarrow{Ktd} Mx + My \qquad (8)$$

The K's with various subscripts are the specific reaction rates of the individual steps. 'I' denotes the initiator molecule, and 'M' the monomer molecule.

For the two termination steps, an overall rate of Kt is adopted, and for the propagation steps a common Kp is assumed. This is usually justified except for the few steps when the chains are very short.

One further assumption is made, that is the initiation process as a whole involving both Kd and Ka, Kd is the rate determining step.

For this reaction scheme and with the above assumptions then:

$$\text{Rate of initiation} = Vi = \frac{d[M^{\bullet}]}{dt} = 2fKd[I] \qquad (9)$$

$$\text{Rate of termination} = Vt = -\frac{d[M^{\bullet}]}{dt} = 2Kt[M^{\bullet}]^2 \qquad (10)$$

IF the concentration of free radicals remain constant throughout the major part of the reaction (steady state) these two rates will be equal.

$$[M^{\bullet}] = \frac{f\,Kd\,[I]^{\frac{1}{2}}}{Kt} \qquad (11)$$

The rate of propagation Vp is given by:

$$Vp = -\frac{d[M]}{dt} = Kp[M][M^{\bullet}] = Kp\left(\frac{f\,Kd\,[I]}{Kt}\right)^{\frac{1}{2}}[M] \qquad (12)$$

The rate of polymerisation, which is given by the rate of propagation, is proportional to $f^{\frac{1}{2}}[I]^{\frac{1}{2}}[M]$.

The factor f is not, in general, independent of the monomer concentration $[M]$.

(f is the fraction of radicals which successfully initiate chains.)

Two limiting cases are possible:

(1) When the initiator efficiency is high $f \longrightarrow 1$. f is independent of $[M]$ and the overall rate is proportional to $[M]$.

(2) When the initiator efficiency is low, f may be proportional to $[M]$ when the overall rate is proportional to $[M]^{\frac{3}{2}}$

The overall rate constant $Kp \left[\frac{Kd}{Kt}\right]^{\frac{1}{2}}$ may be determined experimentally.

Kd may be found by studying the decomposition of initiator, but $\left[\frac{Kp}{Kt}\right]^{\frac{1}{2}}$ cannot be separated into its constituent constants without recourse to additional non-steady state experiments.

Kinetic theory suggests the rate of polymerisation is proportional to the square root of the initiator concentration. This is seen in the results obtained using styrene as the reactive monomer. The initial rate is found to be proportional to the square root of the benzoyl concentration.

In the polymerisation of methyl methacrylate and vinyl acetate it is found that after a constant reaction rate an accelerated reaction then occurs. This increase in reaction rate begins at quite a low conversion when the viscosity of the polymer is low. The viscosity of the polymer depends largely upon the molecular weight, which

in turn depends upon reaction temperature, initiator concentration and the presence of any chain transfer agent.

The accelerated rate is caused by the reduction in chain termination due to the higher viscosity of the reaction medium. The resultant increase in reaction rate often called the gel effect is most noticeable in methyl methacrylate, but the effect is reduced in the case of other monomers including styrene.

1.3 HOMOPOLYMERISATION

It is well established (1) that the kinetics of the process is similar to that of a bulk polymerisation of the monomer in the same polymerisation conditions, ie reaction temperature, initiator/monomer ratios are the same (1).

The kinetic equation for bulk polymerisation which yields polymer soluble in the monomer by the thermal decomposition of free radicals initiators holds true for similar suspension polymerisation (1).

$$Rp = Kp(f\ Kd\ [I]\ /Kt)^{\frac{1}{2}}\ [M] \qquad (13)$$

Where :

Rp = Rate of polymerisation
Kp = Velocity coefficient for the polymerisation
Kt = Velocity constant for termination (disproportion and combination).
[M] = Monomer concentration
[I] = Initiator concentration
Kd = Velocity of decomposition of initiator
f = Constant - such that fKd [I] = Ri
(The rate of initiation)

Where the polymer is insoluble in the monomer the following equation holds (2).

$$C = \left[\frac{1}{q}\left(qK[I]^{\frac{1}{2}}t + \frac{q^2k^2}{2!}([I]^{\frac{1}{2}}t)^2 + \frac{q^2k^2}{3!}([I]^{\frac{1}{2}}t)^3 + \text{---}\right)\right] \quad (14)$$

Where c = overall degree of conversion
K = rate constant $K = Rpd/[I]^{\frac{1}{2}}$
t = reaction time in hours
q = ratio of the rate of polymerisation in the precipitated phase to that in the dilute phase, times the fraction of the overall conversion taking place in the precipitated phase minus that same fraction.

Since the same kinetic mechanisms are operative in both bulk and suspension polymerisations, the molecular weights and molecular weight distribution obtained by these two processes will also be identical.

1.4 COPOLYMERISATION

When two different monomer A and B, which separately homopolymerise readily, are mixed and heated with an initiator more complex reactions are possible. The rate of copolymerisation is usually slower, but cannot be predicted from the rates of homopolymerisation.

Instead of the single propagation reaction there will now be four reactions, from two different monomers, adding to two different radicals, which may be given rate constants as follows:

$$\sim\sim A^{\bullet} + A \xrightarrow{K_1} \sim\sim A^{\bullet} \quad K_1/K_2 = r_1 \quad (15)$$

$$\sim\sim A^{\bullet} + B \xrightarrow{K_2} \sim\sim B^{\bullet} \quad (16)$$

$$\sim\sim B^{\bullet} + B \xrightarrow{K_3} \sim\sim B^{\bullet} \quad K_3/K_4 = r_2 \quad (17)$$

$$\sim\sim B^{\bullet} + A \xrightarrow{K_4} \sim\sim A^{\bullet} \quad (18)$$

The two monomers do not enter the copolymer in the proportion to their concentration in the monomer mixture, but exhibit a pronounced tendency towards one specific reaction. The copolymer formed at any instant will have a different composition from that of the monomer mixture and therefore the copolymer structure will change with conversion.

The values of r_1 and r_2 for a particular combination of two monomers M_1 and M_2 are called monomer reactivity ratios and are determined by the analysis of copolymers.

A value of $r_1 > 1$ indicates that a polymer radical reacts more readily with a monomer of its own type than with the other.

Monomer reactivity ratios are little affected by temperature, chain transfer agents, solvent etc, but only apply to free radicals initiated copolymerisations.

1.5 REACTIVITY AND STRUCTURE OF MONOMERS AND RADICALS

The order of reactivity of olefins towards free radicals is a function of the olefin type, but also depends on the nature of the attacking radical.

This is illustrated by the tendency of many monomers to alternate in a copolymer chain.

The two factors, general reactivity and alternating tendency are predominant in the behaviour of monomers in copolymerisation.

As was shown earlier, the product of the monomer reactivity ratios is a measure of the tendency of a monomer to alternate. IF the monomer shows the same reactivity to all radicals $r_1r_2 = 1$ there is no tendency to alternate, complete alternation implies that $r_1r_2 = 0$.

It is possible to arrange monomers in a series such that two monomers further apart in the series have a greater tendency to alternate. This is primarily due to the polarity of the double bond in the monomer. The order of monomers closely parallels the order of the tendencies of substituents around the double bond to donate electrons (hydrocarbon) or to withdraw them (carbonyl). In general the origin of the order of reactivity of monomers lies in the resonance stabilisation of the transition during the addition to a radical. The greater the resonance energy of the resulting radical after addition, the more reactive is the monomer.

1.5.1 THE ALFREY - PRICE EQUATION

Alfrey and Price (3) attempted to express the factors of general reactivity and polarity quantitatively. The rate constants (for copolymerisation) are in the form:

$$K_{12} = P_1 \, Q_2 \, e^{-e_1 e_2} \qquad (19)$$

Where P_1 is the general reactivity of the radical M_1, Q_2 the reactivity of the monomer, M_2, and e_1 and e_2 are proportional to the electrostatic interaction of the

permanent charges on the substituents in polarising the double bond.

This is analogous to Hammetts equation (4) for the effect of nuclear substituents on the reactivity of aromatic compounds.

Since $r_1 = (Q_1/Q_2)e^{-e_1(e_1 - e_2)}$ (20)

$r_2 = (Q_2/Q_1)^{e^{-e_2(e_2 - e_1)}}$ (21)

and $r_1 r_2 = e^{-(e_1 - e_2)^2}$ (22)

The Alfrey Price equation assumes that the same value of e applies to both monomer and radical.

It is possible to assign values to Q and e for a series of monomers from data on copolymerisation experiments and compute values of r_1 and r_2. A problem however is the large uncertainty in Q and e using standard experimental technique.

1.6 THE POLYMER MOLECULE IN SOLUTION

In solution the polymer molecule is a randomly coiled mass which because of possible rotations about single bonds, may adopt conformations which may effectively occupy many times the volume of the dissolved segment alone.

The size and the degree of extension of the molecular coil are dependent on the polymer solvent interaction forces. In a good solvent where these forces are strong and the interaction between polymer and solvent is favoured the coils are extended. In a poor solvent the reverse may be the case.

The size of the randomly coiled molecule is usually defined either by root mean square end-to-end distance $(\bar{r}^2)^{\frac{1}{2}}$, or by the radius of gyration $(\bar{s}^2)^{\frac{1}{2}}$, the root mean square of distance of the elements of the chain from its centre of gravity (this last term is specially applicable to non-linear chains).

In a polymeric solution there are present many polymer chains differing greatly in molecular weight.

Methods of molecular weight determination applicable to polymers mostly depend upon physical measurements on dilute polymer solutions. They usually involve an extrapolation of an appropriate quantity to infinite dilution. Here the polymer molecules behave independently of one another and the effects of interaction with the solvent are minimised.

Viscosity is not a direct measure of molecular weight but it can be related to molecular weight in a useful manner for some polymers.

1.6.1 MEASUREMENT OF COLLIGATIVE PROPERTIES

Colligative properties which can be measured conveniently include the following:

(1) Ebulliometry (boiling point elevation)

The temperature difference ΔT_b required to restore the vapour pressure to its equilibrium value at the boiling point of the pure solvent is measured.

It can be shown that:

$$\left(\frac{\Delta Tb}{c}\right)_{c=o} = \frac{RT^2}{P\,Lv} \quad \frac{1}{\bar{M}n} \qquad (23)$$

Where Δ Tb is the elevation in boiling point of the pure solvent due to the presence of a solute at a concentration of c, and P and Lv are respectively, the density and latent heat of vaporisation of the solvent. $\bar{M}n$ is the number average molecular weight.

(2) Depression of freezing point

Similarly in the cryoscopic or freezing point depression method, one measures the temperature lowering ΔTf necessary to make the activity of solvent in the solution equal to its activity in the pure state at its freezing point.

$$\left(\frac{\Delta Tf}{c}\right)_{c=o} = \frac{RT^2}{P\,Lf} \quad \frac{1}{\bar{M}n} \qquad (24)$$

Where Δ Tf is the lowering in freezing point of the pure solvent due to the presence of a solute at a concentration of c and P and Lf are, respectively, the density and latent heat of fusion of the solvent. Although the boiling point and freezing point methods are suitable, their application to polymers is difficult; and furthermore, the polymer may decompose during boiling, or become insoluble before the freezing point of the solution is reached.

(3) Osmometry

In the measurement of osmotic pressure the activity of the solvent in the solution is restored to

that of the pure solvent by applying an osmotic pressure π to the solution.

The simplest type of osmometer consists of two half cells, one containing the solvent, and the other the solution, separated by a semi-permeable membrane. Initially the heights of the liquids in the measuring capillaries are set equal. Solvent then flows across the membrane into the solution, causing a pressure head to develop. The equilibrium pressure head is the osmotic pressure (π) of the solution, and it is related to $\bar{M}n$ the number average molecular weight by:

$$\frac{\pi}{R\,T\,c} = \frac{1}{\bar{M}n} \qquad (25)$$

Where c is the polymer concentration, R is the gas constant, and T the temperature (^{o}K).

Equation (25) refers to an ideal solution, however most polymer solutions do not behave ideally and their behaviour is represented by:

$$\frac{\pi}{R\,T\,c} = \frac{1}{\bar{M}n} + A_2C + A_3C^2 + \text{----} \qquad (26)$$

Where A_2 and A_3 are the second and third virial coefficients respectively. The virial coefficients are a measure of the departure from ideality due to the interactions between polymer molecules. Typical semi-permeable membrane for polymer work include Cellophane for non aqueous solutions and collodion for aqueous solutions.

In practice the number average molecular weights which lie between 10,000 - 100,000 are usually determined by these methods.

In all three cases, the quantities to be measured at a given concentration C viz ΔTb, ΔTf and π decrease with increasing molecular weight.

Colligative properties yield a number average weight $\bar{M}n$; other techniques such as light scattering depend on the mass of the molecule in solution and so give a weight average value, $\bar{M}w$.

The spread of molecular weight in the distribution curve can be characterised by the ration $\bar{M}w/\bar{M}n$.

$\bar{M}w$ is usually obtained by light scattering and in addition this technique gives information about the shape and actual size of the dissolved polymer molecule.

Measurement of viscosity is experimentally rapid, simple and accurate and can be used to give $\bar{M}w$ but the method is not absolute and calibration is required.

The most important viscometric quantity is the specific viscosity nsp (which depends on concentration) $(nsp = Ac + Bc^2)$, also $(nsp = n\ rel - 1)$ (27)

Where n rel, the relative viscosity is the ratio viscosity of solution/viscosity of solvent. c = the concentration. A plot of nsp/c is linear and the value at zero concentration is known as the limiting viscosity number. The empirical relation $[n] = K_1 \bar{M}w^a$ is normally used where K_1 and a are constants for a given polymer - solvent system.

$\bar{M}w$ is easily calculated from a measured $[n]$ value; viscosity measurements on polymer solutions are usually made in a capillary viscometer.

There are several ways in which the molecular weight distribution of a polymer can be determined experimentally. Fractionation of the polymer into narrow molecular distributions is carried out in several different ways. The simplest example of this method is by fractional precipitation. In this method the polymer is dissolved in a good solvent, to which a non solvent is gradually added. As the solubility of a polymer is inversly related to molecular weight, the first precipitate contains largest polymer molecule.

An alternative method is sometimes used. This is known as gel permeation chromotography. The length of time that a polymer molecule takes to pass down the column is related to its molecular size and shape.

The column is usually calibrated by using polymer samples of known molecular weight. Finally, other methods include the rate of sedimentation of the polymer solute, and end group analysis. (This depends on the chemical or physical identification of specific end groups which occur in each molecule.)

The viscosity of the aqueous phase containing the dissolved suspending agent was measured in the present investigations and values for $\bar{M}w$ obtained. The effect of mechanical energy (high speed stirring) on the molecular weight was investigated and reported later in Chapter 2.

1.7 THE PHYSICAL SYSTEM

1.7.1 THE AQUEOUS PHASE

Suspension of monomer droplets in water is achieved by mechanical agitation usually stirring, in the presence of a stabiliser. Stabilisers may be inorganic compounds (for instance sparingly soluble carbonates and oxides) or high molecular weight organic materials. The stabiliser plays no significant role in the mechanism of reaction: from the kinetic point of view suspension polymerisation is simply a convenient method of carrying out a very large number of minute bulk reactions in such a manner that the heat of reaction is readily dissipated.

The suspending agent must perform its function during the whole course of the polymerisation particularly at the critical phase when the droplets contain enough dissolved polymer to become syrupy.

As the viscosity increases the droplets are no longer broken up easily by stirring and because they are not solid will stick together unless protected by the stabiliser.

The stabiliser can also affect the particle size, shape and clarity of the product formed. Other factors which can affect clarity include the solubility of water in the monomer and the monomer in water.

The use of inorganic powders as suspension stabilisers can produce a very narrow range of particle

size compared to the water soluble type. A particular problem encountered in the use of inorganic powders is the difficulty of their separation in the final stages of polymerisation, usually an acid is used to remove the powder and the product is then separated by filtration, washed and dried.

1.7.2 MECHANISM OF SUSPENSION STABILISERS

Whilst at the present time, there is no theory which relates stabiliser structure and properties to its ability to stabilise a specific polymerisation process, there are several factors which are common to most protective colloids used.

Generally on dissolving in water the viscosity of aqueous phase is increased by the protective colloid. Some workers have suggested that it is the increase in the viscosity of the continuous phase that is principally responsible for giving good dispersion stability.

The effect of an increased aqueous phase viscosity is to increase the drainage time of the film between the droplets; this will result in an increased resistance to droplet coalescence. Whilst this can affect the equilibrium relationship between dropbreak up and drop coalescence in a stirred tank there is no direct evidence that this alone is a principal mechanism for achieving stability.

The nature of the interface has been shown to exert a considerable influence on various interfacial

phenomena such as interfacial tension (5,6) micellisation and solubilisation (7) surfactant adsorption (8,9) and formation and stability of polar emulsion particles (10, 11, 12). The effect of polarity on surfactant adsorption has received much attention in recent years (13,14,15,16). The polarities of the monomer-water and polymer-water interfaces are believed to govern surfactant and colloid adsorption and very probably particle stabilisation (10-12).

Several workers have attempted to correlate the polarity of monomer (polymer) - water interface to monomer water solubility (12-14) and monomer water interfacial tension(11,13).

Paxton (9) suggested that the area per molecule of a surfactant adsorped onto a polymer surface is related to the polarity of the polymer.

The use of interfacial tension to obtain data about surfactant adsorption is discussed in detail later, when the energetics involved in the adsorption of the colloid from the aqueous phase at the interface is related to the polarity, and ultimately to the final particle size in a suspension polymerisation.

The adsorped colloid layer also possesses a viscosity, and H J Karan (17) examined the viscosity of an adsorbed polymeric film at an interface using an interfacial viscometer. Karan showed the significance of interfacial viscosity upon drop break up behaviour in a liquid-liquid system, and found that the suspending agent

made drop break up more difficult. The interfacial properties of the suspending agent are more important than its effect upon the aqueous phase viscosity. For example small amounts of some colloids can give adequate stability for some monomers and polymers, while higher concentrations of a different type which increase the aqueous viscosity toa greater degree may fail to provide sufficient protection for the polymerising system.

1.8 THE MONOMER PHASE

Monomers or mixtures of different monomers which are insoluble or only slightly soluble in water are used in a suspension polymerisation.

These include monomers such as styrene and the acrylic types (acrylate and methacrylate).

Vinyl chloride can be made by a suspension process if this is carried out under pressure.

The choice of initiator used depends to a large extent upon the temperature range, which for systems at atmospheric pressure means that a low temperature type such as benzoyl peroxide or an azo type must be used. It is advantageous to choose a fairly active initiator which will allow a rapid passage through the semi solid stage in the polymerisation, although good temperature control is necessary if the exothermic reaction is not to get out of control.

Generally if the temperature exceeds a critical value the protective colloid becomes de-adsorped and the

system becomes unstable and coalescence occurs. Chain transfer agents which are soluble in the monomer phase are often used to control the molecular weight of the product.

One of the most active transfer agents used are the aliphatic mercaptans, although their foul odour characteristics can give problems in the final product for certain applications (eg. foodstuff packing). The behaviour of a few common monomers in an aqueous suspension polymerisation is now to be discussed to illustrate the types of problem involved in the problem.

1.8.1 STYRENE

For various reasons such as its ready availability, commercial importance, general chemical behaviour and relatively reproducible kinetic behaviour this monomer has been studied more extensively than most.

The first systematic kinetic investigations of the uncatalysed polymerisation of styrene were published about 1937 .

Breitenbach and Rudorfer (18) examined the reaction at 100°C in bulk and various solvents (in vacuum). Their results showed that in dilute solutions the reaction was second order, while in the bulk process the reaction seemed to follow a first order course. These results were confirmed by Schulz and Huseinann (19) in an inert atmosphere of nitrogen.

The second order dependence is accounted for

if the thermal initiation reaction is second order; is $I = K_i [M]^2$ (Where I = rate of initiation).

The general rate equation; $$-\frac{d[M]}{dt} = Kp[M]^2 \left\{ \frac{Ki}{Ktc + Ktd} \right\}^{\frac{1}{2}} \quad (28)$$

To account for the apparent first order dependence in the bulk polymerisation it is necessary to replace the monomer concentration by its thermodynamic activity.

The difference between concentration and activity is much greater in the case of a bulk process than in a dilute solution.

In a catalysed polymerisation the polymerisation of styrene initiated by the thermal decomposition of molecules which yield free radicals is shown to be half order with respect to catalyst concentration for a wide variety of substances.

The determination and interpretation of the order of the catalysed reaction with respect to styrene have given problems. The order seems to be intermediate between 1 and 1.5. Two alternative explanations have been put forward. Schulz and Husemann assume that the catalyst forms a complex with the monomer. If the equilibrium constant for its formation is Kc and $[M]$, $[Cat]$ $[c]$ represent the monomer, catalyst and complex concentration then:

$$[c] = Kc\,[Cat]\,[M]/(1 + Kc\,[M]) \quad (29)$$

The rate of initiation is assumed to be equal to the rate if decomposition of the complex ($Kc[C]$).

The other (and generally preferred) explanation was proposed by Matheson (20). It is proposed that a fraction of the radicals formed in pairs from the catalyst recombine by a cage effect before escaping from each others proximity. This is a first order combination being proportional to the number of cages.

Thus if $Kd[Cat]$ is the rate of catalyst decomposition, then:

$$I = \frac{r\,Kd\,[Cat]\,[M]}{1 + r\,[M]} \qquad (30)$$

Where r = ratio of the velocity coefficients for reaction of a radical with a monomer and for mutual reaction of two primary particles.

1.8.1.1 MECHANISM OF COMPONENT REACTION INITIATION

There are two possible types of reaction by which a radical R•c produced by decomposition of a catalyst can attack a styrene molecule.

(1) Hydrogen transfer

$$R^{\bullet}c + CH_2 = CH\,\emptyset \longrightarrow RcH + CH_2 = \dot{C}\emptyset \qquad (31)$$

(2) Addition

$$R^{\bullet}c + CH_2 = CH\,\emptyset \longrightarrow RcCH_2 - \dot{C}H\emptyset \qquad (32)$$

or

$$R^{\bullet}c + CH_2 = CH\,\emptyset \longrightarrow RccH\emptyset - \dot{C}H_2 \qquad (33)$$

Addition is the usual mode of reaction as shown by the incorporation of catalyst fragments into the polymer formed.

Propagation

Consideration must be given to the orientation of the addition in the propagation reaction

$$R\cdot + CH_2 = CH\,\emptyset \longrightarrow R - CH_2 - \dot{C}H\emptyset \qquad (34)$$

or $$R\cdot + CH_2 = CH\,\emptyset \longrightarrow R - CH\emptyset - CH_2 \qquad (35)$$

or a combination of the two.

The first is most likely because of the additional resonance stabilisation of the radical formed which has various cononical forms such as:

Transfer

(1) To monomer

Here it must be decided whether a hydrogen atom is transferred to or from the monomer molecule.

$$R - CH_2 - \dot{C}H\emptyset + CH_2 = CH\emptyset \longrightarrow R - CH = CH\emptyset + CH_3 - \dot{C}H\emptyset \qquad (36)$$

$$R - CH_2 - \dot{C}H\emptyset + CH_2 = CH\emptyset \longrightarrow R - CH_2 - CH\emptyset + CH_2 = \dot{C}\emptyset \qquad (37)$$

It seems likely that the first mechanism is correct because in case 2 branched structures are more likely but not usually observed.

Transfer to polymer

Chain transfer by abstraction of a hydrogen atom from a polystyrene molecule will lead to a branched structure.

$$R^{\bullet} + Rm - CH_2 - CH\emptyset - Rn \longrightarrow RH + Rm - CH_2 - \dot{C}\emptyset - Rn \quad (38)$$

The occurrence of such transfer reactions has been demonstrated by the use of radioactive tracer techniques.

Transfer to solvents and other additives

The transfer reaction depends on the substance concerned, usually a hydrogen is abtracted but other atoms or even groups may be split off.

$$R^{\bullet} + C_2H_5SH \longrightarrow RH + C_2H_5S^{\bullet} \quad (39)$$

$$R^{\bullet} + CBr_4 \longrightarrow RBr + Br_3C^{\bullet} \quad (40)$$

$$R^{\bullet} + R'SSR' \longrightarrow RSR' + R'S^{\bullet} \quad (41)$$

$$R^{\bullet} + (C_6H_5OCO)_2 \longrightarrow ROOC\ C_6H_5 + C_6H_5\ COO^{\bullet} \quad (42)$$

The relative strength of the bonds broken and formed as measured by the bond dissociation energies will be an important factor in determining the rate of chain transfer.

Termination

The question of whether the termination reaction in styrene involves combination or disproportionation of two radicals is usually discussed with reference to the determination of the absolute velocity coefficients - since the choice of reaction route will affect the numerical

value obtained.

Usually it was found that all chains end by coupling rather than disproportionation (tracer analysis).

1.8.2 METHYL METHACRYLATE

Next to styrene, methyl methacrylate has been the most extensively investigated monomer largely because of its industrial importance.

It exhibits broadly similar kinetic characteristics as styrene, but in addition, certain of its polymerisation characteristics (gel effect) are not shared by styrene.

The rate of reaction in an uncatalysed reaction seems to be much lower than that for pure styrene at the same temperature.

In a catalysed polymerisation Norrish and Brookman (21) examined the polymerisation using benzoyl peroxide and found it to be of zero order with respect to monomer during the early stages but at about 20% conversion a marked acceleration was noted. Schulz (22) followed the course of the peroxide initiated reaction by dilatometric and gravimetric methods. He found that during the early stage of polymerisation the rate is proportional to the monomer concentration and to the square root of the initiator concentration. Trommsdorf provided experimental confirmation that the viscosity of the reaction medium was of great importance in the production of gel effect at higher conversion levels. According to the generally

accepted explanation of the gel effect, increasing viscosity of the medium can eventually result in the rate of diffusion of radicals becoming a controlling factor in the rate of mutual termination. At high viscosities therefore this will be much reduced, but the rate of the propagation reaction (which involves only one large radical) will be less affected. Hence, the net result will be a progressive increase in the rate of polymerisation. At the present time no adequate theory for diffusion controlled reactions of large molecules has given a satisfactory quantitative interpretation of these effects.

1.8.2.1 MECHANISM OF COMPONENT REACTIONS

The thermal initiation is second order with respect to monomers similar to styrene.

In the propagation step the energetically and sterically favourable head to tail addition occurs in spite of possible steric interference between substituent groups of adjacent residues.

The mode of addition is probably similar to that of styrene, a radical of the type;

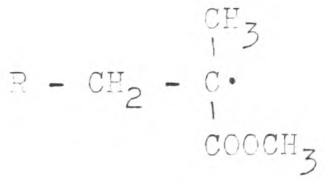

being energetically favoured because of a small amount of resonance stabilisation involving the substituent groups.

The rate coefficient for transfer to monomer is lower than in styrene but transfer is presumed to take place by a similar type of mechanism. Schulz (22) investigated transfer to polymer using added polymer as a transfer agent. Using polymers of different molecular weight Schulz was able to show that transfer at a polymer unit at the end of the chain occurred at a different rate from transfer to other chain units. This was ascribed to the presence of an unsaturated end group arising from the disproportionation reaction in the termination step, since polystyrene (formed by a combination reaction) does not show this effect. The coefficient for transfer to polymer is low, indicating that branching is effectively absent in polymers formed at low conversions.

Using C^{14} labelled initiator Bevington et al (23) were able to show that both types of termination reaction occurred, (ie disproportionation and combination) but later work by Bamford and Jenkins (24) showed that at 90°C disproportionation occurred about ten times as frequently as combination.

1.9 POLYMERISING CONDITIONS

The factors which influence the properties of a polymer produced in a suspension process can be listed as follows:

(1) Temperature
(2) Initiator type and concentration
(3) Monomers used
(4) Presence of transfer agents

The degree of polymerisation, configuration and structure of the polymer are all related to the reaction temperature.

The temperature also influences the decomposition rate of the initiator employed.

IF the temperature is too high, this causes an increase in the rate of polymerisation which usually produces a low molecular weight polymer having increased chain branching, and a greater molecular weight distribution.

The temperature must also be controlled within narrow limits because the adsorbed suspension colloid can be de-adsorbed if the temperature rises above a critical level. This will produce complete coalescence of the monomer droplets resulting in batch agglomeration.

A reaction temperature range for most monomers is between 70 - 85°C for most processes carried out at atmospheric pressure. Above 85°C many monomers produce an azeotrope with water which will reflux strongly, and is difficult to incorporate into the system.

Most monomers or mixtures of monomers require an optimum reaction temperature which corresponds to their reactivity and the initiator employed.

This temperature must produce a final product having the desired physical and chemical properties.

The product molecular weight can be controlled if necessary by the addition of chain transfer agents.

The choice of monomers used clearly influence the physical properties obtained. By careful selection of the monomers, considerable control of important properties (flexibility, solubility etc) is possible.

1.9.1 VOLUME FRACTION

The monomer volume fractions normally used in a suspension process lie between 10 - 45%.

Lower ratios are employed in order that the heat of reaction can be removed quickly.

The use of higher ratios clearly allows the economics of the process to be improved.

The volume fraction is sometimes also used to control the final particle size of the product.

Under Newtonian conditions it has been shown (25) that an increase in volume fraction produces an increase in particle size. The present investigations show that the reverse is true for a non-Newtonian suspending agent.

1.9.2 PROCESS VARIABLES

Process variables which depend upon the design and operation of the agitation system must also be considered. These may be listed as follows:

(1) Volume fraction of monomer
(2) Stirrer size, shape and speed
(3) Reynold s number
(4) Monomer and aqueous phase viscosities
(5) Weber number
(6) Reactor shape
(7) Liquid level in the reactor
(8) Flow characteristics of the aqueous phase (ie Newtonian or non Newtonian flow)

1.9.3 AGITATOR SPEED

The effect of agitator speed upon the final particle size was investigated for a Newtonian system by Topping (25) using methyl methacrylate as the monomer. The particle size was found to be related to the stirrer speed by the following equation.

$$d = CN^{-0.93} \quad (\text{at } \emptyset = 0.10) \tag{43}$$

$$d = CN^{-1.0} \quad (\text{at } \emptyset = 0.20) \tag{44}$$

Vermeulen (26) showed that droplet size was related to agitator speed by $d = CN^{-1.2}$ for liquid - liquid systems.

Later investigations by Topping (25) showed that the relationship existing between the variables displayed in the following equation was true for a suspension polymerisation.

$$\frac{d}{L\emptyset} = C_1 \left(\frac{N^2 L^3 P^1}{\delta}\right)^{-0.6} \tag{45}$$

Where
- L = Stirrer diameter (cm)
- N_1 = Stirrer speed (rpm)
- P^1 = Density (gm/cc)
- δ = interfacial tension (dynes/cm)
- C_1 = Constant
- d = Sauter mean diamter (microns)
- $\emptyset$ = Volume fraction of monomer phase

The work was extended and the $\frac{d}{L\emptyset}$ function was correlated with the Weber and Reynold s number as follows:

$$\frac{d}{L\emptyset} = K_1 \, We^a \, e^{B/Re} \tag{46}$$

Where K_1 = constant
a = -0.68
b = 67.4
d = Sauter mean diamter
L = Stirrer length
$\emptyset$ = 0.20 (volume fraction)

This equation was found to apply for Reynold s number up to 9000.

When $Re > 9000$ $\frac{d}{L\emptyset} = K_2(We)^c$ (47)

The particle size is independent of the molecular weight.

1.9.4 DROP BREAK UP/COALESCENCE EQUILIBRIUM

The process consists of a break up and drop coalescence equilibrium which occurs mainly in the turbulent region near the stirrer making the process fairly insensitive to vessel shape.

The above model was tested over a scale range of 1 Kg to 5000Kg of charge and found to be valid in all cases.

The present investigations extend the model to take into account the non Newtonian system found with high molecular weight protective colloids.

1.9.5 TREATMENT OF THE FINAL PRODUCT

The final product is usually separated from the aqueous phase by filtration or a centrifuge. This removes most of the water but sometimes a wash process is incorporated to remove any residual suspending agent and additives. The final drying is usually achieved using a fluidised bed or ring drier.

CHAPTER 2

PHYSICAL DATA

2.1 SUMMARY

Aqueous solutions of a high molecular weight polyacrylamide solution were investigated for rheological behaviour.

It was established that the suspending agent produced non Newtonian properties over the concentration range examined, and behaved both as a Bingham fluid and a pseudo plastic.

From the experimental data obtained using two different viscometer types, it is possible to estimate Reynold s number for an agitated system at a specified temperature.

Interfacial tension measurements were made using the Sessil℮ drop method.

The effect of suspending agent concentration and different monomer types on interfacial tension were evaluated. The effect of an inorganic salt on both viscosity and interfacial tension were examined.

Finally the behaviour of a polyacrylamide solution under high shear was investigated. It was shown that bond breaking occurs with a corresponding reduction in molecular weight of the molecules in solution.

2.2 INTRODUCTION

Rheology is defined as the science of the flow and

deformation of materials.

In this work however the term will be restricted to fluid rheology.

For many simple fluids, the study involves the measurement of viscosity. For such fluids, the viscosity depends primarily upon the temperature and hydrostatic pressure. The rheology of polymer solutions, however, is much more complex because polymeric fluids show non ideal behaviour.

In addition to having complex shear viscosity behaviour, polymeric fluids also show elastic properties, normal stress phenomena and prominent tensile viscosities. All these rheological properties depend upon:

(1) The rate of shear
(2) The molecular weight
(3) Polymer structure
(4) Concentration
(5) Temperature
(6) Presence of any additives.

A study of polymer operations requires a knowledge of the relationships that exist between the processing variables and the mechanical and flow properties present.

The following schematic figure shows the important inter-relationships.

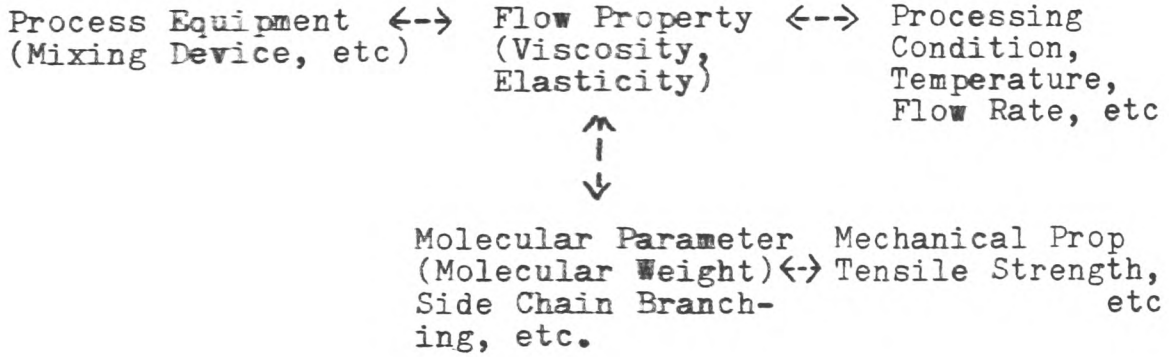

In the present work, rheological behaviour is important since it is believed to influence the behaviour of monomer droplets in a stirred reaction vessel.

Ideal fluids are called Newtonian, and their viscosity is independent of the rate of shear. The use of a Newtonian fluid for the preparation of suspension polymers has been investigated by Topping (25) and a correlation between particle size and physical properties of the system established. The Reynolds and Weber numbers were both incorporated into an experimental model.

A characteristic of some polymer fluids, including high molecular weight polyacrylamide, is their non Newtonian behaviour whereby the apparent viscosity decreases as the rate of shear increases.

Suspension polymerisation involves a dynamic equilibrium between monomer break up and drop coalescence. It is thought that the non Newtonian behaviour of the continuous phase can influence the point of equilibrium and produce new inter-relationships between the processing variables - including flow and molecular parameters and the final particle size.

An important physical parameter is polymer adsorption onto a monomer interface. The effect of the adsorption process is to produce changes in the interfacial tension which is generally reduced. Interfacial tension is very important since it is fundamental to the question of drop break up and coalescence.

To sum up, given a flow situation, a better under-

standing of both the rheological behaviour and surface properties of the protective colloid is essential to successful processing of a suspension polymerisation. In this chapter fundamental studies of both rheology and interfacial tension are described.

2.3 RHEOLOGY - BACKGROUND INFORMATION

2.3.1 THE POLYMER MOLECULE IN SOLUTION

The suspending agent used in a suspension polymerisation is a high molecular weight polymer. In the present work, polyacrylamide was used and this was supplied as a powdered solid.

The polymer chain is linear, and when fully extended is very long compared with its cross sectional area.

The polymer dissolves in water to produce an aqueous solution which exhibits non Newtonian behaviour. The process of solution formation occurs in two stages:

(1) On initial contact with water, the regular structure of the polymer changes, swelling up to form a gel. In this gel, the polymer molecules remain compact to form a three dimensional structure throughout which the water can move freely. The addition of more water breaks the contacts between the polymer molecules completely, which then become solvated and pass into solution. In this state, each polymer molecule is surrounded by a layer of solvent molecules which are held to it by hydrogen bonds or other dipolar molecules.

If the contact between the polymer molecules is very strong because of either hydrogen bonding or

crystallinity then the gel will not go into solution. In liquid water the molecules are not in complete random motion, but exist in areas of ordered structure which are termed flickering clusters. The clusters are highly hydrogen bonded regions consisting of about 60 water molecules and exist for only 10^{-11} seconds.

The cluster is generally spherical in shape; its size depends on the temperature, increasing as the temperature is reduced.

When any solute is added to water the arrangement of the ordered and disordered regions is altered. The ease with which the polymer dissolves in water depends on these resultant interactions.

In general, ionic and polar solutes changes the equilibrium towards more unbonded water, whilst non polar solutes will increase the proportion of molecules in clusters.

The unbonded state is more stable so that ionic and polar solutes readily dissolve in water. Because non polar molecules increase the unstable state they interact with each other rather than with the water to form hydrophobic bonds.

In solution, the polyacrylamide is - randomly coiled. The size and degree of extension depends upon the polymer - solvent interaction forces.

The size of a randomly coiled polymer is usually given by the root mean square end to end distance $(r_2)^{\frac{1}{2}}$ or the radius of gyration $(s^2)^{\frac{1}{2}}$.

For a branched polymer solution there are many chain ends, and a branched polymer will be less extended than a linear one of the same molecular weight. As the branching becomes more extensive the number of possible conformations becomes less and thus the random coil structure is replaced by one in which the polymer is regarded as a fairly dense - spherical structure.

2.3.2 RHEOLOGICAL MODELS

Rheological properties of polymeric materials are influenced by the molecular weight, the molecular weight distribution and the degree of long chain branching.

A theoretical development of the relationship between molecular parameters and rheological properties is far from complete but important progress has been made by a number of investigators (27 - 32).

Any satisfactory molecular theory should provide a basis for relating rheological properties to details of molecular structure.

Bueche and Harding (33) suggested a method which permits the absolute molecular weight to be obtained from the measurement of the viscosity shear rates.

Merefee and Peticolas (34) have shown how it is possible to obtain an estimate of the molecular weight distribution.

Other workers (35,36,32) have shown how the effect of long chain branching may be taken into account to describe the rheological properties of polymers.

2.3.2.1 THE MOLECULAR VISCOELASTIC THEORY OF POLYMERS

The development of the molecular viscoelastic theory is discussed with regard to the properties of polymer solutions.

Rouse (27) developed a molecular theory for dilute solutions of linear polymers.

In his theory the polymer molecule is divided up into N equal submolecules. Each submolecule is a portion of polymer chain just long enough so that at equilibrium the separation distance of its ends, to a first approximation is a Gaussian probability function. Then the polymer molecule is considered to be replaced by a chain of (N + 1) identical beads joined together by N completely flexible spring segments. Such a spring and bead model is schematically shown in Fig 4.

With the aid of chemical potential and orthogonal transformation of coordinates, Rouse was able to derive the following equation for the relaxation time λ_p of the segment.

$$\lambda_P = \frac{6(\eta_o - \eta_s)M}{\pi^2 p^2 c R T} \quad (p = 1, 2, 3, \text{---}N) \qquad (48)$$

Where η_o is the zero-shear viscosity, η_s the viscosity of solvent, c the concentration, M the molecular weight, R the gas constant and T the absolute temperature.

The components of the complex viscosity for

oscillatory shear flow are given by:-

$$n(w) = n'(w) - in''(w) \tag{49}$$

$$n'(w) = ns + cKT \sum_{p=1}^{N} \frac{\lambda_p}{1 + w^2\lambda_p^2} \tag{50}$$

$$n''(w) = cKT \sum_{p=1}^{N} \frac{w\lambda_p^2}{1 + w^2\lambda_p^2} \tag{51}$$

Where w = frequency of oscillation
K = Boltzmanns constant
$n^1(w)$ = dynamic viscosity

Zimm(37) also considered the bead segment model (ie (N + 1) beads connected by N segments). Again each segment is assumed to have a Gaussian probability function and it is further assumed that the force exerted on the fluid by the bead is proportional to the velocity of the bead moving in the fluid.

Zimm combined the method of Kirkwood and Riseman (38) which takes account of the hydrodynamic interaction with the normal coordinate formalism of Rouse.

Zimm examined two limiting cases;

(i) Vanishing hydrodynamic interaction
(ii) Dominant hydrodynamic interaction

The free draining limit is identical to the result developed by Rouse.

In steady shearing flow, the Rouse and Zimm theories give the fluid viscosity as:-

$$n - n_s = cKT \sum_{p=1}^{N} \lambda_p \qquad (52)$$

Neither theory fully describes the shear dependent viscosity of polymeric materials.

Bueche (29 39) also developed a theory based on the consideration that a polymer molecule is divided into a large number of submolecules each of which behaves like a small mass attached to a linear spring. Bueche then developed a model for the displacement of each submolecule relative to its equilibrium position. For a shear field Bueche calculated dissipation from the displacement for each submolecule which is a product of the force and velocity relative to the solvent.

Summing the dissipation over the entire molecule gives the following expression for viscosity:

$$\frac{n - n_s}{n_o - n_s} = 1 - \frac{6}{\pi^2} \sum_{n=1}^{N} \frac{\dot{\gamma}^2 \lambda_1^2}{n^2(n^4 + \dot{\gamma}^2\lambda_1^2)} \left(2 - \frac{\dot{\gamma}^2 \lambda_1^2}{n^4 + \dot{\gamma}^2\lambda_1^2}\right) \qquad (53)$$

Where n_o is the viscosity of the polymer in the limit of zero shear rate
n_s = the viscosity of the solvent
$\dot{\gamma}$ = shear rate
λ_1 = Bueche time constant

$$\text{Where} \quad \lambda_1 = \frac{12(n_o - n_s)M}{\pi^2 cRT} \qquad (54)$$

can be considered a characteristic relaxation time of the molecule.

The Bueche theory gives a shear dependent viscosity where as the Rouse and Zimm theories do not.

Williams (40) extended the Zimm theory to derive the normal stress difference $(r_{11} - r_{22})$ for steady shearing flow, which is given by :

$$(r_{11} - r_{22}) = \frac{2\,c\,R\,T}{M}\,\dot{Y}^2 \sum_{p=1}^{N} \lambda_p^2 \qquad (55)$$

Where $\dot{Y}$ is the shear rate and M the molecular weight.

This equation shows that $(r_{11} - r_{22})$ is proportional to $\dot{Y}^2$ for a given material and shows clearly the dependence of $(r_{11} - r_{22})$ on molecular weight M, the concentration c, and the temperature T of the fluid.

Both the Rouse and Zimm theories hold for moderately dilute polymer solutions, depending on the solvent used (41,42,43).

2.3.2.2 NETWORK AND ENTANGLEMENT THEORIES

A network theory was developed by Lodge (44) for concentrated polymer solutions. The assumptions made in deriving the theory are:-

(i) A homogeneous network prevails in a polymer solution at rest.

(ii) The Helmholtz free energy is made up of contributions from an entropy change.

(iii) Thermodynamic equilibrium with respect to network configuration exists.

(iv) The concentration of functions is unaffected by the flow of the solution.

For steady shearing flow, Lodge (44) derived the following equations for viscosity and nomal stress difference.

$$n = 2 K T N_1 (T, C) \tag{56}$$

$$r_{11} - r_{22} = 2 K T N_2 (T, C) \dot{Y}^2 \tag{57}$$

$$\text{Where } N_r(T, C) = \int_{t^1 = -\infty}^{t^1 = t} N(t - t^1, T, c) (t - t^1)^r dt^1 \qquad (r = 1, 2 \text{ ---}) \tag{58}$$

$N(t-t^1, T, C)$ is the concentration of functions for the group of chains which joins the network during the time interval $(t^1, t^1 + dt^1)$, K the Boltzmanns constant, C the concentration, and T the absolute temperature.

Lodge made two additional assumptions, namely K is such that all segments have the same probability λ_{kn} of leaving the network per unit time, and all segments are created at a constant rate per unit volume LKn.

Then Lodge obtained:-

$$N (t - t^1) = \sum_{K, n} L_{Kn} e^{(t - t^1)/\lambda k n} \tag{59}$$

$$\text{and } n = 2 K T \sum_{K, n} N_{K n} \lambda_{k n} \tag{60}$$

$$(r_{11} - r_{22}) = - 4 K T \dot{Y}^2 \sum_{K,\ n} N_{Kn} \lambda^2_{Kn} \qquad (61)$$

Where N_{Kn} is the number of K type, n^{th} link segments in the network per unit at any instant, and:-

$$N_{Kn} = L_{Kn} \lambda_{Kn} \qquad (62)$$

It is seen that the Lodge theory predicts the fluid viscosity η as independent of the shear rate $\dot{Y}$, and it predicts the normal stress difference $(r_{11} - r_{22})$ as proportional to the square of the shear rate.

Grassley (32,45) developed a theory - considering the dynamics of entanglement formation between pairs of molecules and its influence on the density of entanglements during steady deformation. For an entanglement to exist two molecules must pass within a critical distance for a finite time.

The theory gives the following equations for fluid viscosity in steady shearing flow.

$$n/n_o = (2/\pi)\left\{ \cot^{-1} \theta + \left(\theta(1 - \theta^2)/(1 + \theta^2)^2\right)\right\} \qquad (63)$$

$$\text{Where } \theta = (\lambda_o \dot{Y}/2)\ (n/n_o) \qquad (64)$$

Where η_o = zero shearviscosity
$\dot{Y}$ = shear rate
λ_o = relaxation at zero shear rate

For large values of θ , Grassley derived the

viscosity at high shear rates as;

$$n = (\text{constant}) M^{0.1} \left|\dot{\gamma}\right|^{-3/4} \qquad (65)$$

This indicates that at high shear rates, the viscosity is a very weak function of molecular weight and is proportional to $(\dot{\gamma})^{-3/4}$.

The decrease in viscosity is attributed to a decrease in the polymer entanglement.

The Grassley molecular theory also predicts the normal stress difference $(r_{11} - r_{22})$

$$(r_{11} - r_{22}) = f(M, T, \eta_o)\, \dot{\gamma}^2 \qquad (66)$$

in which $f(M, T, \eta_o)$ is a function of the molecular weight M, temperature T, and the zero shear viscosity, and contains unknown parameters of the model such as the friction coefficient associated with entanglement, the entanglement density at zero shear rate, and the entanglement sphere radius.

2.3.3 DEPENDENCE OF RHEOLOGICAL PROPERTIES ON MOLECULAR PARAMETERS

Consider the Bueche theory, this permits the correlation of the reduced viscosity $(\eta - \eta_s) / (\eta_o - \eta_s)$ with molecular weight M, temperature T, concentration c, zero shear viscosity η_o.

Since the characteristic time constant λ_1 contains all these parameters, λ_1 can be considered a factor which relates η with $\dot{\gamma}$.

It is generally accepted that the primary effect of shear is a breaking down of molecular interactions arising from chain entanglements. Since chain entanglement is a function of both size and number of molecules, the molecular weight and the molecular weight distribution are controlling factors in determining the viscosity of polymeric materials.

In most polymeric solutions and melts the viscosity is independent of shear rate at sufficiently low shear rates. As the shear rate is increased, the viscosity begins to decrease from its low shear value η_o.

Fox and Flory (46,47) were the first to show that the zero shear viscosity η_o of concentrated polymer solutions and melts of linear polymers is proportional to the molecular weight M below a critical value Mc, whereas above Mc it increases rapidly and becomes proportional to $M^{3.4}$.

$$\eta_o = \begin{cases} K\,M & M < Mc \\ K\,M^{3.4} & M > Mc \end{cases} \qquad (67)$$

This is schematically shown in Fig 5. The critical molecular weight Mc corresponds to a value beyond which molecular entanglements begin to dominate the resistance to flow. In the case of polymer solutions, both K and Mc change if a solvent is added to the polymer.

The above equation applies to polymers with different molecular weight distributions if M is replaced in the equation by the weight average molecular weight $\bar{M}w$.

From a rheological standpoint it is possible to interpret the critical molecular weight (Mc) as a constant,

signifying the lower limit of molecular weight for which non Newtonian flow can be observed. It would be expected that the onset of non Newtonian behaviour is strongly dependent on the molecular weight and the molecular weight distribution.

The literature indicates that above a critical molecular weight Mc, the onset of non Newtonian behaviour occurs at lower shear rates as molecular weight increases and as the molecular weight distribution broadens.

2.3.3.1 VISCOSITY - SHEAR RATE CURVES

Viscosity - shear rate curves for polymer solutions of different concentration can easily be obtained from experimental data.

Typical viscosity - shear rate curves are shown in Fig 6.

These curves show that dilute solutions remain Newtonian in behaviour to higher rates of shear than do more concentrated solutions.

The solvent reduces the number of entanglements by increasing Me (Molecular weight between entanglement points).

Reducing the number of entanglements at a given rate of shear reduces the amount of orientation of molecular segments. Since the orientation of molecular segments is the major cause of non Newtonian behaviour adding a liquid to a polymer should increase the rate of shear at which non Newtonian behaviour becomes noticeable.

Both the dynamic viscosity and the shear modulus increase with polymer concentration.

The lower the concentration, the higher the frequency at which non Newtonian behaviour (as revealed by a decrease in viscosity with frequency) becomes apparent. At low concentration few entanglements exist, but the solution will still show some elasticity and a low elastic modulus. The elasticity results from distortion of the coiled molecules by the shearing field with resultant orientation of some of the molecular segments. When the flow stops, the deformed molecules quickly revert back to their coiled state.

In concentrated solutions, the shear modulus increases much more rapidly than the first power of the polymer concentration.

A plot of viscosity against shear rate for samples of a polymer solution can give useful information on the degree of long chain branching. For example consider low and high density polyethylene (Fig 7).

A plot of melt viscosity versus shear rate is shown for both high and low density polyethylene.

The much lower melt viscosity of low density polyethylene is attributable to the presence of much long chain branching.

2.3.4 NORMAL STRESS

Normal stress is a rheological phenomenon encountered with non Newtonian fluids. The normal stresses generally develop at right angles to F, the applied force, when the material is sheared (Fig 8).

The first normal stress difference ($\sigma_{11} - \sigma_{22}$) tends to force the shear plates apart.

to create bulges in the polymer at the edge of the plates either parallel or perpendicular to the direction of the applied force.

The following definitions and relationships apply to normal stresses.

$$\sigma_{11} + \sigma_{22} + \sigma_{33} = 0 \qquad (68)$$

$$\sigma_{11} - \sigma_{22} = \text{first normal stress difference} \qquad (69)$$

$$\sigma_{22} - \sigma_{33} = \text{second normal stress difference} \qquad (70)$$

The cone and plate rheometer can be used to measure directly the normal stress which tends to force the cone and plate apart.

The difference between the first and second normal stress is given by:

$$\sigma_{11} - \sigma_{22} = \frac{2N}{\pi R^2} \qquad R = \text{Radius of Cone} \qquad (71)$$

Where N = normal (axial) force trying to separate the cone and plate.

Normal stresses result from the orientation of chain segments, and chain entanglements greatly enhance the ease of orienting the segments during deformation.

The first normal difference $\sigma_{11} - \sigma_{22}$ is defined as being (+) if the forces tends to push the retaining plates apart during shear of a fluid between plates moving parallel to one another.

The normal stress differences increase with the square of the shear.

$$\sigma_{11} - \sigma_{22} = \psi_1 \dot{\gamma}^2 \tag{72}$$

$$\sigma_{22} - \sigma_{33} = \psi_2 \dot{\gamma}^2 \tag{73}$$

The first and second normal stress coefficients ψ_1 and ψ_2 may be functions of the rate of shear. Normal stresses produce a number of phenomena not found with Newtonian liquids. For example, when a polymer is extruded from an orifice, a capillary or slit, the diameter or thickness is much greater than the diameter of the hole. This is called die swell.

Another phenomenon due to normal stresses is the ascending of polymer liquids up rotating shafts. In contrast rotating shafts in Newtonian liquids cause a depression of the liquid surface because of centrifugal forces.

Fig 9 shows the creep of a polymeric liquid up the rotating inner cylinder of a coaxial cylinder viscometer.

Normal stress measurements are difficult to make.

The first normal stress is generally positive and at high rates of shear may exceed the value of the shear stress.

A positive first normal stress difference ($\sigma_{11} - \sigma_{22}$) means that the tension resulting from the molecular orientation is parallel to the flow stream lines. The second normal stress difference ($\sigma_{22} - \sigma_{33}$) is generally negative and its value is very small. (See Fig 10.)

Two polymers of almost identical viscosity characteristics may exhibit quite different behaviour under actual processing conditions.

Meissner (48) found that three polyethylenes of nearly the same viscosities and molecular weight distribution behaved quite differently when used to make blown film.

The rheological differences between the polymers showed up in the first normal stress differences and in the extensional viscosities.

Bird and coworkers (49) have developed a procedure for calculating both the first normal stress difference and die swell of a polymer from the shear rate dependence of the viscosity.

In the present investigations, concentrated solutions of polyacrylamide 2% exhibited unusual flow behaviour ie, climb up on the rotating stirrer shaft thus indicating a fairly large normal stress difference due to a high fluid elasticity.

The behaviour of stirred solutions with a large normal stress difference is such that sometimes regions of poorly mixed solution will exist in definite regions of a vessel symmetrically arranged to the stirrer (50).

No evidence of this however has been observed in the experimental work carried out using polyacrylamide solutions up to 2% by weight.

2.4 MEASUREMENT OF VISCOSITY

2.4.1 INTRODUCTION

Viscosity depends on molecular size particularly chain length andthe magnitude of intermolecular forces. An ideal liquid (Newtonian) cannot withstand the smallest stress, but flows at a rate which is proportional to the applied stress.

$$\text{Dynamic viscosity} = \frac{\text{shear stress}}{\text{shear rate}} \quad \frac{(\text{Dyne/cm}^2)}{(\text{sec}^{-1})} \qquad (74)$$

Although shear stress and strains vary throughout the liquid in an agitated vessel, the viscosity of a Newtonian liquid will be the same at all points in the vessel. The apparent viscosity of a non Newtonian liquid at any point depends on the magnitude of either the shear stress or shear rate and may also depend upon the previous history of the liquid.

The shear rate is greatest in the immediate vicinity of the agitator and decreases with distance from the agitator.

The effect of shear rate on apparent viscosity will determine the viscosity profile throughout the vessel. The term viscosity has no meaning for a non Newtonian fluid unless related to a particular shear rate . An apparent viscosity μa can be defined as follows;

$$Ua = \frac{R}{\dot{Y}} \qquad (R = \text{shear stress}) \qquad (75)$$

When the apparent viscosity μa decreases with an increase in shear rate $\dot{Y}$ the fluid is said to be pseudo-

plastic. When Ua increases with an increase in $\dot{Y}$ the fluid is said to be dilatant.

Another type of non Newtonian fluid is the Bingham fluid. A plot of R against $\dot{Y}$ on Cartesian Coordinates for a Bingham fluid is a straight line having an intercept Rb on the shear stress axis called the Yield stress. Rb is the stress which must be exceeded before flow starts. The fluid at rest contains a three dimensional structure of sufficient rigidity to resist any stress less than the yield stress (Fig 6a) When this stress is exceeded the system behaves as a Newtonian or a non Newtonian fluid under a shear stress (R - Rb). For Bingham fluids the slope of the shear stress, shear rate plot is called the coefficient of rigidity.

Pseudoplastics, dilatants and Bingham fluids are examples of time independent non Newtonian fluids (The apparent viscosity depends only on the rate of shear at any particular moment and not on the time for which the shear rate is applied). For a certain class of fluids the apparent viscosity continues to change as a function of the time for which the particular shear rate is applied. These are known as time dependent non Newtonian materials. Fluids which become more pseudoplastic with time at constant shear rate known as thixotropic fluids. Their structure progressively breaks down with time at a constant shear rate. Thixotropy is a reversible process and eventually a dynamic equilibrium is reached where the rate of structural breakdown is balanced by the simultaneous rate of reformation. A minimum value of the apparent viscosity is reached at

any constant rate of shear.

Many fluids show thixotropic behaviour in addition to being pseudoplastic or even dilatant.

Most thixotropic fluids will recover their original viscosity if allowed to stand for a sufficient length of time. Some fluids will revert almost immediately, while others might take several hours.

Fluids which become more dilatant with time at a constant shear rate are known as rheopectic fluids. In this case small shearing helps the formation of structure, while above a critical point breakdown occurs. If the shearing rate is rapid, the structure does not form. In general the apparent viscosity of rheopectic fluids increase with time to a maximum value at a constant rate of shear. Another important group of non Newtonian fluids are visco elastic fluids. This exhibit both viscous and elastic properties.

For Newtonian fluids the shear rate, $\dot{Y}$, is a linear function of the shear stress, R.

$$\dot{Y} = \frac{R}{U} \qquad (76)$$

For non Newtonian fluids the relationship between $\dot{Y}$ and R is more complex and for time independent fluids can be written as:

$$\dot{Y} = f(R) \qquad (77)$$

Attempts have been made to produce mathematical models to represent the rheological behaviour of non Newtonian fluids. The simplest and most commonly used relationship is the power law equation.

$$R = K (\dot{Y})^n \qquad (78)$$

Where K is called the consistency coefficient and n the power law index. Fluids which obey the above equation are called power law fluids. For pseudoplastic fluids $n < 1$ and for dilatant fluids $n > 1$. In the case of Newtonian fluids n = 1 and K becomes the coefficient of dynamic viscosity .

2.4.2 METHODS OF MEASURING VISCOSITY

The viscosity of a fluid may be defined qualitatively as the resistance to flow. In order to induce flow a force must be exerted on the fluid so that the viscous forces of mutual attraction between molecules are overcome and the molecules displaced relative to each other. The stronger the molecular force the smaller the amount of flow for a given applied force (ie the greater the viscosity of the fluid).

The foundations of viscosity measurement were laid by Newton when he postulated that the rate of flow is proportional to the applied stress.

The Newtonian model of flow considers two parallel planes at unit distance apart with the space between them filled with liquid.

The viscosity is defined as the tangential shearing force per unit area that will produce a unit velocity gradient. This is written:

$$r = n \frac{dv}{dr} \qquad (79)$$

Where r is the tangential shearing force per unit area (or shearing stress) in dynes/cm^2; $\frac{dV}{dr} = D$ the velocity gradient (or rate of shear) in sec^{-1}; the proportionality constant n is the coefficient of viscosity in poises.

Viscosity may be determined by measuring either the rate of shear caused by a known shear stress or the shear stress required to induce a known rate of shear. The poise is the absolute unit of dynamic viscosity n ($ML^{-1}T^{-1}$) as distinct from the stoke, which is the unit of kinematic viscosity v(L^2T^{-1})

$$v = \frac{n}{p} \qquad (80)$$

Where P is the density of the fluid in g/cm^3

The kinematic viscosity is used with viscometers in which the measurement is influenced by the density of the fluid eg the gravity dependent capillary viscometers.

Low viscosities are usually expressed in centipoises or centistokes (water at 20^{o}C $\sim$ 1 centipoise).

The variation in viscosity is great, ranging from water at 10^{-2} poise to pitch, plastics etc at 10^6 - 10^{12} poise.

No single viscometer can cover the entire range of viscosity and this factor coupled with the diverse nature of non Newtonian flow properties has led to the development of a multiplicity of viscometer types, the majority of which are designed to cover a small part of the range or a particular type of fluid. Unfortunately some instruments are calibrated in arbitary units uniquely related to the particular design of viscometer. This makes the correlation of data obtained with different viscometers difficult.

It is convenient to classify viscometers according to the type of physical measurement employed. The most important types are outlined as follows:-

1. Measurement of the rate of flow of a fluid in a capillary or tube (eg the Ostwald viscometer)

2. The rate of motion of a solid through the sample fluid (eg falling sphere viscometer).

3. Rotational Viscometers.

(a) Measurement of the torsional couple on a suspended solid element due to the viscous force transmitted through the subject medium by a second element in motion. This principle is used in coaxial cylinder viscometer of the Couette - Hatschek type, in which the outer cylinder is continuously rotated and the angular deflection of the inner cylinder measured by a torsion spring (ie measurement of the applied stress necessary to maintain a known shear rate).

(b) Measurement of the velocity of a cylinder or similar element immersed in the fluid. The Searle and

stormer viscometers are typical examples. They are coaxial cylinder viscometers with a fixed outer cylinder, the inner being driven by a pulley and weight. The rotational velocity is inversely proportional to the viscosity of the fluid in the annulus (ie measurement of the shear rate due to a known applied stress).

(c) Measurement of the reaction torque due to viscous traction on a solid element rotating at a known rate in the fluid. The Ferranti-Shirly cone and plate viscometer operates on this principle, the rotating element being a disc with a slightly conical face.

In the Brookfield viscometer, the torque on a rotating cylinder or disc immersed in the fluid is measured ie measurement of the applied stress necessary to maintain a known shear rate.

4 Measurement of the damping of a vibrating element immersed in the fluid. The ultraviscon measures the decrease of free vibrations of a need oscillaing at ultrasonic frequency in the longitudinal mode.

2.4.3 THE FERRANTI SHIRLY CONE AND PLATE VISCOMETER

The essential elements of the cone and plate viscometer are shown in Fig 11.

In the figure 'a' is a slightly conical disc, the apex of which touches the surfaces of the flat plate 'b'.

The sample fluid is contained in the narrow gap between the cone and plate.

Either the cone or the plate may be driven at a known speed whilst the torsional couple on the other member is measured. It has certain advantages to operate with

the plate rigidly constrained while the torque on the cone at a constant speed is measured. In this way, temperature control of the plate is facilitated by circulation of water from a constant temperature bath.

The rate of shear at any radius 'r' is given by the ratio of linear viscosity Ω r to the gap width C. Since both these quantities are proportional to the radial distance, the shear rate is constant throughout the entire measured sample.

2.4.3.1 METHOD OF OPERATION

Measurements can be made with the Ferranti-Shirly cone and plate system by 3 methods:

(a) Shear stress measurement at manually set shear rates.

(b) An X-Y recording showing shear stress (x) versus shear rate (Y) employing the programmed increasing and decreasing rate of shear.

(c) An X-Y recording showing shear stress (x) versus time (Y) at a constant shear rate using programmed control.

2.4.3.2 MANUAL OPERATION

In a cone-plate viscometer the position of the cone with respect to the plate is critical, and the initial setting must be a precise operation as movements of the plate are controlled to within ·0001 inches. The apex of the cone must just touch the plate, and the plate position is adjusted at the required operating temperature according to instrument manual.

The sample size must be sufficient to fill the gap between the cone and plate and is placed on the centre of

the plate.

The plate is raised slowly into the operating position and the speed control turned to give the desired RPM for the first reading which is recorded. The speed control is again turned to give the new RPM setting and the reading noted.

A series of readings are taken at different cone speeds until the maximum desired speed is reached.

Three different cones are available to extend the range of the instrument.

$$\text{Shear Stress } '\tau' = \frac{3T}{2\pi R^3} \qquad (81)$$

$$(\text{dyne/cm}^2 \times \frac{\text{Instrument}}{\text{Reading}} \times \frac{\text{Scale}}{\text{Reading}})$$

Where T = Torque spring constant (dyne cm/div)
R = Radius of cone (cm)

Shear Rate Constant 'D'

$$D = \frac{\Omega}{\psi} \qquad \Omega = \text{Angular Velocity (Rod/sec)} \qquad (82)$$

ψ = Cone Angle (Radians)

$$D = \frac{\text{RPM} \times 2\pi}{\psi \times 60} \ (\text{Sec}^{-1}) \qquad (83)$$

$$= \text{constant} \times \text{RPM} \ (\text{Secs}^{-1}) \qquad (84)$$

CONE CONSTANTS

$$\text{The viscosity } \eta \ (\text{poise}) = \frac{3\psi}{2\pi R^3} \times \frac{G}{\Omega} \qquad (85)$$

Where ψ = Cone angle (Radians)
Ω = Angular Velocity (rad/sec)
R = Radius of Cone (cm)
G = T x Reading 600
T = Torque spring constant
(dyne cms/div on 600 Range)

For the Large Cone ψ = 20'25" = 0.0059526 Radians
R = 3.5 cm T = 2002.22

$$CL = \frac{3}{2\pi \times .1047} \times \frac{\psi T}{R^3} \qquad (86)$$

$$= 4.562 \times \frac{2002.22 \times .0059526}{42.88}$$

$$= 1.268$$

For the Medium Cone ψ = 20'25" = 0.0059531 R = 20cm
T = 2002.22

$$CM = \frac{4.562 \times 2002.22 \times .0059531}{8}$$

$$= 6,795$$

For the Small Cone ψ = 22'24" = ·0065315 Radians

R = 1.0

$$CS = \frac{4.562 \times 2002.22 \times 0.0065315}{1.0}$$

$$= 59.66$$

$$\text{Viscosity (Poises)} = \frac{\text{Scale Reading x Cone Constant x Range}}{\text{Speed}} \qquad (87)$$

at fixed speeds for standard shear rates this simplifies to:-

Viscosity = Scale Reading x K x Range (88)

Results obtained using the cone and plate viscometer are reported in the tables 1 - 5.

2.4.4 THE COAXIAL CYLINDER VISCOMETER

The multiplicity of non Newtonian substances encounted vary so greatly in flow behaviour and degree of anomaly that no single viscometer can be applied satisfactorily to all of them.

The choice of a suitable viscometer for the investigation of a particular type of non Newtonian fluid is facilitated by a study of the shear conditions within the viscometer and their effect on the rheological properties of the subject liquid.

The fundamental difficulty in the determination of non Newtonian flow properties lies in the ability of these fluids to sustain shear without changing the properties which one is trying to measure.

Since the fluid must be sheared in order to make the measurement reproducible experimental data must be obtained by observing two principle conditions:

1. The rate of shear should be uniform throughout the measured sample.

2. A consistent experimental procedure should be adopted, including the previous history of the sample fluid and the amount and duration of the shear.

There are very few viscometers capable of imposing truly constant shear conditions. The band viscometer probably comes closest, with the coaxial cylinder also producing a uniform shear rate in common with the cone and plate type.

The optimum design of viscometer requires that the end effects be reduced to negligible proportions and the cylinder clearance to a minimum.

The first condition is a corollary of the second but with a few exceptions these two requirements are rarely attained in the same viscometer.

A large number of coaxial cylinder viscometers in common industrial use depart widely from this optimum design.

An examination of the flow conditions in a typical viscometer of this type emphasises the difficulties which arise when the sample fluid is non Newtonian. Fig 12 shows schematically a viscometer in which the inner cylinder rotates within a stationary outer cylinder; the thin lines represent the path length through which the shear forces act.

It is clear that widely divergent shear rates exist, ranging in fact, from zero at the axis of rotation to maximum at the perimeter of the inner cylinder. It follows that a non Newtonian fluid having the typical flow characteristic shown in Fig 12 will attain varying viscosity levels in different regions of the sample as indicated by the points A1, B1, and C1.

The total torque on the cylinder will be some complex function of a multiplicity of diverse shear forces, the distribution of which will depend on the flow characteristic. If it is wished to compare the flow data with another fluid having a different characteristic, the distribution of the forces will change and a valid comparison

cannot be made.

This is shown by curve 2 in Fig 13: the difference in viscosity level between B and C in the viscometer is now much greater than the first fluid sample.

These difficulties are often masked by the fact that such a viscometer may be capable of repeating results on different samples of the same fluid with reasonable accuracy.

If means are employed to minimise the end effect errors, a correction can be applied for the variation of shear rate across the annular gap for most type of non Newtonian flow.

The shear rate is proportional to the reciprocal square of the cylinder radius so that for a well designed viscometer where the ratio of the cylinder radii $\frac{R1}{Ro}$ is $\frac{0.9}{1}$, the shear rate variation is about 20%.

For a non Newtonian fluid the variation could be as high as 250%, the actual magnitude and distribution being a function of its flow properties.

2.4.4.1 METHOD OF OPERATION

The instrument used for the investigations was the Rotovisk D.

$$\text{Shear Rate } D = M \times n \quad \sec^{-1} \tag{89}$$

$$\text{Shear Stress } r = A \times S \quad \text{dyne/cm}^2 \tag{90}$$

$$\text{Viscosity } (n) = \frac{G \times S}{n} \quad CP \tag{91}$$

Where n = test speed
s = indicated scale value

Attachment MV1 was used with a 500gm measuring head to obtain calibration values for M, A and G.

These are listed as follows:-

M = 2.35

A = 29.80

G = 1268

The speed was selected, and the reading obtained from the scale. The sample temperature was noted.

2.5 FUNDAMENTAL STUDIES OF THE AQUEOUS PHASE

The object of this work is to collect and present experimental information concerning the fundamental physical and rheological properties of an aqueous solution containing the dissolved suspending agent used in the suspension polymerisation studies reported later.

The following experiments were carried out:-

1. A study of the rheological behaviour of an aqueous solution containing dissolved high molecular weight polyacrylamide.

2. To examine the influence of simple inorganic ions upon an aqueous solution of the suspending agent.

3. To determine the molecular weight of the suspending agent and investigate the effect of stirring speed on the aqueous solution.

2.5.1 THE EFFECT OF SUSPENDING AGENT CONCENTRATION ON THE RHEOLOGICAL PROPERTIES OF THE AQUEOUS PHASE

2.5.1.1 SAMPLE PREPARATION

Aqueous solutions of high molecular weight polyacrylamide were prepared by slowly adding the granulated

solid to a reaction flask containing 2 litres of water. The water was stirred at 150 rpm, and the solid added slowly to prevent the accumulation of lumps which can be difficult to dissolve. The temperature was kept at 20°C during the dissolving stage.

Samples containing between 0.5% - 2% wt/wt of polyacrylamide were prepared in this way.

2.5.1.2 EXPERIMENTAL METHOD

Measurements of the shear rate, shear stress and apparent viscosity were made using the cone and plate and coaxial cylinder viscometers. Measurements were carried out at 75°C (the usual reaction temperature of a suspension polymerisation process).

Using the coaxial cylinder viscometer additional measurements were also obtained in the presence of styrene monomer at 75°C, dispersed as small droplets in the aqueous phase at 0.3% monomer volume fraction.

2.5.1.3 RESULTS

Rheological data obtained using the cone and plate viscometer are reported in tables 1 - 5. Similar data for the coaxial cylinder are reported in tables 6 - 12.

2.5.1.4 DISCUSSION OF RESULTS

(a) Cone and Plate Data

Tables 1 - 4 gives data for shear rate, shear stress and apparent viscosity of 4 solutions of concentration range 0.5% - 2% wt/wt of polyacrlamide at 75°C.

Figure 14 shows a plot of log apparent viscosity against log shear rate for the 4 solutions.

Details of the graph intercept and slope are given in table 5.

A plot of shear stress against shear rate is shown in Fig 15.

It is clear from this result that the aqueous polymer solution behaves as both a pseudo plastic and a Bingham fluid showing a definite yield stress point.

(b) Coaxial Cylinder Data

Tables 6 - 11 gives data obtained with the coaxial cylinder viscometer at 75°C.

These tables list the shear rate, shear stress and apparent viscosity of 3 polyacrylamide solutions (0.5% - 1.5% wt/wt).

Figure 16 shows a plot of shear stress against shear rate for the 3 aqueous solutions. The Bingham fluid behaviour is less apparent in this plot compared to the cone and plate data (Fig 15). Figure 17 shows a plot of log apparent viscosity against the log shear rate for the 3 solutions. Figures 18-20 show a similar plot for the 3 solutions containing dispersed monomer at 0.2 volume fraction. Details of the slope and intercept for the solutions is given in table 12. A comparison of both cone and plate and coaxial cylinder data is reported in Table 13.

The theories of Bueche (39,28), Graessley (45), Williams (50) and Cross (51) are often used to describe the shear rate dependence of the viscosity.

Graessley and Bueche explicitly assume there are molecular entanglements which decrease as the shear

increases and which are forming and disappearing in a dynamic steady state in a shear field.

The behaviour of solutions 2 and 3 as illustrated in Fig 17 and Figs 18-20 shows such a decrease in viscosity with increasing shear rate.

The most dilute solution (No 1) however shows a different viscosity dependence with shear rate. The viscosity of the solution appears to go through a maximum with increasing shear rate, and is probably due to entanglement effects, or possible a first normal stress difference which may go through a maximum at this particular polymer concentration.

2.5.2 THE EFFECT OF A SOLUBLE INORGANIC SALT (Na_2HPO_4) UPON THE RHEOLOGICAL PROPERTIES OF THE AQUEOUS PHASE

2.5.2.1 SAMPLE PREPARATION

Samples of the suspending agent (polyacrylamide) were prepared as previously described in 2.5.1.1. To these solutions were added weighed quantities of the anhydrous phosphate salt, and the mixture stirred until the solid dissolved.

The rheological properties of each solution was then examined (over a salt concentration range of 1-6% wt/wt).

2.5.2.2 EXPERIMENTAL METHOD

The measurement of shear rate, shear stress, and apparent viscosity were made using a cone and plate viscometer at room temperature.

2.5.2.3 RESULTS

The results obtained are reported in tables 14 - 17 and a plot of shear stress against shear rate is shown in Fig 21.

2.5.2.4 DISCUSSION OF RESULTS

The viscosity of a solution is given by the expression:-

$$\text{Viscosity} = \frac{\text{Shear Stress}}{\text{Rate of Shear Strain}} = \frac{r}{\frac{d\dot{Y}}{dt}} = \frac{r}{\dot{Y}}$$

Where r = shear stress
$\dot{Y}$ = shear rate

If the fluid is not Newtonian, a plot of shear stress against the rate of shear $\dot{Y}$ is not a straight line but a curve.

From Fig 21 it can be seen that in the plot of shear rate against shear stress (in the presence of different salt concentrations) a change in the viscosity occured at a shear rate of $\sim 6X10^{-3}$. The concentration of the salt (disodium hydrogen phosphate) over the range 1 - 6% (by wt) made little difference either to the point of change or the modified viscosity values.

The behaviour of the salt may be explained in terms of the molecular conformation that the polyacrylamide is able to adapt in aqueous solution.

The ions enter the polymer network and influences the molecular interaction forces. The result of this is a new polymer conformation usually results in a change

of polymer shape and volume, and thus viscosity.

From the results obtained it is seen that the effect of the salt is most pronounced at low concentrations, little change occurs as the concentration is increased above 1%.

2.5.3 THE EFFECT OF SHEAR CONDITIONS UPON THE MOLECULAR WEIGHT OF THE DISSOLVED POLYACRYLAMIDE SUSPENDING AGENT

2.5.3.1 SAMPLE PREPARATION

A 2% aqueous solution of high molecular weight polyacrylamide was prepared by gentle stirring for 3 hours at room temperature.

2.5.3.2 EXPERIMENTAL METHOD

Two samples of the prepared aqueous phase were taken and stirred under the following conditions:-

(i) A two litre reaction vessel fitted with a 10cm flat bladed stirrer was used to agitate the solution for six hours at room temperature. A constant stirring speed of 600 RPM was employed.

(ii) A sample of the prepared aqueous phase was taken and stirred using an industrial silverson mixer at 6000 RPM for 5 minutes.

The molecular weight of the polymer solutions before and after shear was evaluated.

The equation used to calculate the molecular weight was:-

$$[\eta] = KM^{\alpha} \qquad (92)$$

Where $[\eta]$ = intrinsic viscosity
M = average molecular weight

K and α = constants

$K = 6.8 \times 10^{-4}$ dL gm^{-1}
$\alpha = 0.66$ at $30^{o}C$

2.5.3.3 CALCULATION OF MOLECULAR WEIGHT

The increase in the viscosity of a dilute polymer solution compared with that of pure solvents depends, among other things, on the molecular weight of the polymer chains and on their degree of coiling or extension.

For substantially linear polymers, the viscosity can be related empirically to the molecular weight.

Though a theoretical treatment of this is available it is too complicated for practical use.

The measurement of a solution viscosity at a given concentration may be made by comparing the time t required for a given volume of solution to flow through a capillary compared with the time, to, for the same volume of pure solvent.

Conventionaly the concentration C is expressed as g per decilitre.

The intrinsic viscosity is by definition independent of C and is of special interest since it allows the viscosity average molecular weight to be found.

2.5.3.4 SOLUTION VISCOSITIES

Common Name	Alternative Name	Symbol and Equation
Relative viscosity	Viscosity ratio	$nr = n/no = t/to$ (93)
Specific viscosity		$n_{sp} = nr-1 = \frac{n-no}{n} = \frac{t-to}{to}$ (94)

Reduced viscosity	Viscosity number	$\eta_{red} = \eta sp/c$	(95)
Intrinsic viscosity	Limiting viscosity number	$[\eta] = (\eta sp/c)_{c=0}$	(96)
		$= \left[(\ln \eta r)/c\right]_{c=0}$	(97)

For low concentrations, $\eta sp/c$ and $(\ln \eta r)/c$ are linear functions of c expressed by the equations.

$$\eta sp/c = [\eta] + K^1 [\eta]^2 c \quad (98)$$

$$(\ln \eta r)/c = [\eta] + K^{11} [\eta]^2 c \quad (99)$$

Where K^1 and K^{11} are constants.
The extrapolation of $\eta sp/c$ and $(\ln \eta r)/c$ to zero concentration give a common intercept $[\eta]$.

Two types of commonly used viscometers are used in this type of work:-

(a) Ostwald-Fenske capillary viscometer

(b) Ubbelohde capillary viscometer

In both types of viscometer, the time required for a volume of liquid (defined by etched marks above and below the bulb) to flow through the capillary is measured.

The Ostwald-Fenske viscometer was used in the present work.

2.5.3.5 RESULTS

The results are reported in table 18. A plot of $\frac{t - to}{cto}$ against c gives a straight line graph where the intercept is the intrinsic viscosity (Figs 22 and 23).

For both un-sheared and sheared solutions the intrinsic viscosity was obtained from the results shown in Fig 22 and Fig 23.

Using $K = 6.8 \times 10^{-4}$ dl gm^{-1}
$\alpha = 0.66$

in the equation $[\eta] = KM^{\alpha}$

The molecular weight of the polymer after stirring at 600 rpm was 7,046,000 while after using the high shear mixer this value reduced to 2,718,000.

The molecular weight of the standard unstirred solution was found to be 7,045,000. Thus simple laboratory agitation does not affect the molecular weight of the suspending agent.

In contrast high shear condition produce bond breaking and a reduction in molecular weight.

2.5.3.6 DISCUSSION OF RESULTS

Several papers (52,53,54) have been published on the degradation of polymer molecules in a solution due to high speed stirring.

In the present investigations the molecular weight decreased after stirring and then remained constant.

The final value will depend on the stirring speed, and is about half of the initial value. These experiments suggest that it is the degradation of the polyacrylamide molecules which is giving the decrease in viscosity. The degradation mechanism of vinyl polymers has been widely described and can be applied to other solutions.

A paper by Jeelinek (55) gives the following formula:-

$$dBi/dt = K(Pi - 1)n_1 \quad \text{For} \quad Pi > P_1 \qquad (100)$$

$$dBi/dt = 0 \quad \text{For} \quad Pi \leq P_1 \qquad (101)$$

Where B_1 = number for shear degradation,
Pi is the degree of polymerisation,
P_1 = the limiting degree of polymerisation,
ni = the number of molecules,
K = rate constant and
t = time

The rate formula of shear degradation is given by:-

$$B_{/no} = \left[(2\ Pr/P_1) - 1\right) - \left[(2\ Pr/P_1) - 1 + K(Pr - P_1)\ldots t\right] e^{-KP}\right] \quad (102)$$

Where No = initial number of molecules and
Pr = initial degree of polymerisation

This equation is based on the assumption that all bonds in the polymer are equally likely to break and that the degree of polymerisation of molecules after degrading are all in the region between 1 and P_1. To apply this equation it is necessary to determine the number of degraded molecules as a function of time. This is best carried out using Gel permeation chromatography and is not covered in the present work.

2.6 INTERFACIAL TENSION

2.6.1 INTRODUCTION

If a liquid surface is physically restrained, the tendency of the system towards a position of equilibrium will be manifested as a tension in the surface of the liquid. This surface tension is mathematically equivalent to the excess Helmholtz free energy of formation of $1cm^2$ of surface, ie the work done in isothermally extending the surface by 'a' cm along a line of 'b' cm against the surface tension Y dynes/cm (abY ergs).

The free energy of formation of an area of surface a b cm^2 is $a \times b \times Y$ ergs, where Y is now the free energy of formation in ergs/cm^2.

When two condensed phases are brought into molecular contact, the molecules in the two surface layers will be subject to forces across the boundary and hence will be nearer to the state of the interior molecules.

However, unless the molecules in the two phases are identical, the surface layers will not in general be in quite the same state as molecules in the respective interior phases. There will, therefore, be a residual excess free energy in each of these surface layers.

The total excess free energy, Y_{12} of the interface between the two phases will be the sum of the two.

$$\text{ie,} \quad Y_{12} = Y_1^1 + Y_2^2 \qquad (103)$$

Where Y_1^1 and Y_2^2 are the residual excess surface free energies of each phase at the interface, not the excess free energies at the condensed phase - air boundary surface.

2.6.2 MEASUREMENT OF INTERFACIAL TENSION

2.6.3 THE SESSILE DROP METHOD

Interfacial tension was measured by the sessile drop method. The apparatus for the measurement is shown schematically in Fig 24.

The heavier aqueous phase was introduced into the monomer phase using a clean pipette. The stand was made of mild steel on which was placed a PTFE ring used to support the drop.

This allowed a regular sized drop to be grown. When the shape of the drop changed no further with time,

the height h and the equatorial radius r of the drop were measured using a travelling microscope.

The difference in density between the phases was obtained using a specific gravity bottle.

2.6.3.1 CALCULATION OF INTERFACIAL TENSION

The calculation of surface tension from measurements of sessile drops or from ascension in capillary tubes may be summarised in the equation:-

$$B\left[\frac{1}{R_1}+\frac{1}{r}\right]=\frac{ho+h}{B} \qquad (104)$$

Where B^2 is the capillary constant, $\frac{\sigma}{gp}$;

h = height from mid point of the surface to the plane of greatest section;
r = radius of the above section;
R_1 = the first radius of curvature of the surface where it meets this section;
ho = capillary elevation at the mid point.

Figure 25 shows a sessile drop and the important parameters h and r.

The method of sessile drops or bubbles is of value when changes in surface tension or interface tension extending over long periods of time have to be measured.

The theory concerning the shape of bubbles underneath a plate or drops on a plate is identical.

The usual measurements are of the height, h from the equator (the maximum horizontal diameter) to the vertex of the drop or bubble.

This height h must be determined with the greatest

accuracy as it is usually only 2 or 3 mm, and the surface or interfacial tension depends on its square. The maximum horizontal diameter of the drop need not be so accurately measured, as it only required for correction of the limiting formula relating h and the measurement of the surface tension.

When bubbles or drops of very large diameter are formed and the diameter is so large that the curvature at the apex can be neglected the following simple formulae is valid.

$$h^2 = \frac{2Y}{g(D-d)} \qquad (105)$$

Where D = density of denser phase
d = density of lighter phase
Y = surface tension (dynes/cm)
g = gravity constant

For drops where this curvature cannot be neglected Verschaffelt (56) and others have given approximate formula for the calculation of the surface tension from h and the diameter of the drop.

Dorsey (57) and Porter (58) have applied Bashforth and Adams (59) calculations and are now given such a way that the surface tension can be calculated quite easily.

The method is independent of the angle between the liquid and the plate, provided that this is not so variable as to distort the bubbles or drop seriously from the ideal figure of revolution about the vertical axis.

With bubbles or drops it is necessary to use very

slightly concave plates or very thin PTFE collars to keep the bubble or drop in position.

A measuring microscope is used for the measurement of h and the drop diameter.

2.6.3.2 THEORY

It is recognised that no simple formula is possible except for very large drops. Formulae have been given by Worthington (60), Ferguson (61) and Rayleigh (62).

Worthingtons formulae is given as follows:

$$\frac{B^2}{r^2} = \frac{\frac{1}{2}\,\frac{h^2}{r^2}}{(1 + \cdot 609\,\frac{h}{r})} \qquad (106)$$

While Ferguson's is equivalent to:

$$\frac{2B^2}{r^2} = \frac{h^2}{r^2} - \cdot 609\left[\frac{2B^2}{r^2}\right]^{3/2} \qquad (107)$$

This equation has to be solved by successive approximations. This is made simpler if we write:

$$\frac{2B^2}{r^2} = \frac{\frac{h^2}{r^2}}{(1 + \cdot 609\left[\frac{2B^2}{r^2}\right]^{\frac{1}{2}})} \qquad (108)$$

This can now be compared directly with Worthington's formula.

Rayleigh obtained an expression:

$$\frac{h}{B} = \sqrt{2} + \cdot 6095 \frac{B}{r} \qquad (109)$$

In each case the curvature at the mid point is neglected, though it is recognised that except for very large drops some allowance is necessary.

For large drops Rayleigh showed how the curvature at the mid point can be calculated and obtained the following values. (See Tables(19)(20)

By means of these methods, an approximate correction for the curvature can be applied to the values obtained using the simple formula.

For very large drops, the simple formula gives:

$$\frac{B^2}{r^2} = \frac{1}{2} \frac{h^2}{r^2} \qquad (110)$$

Where $B^2 = \frac{\sigma}{g \Delta p}$ (111)

σ = interfacial tension
$\Delta\rho$ = density difference
β^2 = capillary constant

Consideration of Fig 26 shows there exists two points of zero correction.

When the radius is very large:

$$\frac{B^2}{r^2} < \frac{1}{2} \; {}^{h^2}/_{r^2} \qquad (112)$$

When the radius is very small:

$$\frac{B^2}{r^2} \longrightarrow \infty \qquad (113)$$

It is seen that a correction is necessary for intermediate values of h^2/r^2.

The best way of achieving this, was found to be as follows:

Plot the values from Adams and Rayleigh on a diagram of r/B vs r/h (58). Thus a curve was obtained which allowed $\frac{B^2}{r^2}$ to be found with considerable accuracy.

For large drops ($h^2/r^2 = \cdot 01$) the correction term Δ is 5% of the principle term.

When $h^2/r^2 = \cdot 05$, $\Delta = 10\%$. at $h^2/r^2 = \cdot 25$ Δ = zero, and this area is the most desirable of any to achieve.

Outside the range given, the correction is least known accurately but σ can usually be found within ±10%.

2.6.3.3 EXPERIMENTAL DETAILS

The method consists of the following steps:

1. Measurement of the drop dimension h and r using a travelling microscope.
2. Calculate h^2/r^2 and obtain a correction factor Δ
3. Using the formula $\frac{B^2}{r^2} = \frac{1}{2} \frac{h^2}{r^2} \pm \Delta$ obtain B^2/r^2 using correction obtained.
4. Calculate σ (interfacial tension) from the relationship.

   $B^2 = \frac{\sigma}{g \Delta p}$ Where ΔP = density difference of phases
5. The density difference is accurately measured at experiment temperature t°c.

2.6.3.4 MATERIALS

The aqueous phase was either water or a polyacrylamide solution. The solution was varied between 0.25 - 2% by wt.

Several different monomers were used either individually or as mixtures as follows:

Styrene
Styrene/n-butyl methacylate 50/50
Methyl methacrylate
Styrene/methyl methacrylate 50/50
Vinyl acetate

2.6.3.5 EXPERIMENTAL METHOD

Interfacial tension was measured by the sessile drop method.

The apparatus used for the measurements is shown schematically in Fig 24.

The aqueous solution was stirred for about 5 minutes at the given temperature, then a small quantity of was introduced into the monomer tank (on to a steel sheet) using a micropipette.

The temperature was checked, and when the shape of the drop was steady and changed no further with time, the height h, and the equatorial radius r of the drop was measured using a microscope fitted with a micrometer eyepiece.

Measurements were made at both 20°C and 75°C.

Δ P the difference in density between the demixed phases was also measured.

2.6.3.6 RESULTS

The interfacial tension was calculated as out-

lined in 2.6.3.3 and the results reported in Table 21.

2.6.3.7 DISCUSSION OF RESULTS

Table 21 shows that the interfacial tension of the monomers examined were within the range 5.0 - 17.0 .

Keeping the temperature and monomer composition constant, and increasing the colloid concentration, was found to reduce the interfacial tension.

Details of interfacial tension (dynes/cm) for a 1.1 styrene/butyl methacylate mixture at 75°C for different colloid concentrations is reported in Table 22.

A plot of interfacial tension against colloid concentration is shown in Fig 27.

A Log/Log plot of this data gives good correlation (Table 23 and Fig 28).

From the data the following correlation was obtained.

$$\delta = 5.6 \times (c)^{-0.118} \quad (\text{at } 75^{\circ}C)$$

Where δ = interfacial tension of styrene/butyl methacrylate mixture 1.1

(c) = concentration of colloid wt%

The effect of monomer composition on the interfacial tnesion at a constant colloid level is seen clearly (Table 21). The polar monomers, ie vinyl acetate and methyl methacrylate have a lower interfacial tension than the less polar monomer styrene.

Mixtures of monomers have intermediate values.

2.6.4 EFFECT OF INORGANIC SALTS ($Na_2 HPO_4$) ON INTERFACIAL TENSION.

2.6.4.1 INTRODUCTION

Previous work carried out by Topping (25) on the nature of chain polyelectrolytes, have shown that the theory of random coils was not strictly applicable to systems containing polar groups (ie COOH). In such polymers expansion of the polymer coils beyond the purely random configuration is produced when ionic groups or ions are introduced into the polymer structure.

Electrostatic repulsion between the segments of the chain then tends to keep them apart to an exent which depends on the proximity of the charged groups, and the ionic concentration of the solution.

This was the case for a medium molecular weight polyacrylamide - modified by carboxyl groups. This polymer in aqueous solution produced Newtonian solutions in which the viscosity was a function of the ionic concentration. The interfacial tension was shown to be an additive function of both polymer and salt. The polymer reduced the interfacial tension, while inorganic salts, particularly (+2) types, increased it up to a maximum corresponding to complete molecular coverage.

Using high molecular weight polyacrylamide (containing no ionic groups) the interfacial tension was examined in the presence of di sodium hydrogen phosphate. Na_2HPO_4, (concentration range 5% - 6.0% wt/wt.

2.6.4.2 EXPERIMENTAL DETAILS

The interfacial tension between high molecular weight polyacrylamide and styrene monomer was measured in the presence of disodium hydrogen phosphate (Na_2HPO_4).

2.6.4.3 MATERIALS

A 0.5% wt/wt solution of polyacrylamide (cyanamid superfloc N-100) was prepared at 20°C by gentle stirring.

The disodium hydrogen phosphate was available as a powder in the anhydrous form.

2.6.4.4 EXPERIMENTAL METHOD

The salt was dissolved in the polyacrylamide solution to produce a series of solutions containing from 1 - 6% salt by weight.

The interfacial tension of each solution was measured using the sessile drop method at 20°C. The apparatus and method used for the measurements was discussed earlier, section 2.6.3.5 (Fig 24).

2.6.4.5 RESULTS

The interfacial tension measurements are reported in Table 24, and a plot of interfacial tension against salt concentration is shown in Fig 29.

2.6.4.6 DISCUSSION OF RESULTS

A plot of interfacial tension at 20°C against various amounts of disodium hydrogen phosphate, showed that at lower concentrations, the interfacial tension was lower than for the salt free solution.

A similar effect was noted by K J Rixon (63) using disodium hydrogen phosphate in an aqueous solution of medium molecular weight carboxyl function modified polyacrylamide.

The decrease in interfacial tension is attributed to positive adsorption of the salt molecules in the surface layer. At higher concentrations the salt becomes negatively adsorbed in the surface layer.

CHAPTER 3

FACTORS AFFECTING THE PARTICLE SIZE IN A SUSPENSION POLYMERISATION PROCESS

3.1 SUMMARY

Five factors have been investigated to establish the relationship between particle size and the important processing parameters.

The five variables chosen were:

1. Stirrer speed
2. Volume fraction of the dispersed phase
3. Interfacial tension
4. Presence of an inorganic salt
5. Reynolds number

The investigation was carried out using laboratory scale apparatus of fixed geometry. It was found that the particle size increases:

a. As the stirrer speed decreased
b. As the volume fraction of phase decreased
c. As the interfacial tension increased
d. As the inorganic salt concentration increased
e. As the Reynolds number increased

3.2 INTRODUCTION

Suspension polymerisation forms the basis for producing commercially important polymers including those of the acrylic esters, methacrylic esters, styrene, vinyl-acetate and vinyl chloride. Most suspension polymerisations are made by the batch process.

In a batch process, a dispersion of a relatively insoluble liquid monomer is produced in an aqueous phase by continuous agitation. The dispersion is unstable and continuous break up and coalescence of the monomer droplets occurs. If agitation is stopped, then the monomer - water system will separate into its respective two phases.

During the polymerisation the system is heated to its reaction temperature ($\sim 75^{\circ}C$), and the monomer droplets react to produce polymer particles, the reaction is initiated by the peroxide dissolved in the monomer phase.

In the early stages of reaction, the monomer droplets tend to remain as a true dispersion until polymerisation proceeds to a point where they become tacky due to dissolved polymer and they then agglomerate on droplet collision.

In practice agglomeration is prevented by the presence of a water soluble polymer called the suspending agent, which adsorbs onto the droplets and particles to provide a protective film between the globules to prevent immediate coalescence.

The final particle size distribution of the solid reaction product is clearly a function of the original droplet size produced in the equilibrium developed between drop coalescence and drop break up in the agitated dispersion.

Factors influencing the particle size are those therefore which influence the equilibrium developed between

the drop break up and drop coalescence processes.

Figure 30 illustrates the method of drop break up as proposed by Taylor (64) and endorsed by Snell (65), Richardson (66) and Winslow and Matreyek (67).

These workers have concluded that the mechanics of suspending insoluble polymerisable "oils" in an aqueous system commences with the bulk monomer being subjected to mechanical agitation.

The effects on the monomeric substance of the resultant viscous drag is to cause elongation to a thread like form with subsequent degeneration into drops, as suggested by Taylor (64).

Simultaneously, through the reverse process of coalescence, the drops tend to revert to the original monomeric mass. In a simple mechanical suspension under a constant overall rate of shear a dynamic equilibrium is quickly established. Clusters of globules held together by weak residual forces, but not fused, tend to disperse under the disruptive stress of an agitated system. Snell (65) showed that effective surface active agents alone will deflocculate these aggregates. With the onset of polymerisation and the accompanying increase in viscosity there is greater resistance to distortion of droplets due to viscous drag, but also a greater tendency towards aggregation through collisions with neighbouring globules.

This latter phenomenon can be minimised by the suspending agent which provides a protective film of molecular proportions.

Figure 30 shows such a drop schematically supporting an adsorbed film of polyvinyl alcohol.

Since the equilibrium process between drop break up and coalescence forms such a fundamental part of the process, the following section examines in detail the drop break up and coalescence mechanisms, both at a plane liquid/liquid interface, and a liquid droplet interface. This study provides the basis for the experimental work described later in this chapter.

3.2.1 BREAK UP OF DROPLETS IN AGITATED DISPERSIONS

In dispersion of two liquids formed by turbulent agitation, break up and coalescence of droplets occurs continuously (68,69,70,71,72).

Break up may be caused either by viscous shear forces or by turbulent pressure fluctuations. For a known flow field, both break up and coalescence have been evaluated theoretically (70,73,74,75,76).

In the case of break up by viscous shear, the droplet is first elongated into a cylindrical thread which then breaks into a number of small droplets (74,75). The critical shear force μ du/dx necessary for break up is obtained from:

$$\mu c \left[\frac{du}{dx}\right] \text{ crit } \frac{d}{\delta} = c\,\emptyset\left[\frac{Ud}{Uc}\right] \qquad (115)$$

Where $\emptyset$ (Ud)/(Uc) is a hyperbolic function describing the stability of a liquid cylinder in a viscous

fluid (77) (26) where:

Uc	=	viscosity of continuous phase
Ud	=	viscosity of dispersed phase
Ø	=	dispersed phase volume fraction
C	=	constant
d	=	diameter of droplet or particle
	=	surface tension
U	=	fluctuating component of velocity

A droplet suspended in turbulent flow is exposed to local pressure fluctuations. For small density differences and similar viscosities of the two liquid phases, the droplet can be assumed to oscillate within the surrounding fluid. An oscillating drop becomes unstable if the kinetic energy Ek is sufficient to make up for the difference in the surface energy between single drop and two smaller drops formed from it by break up (73).

This leads to:

$$Ek/d^2 = \text{constant} \sim 0.26 \qquad (116)$$

In agitated dispersions, where conditions of local isotropy prevail, the kinetic energy Ek of a single oscillating droplet will be proportioned to $Pu^2(d)d^3$ (P = density) Substituting this value for Ek gives:

$$Pu^2(d)d/6 = We = \text{constant} \sim 0.26 \qquad (117)$$

This equation applies to break up of the droplets of diameter d much larger than the microscale of the turbulence (n).

Then the viscous forces may be neglected in comparison with the inertia forces. However if $d < n$ viscous forces predominate and it may be more accurate to use

equation (115), other workers (78) in the study of drop break up have shown:

i. greater drop stability is achieved in systems having a small difference in density between phases.

ii. Low dispersed phase viscosity has no significant effect upon drop break up.

iii. Other important factors which influence the drop break up process have been shown to be:

a. Interfacial tension

b. Continuous phase viscosity

c. Density difference

d. Presence of surfactants etc.

Recent evidence for the action of an adsorbed polymeric film upon the drop break up process is given in the work of H J Karan (17). In his investigations, Karan examined the viscosity of an adsorbed polymeric film at an interface. The films formed were found to be quite viscous relative to the bulk solution. Karan described an interfacial viscometer, and using this apparatus showed the significance of interfacial viscosity upon drop break up behaviour in a liquid - liquid system. In particular the action of a suspending agent which made drop break up more difficult was considered.

Topping (25) investigated factors which influenced drop break up in a suspension process. Apparatus was used which utilised a jet of turbulent liquid to produce drop fragmentation. Under carefully controlled conditions, a jet of high velocity liquid was fired at a single submerged

monomer droplet formed at the end of a hyperdermic needle.

The investigations showed that both inorganic salts and the suspending agent reduced drop break up in a turbulent continuous phase. The two salts examined, Na_2HPO_4 and Na_2SO_4 gave results which suggested that it is their structure making properties in solution that increased the surface rigidity of the drop and thus increasing its resistance to fragmentation.

The suspending agent reduced drop fragmentation in two ways:

1. By damping down the turbulence level on the continuous phase.

2. By being adsorbed onto the monomer surface it produces a viscous film around the drop which can resist the effect of small turbulent eddies which otherwise would cause the drop to fragment.

Increasing the dispersed phase viscosity reduced drop break up. In this case it is the internal viscous forces which resist drop fragmentation.

3.2.2 DROP COALESCENCE

Coalescence studies on droplets have been restricted mainly to the behaviour of a single drop resting at a plane liquid - liquid interface (78 – 80). This system is relatively simple to investigate and provides information concerning the factors important to an understanding of the coalescence process. It is thought that the coalescence process takes place through five consecutive stages (81).

1. The approach of the drop to the interface resulting in deformation of both the drop and interface.

2. Damped oscillation of the drop at the interface.

3. The formation of a film of the continuous phase between the drop and its bulk phase.

4. Drainage of the film, resulting in its rupture.

5. Transference of the contents of the drop (partially or wholly) into the bulk of the phase, from which the droplet was formed.

It is thought , by most workers, that stages 1. and 2. occur very fast, and that the observed time of coalescence is the time taken for stages 3,4 and 5.

Most of the time for coalescence occurs at stage 4, when the drop rests on a thinning film between the interface and itself.

A drop situated at the interface between two liquid phases may coalesce completely or undergo a step-wise coalescence of a single droplet at a plane interface proceeds through the draining and rupture of the film of the continuous phase.

Factors which can affect the drainage and rupture process will therefore control the coalescence process.

The following factors are thought to influence the coalescence time.

(i) Drop Size

The coalescence time increases with increase in drop size. This is because the drop flattens out and this

increases the length of the film between the drop and interface which increases the drainage period.

(ii) Distance of fall of the drop

The distance the drops fall to the interface can affect the coalescence time. Some workers (82,83) have shown that the drop stability increases with increase in distance of fall. This is probably due to the presence of an electrostatic charge acquired during passage through the continuous phase.

(iii) Curvature of the Interface

The curvature of the coalescent drop phase when concave to the drop will be expected to increase resistance to film drainage, this was confirmed by Neilson (83).

(iv) Density difference between the phases

Large differences in density between the drop and the continuous phase causes severe deformation of the drop which will increase the length of the drainage film.

(v) Viscosity ratio of the phases

Any increase in the viscosity of the continuous phase relative to the dispersed phase, will increase drop stability because of the increased resistance to film drainage.

(vi) Interfacial tension

A high interfacial tension will result in reduced drop deformation which will decrease the length of the drainage film, reducing drop stability.

(vii) Temperature

An increase of temperature generally reduces coalescence time unless a change occurs in the coalescence process.

(viii) Vibrational effects

Gillespie and Rideal (79) suggested that vibrations stabilised the drainage film and impeded coalescence. The work of Lang (84) did not support their findings and suggested that vibrations would produce random variations in the observed coalescence times.

(ix) Electrical double layers

The rate of coalescence of drops whose continuous phase contain an electrolyte is lower than the rate observed in the presence of a pure solvent. This is attributed to the formation of electrical double layers at the interface:

1. Between the drop and draining film.
2. Between the draining film and the bulk drop phase.

These double layers tend to retard the flow of draining film due to electrostatic forces on the molecules within these films.

The effect will be greatest when the thickness of the draining film is of the same order as the double layers.

Under these conditions, the apparent viscosity of the continuous phase becomes much greater than the normal viscosity.

(x) The presence of a third component

The presence of an electrolyte in the aqueous phase tends to retard the coalescence of hydrocarbon droplets, probably due to the presence of electrical double layers.

Surface active substances which can be adsorbed at the interface also retard coalescence because of a reduction in film drainage rate.

Solid substances can however promote coalescence by forming a bridge across the draining film which causes rupture of the film.

3.2.3 INTERDROP COALESCENCE

Interdrop coalescence is an important factor influencing the final drop size in a stirred dispersion. It may be expected that as the quantity of continuous phase trapped between the coalescing drops increases, the drainage time will also increase. Thus, factors which affect the drainage and rupture process will also influence the rest time.

In interdrop coalescence, the important factors will include:

(i) The viscosity of the continuous phase;
(ii) The interfacial tension;
(iii) Formation of electrical double layers.

The first accurate measurements of the drainage between curved surfaces were made by Derjaquin and Tilyerskaya (85) (86) and later Van Der Temp (87). They examined the stability of liquid films of analine contain-

ing varying amounts of a higher alcohol which acted as a stabilising agent. The film was formed between hydrogen bubbles and its thickness determined by interferometric technique.

They found that the film thinned rapidly to about 10 microns after which it drained more slowly to 1000 A^{o}. In this latter region, the film became uniform and drained slowly to 300 A^{o} when areas of a very thin film appeared and the film finally ruptured.

Stepwise coalescence have been observed during interdrop coalescence. Mackay and Mason (88) showed that partial coalescence took place when the ratio of the drop diameters was greater than 3.5. For pairs of drops below this diameter ratio, no secondary drops were formed. When the drops were of similar diameter the shock wave produced by the drop collisions caused the final drop to become cylindrical in shape before regaining a spherical shape.

Topping (25) investigated the factors influencing the coalescence of methyl methacrylate monomer droplets in an aqueous phase and found that by keeping other experimental conditions constant, whilst changing the properties of the aqueous phase, it was possible to measure the time of coalescence of liquid drop pairs and the effect that various aqueous phase additives had on the coalescence time.

The main point of interest was the effect that both suspending agent and inorganic salt had upon the coalescence time. Both materials were found to increase the coalescence time. The effect of simple salts (ie

KCl, NaCl, LiCl) on the coalescence was such that at the same molar concentration, the salts became more effective with decreasing cation size. An ion introduced into water interferes with its structure because of the difference between ion-water and the water - water interactions. These effects may be of a steric nature and depend upon the size of the ion or they may be due to changes in the ionic charge distribution. The water molecules in the vicinity of small ions are strongly polarised due to the intense electrical field of the ion, and this effect is superimposed on normal interactions between solvent and solute. The water molecules thus form successive layers around each ion with the first layer firmly oriented.

In the coalescence of monomer droplets in an aqueous continuous phase, the flow characteristics of the intervening film between drops are of great importance and are related to the ionic behaviour discussed above. The effect of inorganic ions upon this flow is of special importance since it can influence the equilibrium drop size in a drop break up/coalescence process.

The electrical forces between ions in adjacent layers of an electrolyte solution will affect the solution viscosity.

A mathematical treatment was first given by Falkenhagen (89 – 91) who showed that a limiting law operates which is of the form:

$$U_{rel} = 1 + A1\sqrt{C} \qquad (118)$$

Where C = concentration in molecules per litre
U rel = relative viscosity

The constant A_1 is a function of solvent properties including ionic charge, mobilities and temperature. Jones and Dole (92) extended equation (118) to include a viscosity coefficient (A_2C)

$$\text{ie } U \text{ rel} = 1 + A_1 \sqrt{C} + A_2C \qquad (119)$$

The A_2 values are strongly correlated with the entropy of solutions of the ions. Negative values are found with ions which exert structure breaking effects on water, eg Rb^+, Cs^+, I^-, ClO_3^-

These negative values of A_2 seldom cause a decrease of more than 10% in viscosity. More typical are fairly large positive values of A_2 found with ions which are strongly hydrated, eg Na^+, Li^+, Mg^{++}

These ions are structure makers and increase the viscosity of water by polarising and electrostricting the water molecules. The ionic radii of some ions and the multivalent nature of others make them structure makers eg L_1^+, Mg^{++}, Al^{++}, PO_4^{--} (Fig 31)

Salts containing small or highly charged ions are the most effective in preventing drop coalescence due to their action on the viscosity of the solution. The importance of the solution viscosity in the coalescence process is clearly seen when the individual ionic values of the coefficient A_2 in the viscosity equation; $U \text{ rel} = 1 + A_1 \sqrt{C} + A_2C$ are correlated with the observed coalescence time Fig 32 (25).

Since valency and concentration of the salt are of importance, the ionic strength can be used to correlate coalescence rates.

The ionic strength is a measure of the intensity of the electrical fields due to the ions in solution and is defined as half the sum of the products of the mobilities of the constituting ions and the square of the valencies. The fact that the properties of both the ions are included is one of the advantages of ionic strength as a correlating quantity.

Figure 33 shows a satisfactory correlation obtained for all the salts using ionic strength as the correlating parameter.

The work shows clearly that the degree of coalescence of the air bubbles in water decreases on the addition of inorganic salts. The decrease depends on the valency of the ions and on the concentration of the salt.

Thus the mechanism of coalescence retardation can be explained on the basis of ion-water interactions.

3.2.4 OTHER REPORTED WORK

A quantitative basis for the dispersion of stirred immiscible liquids was given in the work of Vermeulen, Williams and Langlois (26).

For geometrically similar mixers and equal volume proportions of the two liquid phases, it was found that the mean drop size was given by:

$$\frac{d}{L} = K\left(\frac{N^2 L^3 \rho}{\sigma}\right)^{-0.60} \qquad (120)$$

Where d = drop size
L = stirrer diameter
K = constant
N = stirrer speed
P = density difference
o = interfacial tension

A more general equation which takes account of the volume fraction is :

$$\frac{d}{f(\emptyset)L} = K\left(\frac{N^2 L^3 P}{\sigma}\right)^{-0.60} \qquad (121)$$

Where $f(\emptyset)$ is a function of the volume fraction $\emptyset$, and $f(\emptyset) = 1 + 3.3\emptyset$. The term $\left(\frac{N^2 L^3 P}{\sigma}\right)$ is a dimensionless group called the Weber number.

Topping (25) investigated factors influencing the particle size of a suspension polymerisation product in a Newtonian system.

The process variables i.e. stirrer size, speed and interfacial tension were studied using both a laboratory scale suspension system and also large scale reactors ($\frac{1}{2}$ ton and 5 ton capacity). The results obtained were incorporated into an experimental model involving both Weber and Reynolds numbers.

In the present work, stirrer speed, volume fraction, interfacial tension and Reynolds number are investigated in the first instance to assess their importance on the behaviour of a non Newtonian suspension system.

3.3 EXPERIMENTAL DETAILS

3.3.1 MATERIALS

Styrene, methyl methacrylate, n-butyl methacrylate monomers were used in the experimental work. Monomer

supplied were of commercial grade and physical constants were checked before each investigation.

High molecular weight polyacrylamide was used.as the sole suspending agent. It was supplied as a granular solid under the commercial name Superfloc PW G^{N-100} (supplied by Cyanomer UK Ltd). The molecular weight was found to be 7×10^6. Mains water was used for the experimental work, whilst the initiator used was a commercial grade of Benzoyl peroxide (70% water damped).

3.3.2 EQUIPMENT

To study the effects of the polymerisation variables it was necessary to use a suitable laboratory system. Figure 34 shows a schematical diagram of the complete experimental set up.

The system was based on a two litre reaction flask. The separate reaction lid had five inlet ports, into which various other items could be fitted (eg reflux condenser). The reaction lid and vessel were joined using a greased ptfe gasket and held together by a spring clamp.

The stirrer employed was a flat bladed T shape.

The agitator shaft passed through a ptfe stirrer gland and was connected to a laboratory stirrer motor (speed variable 0-600 RPM).

The stirrer speed was checked using an optical tachometer.

The vessel was heated by a thermostatically controlled electrical heating mantle.

The mantle was supported on a laboratory jack which allowed it to be raised or lowered during the reaction if an exotherm occurred and the reaction temperature rose quickly.

3.3.3 OPERATIONAL PROCEDURES

Before making an experimental run, the glass reaction flask was cleaned thoroughly, rinsed and then dried.

The appropriate volume of water was then added to the vessel, the stirrer started and the suspending agent slowly added. After the suspending agent had dissolved the monomer was slowly added to the stirred aqueous phase.

The initiator (benzoyl peroxide) was previously dissolved in the monomer phase. The stirrer was then set to the required speed and the temperature raised to 75°C. Once the reaction temperature was obtained it was carefully controlled during the polymerisation period.

The exotherm experienced depends mainly on the monomer type, styrene giving a slow gentle reaction over a 3 hour period, while methyl methacrylate was characterised by a rapid strong exotherm in the final stage of a one hour reaction.

Once the reaction was completed and the solid product formed, the reaction temperature was raised to 80 - 85°C for one hour to complete the polymerisation.

At the end of the polymerisation the reactants were cooled to 25°C before filtration and washing. The solid product was then allowed to dry slowly on absorbent paper.

Analysis to determine the mean particle size was then carried out using a set of British standard sieves.

A series of exploratory polymerisations were needed to establish the level of suspending agent, stirrer speed etc, needed to maintain a stable product for each monomer. A typical recipe was thus obtained and this is shown as follows for styrene.

Aqueous Phase

Water	800.0
Polyacrylamide suspending agent	8.0

Organic Phase

Benzoyl peroxide (70% water damped)	11.0
Monomer	188.0

2 litre reaction vessel
Monomer volume fraction $\emptyset = 0.2$

Stirrer details ⊥ shape
Diameter 10.00 cm
Thickness 0.75 cm

3.4 RESULTS

3.4.1 EFFECT OF AGITATOR SPEED UPON PARTICLE SIZE

The effect of agitator speed upon the final particle size of the beads produced in a suspension process was examined for two different monomer volume fractions. In each experimental investigation the stirrer speed was varied between 300 and 600 rpm, the stirrer diameter and shape remaining constant.

The results obtained are reported in table 25 and are displayed in a plot of log d and log N (Fig 35 and 36). From the results it can be seen that the particle size decreased as the stirrer speed was increased. This increase

is not however significantly large particularly if compared to that obtained in a Newtonian system using a low molecular weight polyacrylamide as suspending agent. Thus the stirrer speed is not a major influence in the control of the final particle size.

From these results the particle size d is related to stirrer speed N by the equation;

$$d = C\,N^{-0.15} \quad \text{(Volume fraction} = 0.2) \quad (122)$$

$$d = C\,N^{-0.06} \quad \text{(Volume fraction} = 0.3) \quad (123)$$

The relationship between d and N for a Newtonian system was previously investigated by Topping (25). The results obtained in such a system were in good agreement with Vermeulen results (26), obtained for droplet size in an agitated liquid - liquid dispersion. These results can be compared with the results obtained in this investigation using non Newtonian conditions.

SYSTEM	TYPE	RELATIONSHIP
Liquid/Liquid dispersion (Vermeulen)	Newtonian	$d = C\,N^{-1.2}$
Suspension (Topping)	Newtonian	$d = C\,N^{-1.0}$
Suspension (Topping)	Non Newtonian	$d = C\,N^{-.15}$ $\phi = 0.2$ $d = C\,N^{-0.06}$ $\phi = 0.3$

From the results it can be seen that for Newtonian conditions the particle size is more sensitive to stirrer speed. This is to be expected since such a system shows increased turbulence compared to a non Newtonian system; as

the level of turbulence influences the equilibrium between drop break up and coalescence, high values cause a shift to a smaller drop size.

In the non Newtonian system the turbulence is largely damped out, and the equilibrium between drop break up and coalescence is only slightly effected.

3.4.2 EFFECT OF MONOMER VOLUME FRACTION UPON PARTICLE SIZE

A series of experimental runs were carried out using the same reaction vessel and stirrer, the only variable being the monomer volume fraction employed.

The investigation was carried out at two different stirrer speeds (ie 300 and 600 rpm). The results obtained are reported in Table 26 and plotted in Fig 37. From the results it is clear that the particle size decreases with increasing monomer volume fraction, and this trend is evident at both stirrer speeds employed.

This result is completely different from that observed in a Newtonian system. Such a system was investigated by Topping (25). It was found for such a system that the particle size increased with the monomer volume fraction in an approximately linear manner. The influence of the monomer volume fraction clearly contrasts the physical behaviour of the two systems.

In a Newtonian system good mixing occurs throughout the vessel, and while drop break up and coalescence is limited to the region of turbulence near the agitator,

most of the dispersion achieves equilibrium quickly. Increasing the monomer volume fraction leads to increased drop coalescence, giving the observed increase in the final particle size.

In the non Newtonian system however mixing is very poor and is confined to the volume swept out by the stirrer. The viscosity within this region is also reduced due to the shear, and the monomer droplets trapped within this zone are subject to repeated collisions with the stirrer, eventually leaving the zone much reduced in size.

Whilst the droplets reside outside the swept volume of the stirrer, droplet coalescence is unlikely due to the high viscosity in the low shear volume and the consequent reduced mobility of individual drops.

3.4.3 EFFECT OF INTERFACIAL TENSION UPON PARTICLE SIZE

The importance of interfacial tension and its measurement was discussed earlier in chapter two. Interfacial tension is a function of both the aqueous phase and monomer phase compositions. In the aqueous phase, it is the presence and concentration of the colloid or inorganic salt which is important, whilst it is the monomer type which largely controls the interfacial contribution of the organic phase (in particular the presence of polar groups on the hydrocarbon chain).

Temperature also affects the interfacial tension; generally it is decreased if the temperature is raised.

It is clear that the particle size is influenced

by the interfacial tension, and the values of interfacial tension in the present investigations were produced by variation of both the aqueous and monomer compositions.

Two important points are:

1. The suspending agent has been shown earlier to alter the interfacial tension; increasing its concentration reduced the value of interfacial tension.

2. Since interfacial tension depends upon the particular monomer used, changing the monomer will also change the interfacial tension value.

In the present investigations, changes in interfacial tension produced by the above methods were correlated with the observed particle size.

3.4.3.1 (i) CHANGING THE AQUEOUS PHASE COMPOSITION

Formulations of fixed monomer type and volume fraction were produced in which the suspending agent concentration was varied.

The interfacial tensions were then measured using the apparatus and method described in Chapter 2.

The mean particle size for each formulation was measured using standard British sieves. The experimental details and results are listed in Tables 28/27.

It was found that the mean particle size was reduced as the interfacial tension was reduced.

(ii) CHANGE OF MONOMER TYPE

A simple weight for weight replacement was carried out using a different or mixture of different monomers.

The interfacial tension of all these systems were checked before each test.

The monomers examined were as follows:-

1. Styrene
2. Styrene - n Butyl Methacrylate (Copolymer)
3. Methyl Methacrylate
4. Styrene - Methyl Methacrylate (Copolymer)

Copolymers were also produced without difficulty. and the results obtained are reported in Table 28 and plotted in Fig 39. The particle size is related to the interfacial tension by the relationship;

$$d = 5.49 \times 10^{-4} (\sigma)^{7.56} \qquad (124)$$

Where d = particle size (mean) microns
σ = interfacial tension (dynes/cm)

3.4.4 EFFECT OF AN INORGANIC SALT (Na_2HPO_4) UPON THE PARTICLE SIZE

The effect of an inorganic salt upon the interfacial tension was reported in 2.4.5 (Table 24). A plot of interfacial tension against various amounts of disodium hydrogen phosphate is shown in Fig 29. This plot shows a minimum interfacial tension at a salt concentration of approximately 1.5%.

A series of polymerisations were made at salt (Na_2HPO_4) concentrations of 0%, 0.5%, 1%, 1.5%, and 2%. The colloid level was left unchanged at 1.0%. The stirring speed and stirrer geometry was also left unchanged.

The results are reported in Table 29. From the

results it is clear that the particle size increases (Fig 38) steadily with the salt concentration, no minimum in particle size was observed. The action of inorganic salts on drop break up and coalescence was investigated by Topping (25). Using two different inorganic salts, disodium hydrogen phosphate Na_2HPO_4 and sodium sulphate Na_2SO_4 he found that drop break up was reduced in experiments which employed a jet of turbulent liquid to produce drop fragmentation.

In other experiments Topping (25) found that inorganic salts could also influence droplet coalescence. Na_2HPO_4 was found to be more effective than simple salts (NaCl) in reducing coalescence.

The monovalent salts were found to become more effective with decreasing cation size. In the present investigations, the behaviour of the salt can be explained by its effect on the equilibrium drop size. By reducing drop break up the final particle size became progressively larger with increasing salt concentration.

3.4.5 EFFECT OF REYNOLDS NUMBER ON THE PARTICLE SIZE

3.4.5.1 (i) INTRODUCTION

Because of its very high molecular weight, the polyacrylamide suspending agent when dissolved in water produces a viscous solution which behaves in a non Newtonian manner.

The viscosity of the aqueous solution increases quickly with colloid concentration and at 2% produces a gel like fluid.

The behaviour of this fluid was shown earlier to have the properties of a Bingham fluid exhibiting a definite yield point, and also the properties of a pseudoplastic fluid.

The effect of colloid concentration on the rheological properties of the fluid was examined using both the cone and plate and coaxial cylinder viscometers.

These results are reported in Table 1 - 12 and discussed in Chapter 2 Section 2.5.1.

A liquid moves through regions of varying shear conditions while circulating in a reactor, and if the fluid has non Newtonian properties then this can have important effects. In particular pseudoplastic fluids such as the polyacrylamide behave as if their viscosity is low when near the impeller and high when some distance from it. One result of this is that the impeller tends to rotate in a small circulating vortex of highly sheared fluid while the main bulk of the liquid scarcely moves at all.

Any effective mixing of the liquid will thus inevitably be accompanied by excessive shearing of at least some of the fluid. To counter the effect of local thinning associated with high speed agitators in pseudoplastic fluids, frequent use is made in industry of agitator designs that sweep the volume of the vessel, ie, gate, anchor and paddle types. The liquid flow pattern established in reactions generally shows an asymetry in the vicinity of the stirrer blade (91) the extent of which will depend on the Reynolds number (91).

The value of the Reynolds number will thus influence both the circulation of the liquid in the vessel and the degree of turbulence produced at the agitator blade.

The equilibrium developed in a dispersion between drop break up and coalescence is generally regarded to be limited to the area of turbulence associated with the agitator. Drop break up may be caused either by viscous shear forces or by turbulent pressure fluctuations, while interdrop coalescence is a function of the viscosity of the continuous phase, the number of droplet collisions, the interfacial tension and the formation of electrical double layers.

3.4.5.2 CALCULATION OF REYNOLDS NUMBER

One form of generalised Reynolds number is:

$$Re = \frac{L^2 N^{2-n} P}{K} \; 8\left[\frac{n}{6n + 2}\right]^n \qquad (125)$$

Where L = Stirrer diameter
P = Density
n = Exponent for power law fluid model
K = Constant for power law model

This equation reduces to the conventional Reynolds number when n = 1

Both n and K can be obtained from rheological data as follows:

The shear rate $\dot{Y}$ is given by the expression

$$\dot{Y} = L \times rpm \quad (L = \text{Stirrer diameter}) \qquad (126)$$

This expression allows the apparent viscosity

(U_{APP}) to be plotted against shear rate $\dot{Y}$.

The shear stress R is given by:

$$R = -K(Y)^n \quad \text{(Power law fluid)} \tag{127}$$

$$R = -U_{APP}\dot{Y} \quad \text{(Newtonian apparent)} \tag{128}$$

$$\text{Therefore } U_{APP} = K(Y)^{n-1} \tag{129}$$

$$\text{Where } U_{APP} = NS/m^2 = \frac{\text{Poise}}{10} \tag{130}$$

$$\text{Thus Log } U_{APP} = \text{Log } K + (n-1) \text{ Log } \dot{Y} \tag{131}$$

A plot of Log U_{APP} against Log $\dot{Y}$ gives the slope (n-1) which allows n to be obtained, and the intercept (Log K) gives the value for K.

3.4.5.3 DISCUSSION

In the present investigation, a series of polyacrylamide solutions were examined for rheological properties (Tables 1 - 12).

Figure 14 shows a plot of Log U_{APP} against Log $\dot{Y}$ for the four solutions using cone and plate data.

Figure 17 shows the same plot using data from the coaxial cylinder viscometer.

Table 5 and Table 12 records both the intercept and observed slope for the above data. Using laboratory data, the Reynolds number was calculated and reported in Tables 30 and 31, for both viscometer types. (Fig 40)

Finally the calculated Reynolds number and the observed particle size 'd' for a series of different monomer systems is reported in Table 32 and 33.

Using the results reported in Tables 32, 33, a plot of Log Re against Log d is shown in Fig 41. This figure shows Re data obtained from both viscometer types plotted against the same monomer system (Styrene - n Butyl Methacrylate 50/50).

It can be seen that both viscometer types produced data which give lines of similar slope and differed mainly in the value of the intercept.

Complete agreement between the different viscometer types is not expected, since shear conditions in the instruments are not identical.

The relationship between particle size and Reynolds number is given by:

$$d = 0.43 (\text{Re})^{0.64} \quad \text{(Cone and plate)} \qquad (132)$$

Where d = mean particle size
monomer = styrene/n Butyl methacrylate

A further series of experiments were carried out using different monomer systems - these results are reported in Table 34.

The result of plotting Log Re against Log d for all monomer systems is shown in Fig 42. In this figure a series of lines are produced, each line corresponding to a constant polarity dictated by the polymer composition.

The order of the lines produced in this plot also follows the monomer order in the interfacial tension data (Tables 21,28).

Thus Fig 42 shows clearly the dependence of particle size on both interfacial tension and the Reynolds number.

These results confirm that Reynolds number is one important factor controlling the mean particle size in a non Newtonian suspension polymerisation.

The Reynolds number probably controls the particle size by its influence on the flow conditions within the vessel which will effect the drop break up coalescence equilibrium.

CHAPTER 4

DEVELOPMENT OF AN EXPERIMENTAL MODEL FOR A SUSPENSION PROCESS CARRIED OUT UNDER NON NEWTONIAN CONDITIONS

4.1 SUMMARY

An experimental model is presented which incorporates dispersed phase volume fraction, stirrer speed, interfacial tension, Reynold s number and polymer polarity.

The particle size is determined by the process of drop break up and coalescence. Normally an equilibrium exists between these processes.

The equilibrium is a function of the Reynold s number in non Newtonian conditions.

The monomer polarity controls the adsorption of the protective colloid onto the droplet and thus controls the interfacial tension at a fixed colloid concentration.

Interfacial tension is an important factor controlling particle size since it influences both the drop break up and drop coalescence processes.

4.2 INTRODUCTION

4.2.1 THE SUSPENSION POLYMERISATION PROCESS

In Chapter 3 evidence was presented which related the final product particle size to the process of drop break up and coalescence diving a suspension polymerisation.

The particles which are formed during the process are generally spherically shaped with diameters of between 0.1 - 0.3 mm.

Small amounts of a protective colloid are normally used to prevent the particles coalescing.

In the initial stages of polymerisation the reaction mixture is a dispersion of monomer droplets in a continuous phase.

These monomer droplets gradually change into a solid reaction product with the evolution of heat. The final bead size is related to the equilibrium drop size.

The conditions necessary to create a stable dispersion of liquid globules in a continuous liquid medium are as follows:

(a) Agitation must be sufficiently intense to maintain separation of all droplets.

(b) A protective film must be present between the suspended droplets and the continuous phase to prevent total coalescence.

(c) In a stable dispersion, a dynamic equilibrium exists between drop break up and coalescence.

For a fixed geometry of reaction vessel the minimum stable size of droplet will depend on agitator design, speed, and the properties of the phases.

A study of the effect of the suspending agent upon particle size distribution was carried out by Winslow and Miatreyek (92).

They examined the effect of polyvinyl alcohol stabiliser on particle size distribution in the suspension polymerisation of divinyl benzene. It was found that with increasing concentration of polyvinyl alcohol the bead size decreased. The degree of hydrolysis of the suspending agent was also found to affect particle size. For example, 80% hydrolysed polyvinyl acetate was found to give smaller beads than polyvinyl alcohol free of acetate groups. This effect was attributed to the greater emulsifying action of the polymer containing acetate groups.

The viscosity of the aqueous phase was also found to be an important factor that affected the particle size. The higher aqueous phase viscosity produced by partly saponified polyvinyl acetate, was found to give beads of very small particle size. The viscosity factor, however, was not always the major influence, since low viscosity grades of polyvinyl alcohol (even in concentrations as low as 0.005%) hindered agglomeration of the droplets, and stabilised the resulting dispersion at low values of droplet size.

Of equal importance in influencing the particle size are the process parameters employed throughout the polymerisation. An extensive study of the suspension polymerisation of methyl methacrylate, styrene and vinyl acetate was made by Hopff and Coworkers (93, 94).

They developed the following empirical equation relating particle size to the important process variables.

$$\text{Log Lo} = \frac{a^1}{nDh} + b^1 n \log n + b^1_D - \log \bar{D} + b^1 n \log Nn \qquad (133)$$

Where Lo = particle size
$\bar{D}$ = vessel diameter
Nw = viscosity of protective colloid solution
n = the revolution per minute of the agitator

a^1 and b^1 are constants

The work of Hopff shows the dependence of particle size on agitation rate, and also the importance of the aqueous phase viscosity. It does not however offer a complete explanation of the factors influencing particle size, since the ability of a protective colloid to prevent coalescence is dependent on factors other than just the viscosity of the aqueous phase.

A theoretical model of the process was put forward by Church and Shinnar (95). They related the minimum particle diameter

with the average maximum possible energy input, and derived the following equations.

$$d \text{ min} = K_1 \frac{A(h)}{\delta} \qquad (134)$$

$$E \text{ max} = \frac{K_2 \, \delta^4}{A(h)^{5/2} \, p^{3/2}} \qquad (135)$$

Where K_1 and K_2 are constants dependent upon the design of the agitator system, d min is the minimum

particle diameter that can be stabilised, E max is the average maximum possible energy input.

A(h) is the energy required to separate two droplets of unit radius from an initial distance, (ho) to infinity, and is strongly influenced by substances which are surface active. $\acute{o}$ is the interfacial tension, P is the density of the system.

Experimental data supporting the theoretical predictions of Shinnar and Church were provided by Sullivan and Lindsey (96). They pointed out however, that there can only be correlation between average drop sizes, since in a stirred tank there is a non-uniform energy dissipation rate throughout the entire agitated mass and a monodispersed dispersion will not be produced.

More recent work (93) postulates that the mean diameter of a particle produced by a suspension technique is a function of the ratio of liquid level to a centrally located agitator blade of width P^1, the phase viscosity ratio (ie, ratio of initial monomer viscosity to viscosity of aqueous phase), the ratio of the monomer to water densities and the Reynolds and Weber numbers.

The dependence of particle size on stabiliser structure and concentration, must modify any relationship between the various physical variables such as stirring speed, volume fraction etc.

An experimental study of a suspension polymerisation process has to consider the following variables in

assessing the suspension stability and mean particle size of the beads produced during the process:

(1) Type and molecular weight of the suspending agent.

(2) Concentration of suspending agent.

(3) Agitator design.

(4) Agitation rate.

(5) Baffle design and position.

(6) Water-monomer volume ratio.

(7) Reaction temperature.

(8) Reaction time (type and concentration of the free radical initiators used).

(9) Effect of additional surfactants and electrolytes.

(10) Interfacial tension between the two phases.

The effect of each variable, or the combined effects of two or more of these variables produces a very complex problem for analysis.

In the present work which examines the suspension process using non Newtonian conditions, an additional factor to be considered, is the effect of the shear rate on the rheology of the continuous phase. This is now discussed in the following section.

4.2.2 THE EFFECT OF SHEAR RATE ON THE RHEOLOGY OF THE AQUEOUS PHASE

The viscosity of a Newtonian liquid is independent of the shear to which it may be subjected. Thus

although the shear stress and strains vary greatly throughout an agitated liquid in a vessel, the viscosity of a Newtonian liquid will be the same at all points in the vessel. In contrast the apparent viscosity of a non Newtonian liquid at any point in the vessel depends on the magnitude of either the shear stress or the shear rate at that point, and may also depend upon the previous history of the liquid, since some polymer solutions exhibit rheological behaviour due to hydrogen bonding which is a time dependent function.

The shear rate is greatest in the immediate vicinity of the agitator and decreases with distance from the agitator.

The effect of shear rate on the apparent viscosity will determine the viscosity profile throughout the vessel since this will influence the mixing process. The rheological character of a time independent non Newtonian liquid can be shown on a plot of shear stress R against shear rate $\dot{Y}$. The apparent viscosity Ua at a particular shear rate $\dot{Y}$ is given by

$$Ua = \frac{R}{\dot{Y}} \qquad (136)$$

If the apparent viscosity Ua decreases with increasing shear rate $\dot{Y}$ the liquid is pseudoplastic. Conversly, if Ua increases with increasing $\dot{Y}$ the liquid is dilatant.

For a Newtonian liquid the ratio $R/\dot{Y}$ is constant. A third type of independent non Newtonian liquid is the Bingham fluid.

The plot of shear stress against shear rate is a straight line having an intercept Rb on the shear stress axis called the yield stress.

Fig (6a) shows these different types of behaviour in a plot of shear stress R against shear rate $\dot{Y}$. In a Bingham fluid the liquid at rest contains a three dimensional structure of rigidity to resist any stress less than the yield stress. However, when the stress is exceeded the system would be expected to behave as a Newtonian liquid under a shear stress R - Rb. For many non Newtonian liquids the shear stress is related to the shear rate by the equation:

$$R = K(\dot{Y})^n \qquad (127)$$

Where K = consistency coefficient and n the power law index.

The apparent viscosity of a pseudoplastic fluid will decrease immediately when the rate of shear is increased.

Consider the behaviour of the polyacrylamide suspending agent examined in the present work. This polymer behaves as a Bingham fluid initially, but when the yield stress has been exceeded the solution then behaves as a pseudoplastic liquid which will obey the power law.

$$Ua = \frac{R}{\dot{Y}} = K(\dot{Y})^{(n-1)} \qquad (129)$$

Thus $\log_{10} \mu a = \log_{10} K + (n - 1) \log_{10} \dot{\gamma}$ (131)

Since for pseudoplastic liquids $n < 1$ a plot of apparent viscosity μa against shear rate $\dot{\gamma}$ on a log - log scale gives a staight line of negative slope.

Figure 17 shows such a plot for the polyacrylamide solution used in this work but in this case, the true power law relationship does not apply.

In an agitated vessel, the shear rate $\dot{\gamma}$ decreases with distance from the agitator. Thus, the apparent viscosity of the pseudoplastic liquid increases as a function of the distance from the agitator blades.

This progressive increase in apparent viscosity with distance away from the stirrer tends to dampen eddy currents which produce drop break up and coalescence in a shear field. In 1957 Metsner and Otto (97) found the average liquid shear rate in an agitated vessel to be related to Impeller Speed N by the equation:

$\dot{\gamma} = KN$ Where K = constant (137)

This applies for a non Newtonian fluid. If K is known, together with the relationship between apparent viscosity μa and shear rate $\dot{\gamma}$ for the agitated liquid, it can be used to calculate the apparent viscosity of a non Newtonian liquid.

4.2.3 REPORTED INVESTIGATIONS OF THE SUSPENSION POLYMERISATION PROCESS CARRIED OUT UNDER NEWTONIAN CONDITIONS

The particle size of the beads produced in a suspension polymerisation process is thought to depend upon factors which influence the equilibrium drop size produced in the first stages of monomer dispersion.

Mechanical agitation of the imiscible liquids creates a two phase system consisting of small droplets dispersed in a continuous phase. The equilibrium droplet size distribution depends on many factors including physical properties (density, interfacial tension and viscosity), geometric parameters (vessel, agitator and baffles) and operational parameters (agitation speed and temperature).

The interfacial area between the two phases under Newtonian conditions was examined by Vermeulen (26) who showed that interfacial area increased with agitation rate. Vermeulen also showed that in the agitation of a dispersion of hydrocarbon in water containing from 10 - 40% of the dispersed phase, the mean drop size could be correlated by the equation.

$$\frac{d}{Lf\phi} = C \ We^{-0.6} \qquad (121)$$

Where $f\phi$ = is the ratio of the actual drop diameter to the diameter at $\phi = 0.1$

We = Weber number

This becomes when modified

$$\frac{d}{L\phi} = C_1 \left(\frac{N^2 L^3 P^1}{\sigma}\right)^{-0.6} \qquad (138)$$

Where d = mean drop size (microns)
L = length of the agitator blade (cm)
N = agitator rate (Rev/sec)
C_1 = constant
P^1 = mean density of dispersion (gm/cc)
σ = interfacial tension (dynes/cm)
$\emptyset$ = volume fraction of dispersed phase.

The application of this equation to several immiscible liquid dispersions showed good agreement (26).

All the solutions examined by Vermeulen were Newtonian in character and it must be concluded that good mixing occurred throughout the vessel, and equilibrium between drop break up/coalescence was quickly established.

Topping (25) adopted this approach and applied it to a system of immiscible liquids one of which is undergoing continuous reaction on being converted into an insoluble reaction product.

It was found that when considering the influence of dispersed volume fraction, interfacial tension, stirrer speed and size on the mean particle size produced by the suspension polymerisation of methyl methacrylate that the Sauter mean particle size d give very good correlation in a plot of log $\frac{d}{L\emptyset}$ against log $(\frac{N^2L^3P^1}{\sigma})$. The observed slope of the line was given by n = -0.54. The small difference between this result and the Vermeulen data based on droplets is attributed to a contraction in particle size when the liquid changes to a solid reaction product. The stabiliser employed by Topping was a medium molecular weight modified polyacryamide of

molecular weight approximately 0.5×10^6. The polyacrylamide was essentially ionic, modified with carboxyl groups, giving anionic ions along the polymer chain. This property effectively controls the conformation of the polyacrylamide when it is adsorbed on the surface of the monomer droplet. The aqueous phase produced using this type of polyacrylamide was found to give Newtonian behaviour, with the reaction mixture exhibiting good flow and mixing throughout the reaction vessel. Topping also showed that the level of turbulence was of importance and it was also found that the Reynolds number influenced the mean particle size when it was reduced below 9000.

The $\frac{d}{L\phi}$ function was correlated with the Weber and Reynolds number as follows:

$$\frac{d}{L\phi} = K_1 \, We^a \, e^{b/Re} \qquad Re < 9000 \qquad (139)$$

Where K_1 = constant
a = -0.68
b = 67.4
d = sauter mean diameter
L = stirrer length
ϕ = 0.20 (volume fraction)

$$\frac{d}{L\phi} = K_2 \, (We)^c \qquad Re > 9000 \qquad (140)$$

Attempts to correlate the complete range of data with changes in Weber number, and volume fraction were unsuccessful. Two relationships examined were of the form

(a) $$\frac{d}{L\phi} = K_1 \, We^a \, \phi^b \qquad (141)$$

(b) $$\frac{d}{L\emptyset} = K_1(1 + K_2\emptyset)\, We^a \qquad (142)$$

In the Newtonian conditions employed it was found that vessel size had little effect upon the final mean particle size. This indicates that the break up/coalescence equilibrium remained unchanged despite changes in the stirrer diameter tank diameter.

The drop break up coalescene equilibrium is clearly a function of the stirrer diameter but not the total flow within the vessel under Newtonian conditions. It also suggests that the drop break up/coalescence mechanism is largely confined to the region of high turbulence within the region of the stirrer diameter. Further support for this conclusion came from Topping's results when the suspension process was scaled up from a 1 kg laboratory scale to 5000 kg. It was found that despite the very great differences in vessel shape and size there was good agreement between the measured and predicted particle size distribution.

Topping also examined other properties including the moledular weight of the polymer. It was found that molecular weight had little effect on the mean particle size.

This suggests that it is polymer polarity and not molecular weight which controls the adsorption of the suspending agent.

The adsorption of the suspending agent strongly influences the interfacial tension between phases, and

thus affects the final mean particle size.

Adsorption of the suspending agent produces a viscous film at the interface and it is this mechanism which in part is thought to prevent bead agglomeration during the suspension process.

4.3 PRESENTATION OF THE EXPERIMENTAL MODEL

In the present work described in this dissertation, the suspending agent used produces non Newtonian conditions in the reaction vessel with corresponding changes in the mixing and flow properties of the dispersion when compared to a Newtonian system. It is thought that the monomer/polymer polarity governs the adsorption of the suspending agent and thus determines the resultant interfacial tension between the two phases.

The use of a high molecular weight polyacrylamide (7×10^6) was thought, would influence the adsorption rate since the orientation of the polymer chains would be more difficult.

The results obtained for interfacial tension measurements however indicated that adsorption was both rapid and complete.

In the present work both Reynolds number and interfacial tension have been examined for correlation with the observed particle size of the polymer beads produced.

It was thought that the Reynolds number will largely control the flow in the reaction vessel thus

effectively influencing the drop break up/coalescence equilibrium.

Since the influence of stirrer speed on particle size was much reduced compared to that observed with Newtonian conditions (25) the influence of Weber number on particle size was not expected or found to be significant.

The influence of monomer volume fraction on the particle size has already been discussed in 3.4.2. The observed results which indicate that the particle size decreases with increasing monomer fraction confirm that flow and mixing is very poor and is confined to the volume swept out by the stirrer. Droplets of monomer are effectively trapped within this region due to the viscosity gradients present and are subject to repeated collisions which because of hindered drop coalescence produces a reduced droplet size.

Interfacial tension has been shown to be a principal factor affecting particle size and because of its dependence on polymer polarity the relationship between the two will now be discussed.

4.3.1 POLYMER POLARITY

The present investigation attempts to correlate particle size with the interfacial tension for the experimental data obtained using high molecular weight polyacrylamide as the suspending agent in a suspension polymerisation process. Following work carried out by

B E Vijayridran (98) it has been possible to relate the particle size to the fundamental conce pt of polymer polarity. Polymer polarity controls the surfactant/ colloid adsorption which in turn influences the interfacial tension and thus physical properties such as monomer drop break up.

Vijayendran showed that interfacial phenomena such as interfacial tension, surfactant adsorption etc, are influenced by the nature of the interface.

The polarities of the monomer/water and polymer/ water are believed to govern surfactant adsorption and particle stabilisation.

Several workers have attempted to correlate the polarity of the monomer and (polymer)/water interface to the monomer water solubility (99, 100) and monomer/water interfacial tension.

Paxton (101) suggested that the area per molecule of a surfactant on a polymer surface can give useful information as to the polarity of the polymer surface.

The use of monomer water solubility data to estimate polarity is satisfactory, although polar interactions at the monomer/water interface are probably different from those at the corresponding polymer water interface due to the polarity associated with the unsaturation in the molecule. In addition, interactions such as adsorption at the fluid monomer/water interface may be more labile than at a solid polymer/water interface.

Vijayendran considered that in the aqueous phase the driving force for the adsorption of a surfactant molecule at a monomer/water or polymer/water interface is the favourable free energy change associated with the transfer of the hydrophobic portion of the molecule from the aqueous phase to the interface.

The free energy change for such a process will depend upon the nature of the surfactant and the organic phase (monomer or polymer).

The adsorption characteristics of a given surfactant were considered for different interfaces and then it is assumed that any observed differences in the adsorption characteristics are due to the differences in the energy of interaction of the surfactant molecule with the surfaces in question.

The free energy change $\Delta G\ CH_2$ associated with transferring a methylene group from water to an organic phase is a complex function of physical parameters such as miscibility, interfacial tension, dielectric constant of the monomer etc (102), but in some cases the interfacial tension controls the adsorption (103).

In Figure 43 this is clearly seen in the adsorption of hydrocarbon surfactants at various monomer/water interfaces.

In the figure approximate $\Delta G\ CH_2$ values for various acrylate monomers were calculated from data supplied by Yeliseyava and Zhuinkov (99) on the energy

of adsorption of lauryl sulphate at the respective monomer/water interfaces. It is clearly seen that the free energy of adsorption of a surfactant molecule at the monomer/water interface is a linear function of the monomer/water interfacial tension. Vijayredran assumes that a linear relationship is also valid for the corresponding polymer - water interface and so it becomes possible to substitute the free energy of adsorption of the surfactant molecule at various polymer/water interfaces by a function of the interfacial tensions.

Surfactant adsorption at various interfaces is adequately described by Langmuiur adsorption isotherms (101, 104). Using such an isotherm and substituting the energy of adsorption of a surfactant molecule at various polymer/monomer_water interfaces by a function of the respective interfacial tensions γ_{12}, Viyayendran found it possible to obtain a simplified adsorption isotherm as follows:-

$$n = BC \exp f(\gamma_{12})/KT \qquad (143)$$

Where n = saturated adsorption of surfactant (in number of molecules/unit area of the surface
c = concentration of surfactant (in moles/dm^3)
B = constant
K = Boltzmans constant
T = Temperature
γ_{12} = polymer (monomer)/water interfacial tension

This equation is only approximate as it does not take into account electrostatic interactions. However, since the adsorption behaviour involves a given surfactant at various interfaces, Viyajerdran assumed it is reasonable

to suppose that the interactions are constant and that the dominant factor controlling adsorption is the interfacial tension.

The next problem was to relate γ_{12} to the polarity of the polymer surface which was achieved using the following expression:

$$\gamma_{12} = \gamma_1 + \gamma_2 - 2(\gamma_1^d \gamma_2^d)^{\frac{1}{2}} - 2(\gamma_1^p + \gamma_2^p)^{\frac{1}{2}} \quad (144)$$

Where γ_1 = surface tension of water phase
γ_2 = surface tension of polymer phase
γ_1^d γ_2^d = dispersion contribution to water and polymer surface tension
γ_1^p γ_2^p = polar contributions to water and polymer surface tension

The polarity (X^p) is defined following Wu's method (105) as:

$$X^p = \frac{\gamma^p}{\gamma} \qquad \text{also} \qquad X^d = \frac{\gamma^d}{\gamma} \quad (145)$$

and $$X^p + X^d = 1 \quad (146)$$

Where:-

X^d = non polar contribution to surface tension.

By substitution and using numerical values for γ_1, γ_1^p and γ_1^d (1 = water phase) of 72.8, 50.7 and 22.1 MN/M respectively (105) then,

$$\gamma_{12} = 72.8 + \gamma_2 - \left[(4 \times 22.1\, \gamma_2^d)^{\frac{1}{2}} + (4 \times 50.7 \gamma_2^p)^{\frac{1}{2}}\right] \quad (147)$$

By multiplication and division of factors by $\gamma_2^{\frac{1}{2}}$

$$\gamma_{12} = 72.8 + \gamma_2 - \left[(88.4(1 - X^p))^{\frac{1}{2}} + (202.8X^p)^{\frac{1}{2}}\right]\gamma_2^{\frac{1}{2}} \quad (148)$$

expanding $(1 - X^p)^{\frac{1}{2}}$ as a power series and retaining the first two terms

$$(1 - X^p)^{\frac{1}{2}} \simeq \frac{1 - X^p}{2} \qquad (149)$$

Substituting in equation(148) then :-

$$\gamma_{12} = 72.8 + \gamma_2 - \left[9.4 - 4.6X^p + 14.2(X^p)^{\frac{1}{2}}\right]\gamma_2^{\frac{1}{2}} \qquad (150)$$

Thus Vijayendran has obtained a relationship between polymer-water interface and the polarity of the polymer surface, but still contains γ_2 the surface tension of the polymer which is not convenient to use in its present form.

Vijayendran was able to show that γ_2 values do not change as much as the polarity values. For a 20-30% change in γ_2. it is seen that X^p values change by as much as 100%. Further equation (150) shows that the effect of γ_2 may be somewhat compensating due to its additive and subtractive contributions to γ_{12}.

Thus the above equation can be simplified.

$$\gamma_{12} = K^1 - f^1(X^p) \qquad (151)$$

Where K^1 = constant

It was also shown that $\log Am = K^{11} + f^{11}(X^p)$ (152)

where Am = area per molecule of surfactant at saturation adsorption (nM^2) where K^{11} = constant. This means that the log of the area per molecule of surfactant increases with polarity of the polymer surfaces.

This approach was tested by Vijayendran using sodium lauryl sulphate as the surfactant since its area per molecule on various polymer surfaces is known from many studies.

A plot of Am against γ_{12} of the various polymer/water interfaces showed that adsorption of surfactant decreased with decrease in interfacial tension and all the data substantiated the validity of the assumption that the surfactant adsorption from an aqueous solution is related to the interfacial tension of the polymer/water interface. Vijayendran was also able to relate satisfactorily the observed differences in the area per molecule of sodium lauryl sulphate at polymer surfaces to the polarity of the polymer surface and the water-polymer interfacial tension.

Figure 44 shows a plot of γ_{12}(interfacial tension) against X^p (polarity of polymer surface).

This result is of great value and can be used to relate the interfacial tension to the polarity of the polymer under investigation.

4.3.2 APPLICATION POLARITY THEORY TO A SUSPENSION POLYMERISATION PROCESS

Since interfacial tension has already been shown to be one factor controlling particle size, by inference polarity could be equally important.

The experimental results relating the measured interfacial tension with the final particle size are

given in Table 28 and a plot of log 6 against log d size is shown in Fig 39.

It is found that the particle size is related to the interfacial tension by the following expression.

$$d = 5.49 \times 10^{-4} (6)^{7.56} \qquad (153)$$

Where d = sauter mean diamter
ó = interfacial tension (dynes/cm)

The correlation is satisfactory and is valid for both homopolymer and copolymers.

By using Vijayendran's approach it is now possible to relate interfacial tension with polarity, and thus relate the final particle size with a fundamental polymer property in this non Newtonian system.

Table 36 lists the measured interfacial tension values with the polarity of various homopolymers and copolymers at 20°C.

A plot shows that the correlation is quite good considering the various approximations used in Vijayendran derivations. Thus it appears it is possible to relate the polarity of the polymer surface, and the polymer-aqueous phase interfacial tension. (Fig 44)

The final step is to relate the polarity of the polymer directly with the observed particle size. Table 37 lists experimental results obtained with the calculated polarity at 20°C.

The polarity values were taken from Vijayendrans results who calculated them using the method supplied by S Wu (105). A plot of particle size d against the log of

polarity is shown in Fig 45 for different polymer systems.

The results indicate that the data correlation is satisfactory considering that the polarity results relate to 20°C and not the reaction temperature.

(It would be very difficult to measure the polarity experimentally at 75°C).

4.4 CONCLUSIONS

The important conclusions from this analysis are:

(1) the particle size decreased as the stirrer speed increased, but the effect is not significantly large when compared to a Newtonian system.

The particle size d is related to the stirrer speed N by the equation $d = c\ N^{-0.15}$ ($\phi = 0.2$)

(2) The particle size decreases with increasing monomer volume fraction.

This effect was noted at different stirrer speeds.

This result is completely different from that observed in a Newtonian system.

(3) The particle size increases with increasing inorganic salt ($Na_2 HPO_4$) concentration. This behaviour is explained by the effect of the salt on the drop break up/coalescence equilibrium.

(4) The Reynold s number calculated from the rheological properties of the system can be satisfactorily correlated with the particle size. A plot of Log Re against log d for different monomer systems produced a series of lines,

each line corresponding to a constant polarity dictated by the monomer/polymer composition. Theorder of the lines follows the order of the measured interfacial tension and polarity of the monomers used in the experimental work.
(5) The particle size is reduced as the interfacial tension is reduced.

The measured interfacial tension has been shown to be a function of the monomer composition at fixed protective colloid type and concentration.
(6) The particle size is a function of the monomer/polymer polarity at a constant protective colloid concentration.

S E C T I O N 2

CHAPTER 5

EMULSION POLYMERISATION

THE PREPARATION OF SUBMICRON POLYMER PARTICLES AND THE SUBSEQUENT AGGLOMERATION OF THESE PARTICLES

5.1 THE EMULSION POLYMERISATION PROCESS

The earliest investigations of emulsion polymerisation date from 1909, but it was not until 1926 that the use of soaps to stabilise the emulsion was introduced by Fikerscher and other workers (106).

The most important qualitative theory of emulsion polymerisation is attributed to Harkins (107 - 109).

The essential features of the theory are as follows:

1. The principle function of the monomer droplets is to act as a reservoir of monomer, from which monomer molecules can diffuse into the aqueous phase.

2. The principle locus for the initiation of polymer particle nuclei is regarded as the solubilised monomer contained in the micelles. The principle locus for the formation of polymer is regarded as the polymer particles themselves.

3. A small amount of particle initiation can occur within the true aqueous phase. This locus is regarded as being responsible for the formation of almost

all the polymer nuclei when no soap is present.

4. Growth of a polymer monomer particle leads to an increase in its surface area.

5. Continual adsorption of micellar soap onto growing polymer/monomer particles eventually leads to the disappearance of micellar soap as such. This stage is reached relatively early in the reaction (eg between 10% and 20% conversion).

6. Continual imbibition of monomer into growing polymer monomer particles eventually leads to the disappearance of the monomer droplets as a separate phase.

As an extension to the Harkins mechanism of emulsion polymerisation, another theory, ie the Smith Ewart theory (110) bases its model upon the Harkins theory and then endeavours to predict the rate of reaction and its dependence upon the concentration of certain components of the reaction system.

The essential point is that in emulsion polymerisation the polymer particles are not formed by polymerisation of the original monomer droplets since the final latex particles are much smaller and more numerous than the monomer droplets originally present.

In general the rate of polymerisation increases (Fig 46) during stage 1 in which most of the polymer particles are formed: polymer particles are stabilised by the adsorption of surfactant causing the concentration of surfactant in the aqueous phase to fall below the critical miscelle concentration and the surface tension to rise.

The rate remains constant during stage II until at about 60% conversion all the monomer is absorbed into the polymer particles and the monomer droplets disappear from the reaction, the rate then decreasing according to first order kinetics during stage III.

The isolation of single growing polymer radicals in latex particles ($<$ 75nm) accounts for the high reaction rate and molecular weight which are obtained.

In such conditions Smith and Ewart showed that the rate of polymerisation during stage II could be expressed as:

$$Rp = Kp\ N(M)/2L \qquad (154)$$

Where Kp = propagation rate constant
N = Number of latex particles per unit volume
M = molar concentration of monomer in (polymer particles)
L = Avogados number

According to Harkin's theory, particles are formed when the polymerisation of monomer solubilised in a soap micelle is initiated by the capture of a radical formed by decomposition of the initiator in the aqueous phase. Thus new particles cannot be formed when surfactant concentration in the aqueous phase falls below the critical micelle concentration, and the number of latex particles should remain constant from the beginning of stage II. (Since zero order kinetics are observed during stage II, the monomer concentration in the polymer particles must remain constant during this stage).

The presence of micelles is not necessary for the initiation of polymer particles. Aqueous solutions of monomers such as methyl methacrylate, vinyl acetate and even styrene can be polymerised in the absence of surfactants. The polymer precipitates or the latex particles are stabilised by ionic end groups derived from the initiator radicals.

Monomer is absorbed in the polymer phase (or adsorbed on the polymer particles if it does not dissolve in them) and under most conditions the polymer phase soon becomes the chief locus of polymerisation. It has been shown by CP Roe (111) and Van Der Hoff (112) that almost as many particles are formed with concentrations of soap below the critical micelle concentration as above it.

Although high salt concentrations cause coalescence of latex particles (113), lower concentrations of salt increase the number of particles formed by increasing their stability when increased amounts of surfactant are adsorbed. Particle formation continues until the amount of surfactant remaining in solution is insufficient to stabilise newly formed polymer. Polymer precipitated in the aqueous phase then coalesces with existing latex particles instead of nucleating a new particle. Calculations using the Rerjaquin-Landau-Verwey-Overbreek theory of the stability of lyophobic colloids (114) shows that small particles will coalesce with large ones under conditions in which large particles are too stable to coalesce with each other.

The process of particle nucleation in the aqueous phase is described in more detail in the next section, and

this is followed by a discussion of the factors which can influence the agglomeration and flocculation of particles so formed.

5.2 MONOMER SOLUBILITY

At the start of the polymerisation the bulk of the monomer exists as monomer droplets in a separate phase, while only a small amount is present in monomer micelles or in true solution in water.

It is necessary to consider factors which will influence the solubility of the monomer.

The solubility in water of the monomer in a droplet form of radius r is given by:

$$Cr = C_{\infty} \exp\left(\frac{K}{r}\right) \qquad (155)$$

Where

$$K = 2Y\bar{V}m/RT = 2YM/(doRT) \qquad (156)$$

Where Cr = solubility with droplet radius r
C_{∞} = solubility with droplet infinite radius
Y = interfacial tension
Vm = molar volume of monomer
M = molecular weight of monomer
do = density

The solubility rate increases with decreasing radius of the droplet.

If we have present two types of droplets a and b with radius ra and rb where rb $>$ ra, it will be expected that monomer is transported from the 'a' droplets to the 'b' droplets until 'a' droplets have disappeared completely.

The rate of decrease in the radius of the small droplets was shown by Higuchi and Misra (115) to be given by:

$$\frac{dra}{dt} = \frac{-DC_{\infty} K}{do\ ra^2}\left[\frac{nb(rb - ra)}{na\ ra + nb\ rb}\right] \qquad (157)$$

Where na and nb are the numbers of droplets a and b respectively and D is the diffusion coefficient.

From equation (156) the degradation rate is proportional to the solubility of the monomer and to the interfacial tension.

In practice the water will contain emulsifier so that the actual value of C_{∞} may be considerably higher than the value in pure water. The droplet stability is inversely proportional to the cube of the radius.

If the droplet radius r is decreased ten fold, the corresponding change will occur one thousand times faster. If one starts with an equal number of droplets of 0.5 and 1 m and a value of Y = 5 dyne cm^{-1}, c_{∞} = 1g dm^{-3}, M = 100, do = unity and D = 5 x $10^{-6} cm^2\ s^{-1}$, it is calculated that the value of ra will decrease 10% in about 3 minutes.

The rate of disappearance of smaller droplets will be much faster, and for styrene C_{∞} = 0.32g dm^{-3} which suggests it is not possible to prepare droplets in the submicron range.

However, if one has present a small amount of a much more water soluble compound, the rate of degradation of the emulsion will be governed by the diffusion rate of

the more insoluble compound. Changes in the system occur only as fast as the change in distribution of the slowest diffusing component. What happens physically is that it is necessary to wait for the slow diffusion of the more insoluble compounds in order that the more water soluble component shall remain equilibrated among the droplets.

It should be noted that the actual solubility of the more insoluble may be considerably influenced by the presence of the slightly water soluble compound and emulsifier in the aqueous phase.

5.3 PARTICLE NUCLEATION IN THE AQUEOUS PHASE

5.3.1 SMITH EWART THEORY

The classical theory of Smith Ewart (115) has been used to describe the nucleation of particles in an emulsion polymerisation. In accordance with this theory, the nucleation of particles takes place solely in the monomer swollen miscelles which are transformed into polymer particles by absorption of radicals from the aqueous phase.

The following expression was derived by Smith Ewart:

$$N = KS^{0.6} I^{0.4} \qquad (158)$$

Where S = emulsifier concentration
I = initiator concentration
K = constant between 0.37 and 0.53
N = number of latex particles in unit volume

This equation gives a fairly good prediction of particle number for highly water insoluble monomers like styrene within a limited range of particle number.

In the case of with increased water soluble monomers the Smith Ewart expression does not satisfactorily describe particle nucleation.

5.3.2 THE FITCH THEORY

Heller, Klevens, Priest (116) and Fitch (117) (118) proposed a mechanism which suggests that primary particles are formed in the aqueous phase by precipitation of oligomer radicals above a critical molecular weight.

The basic principles of the Fitch theory is that formation of primary particles will take place up to a point where the rate of formation of radicals in the aqueous phase is equal to the rate of disappearance of radicals by capture of radicals by already formed particles: $Pi - Pc = 0$. Fitch et al, derived an expression for the rate of radical capture Pc which implies that Pc is proportional to the surface area of the particles formed.

The theory was applied to describe experimental results using very dilute aqueous systems of methyl methacrylate.

Stabilization of primary particles in emulsifier free systems may be achieved if the initiator produces ionic end groups.

According to the Fitch theory of homogeneous particle nucleation, the addition of emulsifier does not lead to any increase in the number of primary particles formed. It only leads to an increased stability of the primary particles, preventing them from coagulating and

and producing a decrease in the final number of particles.

5.3.3 THE UGELSTAD AND HANSEN MODEL

A model proposed by Hansen and Ugelstad (119) was formulated for a homogeneous nucleation theory where the reaction path of the radicals formed in the water phase is described.

If no emulsifier is present the radicals that are produced by the initiator may:

(i) Add monomer units dissolved in the water phase.

(ii) Be absorbed into an existing polymer particle or be adsorbed onto the surface of the radical.

(iii) Terminate in the water phase with another radical.

(iv) Coagulate with another dissolved radical.

(v) Precipitate as a primary particle if the radical reaches the critical chain length.

If there are surface active species present in the water phase, these may adsorb onto the precipitated primary particles and the particles may be stabilised. Otherwise the surface charge will proably be too small to stabilise the primary particle and they will start to coagulate.

This behaviour will stop when the charge density reaches a level where the particles are stable, and is called limited coagulation.

Their model based on diffusion, propagation and termination steps is now derived.

If no seed particles are present, Hansen and Ugelstad proposed the following differential equations for radical growth, radical capture and formation of primary particles by precipitation.

$$dRi/dt = Pi - kRi \tag{159}$$

$$dRj/dt = kRj-1 - kRj - ktwRjRtot - Rj\sum_{p=1}^{\infty} kcp\ Np \tag{160}$$

$$dN1/dt = kRjcr-1 - N1\sum_{p=1}^{\infty} kfp1Np - kc1\ N1\ Rtot \tag{161}$$

$$dN_2/dt = kf_{11}N_1^2 - N_2\sum_{q=1}^{\infty} kf_{2q}\ Nq + (Kc1N_1 - kc_2N_2)\ Rtot \tag{162}$$

$$dNs/dt = \tfrac{1}{2}\sum_{p=1,\ q=s-p}^{p=s-1} kfpq\ NpNq - Ns\sum_{q=1}^{\infty} kfsq\ Nq + (Kc(s-1)\ Ns - 1 + KcsNs)R_{tot} \tag{163}$$

The particles are divided into a number of classes according to the degree of coagulation. Both the class index and surface charge can change by particle capture.

Where:

P1	=	rate of radical formation from the initiator
R1	=	number of initiator radicals
Rtot	=	R1 + R2 + --- Rjer-1 = total number of growing radicals in the aqueous phase
Ktw	=	termination constant for reaction between two growing radicals
kcj	=	capture constant for a radical of chain length j
N1	=	number of precipitated primary particles
Mw	=	number of moles of monomer in aqueous phase
Rj	=	oligomeric radicals of chain length j
Ns	=	particles of class S
Kcp	=	capture rate constant
Kfpq	=	coagulation rate constant
Rj-1	=	number of growing radicals to total
K	=	KpMw
Ktw	=	termination constant.

Kcp (capture rate constant) is given by the following equation:

$$kcp = 4\pi\ Dw\ rp\ Fp \tag{164}$$

Where:

Dw = mean diffusion constant of oligomers
rp = class radius
Fp = reduction factor of radicals in particles of class P

The coagulation constant Kfpq is given by:

$$kfpq = 4\pi\ Dpq\ rpq/Wpq \tag{165}$$

Where Dpq, the diffusion constant for particles p to q in the aqueous phase is given by:

$$Dpq = Dp + Dq \tag{166}$$

$$= \frac{\bar{k}T}{6\pi nrp} + \frac{\bar{k}T}{6\pi nrq} \tag{167}$$

$$= \frac{\bar{k}T}{6\pi n}\left(\frac{1}{rp} + \frac{1}{rq}\right) \tag{168}$$

Where n is the viscosity of the aqueous phase, rp is given by:

$$rp = r1\ p^{\frac{1}{3}} \tag{169}$$

Where r1 is the radius of the primary particles

$$rpq = rp + rq \tag{170}$$

Thus the total expression for kfpq is:

$$Kfpq = (2\ \bar{K}T/3n)\ (p^{\frac{1}{3}} + q^{\frac{1}{3}})\ (p^{-\frac{1}{3}} + q^{-\frac{1}{3}})/Wpq \tag{171}$$

Wpq is the Fuchs stability ratio expressed by

$$Wpq = 2\int_0^{\infty} \exp\left\{V_{Tpq}/\bar{k}T\right\}\left[du/(u+2)^2\right] \tag{172}$$

Where $V_{T}pq$ is the total potential energy of interaction between p and q particles and $u = 2H/(rp + rq)$ (173)

H is the shortest distance between the particles. $V_{T}pq$ is the total potential energy of interaction between p and q particles.

$V_{T}pq$ is equal to the sum of attractive and repulsive energy. The attractive energy is according to Hamaker (120).

$$V_{APQ} = -\frac{A}{12}\left\{\frac{y}{x^2 + xy + x} + \frac{y}{x^2 + xy + x + y} + 2\ln\frac{x^2 + xy + x}{x^2 + xy + x + y}\right\} \quad (174)$$

Where A = Hamaker constant

$x = H/rp$

$y = rq/rp = (q/p)^{\frac{1}{3}}$

The repulsive potential between two spheres of different size and with surface potentials (ψ_0) have been calculated by Hogg et al (121) by means of the Derjaquin method.

$$V_{Rpq} = \frac{\pi \epsilon\, rp\, rq(\psi_{op}^2 + \psi_{oq}^2)}{rp + rq}\left[\frac{2\psi_{op}\psi_{op}}{\psi_{op}^2 + \psi_{op}^2}\ln\frac{1+\exp\{-kH\}}{1 - \exp\{-kH\}} + \ln(1 - \exp\{-2KH\})\right] \quad (175)$$

Equation (175) is a good approximation for

ψ_0 50 - 60 mV and $kr > 5$

$$\psi_{op} = Qp/[4\pi\epsilon\, rp\,(1 + krp)] \quad (176)$$

Where the total surface charge $Qp = ep$ (177)

For an estimation of the conditions under which equation (175) is valid,

This gives rp = 25 nm at krp = 5. With a value of P = 50, the values of ψ_{op} is from equation (176) = 60mV. These values represent the smallest particle size and higher values of p for which equation (175) and (176) may be applied. The corresponding values for the radius of the primary particle r1 = $25/(50^{1/3})$ = 6.8 nm

For a monomer such as styrene, the size of the primary particles may be considerably lower.

The exact size of the potential energy will be dependent upon the size of the primary particle because the surface charge density of a particle is inversely proportional to the square of its radius.

This value of r is very small at the start of the nucleation process but increases with time due to the propagation reaction. In order to get a qualitative idea of the coagulation kinetics it is not necessary to have the absolute value for the potential energy. (It is far more important that the change in potential with particle size is expressed in relative units.)

The stability ratio Wpq was calculated by numerical integration of equation (172).

Fig (47) shows a contour map where Wpq is a function of p and q for r1 = 2nm and with electolyte concentration of 6.4×10^{-3} N.

It is seen that Wpq $\rangle$ 10^6 when p = q = 100 and this should be sufficiently high to ensure stability. However, W, the Fuchs stability ratio between small and

large particles is always small and may be less than unity when $P < 4$. This indicates that the attractive force exceeds the electrostatic repulsion and the primary particles will always coagulate with all other particles.

The particle size distribution after different reaction times were calculated by Hansen and Ugelstad using the numerical integration of particle nucleation and flocculation equations.

This is shown as a plot of N against P in Fig 48.

The maximum in particle number occurs at a very short time and would in practice be unobserved. However the decrease after the maximum may be pronounced. It should be noted that after the maximum the distribution becomes bimodal. The small particles will have a maximum in the primary particles. This is because primary particles are steadily formed from oligomers. The other maximum will be at larger particle sizes and this is the normal monodisperse distribution that is observed (see election micrographs Fig 60). This review outlines the formation of the monodisperse distribution from the aqueous phase. The present work extends their work and examines the formation of agglomerates produced from the monodisperse particles, and in particular the magnitude of forces which bind together the particles in the formed agglomerate.

It was clear from the micrograph photographs that the size of the particles in the monodisperse distribution were quite regular and little influenced by the concentration of the polyvinyl alcohol. However, the formation of

the agglomerates are very sensitive to changes in the protective colloid type and concentration. The process is thus shown as follows:

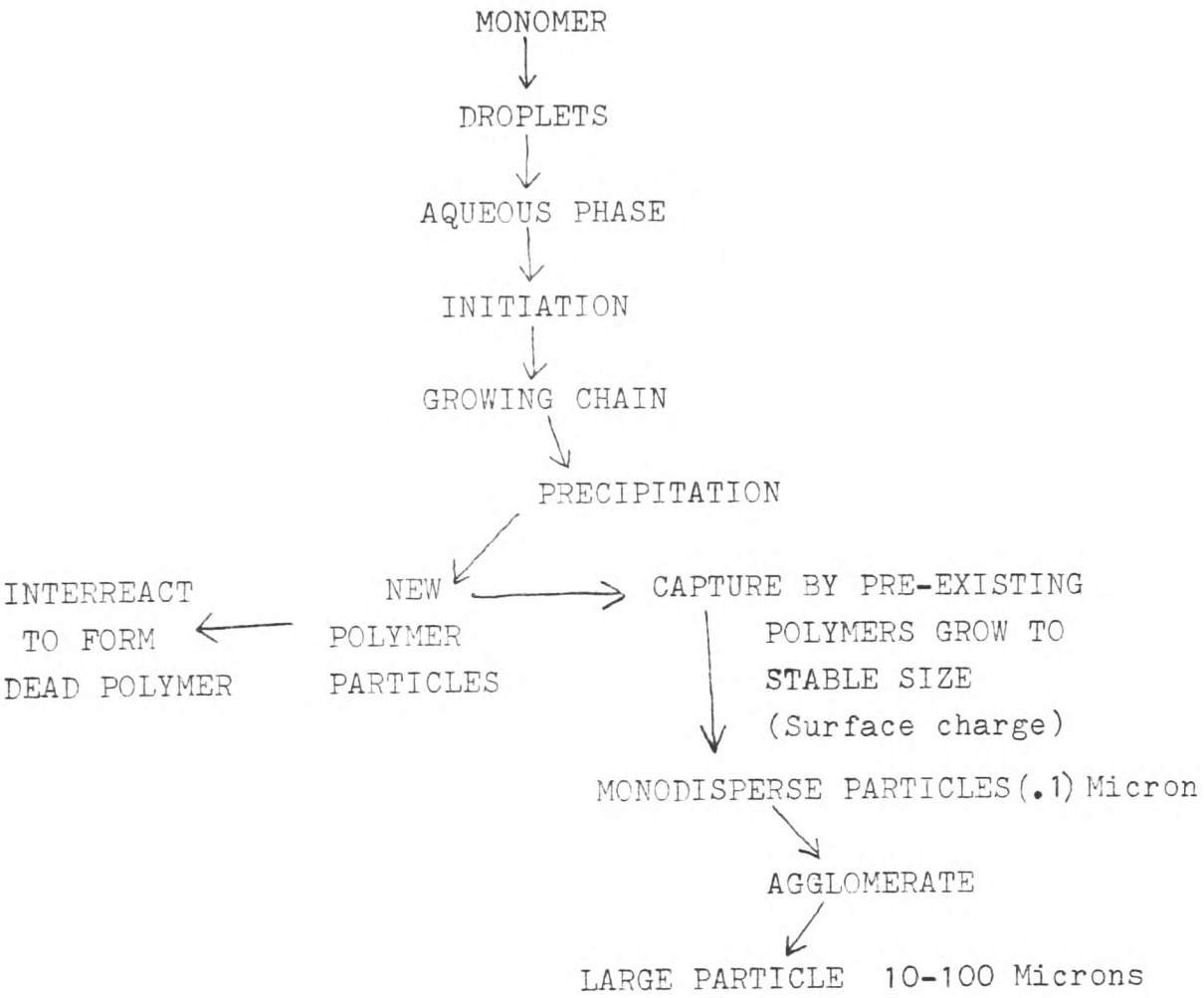

5.4 PARTICLE AGGLOMERATION THEORY

The factors which cause sub micron polymer particles to agglomerate or disperse in a water/polyvinyl alcohol system has been investigated in the present work.

New concepts have been developed which explain the surface energetic relationships causing the dispersion/ agglomeration process. It is generally well known that

lack of surfactant is one reason for agglomeration of the particles under the specific set of experimental conditions employed.

As more surfactant is added the agglomerate particle size becomes progressively smaller and finally achieves complete dispersion of the individual polymer particles when sufficient dispersant has been added.

The best method of dispersing a liquid to produce a small droplet suspension is by the use of surface active agents.

The use of solubility and dispersion parameter data allows some insight into the correct choice of colloid to be used.

The head of the surfactant molecule must match the dispersion parameter of the solid surface, while the tail of the surfactant molecule must match the solvent.

The two molecular ends are held together by chemical, ionic or other strong bonds.

In the present work polyvinyl alcohol was used as the surfactant, although in this case it acts as a protective colloid rather than a true surfactant molecule.

In the aqueous solution, the polymer particles produced by reaction adsorb polyvinyl alcohol on to their surface.

The adsorption of the PVA has been shown to be a function of concentration and type of grade used.

When no molecules of such a dispersant are present, (or are present in low concentrations) such that the

surface of the polymer particle is not covered completely, then agglomeration of the particles occurs; this is shown in Fig 51.

When the agglomeration process (due mainly to Brownian Motion in a unstirred system or kinetic energy in a stirred system) has reached the final stage the agglomerate will have grown to such a size that sufficient surfactant molecules are available to protect the agglomerate and it will not grow further in size.

It is clear that the polymer particles in the agglomerate are held together by surface forces and under sufficient shear conditions it should be possible to reverse the agglomeration process and produce the individual particles.

However, when shear is stopped the particles will agglomerate again to the equilibrium size depending on the type and concentration of surfactant present.

Generally, a dispersion which consists of agglomerate particles is fairly uniform in size. The following explanation is offered:

If small particles co-exist in the presence of larger agglomerates they would require a disproportionately large number of the dispersing molecules present to produce a stable system. Thus, equilibrium conditions tend towards a uniform agglomerate size where each unit of agglomerate has its fair share of dispersing molecules, commensurate with the total area that these molecules can cover.

If this concept of the surface layer of the dispersing molecules is correct a quantitative relationship should exist between the amount of colloid present, the relative surface area of the agglomerate, and the relative agglomerate size.

From basic considerations, the surface covered by the dispersing molecules should be directly proportional to the amount of colloid present. It is shown later (7.3.7) that the total concentration of protective colloid is proportional to the reciprocal of the agglomerate size for a given concentration of polymer particles. Figure 64 shows a plot of agglomerate size dependence on added protective colloid. The good correlation indicates that the system behaves as expected with an equilibrium agglomerate size produced for each level of protective colloid concentration.

5.5 AGGLOMERATE SIZE AND FLOW PROPERTIES

The factors affecting the dispersion and agglomeration process have been examined by WK Asbeck (122).

Asbeck considered an agglomerated particle, Fig 52, suspended in a unit shear field. The unit shear stress, r_A, required to break the agglomerate is proportional to the number of pairs of individual particles across the major cross sectional area parallel to the shear field, and also the sum of the forces of attraction between these individual particles and the concentration of such agglomerates in the unit shear field and is given by:

$$r_A = \left(\frac{D}{d} - 1\right)^2 fA \, \phi \, (C) \qquad (178)$$

Where $(\frac{D}{d} - 1)$ is the reduced relative hydraulic diameter of the agglomerate. f_A is the force of attraction per unit area between the sum of the individual particles in the agglomerate, and $\phi(C)$ is a function of the concentration of the particles in suspension.

$$\text{Since, } f_A = \frac{fa}{d^2} \tag{179}$$

Where d = distance of separation
f_A = force of attraction per unit area between the sum of the individual particles in the agglomerate.

fa = average force of attraction between any pair average particles.

Taking roots of equation (178) then:

$$r_A^{\frac{1}{2}} = (\frac{D}{d} - 1) \quad f_A^{\frac{1}{2}} \quad \phi(C)^{\frac{1}{2}} \tag{180}$$

but by definition,

$$r_A^{\frac{1}{2}} = n_A^{\frac{1}{2}} \quad \dot{Y}^{\frac{1}{2}} \tag{181}$$

Where n_A = contribution to the viscosity caused by the break up of the agglomerate, and $\dot{Y}$ is the shear rate therefore;

$$n_A^{\frac{1}{2}} = \frac{(\frac{D}{d} - 1) \quad f_A^{\frac{1}{2}} \quad \phi(C)^{\frac{1}{2}}}{\dot{Y}^{\frac{1}{2}}} \tag{182}$$

A plot of $n_A^{\frac{1}{2}}$ against $\frac{1}{\dot{Y}^{\frac{1}{2}}}$ will thus give a straight line with the intercept on the $n_A^{\frac{1}{2}}$ axis equal to the viscosity of the system when all the forces of agglomeration have been overcome and only the viscosity due to the presence of the individual particles in a monodispersion

remain. (Such a plot is shown in Fig 62 and Fig 63). The latter can be designated $N_\infty^{\frac{1}{2}}$, the residual viscosity at infinite shear rate. The total viscosity is the sum of the individual viscosity contributions.

$$n^{\frac{1}{2}} = n_\infty^{\frac{1}{2}} + n_A^{\frac{1}{2}} \qquad (183)$$

The slope of the curve is given by:

$$\text{Slope} = r_A^{\frac{1}{2}} = \left(\frac{D}{d} - 1\right) f_A^{\frac{1}{2}} \phi(C)^{\frac{1}{2}} \qquad (184)$$

The concentration function $\phi(C)^{\frac{1}{2}}$ can be evaluated in terms of the viscosity at infinite shear rate, $n_\infty^{\frac{1}{2}}$ where the particles are monodisperse.

To evaluate $\phi(C)^{\frac{1}{2}}$ Asbeck developed a simple cell model of the form:

$$n_\infty = n_o \left\{ 1 + \frac{r\,C}{U_r} \Big/ \left[1 - \left(\frac{C}{U_r}\right)^{\frac{1}{3}} \right] \right\} \qquad (185)$$

Where:

n_o = The Newtonian viscosity of the supernatant liquid

C = The per cent by volume of the suspended monodisperse particles.

U_r = A rheological packing factor which is very nearly equal to the Ultimate Pigment Volume Concentration for particles in the monodisperse state.

r = A shape factor which for most spherical or nearly spherical particles approaches the ratio of the area of a circle within a circumscribed square or:

$$r = \frac{\pi}{4} = 0.7854 \qquad (186)$$

When the concentration of particles is zero, the residual viscosity is obviously that of the supernatant liquid or n_o.

The concentration function in terms of the reduced equivalent rheological values then simply becomes:

$$\phi(C)^{\frac{1}{2}} = (n_\infty{}^{\frac{1}{2}} - n_o{}^{\frac{1}{2}}) \Big/ n_o{}^{\frac{1}{2}} \tag{187}$$

which is equal to:

$$\phi(C)^{\frac{1}{2}} = \left\{ \frac{rc}{Ur} \Big/ \left[1 - \left(\frac{c}{Ur}\right)^{\frac{1}{3}} \right] \right\}^{\frac{1}{2}} \tag{188}$$

The overall relationship between the viscosity of a dispersion of agglomerated particles suspended in a Newtonian liquid then becomes:

$$n^{\frac{1}{2}} = n_\infty{}^{\frac{1}{2}} + \left(\frac{ra}{Y}\right)^{\frac{1}{2}} \tag{189}$$

where $$r_\infty{}^{\frac{1}{2}} = no^{\frac{1}{2}} (1 + Z)^{\frac{1}{2}} \tag{190}$$

$$ra^{\frac{1}{2}} = \left(\frac{D}{d} - 1\right) f_A{}^{\frac{1}{2}} (1 + Z)^{\frac{1}{2}} \tag{191}$$

and:

$$(1 + Z)^{\frac{1}{2}} = \left\{ 1 + \frac{\frac{rc}{Ur}}{1 - \left(\frac{c}{Ur}\right)^{\frac{1}{3}}} \right\}^{\frac{i}{2}} \tag{192}$$

Equation (185) has the same form as the semi-empirical equation proposed by Casson (123). The equation in this form has been substantiated with a considerable amount of practical data by Asbeck.

The formally derived Casson equation has proved to be of little value since the unrealistic assumptions

were made that the agglomerated particles consist of rod like clusters, and that these rods can pack so tightly that their critical Pigment Volume Concentration (CPVC) will be equal to 100%, signifying that no liquid will normally remain within the tightly packed agglomerate. Asbeck showed that both these assumptions were incorrect.

Using Asbeck's simple cell model it becomes possible to predict the shear rate sensitive viscosity of any dispersion in a Newtonian liquid, since all of the factors are either known or can be measured independently.

Conversely, the force of attraction between the individual particles making up an agglomerate can now be measured directly by rheological means alone.

Thus $n_o^{\frac{1}{2}}$ the viscosity of the carrier liquid is measured, and $n_\infty^{\frac{1}{2}}$ found by experiment. $n_A^{\frac{1}{2}}$ is obtained from $r_A^{\frac{1}{2}}$ and $\dot{Y}$ data. D and d, the agglomerate and primary particle size can be measured (using the coulter counter and SEM). Hence $f_A^{\frac{1}{2}}$ and fa (the bonding energy between particles) can be calculated.

CHAPTER 6

PHYSICAL DATA

6.1 SUMMARY

The physical and chemical properties of polyvinyl alcohol are related to its chemical structure and the behaviour of its aqueous solutions are discussed from this aspect.

Interfacial chemical properties of solutions are also discussed and correlated with their protective colloid properties.

A short report of their effects on the kinetics of a polymerisation are described.

The properties of the aqueous phase are discussed together with the measurement of rheological properties and interfacial tension.

6.2 INTRODUCTION

6.2.1 POLYVINYL ALCOHOL

6.2.2 STRUCTURE

Polyvinyl alcohols are manufactured by a continuous process involving polymerisation of vinyl acetate and partial or complete hydrolysis of the intermediate polyvinyl acetate or polyvinyl alcohol.

Varying the degree of polymerisation and the extent to which acetate groups along the polymer chain are replaced by hydroxyl groups, results in a series of resins with a range of properties.

There are a large number of commercially available grades of polyvinyl alcohol. The classification falls into three groups:

1. A fully hydrolysed group with a degree of hydrolysis $>$ 98%.

2. A partly hydrolysed sub group: 87-89% hydrolysed.

3. A partly hydrolysed sub group: 80%.

Another classification is based on the viscosity at 20°C of a 4% aqueous solution of polyvinyl alcohol.

The major groups form the following viscosity classification:

1. A low viscosity group of approximately 5 cp.

2. A medium viscosity group of 20 to 30 cp.

3. A high viscosity group of 40 to 50 cp with a sub group of about 60 cp in certain types.

Between the medium and low viscosity groups is a sub group of viscosity 10 to 20 cp.

In terms of molecular weight, the types can be classified into major groups of degree of polymerisation of approximately, 500, 1700 and 2000 with sub groups of 1000 and 2400. Thus the number of grades of polyvinyl alcohol can be classified by three groups relating to

degree of hydrolysis and four or five groups classified by molecular weight.

6.2.3 PHYSICAL PROPERTIES OF POLYVINYL ALCOHOL (PVA)

Polyvinyl alcohol is always used in aqueous solution. Its solubility in water depends on its degree of polymerisation and the degree of hydrolysis.

Hydrogen bonding between intra and intermolecular hydroxyl groups can impede solubility.

Residual acetate groups in partly hydrolysed PVA are essentially hydrophobic and weaken the intra and intermolecular bonds which then increase the water solubility.

The relation between the degree of hydrolysis and the solubility of PVA at a fixed molecular weight (1700) is shown in Fig 53. The presence of as little as two to three molecular per cent of residual acetate groups in the structure causes significant changes in the solubility of PVA from 60°C.

Partly hydrolysed polyvinyl alcohol dissolves only slightly, but approximately 97% hydrolysed PVA dissolves completely in water.

Heating to at least 80°C is required to dissolve a completely hydrolysed grade. A 20°C, polyvinyl alcohol less than 88% hydrolysed dissolves almost completely in water but the solubility decreases with increasing hydrolysis.

The solubilities of typical commercial grades of polyvinyl alcohol at various temperatures is shown in Fig 54. The molecular weight spread lies between 500 and 2400 and the polymers are 98, 88 and 80% hydrolysed.

The solubility of 98% hydrolysed polyvinyl alcohol (usually known as fully hydrolysed grade) is slightly increased as the degree of polymerisation is decreased, but that of (88%) partly hydrolysed polyvinyl alcohol is relatively independent of the degree of polymerisation.

With 80% hydrolysed polyvinyl alcohol the solubility at low temperature is far higher than that of 88% hydrolysed polyvinyl alcohol, but decreases rapidly above $40^{\circ}C$.

6.2.4. VISCOSITY BEHAVIOUR OF AQUEOUS SOLUTIONS OF POLYVINYL ALCOHOL

Figure 55 shows the relations between the viscosity of commercial grades of polyvinyl alcohol in aqueous solution and the degree of hydrolysis, degree of polymerisation, temperature and concentration.

Naito (124, 125) has discussed the molecular theory of aqueous solutions of completely hydrolysed grades of polyvinyl alcohol, and has showed that in the viscosity concentration relation shown in Fig 56 an inflexion point at 2-4% concentration can be observed.

It has been suggested that the structure of polyvinyl alcohol before the inflexion point differs from that above it. Below the inflex ion point it is thought that

each molecule is dispersed in water in the form of thread filled spheres containing water, while above the critical concentration entanglement of polymer chains occurs; this effect increases with concentration such that at 10-20% a structure exists such that chain entanglement stabilise at an equilibrium condition.

Viscosity Stability

Aqueous solutions of polyvinyl alcohol of 98-99 per cent hydrolysed (molecular weight 1700-1800) polyvinyl alcohol increase in viscosity with time and can gel.

The rate of this increase in the viscosity increases with concentration, and decreases with temperature. However, the viscosity of 88% hydrolysed grades is stable with time.

The increase of viscosity of the 98-99% hydrolysed grade is related to time as follows:

$$nt = No\ (1 + \alpha t) \qquad (187)$$

No = apparent viscosity after dissolving
nt = apparent viscosity after t hours
α = viscosity increase coefficient

This behaviour is not seen using the polyvinyl grade 52-22, the type employed in the investigations described later in this section.

Effect of Shear on Viscosity

It is well known that aqueous solutions of polyvinyl alcohol exhibit non Newtonian viscosity characteristics.

By investigation of the effects of shear on the viscosity of aqueous solutions of polyvinyl alcohol of various concentrations and degrees of polymerisation, Naito and Coworkers (126, 127) concluded that a dilute (less than 5 gm/litre) aqueous solution of polyvinyl alcohol of molecular weight 3000 can be considered Newtonian with a velocity gradient in a low shear region from 400-500 sec^{-1}. However, the shear effect increases with increase in concentration and Naito found that there was a critical concentration above which polymer entanglements are broken.

6.2.5 INTERFACIAL CHEMICAL PROPERTIES

6.2.5.1 SURFACE TENSION

Aqueous solutions of partly hydrolysed grades of polyvinyl alcohol with hydrophobic acetate groups and hydrophilic hydroxyl groups have a lower surface tension than those of fully hydrolysed grades.

Hayashi, Nakano and Motoyamra (128) in their work on the protective colloid action of polyvinyl alcohol with different degrees of hydrolysis and the distribution of acetyl groups investigated the effect of surface tension. Figure 57 shows that there is a slight decrease in the surface tension γ of fully hydrolysed grades of polyvinyl alcohol, but partly hydrolysed grades decreased with increased residual acetyl group content.

6.2.5.2 PROTECTIVE COLLOID PROPERTIES

When polyvinyl alcohol is used as a stabilising agent in emulsion polymerisation, it fulfils the dual function of smulsifying the monomer and stabilising the polymer particles formed during the process.

Polyvinyl alcohol has yielded useful products when used as stabiliser with vinyl acetate only, but, with other monomers, it is used in conjunction with other surfactants.

The protective colloid properties of partly hydrolysed grades increase with decreasing degree of hydrolysis and more block-like intermolecular distribution of residual acetate groups is obvious from surface tension data. Hayashi, Nakano and Motoyamra (129), verified this by a study of gold colloids and by various properties of polyvinyl acetate emulsions.

Table 38 shows the protective colloid properties of partly hydrolysed PVA, made using different hydrolysis solvents in relation to the properties of gold colloids.

The gold number is the quantity of colloid required to stabilise a gold solvent to the addition of a given amount of electrolyte.

As the ratio of benzene to methanol in the hydrolysis increases, and the distribution of the residual groups is more blocklike, the gold number is lower and the protective colloid properties are improved.

Polyvinyl acetate emulsions polymerised with polyvinyl alcohol shown in Table 38 as an emulsion stabiliser

have the following properties.

The emulsion viscosity is in the order:

$$A > B > C > D$$

The particle size of the emulsion is in the order:

$$A < B < C < D$$

The stability of the emulsion to sodium sulphate addition is in the order:

$$A < B < C < D$$

Thus the more block-like the distribution of the residual acetyl groups of PVA (A-->D) the smaller the particle size after polymerisation, the greater the viscosity and the better the stability to salting out.

The importance of the degree of blockiness is further illustrated by the gold number (ie the quantity of colloid required to stabilise a gold solvent to the addition of a given amount of electrolyte; the reciprocal of the gold number increases as the degree of stabilisation rises:. From the gold number given in Table 38 it can be seen that as the blockiness of the acetyl groups increased the degree of protectivity rose.

6.2.6 POLYVINYL ALCOHOL AS AN EMULSIFIER AND PROTECTIVE COLLOID

The function of the polyvinyl alcohol when used as a stabilising agent is to emulsify the monomer and stabilise the polymer particles produced during the reaction.

A series of water soluble hydrolysed polyvinyl acetates was examined by Capitani and Pirrone (130) in the emulsification of vinyl acetate. They concluded that medium molecular weight partially saponified polyvinyl acetate was the most effective surfactant. Shiraishi (131) estimated the efficiency of emulsification of vinyl acetate from the monomer emulsion viscosity and found it to increase with the degree of blockiness of the polyvinyl alcohol and with acetyl content up to about 20 per cent molar (ie 80 mol per cent hydrolysed polymer).

Styrene was included in a study of the stability of drops of organic liquids as suspended in solutions of various colloids, one of which was polyvinyl alcohol.

It was found that the half life of the drop varied with the concentration of the colloid (88% hydrolysed PVA, high molecular weight) in water. The emulsification of styrene in aqueous polyvinyl alcohol solutions has been further studied by Gromov and Coworkers (132). Using partly hydrolysed polyvinyl acetate, they found that the surface activity at the styrene-water interface increased slightly with temperature (132), between 20°C and 80°C (as also occurred with 88% hydrolysed PVA with other monomers), but that the life time of the styrene drop decreased substantially (133). The life of the styrene drop increased with the polyvinyl alcohol concentration and was highly sensitive to the addition of various salts.

The drop stability was also found to be a function of the pH. Adjustment of the pH with HCl affected the

stability as well as the rheology of the polyvinyl alcohol solutions.

Using toluene, a maximum total drop area was detected at a polyvinyl alcohol concentration in the region of 5-6% for a variety of polyvinyl alcohol types.

A maximum was also found at 10-12 mol per cent acetate content in the optimum concentration range (134)

This behaviour is probably related to the configuration of the polyvinyl alcohol molecule in aqueous solution.

Both cations and hydrogen ions will be expected to have an effect on the polymer configuration as they will change the hydrogen bonding on entering the polymer network.

The protective power of polyvinyl alcohol is due in part to the configuration of the molecule. It has been shown from surface tension measurements, that at low concentrations ($<$ 0.020% by Wt), the molecules are oriented horizontally at the interface, but are oriented vertically at higher concentrations.

Work on carbon black dispersions in low concentrations of polyvinyl alcohol suggest that the colloid is attached to the hydrophobic surface at only a few points, and that complete coverage of the surface is not required to achieve dispersion in water (135).

Other studies have been concerned with the solvation of the molecule, flow birefringence and determinations using light scattering techniques suggest some form of association in aqueous solution (136).

Peters and Fasbender (137) have shown the existance of a solvate layer by couette viscosity tests on 10% aqueous solutions of polyvinyl alcohol (molecular weights = 20,000, 85,000 and 180,000) between 20°C and 50°C. The effective rheologically immobile volume per unit weight of dissolved substance owing to the solvate cover of the macromolecule increased with decreasing concentration, reaching a maximum of 38.5 - 40.4 ml/g at infinite dilution at 20°C. This corresponded to 94-99 molecules of water per monomeric unit of vinyl alcohol (138). Using hydrophobic surfaces such as paraffin, Lyblema (139) found that the adsorption at low concentration of an 88% hydrolysed grade of PVA was higher than that of a 98% hydrolysed material. He also noted pseudomicelle formation of the latter at a concentration of about one part in 10^6 but not with the 88% hydrolysed grade.

The use of different types of polyvinyl alcohol as protective colloid in the emulsion polymerisation of vinyl acetate was studied by Hayashi and workers (140). It was possible to show that the stability increased with the acetyl content and the blockiness of the distribution of the acetate groups.

Fischer (141) found that the addition of small quantities of water soluble polymeric compounds could cause agglomeration in polymer emulsions but larger quantities promoted stability. The minimum quantity of polyvinyl alcohol required to assist the stability of a polystyrene emulsion was 3.2% of the weight of polystyrene.

Fischer proposed that the agglomeration occurred when the adsorption layers were not saturated, and that the repellent effect between particles could be explained by the configurational entropy. The good stabilising property of partially saponified polyvinyl acetate as against 100% polyvinyl alcohol and partially acetylate polyvinyl alcohol has been demonstrated by measurement of the gold number (142), coalescence studies on liquid drops (140), and solubilization of an oil soluble dye.

Hayashi, Nakano and Motoyama (142) showed that for fully hydrolysed polyvinyl alcohol a logarithmic relationship exists between the gold number (N = 1 to 100) and the degree of polymerisation ($\bar{P}$ = 3000 to 1000) such that

$$\log N = 4.2 - 1.2 \log \bar{P} \qquad (188)$$

6.2.7 KINETICS OF POLYMERISATION

It has been reported by Motoyama and workers (143) that in the emulsion polymerisation of vinyl acetate, the rate of polymerisation was greater with partly hydrolysed polyvinyl acetate than with fully hydrolysed polyvinyl alcohol.

Using ammonium persulphate

$$Rp = [PV - OH]^{0.25} [M] [I] \qquad (189)$$

Where Rp = rate of polymer
[M] = monomer concentration
[I] = initiator concentration

For styrene, Schuller reports (144)

$$Rp \propto [PV - OH]^{0.7} [M] \qquad (190)$$

Where $[M]$ is monomer concentration in the particle, also :-

$$Rp \propto (\bar{P}_{PV - OH})^{1.5} \qquad (191)$$

Where $\bar{P}_{PV-OH}$ = average degree of polym.

6.3 PROPERTIES OF THE AQUEOUS PHASE

In the present work, the aqueous phase (a solution of polyvinyl alcohol in water) is examined for viscosity and other rheological properties.

This information is needed to supply data from which the interparticle bonding force can be calculated for the polymer dispersions. Although most of the experimental work involves measurement on particle dispersions, it is necessary to know, in detail, the effect that the solvent (PVA solution) is having in the process so that a complete understanding of the process is obtained.

6.3.1 MEASUREMENT OF VISCOSITY

Viscosity measurements were carried out using the cone and plate viscometer described in Chapter 2. Experimental investigations were made on aqueous polyvinyl alcohol solutions and also agglomerated dispersions produced by the polymerisation of styrene using polyvinyl alcohol as stabiliser.

Results are reported in Tables 43 - 58.

6.3.2 MEASUREMENT OF INTERFACIAL TENSION

The interfacial tension was measured using both the drop volume and sessile drop methods. Results are reported in Table 39.

6.4 PARTICLE SIZE MEASUREMENT

The measurement of particle size and particle size distribution is necessary for characterising a latex or any suspension. The importance of this physical characteristic is realised when one examines the physical properties controlled by particle size and size distribution.

The rheological properties of suspensions are affected mainly by the particle size of the reaction product.

6.4.1 ULTIMATE AND AGGLOMERATE SIZE

In the present work the agglomerate size was measured using a Coulter counter. The primary or individual particle size was obtained using a scanning electron microscope.

6.4.2 THE COULTER COUNTER

The coulter counter is capable of measuring particle size and distribution of both aqueous and non aqueous suspensions in the range of 0.2μ to 200μ .

Detection is based upon drawing the suspension of particles in a conducting medium by a slight vacuum created by unbalancing a mercury-u-tube connected to a small orifice, the working sensitivity.is 2-40% of the orifice

diameter. An electrode current established on either side of the orifice is altered only momentarily when a particle passes through the orifice. This current change is detected as a pulse in a discriminating circuit. The pulse height is proportional to the resistance change as the particle passes through the orifice.

By gradually increasing the sensitivity of the pulse height a cumulative count of particles larger than a given size can be made over the range of the instrument sensitivity.

The advantages of the method may be listed as follows:

1. Small sample required.
2. A large number of particles counted.
3. Very fast automatic with latest model.
4. Either number or weight average can be computed.

A few limitations may be mentioned:

1. Several orifice sizes needed to cover the range of particle sizes.
2. Each orifice must be calibrated with a monodisperse system of known size.
3. Particle concentration must be kept low enough to avoid coincident passage of two or more particles. (Which would be counted as one larger particle).

Results obtained are reported in Tables 42 and 56.

6.4.3 ELECTRON - MICROSCOPE

The electron microscope with its great resolution is useful in sizing particles below 10,000°A. Magnification as high as 500,000X is practical since the resolution on modern instruments is in the order 2 - 7Å.

A drop of highly dilute suspension (15^{3} - 10^{5}) g/cc is placed on a collodion coated screen of about 200 mesh and allowed to dry: the dried specimen is then examined and the particles photographed. The size of the photographed particles is then determined and from the magnification employed the particle size is compiled.

One of the chief problems in electron microscopy is the temperature of the sample which is about 100°C but can reach 200°C.

Thus many latexes can shrink or even melt where the glass transition temperature is exceeded.

The electron microscope used is located at the Polytechnic of Wales.

Photographs obtained with the instrument are shown in Figs 59 - 64 and described with the various experimental results.

CHAPTER 7

EXPERIMENTAL RESULTS

7.1. SUMMARY

The factors which cause polymer particles to agglomerate or disperse have been investigated for the emulsion polymerisation using benzoyl peroxide as initiator and polyvinyl alcohol as the protective colloid.

Variables examined were:

1. Stirrer speed
2. Stirrer size
3. Colloid type and concentration
4. Monomer type

The investigation was carried out using laboratory scale apparatus which employed a fixed stirrer geometry. It was found that agglomerate size depends on colloid concentration, but little difference was detected in the size of the submicron primary particles. Stirring speed had an effect on the polydispersity of the primary submicron particles and caused a reduction in agglomeration size with increased agitation rate.

The agglomerate size was sensitive to both the type and concentration of the protective colloid. From rheological data, it was shown that an equilibrium exists between the agglomeration and dispersion processes.

It was confirmed that the bonding energy between

particles in an agglomerate for one particular colloid type was independent of the colloid concentration and thus supports the theory that the protective colloid is found only on the surface of the agglomerate and that the process only stops when there is sufficient surface coverage.

Finally, it has been shown that the presence of a reactive difunctional monomer produces particles which agglomerate in a specific manner and produce fibres up to 2 cm in length. Under the influence of high shear on the surface of the stirrer the ultimate particles grow in a linear manner until broken up by the turbulence. It was established that the bonding energy between particles in these linear agglomerates were of much smaller magnitude to those involved in the spherical agglomeration of primary particles.

7.2 INTRODUCTION

This investigation relates to the main factors thought to influence both the ultimate and final agglomerate size in a dispersion, when an unsaturated hydrocarbon is transformed into a solid reaction product, which then agglomerates into spherical agglomerate particles. At an early stage in the reaction, the main factors thought to influence the drop size of the mobile droplets are:

1. Type and concentration of surfactant used.
2. Stirrer size and geometry
3. Stirrer speed
4. Volume fraction of dispersed phase
5. Interfacial tension

6. Reaction temperature

7. Monomer type and solubility

The size of the monomer droplets will depend upon the equilibrium developed between the process of coalescence and drop break up. However in this process (in which styrene and polyvinyl alcohol were chosen as monomer and protective colloid respectively) the principal reaction product was not to be bead particles but spherical agglomerates.

Using a monomer soluble dye, it was clearly shown that the reaction did not originate in the monomer/aqueous interface, but proceeded by direct initiation in the aqueous phase. The primary particles ~(0·2 μ) formed, and agglomerated to a critical size, which depended upon the type and concentration of the polyvinyl alcohol employed.

The size of the agglomerate and the primary particles nucleated in the aqueous phase were investigated in the present work and an estimate of the forces necessary for particles to bond in the agglomerate obtained.

The possibility of other agglomeration processes occurring which can produce a final product not necessary of spherical shape was also considered. By changes in polymer polarity and chemical structure, it was found that unusual adsorption patterns can be obtained which leads to the formation of fibre agglomerates. Thus factors which can influence the primary particle size, and the final agglomerate size and shape include the following:

1. Type and concentration of colloid used
2. Relative volume of the phases
3. Type and rotational speed of the stirrer
4. Interfacial tension.
5. Reaction temperature
6. Monomer type - its solubility in the aqueous phase, its polarity, reactivity and density.

The preparation of the polystyrene dispersions was investigated in the absence of true emulsifiers as the agglomeration process does not take place under these conditions and a stable latex results. For the same reason benzoyl peroxide was used as the initiator since it is not expected to stabilise the latex with fragments of initiator chemically bound to the surface of the particles in the way that a persulphate initiator stabilises emulsions.

Two monomer types were investigated. Styrene was chosen because of its low water solubility and polarity, methyl methacrylate for its increased polarity and water solubility. The reaction system was also modified by the use of difunctional acrylic monomers in later work.

7.3. INVESTIGATION OF FACTORS WHICH INFLUENCE THE FORMATION OF PRIMARY PARTICLES IN THE AQUEOUS PHASE

7.3.1 INTRODUCTION

It is considered that during the polymerisation process oligomeric free radicals are formed by reaction between the monomer and primary free radicals.

However, whereas the Harkins theory (107,108) presents a clear picture of nucleation and growth of latex particles in the presence of emulsifier micelles the corresponding mechanism of nucleation in their absence is still debatable. Several mechanisms have been proposed:

(a) That the growing free radicals in solution become insoluble and precipitate out upon themselves.

(b) That the growing free radicals undergo termination followed by particle nucleation through coagulation of these dead species.

(c) That the growing free radicals achieve a size and concentration at which they become surface active and undergo micellisation.

Which mechanism would describe particle nucleation of a particular monomer depends on the solubility of the monomer and also its hydrophobicity, since these factors would be expected to have a large effect on what occurs in the initial stages - a process occurring in solution.

Hansen and Ugelstad (119) have presented a theory for particle nucleation by precipitation of oligomeric radicals from the water phase. Their model is based on the diffusion, propagation and termination steps and in systems with no or low emulsifier concentration they introduce the term limited coagulation to describe the process.

In the present work, particle formation in the presence of a low concentration of polyvinyl alcohol was examined.

The polyvinyl alcohol is added to control the agglomeration process which occurs after the polymerisation of the monomer in the aqueous phase.

The initiator employed in the investigation was benzoyl peroxide. This was used to avoid complications associated with the use of the usual water soluble persulphates. In the presence of a persulphate initiator the latex particles are stabilised by ionic end groups derived from the initiator radicals.

Benzoyl peroxide is normally used in suspension processes since it is monomer soluble and is generally thought of as insoluble in water.

However, the use of benzoyl peroxide in the present work has given results which suggest that the initiator is transferred to the aqueous phase by mass transfer at a rate fast enough to sustain polymerisation. Since the production of primary particles and their subsequent removal from the aqueous phase by agglomeration takes place at a substantial rate, then mass transfer of both monomer and initiator through the aqueous phase must take place during reaction.

A series of experiments were carried out to investigate the reaction mechanism, and, in particular to establish the rate determining step for mass transfer of the initiator through the aqueous phase.

7.3.2 MASS TRANSFER OF BENZOYL PEROXIDE TO THE AQUEOUS PHASE

7.3.2.1 EXPERIMENTAL

7.3.2.2 MATERIALS

Industrial water was used, styrene of commercial grade was employed as the monomer.

Polyvinyl alcohol (Dupont - Elvanol 52-22) grade was used as the protective colloid.

Benzoyl peroxide 70% (water damped grade) was employed as the initiator.

7.3.2.3 PROCEDURES

Preparation of the dispersion was carried out at 80°C unless otherwise stated. The prescribed amount of water was charged to a one litre flask fitted with a stirrer and heated to 60°C when the polyvinyl alcohol was added.

After the completion of the dissolution, styrene monomer, was added, and the reaction mixture stirred for 30 minutes.

Next the initiator (benzoyl peroxide) was added and the reaction mixture stirred for a further 30 minutes. The aqueous phase was then separated from the monomer using a separation funnel.

Finally after filtration, a clear solution of the aqueous phase was obtained.

The weight of the aqueous phase was then measured and placed in a reaction vessel with the appropriate weight of styrene monomer.

The mixture was heated (with stirring) to 80°C, when the solution became cloudy due to precipitated polymer after about 5 minutes. No further change was noted and the experiment was concluded after 45 minutes.

7.3.2.4 DISCUSSION

Since the reaction mixture produced a small amount of polymer it must be concluded that some of the initiator was retained in the aqueous solution.

Thus although benzoyl peroxide is normally only employed as an initiator in the monomer phase, mass transfer makes it effective for some aqueous polymerisations.

7.3.3 INVESTIGATION OF THE REACTION PATHWAY USING SOLUBLE DYES

7.3.3.1 EXPERIMENTAL

The following formulation was placed in a stirred reaction vessel.

Water	792.0 grms
Polyvinyl alcohol (52,22)	8.0 "
Styrene	188.0 "
Benzoyl peroxide (70%)	2.8 "
	990.8

dye
(Automate Red B Williams Commercial dyestuff)

Stirrer speed 400 rpm
Stirrer type ⊥ 10 cm diameter

7.3.3.2 PROCEDURE

The aqueous solution was prepared by charging the prescribed amounts of water and polyvinyl alcohol to the vessel, heating to 50°C and stirring for one hour.

The benzoyl peroxide was dissolved in the styrene monomer for use in the reaction vessel. The monomer was charged to the vessel, and the reaction mixture heated to 80°C.

Drops of a monomer soluble dye were added to the stirred system.

Samples of the mixture were taken at 5 minute intervals for examination under a microscope.

7.3.3.3 RESULTS

The preparation of polystyrene dispersions by the initiator process was investigated with benzoyl peroxide as initiator, the reaction was followed using a monomer soluble dye.

It was apparent that the rate of polymerisation increased remarkably after about 10 minutes. The dye coloured monomer droplets were gradually replaced firstly by very fine colourless particles, which then slowly coagulated to a much larger agglomerated particles. In the later stages of reaction all the monomer was used up and no coloured suspension product was noted. Thus the reaction proceeds in the aqueous phase and following homogeneous particle nucleation, coalescence occurs to produce large agglomerated particles as the final reaction product.

7.3.4 INVESTIGATION OF THE EFFECT OF INITIATOR CONCENTRATION ON THE RATE OF REACTION

7.3.4.1 INTRODUCTION

Previous experiments indicate that homogeneous particle nucleation occurs in the aqueous phase even for a relatively water insoluble monomer like styrene. Stabilisation of the primary particles is not achieved using benzoyl peroxide since this does not produce ionic end groups.

Since both the monomer and initiator are insoluble these must pass from the monomer phase by mass transfer to the reaction site.

The mass transfer rate is given by the expression:

$$W = ho \times A \times C \qquad (192)$$

Where :-

ho = mass transfer coefficient
A = interfacial area
C = concentration gradient
W = rate

Thus the reaction rate should show dependence on the initiator concentration if mass transfer of initiator is the rate determining step.

7.3.4.2 EXPERIMENTAL

7.3.4.3 (i) REAGENTS

Industrial water, and commercial styrene monomer were employed throughout.

Benzoyl peroxide (70%) water damped grade was used as the initiator.

Polyvinyl alcohol (du-Pont 52,22) was used as the protective colloid, ie to control the agglomeration process.

7.3.4.4. (ii) PROCEDURE

The following formulation was employed in the investigation.

Water	=	792.0 g		
Polyvinyl alcohol	=	8.0 g		
Styrene	=	188.0 g		
Benzoyl peroxide	=	2.8 g*	*	Initiator Level
		990.8 g		A = 5.6 gm
				B = 2.8 gm
				C = 1.4 gm

The polymerisation was carried out in a laboratory reaction vessel fitted with a stirrer.

Stirrer speed and geometry were unchanged throughout the investigation.

The aqueous phase was first prepared by placing the water and polyvinyl alcohol in the flask and heating to 50°C with stirring. Following the completion of dissolution, the styrene and benzoyl peroxide were added. (The initiator was dissolved in the styrene). The contents were heated 80±1 °C and polymerisation continued until it was substantially completed.

A total of three runs were made, each had the indicated changes in initiator level. Samples were taken frequently and the opacity compared visually with a standard set of opacity samples prepared from an emulsion latex.

The standard samples were arranged such that each was double the concentration of the next in the series.

Sample O was the most concentrated, while sample 5 was the most dilute.

The estimation procedure was kept as simple as possible. Following the sampling, the sample was centrifuged and the monomer removed. The estimation of opacity was made to the nearest 0.5 of the standard set. The results are listed in Table 40 for three runs A, B, C in which the initiator level was doubled and halfed. The actual opacity is plotted against time in Fig 58.

7.3.4.5 DISCUSSION

In Fig 58 a plot of opacity number against time is shown.

The dependence of reaction rate on the initiator level is evident at once, with the increased initiator level producing the fastest reaction rate.

The experiments also show that little reaction occurs within the first 10 minutes, but afterwards the reaction rate is quite fast. It may have been a reasonable prediction to have expected no change in reaction rate if mass transfer of the initiator was a rate step. The results however indicate a change in the concentration gradient.

The overall rate of reaction is controlled by mass transfer of both monomer and initiator simultaneously to the aqueous phase.

7.3.5 THE EFFECT OF AGITATOR SPEED UPON PRIMARY AND AGGLOMERATE PARTICLE SIZE

7.3.5.1 EXPERIMENTAL

7.3.5.2 MATERIALS AND APPARATUS

The monomers used in this work were styrene and methyl methacrylate.

Both monomers were of commercial grade. The inhibitor type and concentration present in the monomers were as follows:

Styrene - 4 tertiary butyl catechol (10 ppm)

Methyl methacrylate - methyl hydroquinol (100 ppm)

The protective colloid employed was polyvinyl alcohol (Du-pont Elavanol grade 52,22).

Tap water was used for all the experimental investigations,

The experimental polymerisation was carried out using the laboratory equipment shown in Fig 34.

The stirrer employed was a flat blade type and the stirrer speed was variable between 0 and 600 rpm.

The reaction mixture was heated by an electrically heated water bath and the stirring speed was set using a stroboscope. The polymerisation systems used are described in Table 41.

7.3.5.3 OPERATING PROCEDURE

Before making an experimental preparation, the glass reaction flask was cleaned, rinsed thoroughly and dried.

The appropriate volume of water was charged, heated to 60°C, and the suspending agent added slowly with vigorous stirring. The initiator (benzoyl peroxide) was dissolved in a weighed quantity of monomer and this organic phase added slowly to the stirred aqueous phase when the polyvinyl alcohol had dissolved.

The stirrer was set to the required speed and the temperature of the contents raised to 80°C.

Temperature control was maintained to within ± 1°C by an external thermostat.

The polymerisation lasted about four hours, after which the product produced was washed, dewatered and dried.

Samples of product were taken to carry out a particle size analysis using the coulter counter and for examination by the scanning electron microscope.

The remainder of the sample was used to carry out various rheological determinations.

7.3.5.4 RESULTS - EFFECT OF AGITATOR SPEED UPON AGGLOMERATE PARTICLE SIZE

The effect of agitator speed upon the agglomerate and primary particle size in the process was examined. The agglomerate size was measured using a coulter counter, while the primary particle size was determined by the electron microscope.

In the experimental investigations, the stirrer speed was varied between 200 and 600 rpm, the stirrer

diameter varied between 4-10 cm, but the shape remained constant.

These results are reported in Table 42 and SEM photographs presented in Figs 59, 60 and 61.

From the results it can be seen that the mean agglomerate particle size decreased with increasing stirrer speed, and two samples showed a bimodal size distribution.

The primary particle size remained between 0.15 - 0.25 μ.

There was no obvious correlation between agitator speed and the primary particle size. Finally, a small sample of the agglomerated product was broken open and the interior examined using the scanning electron microscope. Figure 61 shows one such particle. It is clear that the particle is a true agglomerate consisting of primary particles throughout its volume and are not large beads covered by adsorped primary particles. Methyl methacrylate in contrast to styrene showed no evidence of agglomeration product.

7.3.6 EFFECT OF COLLOID CONCENTRATION ON THE AGGLOMERATE PARTICLE SIZE (STYRENE)

7.3.6.1 EXPERIMENTAL

A series of polystyrene agglomerates were prepared to the basic formulation given in Table 41. In the investigation the polyvinyl alcohol concentration was varied between 0.5% - 4.0%. The aqueous solutions were prepared by dissolving the polyvinyl alcohol granules in water at

60°C using vigorous stirring.

The initiator (70% benzoyl peroxide) was dissolved in the styrene monomer which was then added to the stirred aqueous phase.

The reaction mixture was heated to 80°C, and the reaction completed using a fixed stirrer, speed, size and geometry.

Once the reaction was completed, samples were taken for an evaluation of the agglomerate size 'D' using the coulter counter, the primary particle 'd' size was obtained using the scanning electron microscope.

The rheological properties of both the polyvinyl alcohol solutions, and the final agglomerated dispersions were investigated using a cone and plate viscometer.

The results are reported in Table 43 - 50.

7.3.6.2 DISCUSSION OF RESULTS AND CONCLUSIONS

Figure 62 shows a plot of $\sqrt{\text{viscosity}}$ against $\frac{1}{\gamma^{1/2}}$ for the data given in the above tables.

The plot shows the decrease in viscosity due to the break up of the agglomerated particles as the shear rate is increased. Reducing the shear, it was found possible to reproduce the data, thus indicating that the particles rapidly revert to their maximum equilibrium degree of agglomeration. The polyvinyl alcohol solutions were found to gradually increase in viscosity finally levelling out under conditions of high shear.

From the data it was possible to calculate $\eta_A^{\frac{1}{2}}$ tables 51 - 58 and obtain a plot of $n_A^{\frac{1}{2}}$ against $\frac{1}{\dot{Y}^{\frac{1}{2}}}$ as shown in Fig 63.

η_A is the contribution to the viscosity caused by the break up of the agglomerates and $\dot{Y}$ is the shear rate. From Fig 63, $n_\infty^{\frac{1}{2}}$ the point where all the forces of agglomeration have been overcome can be measured. At $n_\infty^{\frac{1}{2}}$ the viscosity is due to the presence of primary particles in a state of monodispersion.

$\eta_o^{\frac{1}{2}}$ the residual viscosity due to the supernatant polyvinyl alcohol solution (when the concentration of particles is zero) can also be measured under shear conditions.

From these measurements the concentration function $\phi(C)^{\frac{1}{2}}$ can be calculated.

Since a plot of $\eta_A^{\frac{1}{2}}$ against $\frac{1}{\dot{Y}^{\frac{1}{2}}}$ gives a line of slope = $r_A^{\frac{1}{2}} = (\frac{D}{d} - 1)\, f_A^{\frac{1}{2}}\, \phi(C)^{\frac{1}{2}}$ it becomes possible to measure f_A and fa the force of attraction between the individual particles in the agglomerate.

Table 59 shows the calculated value for fa using experimental data for each PVA concentration between 0.5% - 4%.

From these results it can be concluded that the bonding energy between particles in an agglomerate for one particular grade of PVA is independent of the colloid concentration, and thus supports the theory that the protective colloid is found only on the surface of the agglomerate, and that the process only stops when there is sufficient surface coverage.

7.3.7 AGGLOMERATE SIZE RATIO

In the present investigations, it is proposed that the polymer particles in the agglomerate are held together by surface forces.

An equilibrium condition will tend towards a uniform agglomerate size commensurate with the total area that the protective colloid will cover. Thus a quantitative relationship should exist between the colloid concentration and the relative agglomerate size ($\frac{d}{D}$).

Data for both the agglomerate size (D) and the primary particle size (d), together with % PVA level used is given in Table 60.

The result of plotting %PVA against d/D is presented in Fig 64.

From Fig 64 there is quite good correlation and it is clear that the surface area covered by the colloid is important.

7.3.8 INTERFACIAL TENSION

The interfacial tension between a 1% PVA solution (52, 22 type) and the monomer phase was measured using both the sessile drop and drop volume methods, and these results are reported in Table 39.

While the interfacial tension will be important in the early stage of reaction, and will play a part in the drop break up mechanism which can influence the rate of solubility of the monomer in the aqueous phase, the interfacial tension will not play any part in final stages

of the agglomeration equilibrium.

7.3.9 EFFECT OF CROSS LINKING MONOMER ON THE AGGLOMERATION PROCESS

A series of laboratory investigations were carried out using two different diacrylate compounds and two different monomers (styrene and methyl methacrylate).

The composition of the reaction mixture is reported in Table 61.

The effect of changing both the concentration and composition of the PVA was examined. The same reaction vessel and stirrer was used (⊥ - type), and the impeller speed was kept constant.

The reaction temperature was maintained at 80°C. The product of reaction instead of being a spherical agglomerate consisted of (a) normal beads and (b) elongated fibre agglomeration product, seen to be particulate under the SEM (See Figs 65, 66), whilst the beads produced were completely crosslinked and tough, the agglomerate fibres were very brittle breaking down into individual particles with relatively slight mechanical agitation. The high magnification views of the particles obtained with the scanning electron microscope show a perculiar mottled appearance not observed in earlier photographs of the sperical agglomerates. Examination of Table 65 shows that in general which agglomeration process occurs depends on:

(a) The particular alcohol molecular weight and hydrolysis range used.

(b) The polyvinyl alcohol concentration.

(c) The presence of diacrylate monomers.

(d) The concentration of any diacrylate monomer used.

(e) The monomer used.

The formation of the fibre agglomerate is promoted by the presence of the Elvanol (52,22) grade of polyvinyl alcohol.

The use of a reduced molecular weight grade of polyvinyl alcohol was found to give reduced fibre agglomeration at the same concentration level, whilst a high viscosity, high molecular weight type showed a very much reduced effect.

Increasing the concentration of Elvanol (52,22) was found to reduce the fibre agglomeration level. Whilst there was little difference in the effects of the two diacrylate monomers used, their concentration is important, since increasing the concentration reduces the level of fibre agglomeration. Finally while both styrene and methyl methacrylate show fibre agglomeration, only styrene shows spherical agglomeration at a fixed protective colloid type and concentration.

7.3.9.1 ESTIMATION OF THE PARTICLE BONDING ENERGY IN FIBRE AGGLOMERATES.

Previous investigation had shown it possible to measure the force of attraction between polymer particles in a spherical agglomerate. Using high shear conditions in a cone and plate viscometer it was found possible to

break up the spherically agglomerated particles to a state of monodispersion, and from the rheological data obtained, calculate fa the average force of attraction between any pair of particles.

The same approach was adopted for the fibrous agglomerates, since although not spherical, the agglomerates can be made to approximate a spherical shape by the simple grinding of a sample.

7.3.9.2 EXPERIMENTAL

Particles of the fibre agglomerate were taken and ground up to give an approximate spherical distribution of agglomerate. A suspension of these particles in polyvinyl alcohol was then prepared (using the original PVA concentration and original fraction).

The dispersion was then examined for its rheological properties using a cone and plate viscometer.

The agglomerate particle size of the dispersion so produced was determined using a coulter counter, and the primary particle size of the agglomerate evaluated from the scanning electron microscope.

The rheological data is listed in Tables 55, 62 and 63.

7.3.9.3 RESULTS

From the data presented in Tables 55, 62 and 63 a plot of $\sqrt{\text{viscosity}}$ against $\frac{1}{\dot{\gamma}^{\frac{1}{2}}}$ is shown in Fig 67. A further plot of $n_A^{\frac{1}{2}}$ against $\frac{1}{\dot{\gamma}^{\frac{1}{2}}}$ is shown in Fig 68.

From the above data, it was possible to obtain an approximate value for fa. The actual data used in the calculation is reported in Table 64.

The values of fa for both types of agglomerate can now be compared.

Fa (Fibre) = 0.22×10^{-12} dynes per pair

fa (Spherical) = 0.30×10^{-10} dynes per pair

The lower bonding energy for the fibre agglomerate seems reasonable since it supports the earlier observation that these agglomerates are very weak breaking up into primary particles with the slightest mechanical agitation.

7.4 DISCUSSION

The factors thought to influence the final particle size of the agglomerate and primary size have been discussed earlier in the introduction to this chapter.

The present investigation examined the effect of various variables which included stirrer speed, colloid type and concentration.

In the present work the volume fraction of monomer was kept constant, the type and concentration of the polyvinyl alcohol was varied (Table 65).

7.4.1(i) SPHERICAL AGGLOMERATION

In the absence of a divinyl compound, the use of polyvinyl alcohol produced spherical agglomerates of variable size but quite similar primary particle size. Stirring speed seemed to have an effect on particle

(agglomerate) size, decreasing it with increasing stirrer speed.

Methyl methacrylate did not form an agglomerated product. It was established that the process of primary particle formation proceeded via an aqueous intermediate state.

The effect of protective colloid concentration upon the agglomerate and primary particle size is clearly seen in Table 60.

The agglomerate size increases with decreasing cocncentration of polyvinyl alcohol, but there was little effect on the primary particles size except at the lowest colloid concentration.

From rheological means it was possible to measure the force of attraction between individual particles in the agglomerate.

The values of fa remained fairly constant over the concentration range (0.5% - 4%) of the polyvinyl alcohol.

This supports the concept of a skin of protective colloid molecules on the surface of the agglomerate.

7.4.2 FIBRE AGGLOMERATION

This type of agglomeration is produced when there is a difunctional monomer present. The extent of agglomeration is also a function of both protective colloid grade and concentration and also the difunctional monomer concentrations. Monomer type and polymer polarity seem

to have little effect, since both styrene and methyl methacrylate exhibit this type of agglomeration.

The bonding energy between particles in a polystyrene fibre agglomerate was measured and found to be much smaller than the result obtained for a spherical agglomerate.

CHAPTER 8

DEVELOPMENT OF AN EXPERIMENTAL MODEL

8.1 SUMMARY

An experimental model is presented which examines the reaction rate profile of styrene in the absence of an emulsifier, but in the presence of polyvinyl alcohol as a protective colloid. The initiator used was not a water soluble type. It is concluded that both monomer and initiator pass into the aqueous phase by mass transfer, where homogenous particle nucleation of the styrene occurs.

Particle destabilisation occurs which is followed by the coalescence and agglomeration of the polymer particles. The presence of the protective colloid and its effect on the subsequent agglomeration processes is discussed in terms of particle stabilisation theory.

8.2 INTRODUCTION

8.2.1 THE STABILITY OF SUSPENSIONS

The interactions between dispersed particles may be discussed either in terms of the interparticle force $f_1(h)$, or the interaction free energy $G_1(h)$.

Where h is the distance between the pair of particles concerned.

$$f_i(h) = - d G_i (h)/dh \quad (193)$$

The assumption that the stability/instability of a suspension with respect to aggregation, can be discussed in terms of the pairwise interaction is the central premise of the classical DLVO (143, 144) theory of colloid stability.

Vincent (145) considers it a reasonable assumption at low particle volume fractions, but questionable at high values of $\emptyset$ where there may be some long range (spacial) correlations in the positions of the particles with respect to each other. In order to examine $G_1(h)$ (the interaction free energy), it is necessary to know the the various contributions to the interparticle interaction.

(1) <u>All particles - Van der Waals forces</u>

For two spherical particles, Fig 69, radius a, the most widely used approximation for GA, the Van der Waals interaction free energy is:

$$G_A(h) = -\frac{a(A_1^{\frac{1}{2}} - A_2^{\frac{1}{2}})^2}{12h} \qquad (h \ll a) \qquad (194)$$

Where A_1 and A_2 are the Hamaker constants of the particles and solution respectively. Hamaker constants for most materials lie in the range 5 - 100 kT (water 10.6 kT). At contact separation the particles experience the very high repulsion forces associated with electron orbital overlap (the Born repulsion).

(2) Charged particles - electrical double layer interactions

A surface may aquire a net charge by various mechanisms, isomorphic substitution, dissociation, adsorption of ionic surfactants etc. The total surface charge is counter balanced by counter ions some specifically adsorbed in the stern plane (Fig 69), and the rest in a diffuse layer, the effective thickness of which may be taken as k^{-1} where for 1:1 electrolytes.

$$K = \left(\frac{2e^2\ Cb}{\varepsilon\varepsilon_o KT}\right)^{\frac{1}{2}} \qquad (195)$$

Where e is the electronic charge, cb the bulk electrolyte concentration, ε the dielectric constant of the medium and ε_o the permittivity of free space. For aqueous solutions at 25°C, equation (195) predicts the following values for K^{-1}.

$C_b = 10^{-5}$ mol dm^{-3}, K^{-1} = 100nM

$C_b = 10^{-3}$ mol dm^{-3}, K^{-1} = 10 nM

$C_b = 10^{-1}$ mol dm^{-3}, K^{-1} = 1nM

When two particles approach such that their double layers overlap, they experience an increase in free energy (repulsion). Various approximate formulae have been derived for this electrostatic repulsion free energy, G_E .

The following applies in the limit of large particles ($Ka \gg 1$) and low stern layer potentials, ψ_δ ($< \sim 25$ mV)[5].

$$G_E(h) = 2\pi\varepsilon\varepsilon_0 a \psi_s^2 \ln(1 + \exp(-kh)) \quad (196)$$

As an approximation it is common to substitute the electrokinetic potential (ie the zeta potential) for ψ_s in evaluating $G_E(h)$.

The form of $G_j(h)$ $[G_j h = G_a(h) + G_E(h)]$ (197) is illustrated schematically in Fig 70 for particles of diameter $\sim 1\mu$mm and three different (1:1) electrolyte concentrations. At 10^{-5} and 10^{-3} mol dm^{-3}, a maximum exists (G max); at all three electrolyte concentrations a primary minimum (G^1 min) exists, corresponding to close contact (coagulation); at 10^{-3} mole dm^{-3} (but not at either of the other concentrations) a secondary minimum, G^1 min exists but it depends critically on a (only being signigicant for large particles) and Cb.

Thus for Cb $\sim 10^{-5}$ mol dm^{-3} the dispersion will be kinetically stable; G max is sufficiently high that virtually no collisions lead to coalgulation since in effect there is a net repulsion between the particles. For Cb $\sim 10^{-1}$ mol dm^{-3} there is no energy barrier to coagulation, there is a net strong attraction between the particles and coalgulation is essentially irreversible.

The kinetics are second order.

$$d\,Ni/dt = -\vec{K} \sum_{j=1}^{x} N_1 N_j \simeq -\vec{K} N_1^2 \quad (198)$$
$$(t \to 0)$$

Where $\vec{K}$ is the coagulation rate constant and $N_i(t)$ is the number of singlet particles at time t and

$N_j(t)$ the number of j - mers.

In order to evaluate K it is necessary to know both the hydrodynamic interactions (between the particles and the molecules comprising the continuous phase) and the interparticle interactions.

For $C_b \sim 10^{-3}$ mol dm^{-3} even at low particle volume fractions, the situation is complicated by the presence of the secondary minimum; this leads to a weak reversible flocculation.

The kinetics is now much more complex since the deflocculation has to be taken into account. The free energy of aggregation ΔG_{agg} is given by:

$$\Delta G_{agg} = \Delta G_i - T \Delta S^{config} \qquad (199)$$

Where ΔG_i is a function of G min and ΔS^{config} is a configurational entropy term associated with the loss in translational degrees of freedom of the particles.

ΔS^{config} is a function of the particle volume fraction ϕ (decreasing with increasing ϕ).

For primary minimum (strong) aggregation, G' min is so large that $|\Delta G_i| \gg |T \Delta S^{config}|$ and ΔG_{agg} is negative at effectively all ϕ.

For secondary minimum flocculation, however G min is small and at low ϕ it is possible that $T \Delta S^{config} > \Delta G_i$, so that the dispersion is thermodynamically stable.

In establishing the form of the particle curves the long range forces include the Van der Waals interaction and the electrical double layer interaction.

At very small separations ($h < 2$ nM) short range interactions may have to be considered (ie in addition to the Born repulsion at contact separation).

These short range contributions are important in aqueous systems: they may be repulsive or attractive depending on the nature of the particle surface.

These forces are due to the displacement into bulk solution of the water molecules from the vicinity of the solid interfaces as two particles come into contact.

With hydrophilic surfaces there is a net increase in free energy of the water molecules as a result of this displacement process (this is due to the ordered water structure near the surface being broken down).

This leads to a short range repulsion force which may be sufficient to prevent hydrophilic particles coagulating into a deep minimum. With hydrophobic particles this short range interaction contributes a net attraction over and above the dispersion force, and this leads to a deepening of the primary minimum. This arises because the water molecules displaced into bulk solution now decrease their free energy. (In bulk solution there is more opportunity for H bonding)

Steric Stabilisation

In this case an adsorbed layer of polymer molecules surrounds the particles.

The situation is shown schematically in Fig 71 (for neutral particles).

The Van der Waals term G_A is now characterised by three Hamaker constants, appropriate to the three regions shown in Fig 71 but in many practical cases $A_3 \sim A_2$.

When $(h < 2\delta)$, the steric interaction Gs (h) is important. The form of this interaction is complex and still the subject for much debate in the literature (146, 147, 148).

For two spherical particles, stabilised by terminally anchored chains, Nappier (147) derived a complex expression for Gs (h)

$$Gs(h) = \frac{2\pi a K T V_s^2 n^2 \Gamma^2}{V_1} (\tfrac{1}{2} - \chi) S_{mix} - 2\pi a K T \Gamma S_{el} \qquad (200)$$

The first term on the (r h s) of this equation refers to the mixing of polymer segments and solvent molecules in the overlap zone ($h < 2\delta$). The second term refers to the elastic compression of polymer molecules and is thought by Vincent to be significant for $(h < 2\delta)$.

Vs and V_1 are the volumes of the segments and solvent molecule, n is the number of segments per polymer chain, χ is the Flory interaction parameter:

Γ is the number of chains per unit area of surface. S mix and S el are essentially geometric terms which depend on the choice of segment distribution normal to the surface in the adsorbed layer (148, 149).

In low levels of interaction ($\delta < h < 2\delta$) only the mixing term is important, and this depends on Γ^2 and $(\frac{1}{2} - \chi)$.

The function form of Gi (h) = $G_{A(h)}$ + G (h) is shown in Fig 72, it can be seen that this curve is characterised by a single minimum.

For high Γ and ($\chi < \frac{1}{2}$) the value of G min is effectively the value of G_A at $h = 2\delta$. For a given system, therefore, G min is most effectively controlled by varying the molecular weight of the stabilising chains. IF $\chi > \frac{1}{2}$ (Θ conditions are exceeded) there is a significant deepening of the interaction free energy minimum, G min.

The term coagulation/agglomeration is used when it is clear that the particle association process is occuring under the primary maximum conditions, while the term flocculation is used to describe secondary minimum association. Thus coagulation gives a compact aggregate structure while flocculation produces a more open structure.

8.3 DEVELOPMENT OF AN EXPERIMENTAL MODEL

8.3.1 THE NUCLEATION AND GROWTH OF PRIMARY PARTICLES

It is considered that during the polymerisation process oligomeric free radicals are developed by reaction between monomer and primary free radicals in the same manner as in emulsifier containing polymerisation. However, while the Harkins theory (107) gives a clear

picture of nucleation and growth of latex particles in the presence of emulsifier micelles, the corresponding mechanism of nucleation in their absence is still largely unknown but several mechanisms have been proposed:-

(a) That the growing free radical in solution becomes insoluble and precipitate out upon themselves.

(b) That the growing free radical undergoes termination followed by particle nucleation through coagulation of these dead species.

(c) That the growing free radicals achieve a size and concentration at which they become surface active.

It is unlikely that any one of these mechanisms alone would describe particle nucleation for all monomers since the solubility of the monomer and its hydrophobicity would be expected to have a large effect on what is, in the initial stages, a process occurring in solution.

The presence of a poor stabiliser - polyvinyl alcohol will tend to improve the stability of the particles after nucleation.

Fitch and Coworkers (150, 151) have studied the emulsifier free polymerisation of the relatively water soluble monomer methyl methacrylate and consider that the reaction proceeds via mechanism (a) above ie homogenous nucleation. However, in the case of the insoluble monomer styrene, evidence has been presented (152,153,154), that a micellar type nucleation occurs .

In the present investigation, it has been shown that the reaction proceeds via an aqueous intermediate stage (dye experiment), and from the work carried out on reaction rates it can be seen that the reaction curves can be broken down into three sections. Initially the opacity did not increase, the duration of this period being 15-10 minutes. After this period it rose rapidly (interval B) for about 35 minutes, and this was followed by a much slower increase in opacity (interval C). (Fig 73)

INTERVAL A

It is proposed that this interval is attributable to an induction period in the reaction during which time the concentration of trace impurities (free radical scavengers) decreases.

However, the actual formation of any particle nuclei was probably undetected due to their very small size.

INTERVAL B

This period of rapid increase in opacity is attributable both to growth by polymer formation and subsequent monomer inbibition and to particle agglomeration. In the case of a homogeneous nucleation process, it is likely that the initial nuclei would be unstable due to their low surface charge density and flocculation followed by coalescence would occur. In the case of a micellar type mechanism, the initial nuclei would be much more stable owing to a high surface charge density,

but would become unstable through growth by further polymerisation and imbibition of monomer. As the particles continued to form, a point of colloidal instability occurs which is followed by flocculation and coalescence.

This process of stabilisation by flocculation and particle - particle coalescence can continue as long as the polyvinyl alcohol is adsorped onto the particle surface.

The rapid rise in opacity is attributed to both particle agglomeration and polymer formation. Throughout this period, both monomer and initiator pass into the aqueous phase by mass transfer.

INTERVAL C

During this interval slow agglomeration was still occurring but at a much reduced rate compared to interval B.

It is probable that the rate of growth of the polymer particles was governed by the supply of monomer which had to diffuse from the monomer layer.

This would have the effect of reducing the rate of polymer swelling and subsequently the degree of coagulation of the particles.

8.3.2 THE EFFECT OF AGITATOR SPEED ON THE PRIMARY PARTICLE SIZE

Consider the primary particle size obtained from identical formulation, but which were stirred at different

rates (Table 42). The very slow agitator speed (200 rmp) gave a much more polydisperse system compared to the 400 rpm and 600 rpm rates.

This explanation may be attributable to monomer starvation caused by the delay in monomer diffusing from the organic phase.

This is due to the reduced interfacial area of the monomer droplets.

Support for this explanation comes from the work of Munro Et Al (155).

They found that unstirred nucleation in water (emulsifier free) gave particle sizes which were very disperse.

This was in marked contrast to the mono disperse nature of a stirred reaction at a similar initiator concentration and also to a reaction employing monomer saturated water.

8.3.3 THE AGGLOMERATION OF PRIMARY POLYMER PARTICLES FOLLOWING HOMOGENEOUS PARTICLE NUCLEATION

It is considered that during the polymerisation process oligomeric free radicals are formed by reaction between monomer molecules and primary free radicals.

Both the monomer and the initiator have been shown to pass from the dispersed phase to the continuous phase by mass transfer.

The aqueous phase is considered to be fairly saturated with both monomer and initiator, except in the later stages of reaction.

Particle nucleation takes place via a homogeneous nucleation mechanism. The primary particles formed will start to coagulate with others, their actual stability depending on their surface charge, their size and the concentration of any protective colloid present. When the primary particles agglomerate the surface area will decrease, and the protective colloid molecules will become more effective.

When the agglomerates become sufficiently large they will have enough groups on the surface to prevent further agglomeration. This process is termed limited coagulation or agglomeration.

The primary particles produced were generally found to be polydisperse (0.08 - 0.15μm). This is to be expected from consideration of the Hansen and Ugalstad Model for homogeneous nucleation.

The present investigations support the concept of an equilibrium agglomerate size, since the bonding energy measured in agglomerates produced in the presence of different protective colloid levels remained constant, while the agglomerate size depended on the actual concentration of the polyvinyl alcohol used.

The physical stability of particulate suspensions was discussed in some detail in section 8.2.1. The stability against agglomeration is usually achieved by the use of dispersing agents, eg surface active agents of the ionic or non ionic type, macromolecules or

polyelectrolytes. These dispersing agents must be strongly adsorbed onto the particle surface and fully cover them. With ionic surfactants irreversible agglomeration is prevented by the repulsive force generated from the presence of an electrical double layer at the particle/solution interface. Depending on the conditions this repulsive force can be made sufficiently large to overcome the Van der Waals attraction between the particles. With non ionic surfactants and macromolecules such as polyvinyl alcohol, repulsion between particles is ensured by the steric interactions of the adsorbed layers on the particle surface. With polyelectrolytes both electrostatic and steric forces exist.

Figure 74 shows the various energy distance curves obtained with the three types of stabilisation mechanisms, namely electrostatic, steric and the combined case.

For systems stabilised by adsorbed non ionic surface active agents and macromolecules (polyvinyl alcohol is in this class) the energy of interaction distance curve shows a minimum, the depth of which depends on the adsorbed layer thickness, the particle size, and the Hamaker constant.

This type of stabilisation was observed in the present investigations, where the agglomerate size depended on the polyvinyl alcohol concentration. Further evidence is provided by Tadros (156). He showed that the

energy of interaction curves for polystyrene particles (containing adsorbed polyvinyl alcohol) showed a V min which depends on the molecular weight grade used (Fig 75).

The different molecular weight materials produced changes in the adsorbed layer thickness. Short range interactions are also important in the case of a hydrophobic particles like styrene. These forces contribute a net attraction and leads to deepening of the primary minimum. Methyl methacrylate which is a much more hydrophilic polymer did not show spherical agglomeration as did styrene, this is due to short range repulsion forces preventing the more hydrophilic particles coagulating into a deep minimum. The agglomeration process for polystyrene particles has been shown to be a relatively slow process, the diffusion of particles in the agitator force field producing uniform spherical agglomerates.

In contrast the reaction rate of a system containing a difunctional monomer is fast, with the production of polymer particles having a cross linked structure. A characteristic of this type of reaction was the formation of fibre agglomerates, and not spherical agglomerates from the primary particles.

The mechanism for the formation of such agglomerates is unknown, but probably depends on the presence of a pressure wave at the surface of the stirrer blade. It is in such a pressure wave that a linear contact of highly reactive polymer particles would occur. Such a

chain of particles would grow until turbulence and buffeting breaks down the structure to a length determined by the forces present. The bonding energy of the fibre agglomerate particles was measured and found to be much smaller than that observed with spherical agglomeration.

The low bonding energy suggests that the agglomerate is produced as the result of a weak and possibly reversible flocculation process.

With a sterically stabilised dispersion this would mean an adsorbed layer which is not thick and a minimum in the potential energy distance curve which is not deep enough for complete stability. However the type of stabilisation mechanism is unknown in the presence of the difunctional monomer, and the agglomerated product could be electrostatically stabilised, and the result of a secondary minimum in the system.

8.4 CONCLUSION

The important conclusions from this analysis are:

(1) Both monomer and initiator pass into the aqueous phase by mass transfer where homogeneous particle nucleation of the monomer occurs.

(2) Particle destabilisation occurs which is followed by the coalescence and agglomeration of the polymer particles.

(3) The size of the spherical agglomerates produced are a function of the protective colloid concentration (polyvinyl alcohol).

(4) The bonding energy between particles in the agglomerates is independent of the protective colloid concentration and is of the order 0.30×10^{-10} dynes per pair. This suggests that the polyvinyl alcohol is only found on the surface of the agglomerate.

(5) Under high shear conditions the agglomeration process is reversible (cone and plate viscometer data).

(6) The agglomeration process in the presence of a protective colloid can be explained in terms of particle stabilisation theory.

(7) In the presence of difunctional monomers, fibrous agglomerates are produced. The bonding energy between particles is lower than that found in spherical agglomerates and is of the order 0.20×10^{-12} dynes/ particle pair.

REFERENCES

NO

(1) W P Hopenstein and H F Mark J Polymer Sci 1, 127 (1946).

(2) G Talamini. J Polymer Sci, 535 (1966).

(3) T Alfrey Jr, and C C Price. J Polymer Sci 2, 101 (1947).

(4) L P Hammett, 1 bid, 59 95 (1937); L P Hammett, Physical Organic Chemistry, McGraw Hill Book, New York (1940).

(5) D J Donahue and F E Bartell, J Phys, Chem 56 480 (1952).

(6) C O Timmons and W Zisman, J Colloid and Interfac Sci, 28, 106 (1968).

(7) K Shinoda, Surface Science Series Vol II, New York 1967 Chap 1 (Solvent props of surfactant solutions).

(8) F Van Voorst Vader. Trans Faraday Soc 56, 1067 (1960).

(9) T R Paxton, J Colloid Interfac Sci 31, 19 (1969).

(10) V I Yeliseyava, Acta, Chim (Budapest) 71, 465 (1972).

(11) A V Zuikov and A Vasilenko, Colloid J USSR 37,4 640, (1975).

(12) N Sutterlin, H Kurth and G Markert, Makronol Chem 177, 1549 (1976).

(13) V Yeliseyeva and A Zurkov. Emulsion Polymerisation ACS Symposium Series 24. Pirma and Gordon P. 62 (1976).

(14) D Gershberg A 1 ch E I Chem E Symp Ser 3, 4 (1965).

(15) R M Fitch, Off Dig, Fed Soc Paint Technol 37, 32 (1965).

(16) C P Roe, Ind Eng Chem 60, 20 (1968).

(17) H J Warren. J Applied Polymer Sci 18 1693-1769 (1974).

(18) Breitenbach, J W and Rudorfer H,Mh Chem 70, 37 (1937).

(19) Schulz G V and Huseman E, 2 Phys, Chem B 34, 187 (1936).

(20) Matherson, M S J Chem Phys,13 584 (1945).

(21) Norrish, R G and Brookman E F. Proc. Roy Soc A 171, 147 (1939).

(22) Schulz G V and Harbarth G, Makromol Chem 1, 106 (1947).

(23) J Barington, Melville and Taylor. J Polym Sci 12, 449 (1954). 14, 463, (1954).

(24) Bamford CH and Jenkins AD. Nature Lon 176, 517 (1943).

(25) R Topping M Phil Thesis (Polytechnic of Wales).

(26) Vermeulon, Williams and Langbis, Chem, Eng Prog 51, 2 (1955)

(27) P E Rouse Jr, J Chem. Phys 21, 1272 (1953), 22, 1570 (1954).

(28) F Bueche, J Chem, Phys 22, 603 (1954).

(29) B H Zrm, G M Roe and L F Epstein, J Chem, Phys 24, 279 (1956).

(30) W L Petrcolas, J Chem, Phys 35, 2128 (1961).

(31) W L Petrcolas, J Poly Sci 58, 1405 (1962).

(32) W W Grassley, J Chem, Phys 43, 2696 (1965) 47, 1942 (1967).

(33) F Bueche and S W Harding, J Polym Sci 32, 177 (1958).

(34) E Menefree and W L Peticolas, J Chem, Phys 35 946, 951 (1961).

(35) B H Zimm and R W Kilb J Polym Sci 37, 19 (1956).

(36) W L Peticolas and J M Watkins, J Ameri Chem Soc 79, 5083 (1957).

(37) B H Zimm, J Chem Phys 24, 269 (1956).

NO

(38) J G Kirkwood and J Riseman, J Chem Phys 16 565 (1948).

(39) F Bueche, J Chem Phys 22, 1570 (1954).

(40) M C Williams, J Chem Phys 42 2988 (1965).

(41) P E Rouse Jr and K Sittle, J Apply Phys 24 690 (1953).

(42) J D Ferry, M L Williams, M Stern J Chem Phys 58 987 (1954).

(43) B Demallie, M H Birboam, Frederick, Ferry. J Phys Chem 66, 536 (1962).

(44) A S Lodge, Trans, Faraday Soc 52, 120 (1956).

(45) W W Grassley. J Chem Phys 54, 5143 (1971).

(46) T G Fox and P J Flory, J Ameri Chem Soc 70, 2384 (1948).

(47) T G Fox and P L Flory, J Phys Chem 21, 581 (1950).

(48) J Meissner, Pure Appl Chem 42, 553 (1975).

(49) S I Abdel-Khalik, O Hassager and R Bird, Polym Eng Sci 14, 859 (1974).

(50 M C Williams A 1 Ch EJ 12, 1064 (1966).

(51) M Cross J Appl Polymer Sci 13, 765 (1969).

(52) W R Johnson and C Price, J Polym Sci 45, 217 (1960)

(53) R E Harringtom and B H Zimm, J Phys Chem 69, 161, (1965).

(54) Nagashiro and T Tsunodra . Appl Poly Sci 21, 7149 (1977).

(55) H G Jellinek and G White, J Polym Sci 6, 745 (1951).

(56) Proc K AKad. Welensch, Amsterdam 21, 357, 386, (1919).

(57) Dorsey. J Washingtom Acad Sci 18, 505 (1928).

(58) Porter, Phil Mag 15, 163 (1933).

(59) Bashforth and Adams, Physics and Chemistry of Surfaces, N K Adam (3rd Edition) P365.

(60) Worthington 15 Phil Mag (1933)

(61) A Ferguson Phil Mag (1913).

(62) Rayleigh Proc Roy Soc 184 (1915).

(63) K J Rixon, PhD Thesis Polytechnic of Wales.

(64) Taylor, Proc Roy Soc (London), 146A 501 (1934).

(65) Snell, Ind Eng Chem 35, 107 (1943).

(66) Richardson, J Colloid Sci 51, 404 (1950).

(67) F H Winslow and W Matneyek, Ind Eng Chem 43, 1108 (1951).

(68) Park and Blair, Chem Eng Sci 30, 1057 (1975).

(69) P H Clay, Ned AKad, Van Witenskapen Proc 43, 852-865, 979-990 (1940).

(70) J O Hinze, Ibid, 1, 289 (1955).

(71) K Magnusson Chem and Proc Eng 35, 276 (1954).

(72) W A Rodger, V C Trice, J H Rushton, Chem Eng Progr, 52, 515 (1956).

(73) N Bohr, J A Wheeler, Phys Rev 56, 426 (1939).

(74) G I Taylor, Proc Roy Soc (London) A,138, 41 (1932).

(75) I bid, A 146, 501 (1934).

(76) S Tomotika. Ibid A 150, 323 (1935).

(77) 1 bid. A 153, 303 (1936).

(78) D V Smith, MSc thesis Univ of Manchester (1966)

(79) T Gillespie, EK Rideal. Trans Faraday Soc 52, 173 (1956).

(80) G V Jeffreys, G L Hawksley, J Applied Chem, 12 529 (1962).

(81) G V Jeffreys, G A Davies, Recent advances in liquid/liquid extraction.

(82) G V Jeffreys, G L Hawksley, A I Ch E 11 412 (1965).

(83) L E Neilson, R Wall, G Adams, J Coll Sci, 13, 441 (1958).

(84) S B Lang, PhD Thesis Univof California (1962).

(85) D V Derjaquin, A Titijersakaga, Discussion of Fara Soc, 18, 27 (1954).

(86) Second Int Congr of surface Activity Vol 1 Butterworth (1957).

(87) Van Der Temp, J Coll Sci 13, 125 (1958).

(88) D H MacKay, S G Mason, J Chem Eng 41, 203 (1963).

(89) H Falkenhagen and M Dole, M Phys Z, 30 611 (1921)

(90) H Falkenhagen and E Vernon, 1 bid 33, 140 (1932)

(91) F H Winslow and W Matreyek, Ind Eng, chem 43 1108 (1951)

(92) F H Winslow and W Matreyek, Ind Eng Chem 43, 1108 (1951).

(93) H Hopff, H Luessi, P Gerspacher, Mackromol Chem 78, 24 (1964) 78, 37 (1964).

(94) H Hopff, H Luessi, E Hammer, Mackromol Chem 82, 175 (1961), 82, 184 (1965) 84, 282 (1965) 84, 274 (1965) 84, 286 (1965).

(95) Shinnor and Church, Ind Eng Chem 53, 479 (1960) 52, 253 (1960).

(96) D M Sullivan, E E Lindsey, Ind Eng Chem Fundamentals 1, 87 (1962).

(97) Melsner and Otto.

(98) B P Vijayendran, J A Polymer Sci Vol 23, 733-742 (1979).

(99) V Yeliseyeva and A Zuikov, Emulsion polymerisation ACS, Symposiuns Series 24. 1 Pirrma, L Gordon P 62 (1976).

(100) D Gershberg, A 1 Ch E-1, Chem E Sym Ser 3,4 (1965)

(101) T R Paxton, J Colloid Interfac Sci 31, 19 (1969).

(102) S Davies, T Higuchi, J Rytting, J Pharm Pharmacol, 24 (Suppl), 30 P (1972).

(103) F Van Voorst Vader, Trans, Faraday Soc 56, 1067 (1960).

(104) J T Davies, K Rideal, Interfacial Phenomena, Academic Press, New York Chap 4 (1963).

(105) S Wu J Macromol Sci-Rev Macromol Chem C10, 1 (1974).

(106) Fikertscher, H Germens, H P Schuller Angrew Chem 72, 856 (1960).

(107) W D Harkins J Chem Phys 13, 381 (1945).

(108). W D Harkins J Chem Phys 14, 47 (1946).

(109) W D Harkins J Am Chem Soc 69, 1428 (1947).

(110) W V Smith and R H Ewart, J Chem Phys 16, 592 (1948).

(111) L P Roe, Ind Eng Chem, 60, 21 (1968).

(112) Van der Hoff, BME J Polym Sci 44, 241 (1960).

(113) Dunn A S and Taylor P A, Makromol Chem 83, 207 (1965).

(114) B V Deryaquin, L D Landam Acta Phys-chem, URSS 14, 633 (1941), E J Verwey and J T Overbeek (Theory of the stability of lyophobic colloids Amsterdam, Eksvier)(1948).

(115) Review by J Ugelstad, Ellingsen and Kaggerad. Institute of industrial chemistry. Univ of Trondeum Norway.

(116) W J Priest, J Phys Chem 56, 1077 (1952).

(117) R M Fitch, B Preprosil, K J Sprick, J Polym Sci C 27, 95 (1969).

(118) R M Fitch, C H Tsai, Polymer Colloids, M Fitch ed, Plenum, New York P 73 (1971).

(119) F K Hansen and J Ugelstad J Polym Sci 16 1953-1959 (1978).

(120) H C Hamaker, Physica 4, 1058 (1937).

(121) R Hogg, T W Hearly, W Fuerstenan,Trans Faraday Soc 62, 1638 (1966).

(122) W K Asbeck Journal of Coating Technology 49, 635 (1977).

(123) N Casson Rheology of Disperse Systems, Mill C C Edition Perganeon. Press New York pp 84-164 (1959).

(124) R Naito, J Ukida and T Koninarii, Kobunski Kagaku 14, 117, (1957) (CA 52, 1676, 1958).

(125) R Naito, Kobunski Kagaku 15, 191, 195 (1958) (CA 54, 2886, 1960).

(126) National Distiller Brit Pat 976, 613 (1964).

(127) Forbenfabriken Bayer Brit Pat 981, 987 (1965).

(128) S Hayashi, C Nakano and T Motoyama Kobunski Kagaku 21, 300 (1964) (CA 62 9249 (1965)).

(129) S Hayashi, C Nakano, T Motoyanii, Kobunski, Kagaku, 21, 304, 1964 (CA 62 9205 1965).

(130) C Capitani, G pirrone XXX11 e Congres Intem de Chemie Industrielle Compte Rendu, Bruxelles Vol 31, 685 (1955).

(131) M Shirashi Brit Polym J,2,135,(1970).

(132) E V Gromov Kolloid 2h,29 484 (1967).

(133) E V Gromov Kolloid 2h 30 508 (1968).

(134) A Abramzon E V Gromov Kolloid 2h 31 795 (1969).

(135) G A Johnson and K E Lewis Brit Polym J 1, 266 (1969).

(136) Sh Fujishige, J Colloid Sci 13, 193 (1958).

(137) S Peters and H Fasbender, Rheol Acta 3 92 (1963).

(138) S Peters and H Fasbender, Kolloid 2 2 Polym 188 14 (1963).

(139) G Lanveld and J Lyklema. Compte-rend V. Congress Intem Retergence, Barcelonia Vol 2 (1968).

(140) S Hayashi, Ch Nakano, T Moloyani CA 63, 19476 h (1965).

(141) E W Fischer, Kolloid 2, 160 120 (1958).

(142) S Hayashi, Nakano, Motoyami CA 62, 9249 (1965).

(143) Motoyami, Yamamoto, S Okamuri, Kobunski, Kagaku 10, 108 (1953).

(144) Schuller IIIrd, Int Cong Serf (Cologne 1960), Vol 4.

(145) B Vincent, Chemistry and Industry, March (1980)

(146) B Vincent, Adv Colloid Interface Sci, 4 193, (1974)

(147) D H Napper, J Colloid Interface Sci, 58, 390 (1977)

(148) B Vincent and S Whittington, Surface and Colloid Science, E Matijevie (Ed) New York Plenum

(149) D J Harding, J Colloid Interface Sci 35, 172, (1971).

(150) R M Fitch, Polymer Colloid Preprints Nato advanced Study Institute, Tronaheim (1975).

(151) R Watson, R M Fitch, D Baker Polym Preprints, 16 109 (1975).

(152) A R Goodhall, A Wilkinson, J Hearn, J Polym Sci 15, 2193 (1977).

(153) R Cox, A Wilkinson, A Goodhall, J Hearn, J Creasley. J Polym Sci 15, 2311 (1977).

(154) B M Vanderhoff, Advances in Chemistry No 34 P6, ACS publication Washington DC (1962).

(155) D Munro, J Colloid Interface Sci, 68 1 (1979).

(156) T F Tadros, Chemistry and Industry, March (1980).

NOMENCLATURE

A	Haymaker constant (eq 174)
A_1, A_2	Hamaker constants (eq 194)
A_2, A_3	2nd and 3rd viral coefficient (eq 26)
Ac	Coefficient (eq 27)
A	Interfacial area (eq 192)
Am	Area per molecule of surfactant (eq 152)
A	Constant (eq 134)
A_1, A_2	Constant (eq 118)
B	Capillary constant (eq 104)
B	Constant (eq 143)
B_1	Number for shear degradation (eq 100)
Bc^2	Coefficient (eq 27)
C	Overall degree of conversion (eq 14)
C	Concentration term (eq 23)
C	Constant (eq 43)
C	Concentration of junctions (eq 58)
C	Concentration (eq 99)
C	Concentration (moles per litre) (eq 118)
C	Constant (eq 143)
C	% volume fraction of monodisperse particles (eq 185)
C	Concentration gradient (eq 192)
Cr	Solubility (droplet radius r) (eq 155)
$C\infty$	Solubility (droplet infinite radius (eq 156)
CPVC	Critical Pigment Volume Concentration

D	Shear rate constant (eq 82)
D	Shear rate (eq 89)
D	Velocity gradient (eq 79)
D	Density of denser phase (eq 105)
D	Diffusion coefficient (eq 157)
D	Diamter of agglomerated particle (eq 178)
Dw	Mean diffusion constant of oligomers (eq 164)
Dpq	Diffusion constant (eq 165)
$\bar{D}$	Vessel diameter (eq 133)
Ek	Kinetic energy
E max	Average max possible energy input (eq 135)
Fp	Reduction faction (eq 164)
FA	Force of attraction per unit area (eq 179)
Fa	Average force of attraction between a pair of particles (eq 179)
$f_1(h)$	Interparticle force (eq 193)
$G_1(h)$	Interaction free energy (eq 193)
G_e	Electrostatic repulsion free energy (eq 196)
$\triangle G_{agg}$	Free energy of aggregation (eq 199)
h	Drop section (eq 104)
ho	Capillary elevation (eq 104)
ho	Mass transfer coefficient (eq 192)
I	Initiator molecule (eq 1)
I	Initiator concentration (eq 158)
(I)	Initiator concentration (eq 13)
Ka	Specific reaction rate (eq 1)
Kd	Specific Reaction rate (eq 2)

K_p	Specific reaction rate (eq 3)
Ktc	Specific reaction rate (eq 7)
Ktd	Specific rate (eq 8)
K	Rate constant (eq 14)
K_1	Precipitated phase rate constant (eq 15)
K_2	Precipitated phase rate constant (eq 16)
K_3	Precipitated phase rate constant (eq 17)
K_4	Precipitated phase rate constant (eq 18)
K_{12}	Rate constant for copolymerisation (eq 19)
K	Constant (eq 67)
K	Consistency coefficient (eq 78)
K	Constant for power law model (eq 125)
K_1	Constant for power law model (eq 134)
K_2	Constant for power law model (eq 135)
K	Baltzmans constant (eq 143)
K	Constant (eq 158)
K^1	Constant (eq 151)
K^{11}	Constant (eq 151)
Kcj	Capture constant (eq 158)
Kcp	Capture rate constant (eq 158)
Ktw	Termination constant (eq 158)
Kfpq	Coagulation rate constant (eq162)
K_f	Propagation rate constant (eq 154)
Lv	Latent heat of vaporisation (eq 23)
Lo	Particle size (eq 133)
L	Avogadros No (eq 154)
L	Stirrer diameter

$\bar{Mn}$	Number average molecular weight (eq 23)
Mc	Critical molecular weight (eq 67)
M	Molecular weight (eq 67)
M	Average molecular weight (eq 92)
M	Molecular concentration of monomer (eq 154)
Mw	Number of moles (monomer) in aqueous phase (eq 158)
(M)	Monomer concentration (eq 13)
N	Stirrer speed (eq 43)
N	Number of polymer segments (eq 50)
Nw	Viscosity of protective colloid solution (eq 133)
N	Number of latex particles per unit volume (eq 158)
N_1	Number of precipitated primary radicals (eq 158)
N_s	Particles of class s (eq 162)
Nj(t)	Number of singlet particles (eq 163)
N	Number of latex particles per unit volume (eq 154)
P_1	General reactivity of radical (eq 19)
P_1	Limiting degree of polymerisation (eq 100)
P_1	Limiting degree of polymerisation (eq 100)
Pr	Initial degree of polymerisation (eq 102)
Pi	Rate of radical formation from initiator (eq 158)
PVA	Polyvinyl alcohol
Q_2	Reactivity of the monomer (eq 19)
R	Free radical (eq 1)
Rp	Rate of polymerisation (eq13)

Re	Reynold's number
R	Gas constant (eq 23)
R	Apparent viscosity (eq 75)
R	Radius of Cone (cm) (eq 81)
R_1	First radius of curvature (eq 104)
Rp	Propagation rate constant (eq 154)
R_1	Number of initiator radicals (eq 159)
Rtot	Total number of growing radicals (eq 159)
Rj	Oligomeric radicals of chain lengin j (eq 159)
Rcj	Capture constant (eq 159)
$(S2)^{\frac{1}{2}}$	Radius of gyration (p 21)
S	Indicated scale value (eq 91)
S	Emulsifier concentration (eq 158)
S mix	Geometric term (eq 200)
S el	Geometric term (eq 200)
ΔS^{config}	Configurational entropy term (eq 199)
T	Temperature ° (eq 25)
T	Torgue spring constant (eq 81)
ΔTb	Elevation in boiling point
ΔTf	Lowering in freezing point
Ua	Apparent viscosity (eq 75)
U	Viscosity (eq 76)
Urel	Relative viscosity (eq 118)
Uc	Viscosity of continuous phase (eq 115)
Ud	Viscosity of dispersed phase (eq 115)
U	Fluctuating component of velocity (eq 115)
Ur	Rheological packing factor (eq 185)

V_1	Rate of initiation (eq 9)
Vt	Rate of termination (eq 10)
Vm	Molar volume of monomer (156)
Vtpq	Total potential energy of interaction (eq 173)
Vtpq	Sum of attractive/repulsive energy (eq 173)
Vs	Volume of polymer segment (eq200)
V_1	Volume of solvent molecule (eq 200)
We	Weber number
(W)	Frequency of oscillation (eq 49)
Wpq	Fuchs stability ratio (eq 171)
W	Mass transfer rate (eq192)
X^p	Polarity (eq 144)
X^d	Non polar contribution to surface tension (eq 144)
Y	Surface tension (eq 105)
Y_{12}	Total excess free energy (103)
Y_1^1	Residual excess surface free energy (eq 103)
Y_2^2	Residual excess surface free energy (eq 103)
γ_1	Surface tension of water phase (eq 144)
γ_2	Surface tension of polymer phase (eq 144)
γ_1^d	Dispersion contribution to water surface tension
γ_2^d	Dispersion contribution to polymer surface tension
γ_1^p	Polar contribution to water surface tension
γ_2^2	Polar contribution to polymer surface tension
$\dot{\gamma}$	Shear rate (eq 53)

a^1	Constant (eq 133)
b^1	Constant (eq 133)
cm	Centimetre 10^{-2} metre
d	Density (105)
do	Density (eq 105)
d	Particle diameter
d min	Particle diameter (eq 134)
e	Electronic charge (eq 195)
e_1	Constant (eq 19)
e_2	Constant (eq 19)
f	fraction of radicals which successfully initiate chains (eq 9)
g	Gravity constant
n	Viscosity
q	Ratio of the rate of polymerisation)
r	Drop section
r	Radius (eq 104)
r_1	Monomer reactivity ratio (eq 15)
r_2	Monomer reactivity ratio (eq 16)
n	Saturated adsorption of surfactant (eq 143)
n	Number of segments per polymer chain
na, nb	Number of droplets (eq 157)
n	Exponent for power law fluid model (eq 125)
n	revs per min of agitator (eq 133)
n	test speed (eq 91)
$r_{11} - r_{22}$	normal stress difference (eq 55)
$(\bar{r}^2)^2$	Root mean square end to end distance P 21.
rp	Class radius (eq 164)

t	time (solution) (eq 93)
to	time (solvent) (eq 93)
no	zero shear viscosity (eq 48)
ns	viscosity of solvent.(eq 48)
nA	contribution to viscosity caused by agglomerate break up (eq 181)
$n_\infty^{\frac{1}{2}}$	viscosity at infinity shear rate (eq 189)
no	Newtonian viscosity of carrier liquid (eq 185)
n(w)	Complex viscosity (eq 49)
$n^1(w)$	Dynamic viscosity component (eq 49)
$n^{11}(w)$	Dynamic viscosity component (eq 49)
n	Measured viscosity (eq 91)
nr	relative viscosity (eq 93)
n sr	specific viscosity (eq 94)
n red	reduced viscosity (eq 95)
(n)	intrinsic viscosity (eq 96)
ψ	surface potential (eq 174)
ϕc	function of particle concentration (eq 178)
r	shape factor (eq 185)
ε	di electric constant (eq 195)
χ	flory interaction parameter (eq 200)
Γ	number of chains per unit area (eq 200)
δ	thickness of adsorbed layer (p 217)
6	interfacial tension
T_1	Bueche time constant (eq 53)
Ω	Angular velocity (eq 82)

ψ Cone angle (eq 82)

α constant (eq 92)

LIST OF TABLES

LIST OF FIGURES

Figure	LIST OF FIGURES	Page No
16	Plot of shear stress against shear rate of solutions 1-3. Coaxial cylinder data.	331
17	Plot of poise/10 against log shear rate (coaxial cylinder data). (Solutions 1-3.)	332
18	Log of poise/10 against log shear rate. Solution 1 + monomer (coaxial cylinder data).	333
19	Plot of poise/10 against log shear rate. Solution 2 + monomer (coaxial cylinder data).	334
20	Plot of poise/10 against log shear rate. Solution 3 + monomer (coaxial cylinder data).	335
21	Plot of shear stress against shear rate (at various salt levels).	336
22	Plot of $\frac{t - to}{toC}$ against concentration (C).	337
23	Plot of $\frac{t - to}{toC}$ against concentration (C).	338
24	Apparatus for sessile drop measurement.	339
25	The sessile drop method.	340
26	Correction curve $\triangle / \frac{h^2}{r^2}$.	340
27	Plot of interfacial tension against colloid concentration.	341
28	Plot of log interfacial tension against log colloid concentration.	342
29	Plot of interfacial tension against salt concentration.	343
30	Schematic diagram of states of dispersion in suspension polymerisation.	344
31	The effect of inorganic salts upon bubble surface area.	345

Figure	LIST OF FIGURES	Page No
32	Correlation between individual ionic values of the A_2 coefficient and the observed coalescence time for 1-1 electrolyte and methyl methacrylate monomer.	346
33	Plot of surface area against ionic strength (gas bubbles).	347
34	Apparatus for the production of suspension polymers.	348
35	Plot of log particle size against log stirrer speed (vol fraction Θ = 0.2).	349
36	Plot of log particle size against log stirrer speed (vol fraction Θ =0.3).	350
37	Plot of particle size against monomer volume fraction.	351
38	Plot of salt level against particle size.	352
39	Plot of log particle size against log interfacial tension.	353
40	Plot of Reynold's number against colloid concentration.	354
41	Plot of log Reynold's number against log particle size (different viscometers).	355
42	Plot of Reynold's number against log particle size. (All monomer systems).	356
43	Plot of $-\Delta GCH_2$ against interfacial tension.	357
44	Plot of interfacial tension against polarity.	358
45	Plot of log polarity against log particle size.	359
46	Variation of rate dRp/dt, and surface tension with conversion in a emulsion polymerisation.	360

Figure	LIST OF FIGURES	Page No
47	Contour Map of Fuchs stability ratio as a function of class index.	360
48	Particle class distribution after different reaction times.	361
49	The surfactant molecule.	361
50	Particles and dispersing molecules.	362
51	Particles with an insufficient number of dispersing molecules.	362
52	Agglomerated particle suspended in unit shear field.	363
53	Water solubility against degree of hydrolysis (for polyvinyl alcohol).	364
54	Water solubility against temperature for polyvinyl alcohol.	364
55	Plot of viscosity against concentration for polyvinyl alcohol.	365
56	Apparent activation energy of flow En against concentration.	366
57	Surface tension of aqueous solutions of partly hydrolysed PVA.	366
58	Plot of opacity number against time.	367
59	(SEM) (Spherical agglomerates).	368
60	(SEM) The surface of a spherical agglomerate.	368
61	(SEM) The interior of a spherical agglomerate.	369
62	Plot $\sqrt{\text{poise}}$ against $1/\nu^{\frac{1}{2}}$ for spherical agglomerates and PVA solutions.	370
63	Plot of $Na^{\frac{1}{2}}$ against $1/\nu^{\frac{1}{2}}$ for spherical agglomerates and PVA solutions.	371
64	Plot of colloid concentration and agglomerates d/D data.	372
65	(SEM) The fibre agglomerate.	373

Figure	LIST OF FIGURES	Page No
66	(SEM) The surface of a fibre agglomerate.	373
67	Plot of $\sqrt{\text{poise}}$ against $1/\dot{\gamma}^{\frac{1}{2}}$ (fibre agglomerate).	374
68	Plot of $Na^{\frac{1}{2}}$ against $1/\dot{\gamma}^{\frac{1}{2}}$ (fibre agglomerate).	375
69	Interactions between charged particles.	376
70	Functional form of G1(h) for aqueous suspension of charge stabilised particles.	376
71	Steric interactions between polymer covered particles.	377
72	Functional form of G1(h) for a sterically stabilised suspension.	377
73	Plot of opacity against time.	378
74	Total energy distance curves for 3 different stabilisation mechanisms.	378
75	Total potential energy of interaction versus separation for polystyrene latex with adsorbed layers of PVA of various thicknesses.	379

TABLE 1

Rheological Data
Cone and Plate Viscometer

Solution 1 - 0.50% Polyacrylamide Solution (75°C)

Speed	Reading	Cone Constant	Range	Viscosity (Poise)	Poise / 10	Log Poise / 10	Shear Rate Constant	Shear Rate (Sec^{-1})	Log Shear Rate	$\frac{3I}{2\Pi R^3}$	Shear Stress dynes/cm^2
100	4.5	1.2051	X1	0.0542	.00542	-2.2657	17.59	1759	3.2452	22.3	101.25
200	7.0	1.2051	X1	0.04218	.004218	-2.3749	17.59	3518	3.5462	22.3	156.10
300	9.5	1.2051	X1	0.03816	.003816	-2.4184	17.59	5277	3.7224	22.3	211.85
400	12.5	1.2051	X1	0.03766	.003766	-2.4241	17.59	7036	3.8473	22.3	278.75
500	15.5	1.2051	X1	0.03736	.003736	-2.4276	17.59	8795	3.9442	22.3	345.65
600	18.0	1.2051	X1	0.03615	.003615	-2.4419	17.59	10554	4.0234	22.3	401.40
700	20.5	1.2051	X1	0.03529	.003529	-2.4523	17.59	15750	4.1972	22.3	457.15
800	22.5	1.2051	X1	0.03389	.003389	-2.4698	17.59	19600	4.2922	22.3	501.75
900	23.5	1.2051	X1	0.03146	.003146	-2.5023	17.59	23850	4.3775	22.3	524.05
1000	25.0	1.2051	X1	0.03012	.003012	-2.5210	17.59	28500	4.4548	22.3	557.50

TABLE 2

Rheological Data
Cone and Plate Viscometer

Solution 2 - 1.0% Polyacrylamide Solution (75°C)

Speed	Reading	Cone Constant	Range	Viscosity (Poise)	$\frac{\text{Poise}}{10}$	$\frac{\text{Log Poise}}{10}$	Shear Rate Constant	Shear Rate (Sec^{-1})	Log Shear Rate	$\frac{3I}{2\Pi R^3}$	Shear Stress $dynes/cm^2$
100	12.0	1.2051	X1	0.1446	.0144	-1.8397	17.59	1759	3.245	22.3	267.6
200	17.0	1.2051	X1	0.10241	.0102	-1.9895	17.59	3518	3.546	22.3	379.1
300	21.0	1.2051	X1	0.08436	.0084	-2.073	17.59	5277	3.722	22.3	468.3
400	25.0	1.2051	X1	0.07532	.0075	-2.123	17.59	7036	3.847	22.3	557.5
500	29.0	1.2051	X1	0.06989	.0070	-2.155	17.59	8795	3.944	22.3	646.7
600	33.0	1.2051	X1	0.06628	.0066	-2.178	17.59	10554	4.023	22.3	735.9
700	36.0	1.2051	X1	0.06197	.0062	-2.208	17.59	15750	4.197	22.3	802.8
800	38.5	1.2051	X1	0.0579	.0058	-2.237	17.59	19600	4.292	22.3	858.6
900	40.5	1.2051	X1	0.0542	.0054	-2.266	17.59	23850	4.378	22.3	903.2
1000	45.0	1.2051	X1	0.0542	.0054	-2.266	17.59	28500	4.455	22.3	1003.5

TABLE 3

Rheological Data
Cone and Plate Viscometer

Solution 3 - 1.5% Polyacrylamide Solution (75°C)

Speed	Reading	Cone Constant	Range	Viscosity (Poise)	Poise / 10	Log Poise / 10	Shear Rate Constant	Shear Rate (Sec^{-1})	Log Shear Rate	$\frac{3T}{2\Pi R^3}$	Shear Stress dynes/cm^2
100	38.0	1.2051	X1	0.4579	.0458	-1.3392	1759	1759	3.2452	22.3	847.4
200	40.6	1.2051	X1	0.2446	.0245	-1.6115	3518	3518	3.5462	22.3	905.4
300	42.0	1.2051	X1	0.1687	.0169	-1.7728	5277	5277	3.7224	22.3	936.6
400	46.0	1.2051	X1	0.1386	.0138	-1.8583	7036	7036	3.8473	22.3	1025.8
500	50.0	1.2051	X1	0.1205	.0121	-1.9189	8795	8795	3.9442	22.3	1115.0
600	53.0	1.2051	X1	0.1065	.0107	-1.9728	10554	10554	4.0234	22.3	1181.9
700	56.0	1.2051	X1	0.0964	.0096	-2.0159	15750	15750	4.1972	22.3	1248.8
800	59.0	1.2051	X1	0.0890	.0089	-2.0512	19600	19600	4.2922	22.3	1315.7
900	61.0	1.2051	X1	0.0816	.0082	-2.0878	23850	23850	4.3775	22.3	1360.3
1000	64.0	1.2051	X1	0.0771	.0077	-2.1128	28500	28500	4.4548	22.3	1427.4

TABLE 4

Rheological Data
Cone and Plate Viscometer

Solution 4 - 2.0% Polyacrylamide Solution (75°C)

Speed	Reading	Cone Constant	Range	Viscosity (Poise)	Poise / 10	Log Poise / 10	Shear Rate Constant	Shear Rate (Sec^{-1})	Log Shear Rate	$\frac{3\Gamma}{2\Pi R^3}$	Shear Stress $dynes/cm^2$
100	48.0	1.2051	X1	0.5784	.0584	-1.238	17.59	1759	3.2452	22.3	1070.4
200	57.0	1.2051	X1	0.3434	.0343	-1.464	17.59	3518	3.5462	22.3	1271.1
300	63.0	1.2051	X1	0.2531	.0253	-1.597	17.59	5277	3.7224	22.3	1404.9
400	68.0	1.2051	X1	0.2048	.0205	-1.689	17.59	7036	3.8473	22.3	1516.4
500	72.0	1.2051	X1	0.1736	.0174	-1.761	17.59	8795	3.9442	22.3	1605.6
600	76.0	1.2051	X1	0.1526	.0153	-1.816	17.59	10554	4.0234	22.3	1694.8
700	79.5	1.2051	X1	0.1369	.0137	-1.864	17.59	15750	4.1972	22.3	1772.9
800	83.0	1.2051	X1	0.1250	.0125	-1.903	17.59	19600	4.2922	22.3	1850.9
900	86.0	1.2051	X1	0.1152	.0115	-1.939	17.59	23850	4.3775	22.3	1917.8
1000	89.5	1.2051	X1	0.1078	.0108	-1.967	17.59	28500	4.4548	22.3	1995.9

TABLE 5

Rheological Properties

Data from Graphical Plot (Fig. 14) (75°C)

Cone and Plate Viscometer

Colloid Solution	Intercept	Antilog	Slope
No. (1) (0.5% polyacrylamide)	-1.34	0.0457	-0.300
No. (2) (1.0% ")	-0.40	0.3981	-0.444
No. (3) (1.5% ")	0.38	2.3988	-0.7785
No. (4) (2.0% ")	0.48	3.0199	-0.8143

TABLE 6

Rheological Data

Coascial Cylinder Viscometer

Solution 1 - 0.5% Polyacrylamide (75°C)

Speed	Reading	Viscosity (CP)	Poise	Poise / 10	Log Poise / 10	Shear Rate Sec^{-1}	Log Shear Rate	Shear Stress $dynes/cm^2$
1	0					2.3	0.37106	0
2	0					4.7	0.67209	0
4	0.1	31.70	.3170	.0317	-1.4989	9.4	0.97312	2.98
8	0.2	31.70	.3170	.0317	-1.4989	18.8	1.2742	5.96
16	0.5	39.63	.3963	.03963	-1.4019	37.6	1.5752	14.90
32	1.0	39.63	.3963	.03963	-1.4019	75.2	1.8762	29.80
64	1.3	25.75	.2575	.0257	-1.5892	150.4	2.1772	38.74
128	1.7	16.84	.1684	.01684	-1.7737	300.8	2.478	50.66
256	2.5	12.38	.1238	.01238	-1.9073	601.6	2.779	74.50
512	3.7	9.16	.0916	.00916	-2.0380	1203.2	3.0803	110.30
724	4.8	8.41	.0841	.00841	-2.0750	1701.4	3.2308	143.04

TABLE 7

Rheological Data

Coascial Cylinder Viscometer

Solution 1 - 0.5% Polyacrylamide + Styrene monomer $\phi = 0.2$ (75°C)

Speed	Reading	Viscosity (CP)	Poise	$\frac{\text{Poise}}{10}$	Log $\frac{\text{Poise}}{10}$	Shear Rate Sec^{-1}	Log Shear Rate	Shear Stress dynes/cm^2
1	0					2.3	0.3711	
2	0					4.7	0.6720	
4	0					9.4	0.9731	
8	0.1	15.850	.1585	.01585	-1.799	18.8	1.2742	2.98
16	0.2	15.680	.1568	.01568	-1.8047	37.6	1.5752	5.96
32	0.5	19.810	.1981	.01981	-1.7031	75.2	1.8762	14.90
64	0.8	15.850	.1585	.01585	-1.7990	150.4	2.1772	23.84
128	1.0	9.906	.0991	.00990	-2.0040	300.8	2.4782	29.80
256	1.5	7.429	.0743	.00750	-2.1291	601.6	2.7793	44.70
512	2.9	7.182	.0718	.00718	-2.1438	1203.2	3.0803	86.42
724	3.75	6.567	.0657	.00657	-2.1826	1701.4	3.2301	111.75

TABLE 8

Rheological Data

Coascial Cylinder Viscometer

Solution 2 - 1.0% Polyacrylamide (75°C)

Speed	Reading	Viscosity (CP)	Poise	$\frac{\text{Poise}}{10}$	$\frac{\text{Log Poise}}{10}$	Shear Rate Sec^{-1}	Log Shear Rate	Shear Stress dynes/cm^2
1	1.0	1268	12.680	1.2680	.1031	2.3	0.3711	29.8
2	1.0	634	6.340	.6340	-.1979	4.7	.6721	29.8
4	1.5	475.5	4.760	.4760	-.3228	9.4	.9731	44.7
8	2.0	317.0	3.170	.3170	-.4989	18.8	1.2741	59.6
16	2.3	182.3	1.820	.1820	-.7392	37.6	1.5752	68.5
32	3.0	118.9	1.188	.1188	-.9252	75.2	1.8760	89.3
64	3.5	69.34	.6934	.0693	-1.1593	150.2	2.1770	104.3
128	4.5	44.56	0.4458	.0446	-1.3507	300.8	2.4782	134.1
256	6.5	32.19	.3219	.0322	-1.4921	601.6	2.7793	193.7
512	9.0	22.29	.2229	.0223	-1.6517	1203.2	3.0803	268.2
724	11.0	19.26	.1926	.01926	-1.7153	1701.4	3.2308	327.8

TABLE 9

Rheological Data

Coascial Cylinder Viscometer

Solution 2 - 1.0% Polyacrylamide + Styrene monomer $\phi = 0.2$ (75°C)

Speed	Reading	Viscosity (CP)	Poise	$\frac{\text{Poise}}{10}$	$\frac{\text{Log Poise}}{10}$	Shear Rate Sec^{-1}	Log Shear Rate	Shear Stress dynes/cm^2
1	0					2.3	.3711	
2	0					4.7	.6721	
4	0					9.4	.9731	
8	.1	15.85	.1585	.01585	-1.7990	18.8	1.2741	2.98
16	.2	15.85	.1585	.01585	-1.7990	37.6	1.5752	5.96
32	.5	19.81	.1981	.01981	-1.7031	75.2	1.8760	14.90
64	1.0	19.81	.1981	.01981	-1.7031	150.2	2.1772	29.80
128	1.5	14.856	.1486	.01486	-1.8279	300.8	2.4782	44.70
256	2.0	9.906	.0991	.00990	-2.0039	601.6	2.7793	59.60
512	3.0	7.4296	.0743	.00740	-2.1290	1203.2	3.0808	89.40
724	4.0	7.005	.0701	.00701	-2.1543	1701.4	3.2308	119.20

TABLE 10

Rheological Data

Coascial Cylinder Viscometer

Solution 3 - 1.5% Polyacrylamide (75°C)

Speed	Reading	Viscosity (CP)	Poise	Poise / 10	Log Poise / 10	Shear Rate Sec^{-1}	Log Shear Rate	Shear Stress $dynes/cm^2$
1	2.0	2536	25.36	2.536	.4041	2.35	.3711	59.8
2	3.0	1902	19.02	1.902	.2792	4.7	.6721	89.4
4	4.0	1268	12.68	1.268	.1031	9.4	.9731	119.2
8	5.0	792.5	7.925	.7925	-.1010	18.8	1.2742	149.0
16	7.0	554.75	5.5475	.5548	-.2559	37.6	1.5752	208.6
32	7.5	297.18	2.9718	.2972	-.5269	75.2	1.8762	223.5
64	8.0	158.5	1.585	.1585	-.7999	150.4	2.177	238.4
128	10.0	99.06	.9906	.0991	-1.0041	300.8	2.4783	298.0
256	12.0	59.43	.5943	.0594	-1.2259	601.6	2.7793	357.6
512	16.0	39.63	.3963	.0396	-1.402	1203.2	3.0803	476.8
724	12	21.01	.2101	.02101	-1.678	1701.4	3.2301	357.6

TABLE 11

Rheological Data

Coascial Cylinder Viscometer

Solution 3 - 1.5% Polyacrylamide + Styrene Monomer $\phi = 0.2$ ($75^{\circ}C$)

Speed	Reading	Viscosity (CP)	Poise	$\frac{\text{Poise}}{10}$	$\frac{\text{Log Poise}}{10}$	Shear Rate Sec^{-1}	Log Shear Rate	Shear Stress $dynes/cm^2$
1	2	2536	25.36	2.53	.403	2.35	.3711	59.60
2	4	2536	25.36	2.53	.403	4.7	.6721	119.20
4	4	1268	12.68	1.27	.104	9.4	.9731	119.20
8	5	792.5	7.93	.79	-.10	18.8	1.274	149.00
16	5	396	3.96	.396	-.40	37.6	1.5752	149.00
32	5	198	1.98	.198	-.70	75.2	1.8762	149.00
64	6	111	1.11	.118	-.92	150.4	2.1772	178.80

TABLE 12

Rheological Data

Data from Graphical Plot (Figs.17-20)

Coascial Cylinder Viscometer

Solution	Slope	Intercept	Antilog
Soln. 1 A/P	-0.5	-0.5	.3162
Soln. 1 A/P + M/P	-0.44	-0.9	.1259
Soln. 2 A/P	-0.68	+0.4	2.51
Soln. 2 A/P + M/P	-0.428	-0.9	0.1259
Soln. 3 A/P	-0.6538	+0.7	5.012
Soln. 3 A/P + M/P	-0.6538	+0.7	5.012

TABLE 13

The Effect of Protective Colloid Concentration on the Apparent Viscosity (75°C)

Cone and Plate Concentric Cylinder Viscometers

Colloid Concentration % (wt/wt)	Apparent Viscosity (Poise)	
	Cone & Plate	Concentric Cylinder
0.5	0.054	0.317
1.0	0.145	4.76
1.5	0.458	12.68
2.0	0.578	-

TABLE 14

Rheological Data (Cone and Plate Viscometer)

Effect of an Inorganic Salt (Na_2HPO_4)

1% Polyacrylamide Solution

RPM	Reading R	Cone Constant	Range S	Viscosity (Poise)	Shear Rate Constant	Shear Rate Sec^{-1}	Shear Stress Constant	Shear Stress $dynes/cm^2$	Salt Level %	Temp °C
100	8.0	6.795	X1	0.54	17.655	1765.5	119.96	959.68	0	25
200	10.0	"	"	0.34	"	3531	"	1199.60	0	25
300	11.0	"	"	0.25	"	5296.5	"	1319.56	0	25
400	14.0	"	"	0.24	"	7062	"	1679.44	0	25
500	17.0	"	"	0.23	"	8827.5	"	2039.32	0	25
600	20.0	"	"	0.23	"	10593	"	2399.20	0	25
700	23.0	"	"	0.22	"	12358.5	"	2759.08	0	25
800	28.0	"	"	0.24	"	14124	"	3358.88	0	25
900	30.0	"	"	0.23	"	15889.5	"	3598.80	0	25
1000	31.0	"	"	0.21	"	17655	"	3718.76	0	25

TABLE 15

Rheological Data (Cone and Plate Viscometer)

Effect of an Inorganic salt (Na_2HPO_4)

1% Polyacrylamide Solution

RPM	Reading R	Cone Constant	Range S	Viscosity (Poise)	Shear Rate Constant	Shear Rate Sec^{-1}	Shear Stress Constant	Shear Stress $dynes/cm^2$	Salt Level %	Temp °C
100	7.5	6.795	X1	0.51	17.655	1765.5	119.96	899.70	1.0	25°C
200	10.0	"	"	0.34	"	3531	"	1199.60	"	"
300	11.0	"	"	0.25	"	5296.5	"	1319.56	"	"
400	11.5	"	"	0.20	"	7062	"	1379.54	"	"
500	13.0	"	"	0.176	"	8827.5	"	1559.48	"	"
600	15.0	"	"	0.17	"	10593	"	1799.40	"	"
700	16.5	"	"	0.16	"	12358.5	"	1979.34	"	"
800	17.0	"	"	0.14	"	14124	"	2039.32	"	"
900	19.0	"	"	0.14	"	15889.5	"	2279.24	"	"
1000	20.0	"	"	0.14	"	17655	"	2399.20	"	"

TABLE 16

Rheological Data (Cone and Plate Viscometer)

Effect of an Inorganic salt (Na_2HPO_4)

1% Polyacrylamide solution

RPM	Reading R	Cone Constant	Range S	Viscosity (Poise)	Shear Rate Constant	Shear Rate Sec^{-1}	Shear Stress Constant	Shear Stress dynes/cm^2	Salt Level %	Temp °C
100	7.0	6.795	X1	0.48	17.655	1765.5	119.96	839.72	2.0	25°C
200	10.0	"	"	0.34	"	3531	"	1199.6	"	"
300	10.5	"	"	0.34	"	5296.5	"	1259.58	"	"
400	11.0	"	"	0.19	"	7062	"	1319.56	"	"
500	13.0	"	"	0.176	"	8827.5	"	1559.48	"	"
600	15.0	"	"	0.17	"	10593	"	1799.4	"	"
700	16.5	"	"	0.16	"	12358.5	"	1979.34	"	"
800	18.0	"	"	0.15	"	14124	"	2159.28	"	"
900	19.0	"	"	0.14	"	15889.5	"	2279.24	"	"
1000	21.0	"	"	0.14	"	17655	"	2519.16	"	"

TABLE 17

Rheological Data (Cone and Plate Viscometer)

Effect of an Inorganic salt (Na_2HPO_4

1% Polyacrylamide solution

RPM	Reading R	Cone Constant	Range S	Viscosity (Poise)	Shear Rate Constant	Shear Rate Sec^{-1}	Shear Stress Constant	Shear Stress dynes/cm^2	Salt Level %	Temp °C
100	7.5	6.795	X1	0.51	17.655	1765.5	119.96	899.70	6.0	25°C
200	10.0	"	"	0.34	"	3531	"	1199.60	"	"
300	10.5	"	"	0.34	"	5296.5	"	1259.58	"	"
400	12.0	"	"	0.20	"	7062	"	1439.52	"	"
500	13.0	"	"	0.17	"	8827.5	"	1559.48	"	"
600	14.5	"	"	0.16	"	10593	"	1739.42	"	"
700	15.5	"	"	0.15	"	12358.5	"	1859.38	"	"
800	18.0	"	"	0.15	"	14124	"	2159.28	"	"
900	19.0	"	"	0.14	"	15889.5	"	2279.24	"	"
1000	20.0	"	"	0.13	"	17655	"	2399.20	"	"

TABLE 18

Effect of Shear on a Polyacrylamide Solution
Molecular Weight Determination Using Viscosity Data

Concentration gm/100 ml.	to(sec) Pure Solvent	t(sec) Solution	$\frac{t-to}{C\ to}$	$[\eta]_{dt\ c=o}$	K	α
(a) Data - Before Shear						
0.16136	185	857	22.511		6.8×10^{-4} al gm^{-1}	0.66
0.14669	185	800	22.66		"	"
0.12412	185	745	22.51		"	"
0.10757	185	696	22.25		"	"
0.09492	185	664	22.46	22.40	"	"
(b) Data - After High Shear						
0.16136	185	790	20.267		"	"
0.14669	185	715	19.529		"	"
0.12412	185	603	18.203		"	"
0.10757	185	538	17.738		"	"
0.09492	185	480	16.799	12.00	"	"

TABLE 19

Interfacial Tension Data

The Sessile Drop Method

r/B and ho/B Correction Values

$\frac{r}{B}$	$\frac{ho}{B}$
6	0.0149
7	0.0059
8	0.0023
9	0.00089
10	0.00034

TABLE 20

Interfacial Tension Measurement

The Sessile Drop Method

h^2/r^2 and B^2/r^2 Correction Values

$\frac{h^2}{r^2}$	$\frac{B^2}{r^2} - \frac{1}{2}\frac{h^2}{r^2}$		$\frac{B^2}{r^2}$
.948341	+ 7.8485		8.3227
.905923	3.8606		4.3135
.839539	1.8788		2.2986
.789864	1.22456		1.6194
.750063	0.90091		1.2759
.538453	0.19466		0.4638
.426071	0.07331		0.2863
.358633	0.03326		0.2125
.313675	0.01570		0.1725
.281426	0.00666		0.1473
.257040	0.00153	zero connection	0.1300
.237900	- 0.00161		0.1173
.209567	- 0.00492		0.0998

TABLE 21

Interfacial Tension between

Polyacrylamide Solutions and Various Monomers

% Colloid	Composition Monomer Phase	Temp °C	h	r	$\frac{h^2}{r^2}$	Correction Value Δ	PA Density Aqueous Phase	PM Density Monomer Phase	ΔP	Interfacial Tension (Dynes/cm) σ
0.5	St	20	0.506	0.8620	0.3446	0.0275	0.9983	0.9100	0.0870	12.70
0.5	St/BMA 1:1	20	0.4870	0.8125	0.3592	0.0340	0.9983	0.9100	0.0870	12.03
0.0	Water	20	0.5380	0.8870	0.3678	0.0380	1.000	0.9000	0.1000	17.13
0.5	VA	20	0.4700	0.8250	0.3245	0.0200	0.9983	0.9342	0.0641	7.80
0.5	MMA	20	0.4950	0.8250	0.3600	0.0350	0.9983	0.9360	0.0623	8.90
0.5	St/MMA 1:1	20	0.5050	0.8500	0.3529	0.0300	0.9983	0.9230	0.0753	11.02
0.25	St/BMA 1:1	75	0.4800	0.8550	0.3152	0.0060	0.9344	0.8760	0.0594	6.94
0.50	St/BMA 1:1	75	0.4200	0.7000	0.3600	0.0340	0.9371	0.8760	0.0611	6.23
1.00	St/BMA 1:1	75	0.4200	0.9050	0.2154	-0.0025	0.9404	0.8760	0.0644	5.66
1.50	St/BMA 1:1	75	0.4040	0.8300	0.2084	-0.0030	0.9424	0.8760	0.0664	5.43
2.0	St/BMA 1:1	75	0.3900	0.8250	0.2234	-0.0020	0.9447	0.8760	0.0687	5.21
0.50	MMA	75	0.5700	0.9050	0.3967	0.0530	0.9358	0.9110	0.0248	5.00
0.50	St	75	0.4200	0.6750	0.3871	0.0490	0.9359	0.8765	0.0594	6.44

Key to Monomers used:

St = Styrene
BMA = n-Butyl Methacrylate
VA = Vinyl Acetate
MMA = Methyl Methacrylate

TABLE 22

Variation of Interfacial Tension

With Protective Colloid Concentration

Polyacrylamide Concentration % wt/wt	σ Interfacial Tension Dynes/cm	Temperature ^{o}C	Monomer Composition	Monomer Volume Fraction ϕ
0.25	6.94	75	St/BMA 1:1	0.20
0.50	6.23	75	St/BMA 1:1	0.20
1.00	5.65	75	St/BMA 1:1	0.20
1.50	5.42	75	St/BMA 1:1	0.20
2.00	5.20	75	St/BMA 1:1	0.20

Key to Monomers used.

St = Styrens

BMA = n-Butyl Methacrylate

TABLE 23

Correlation of Interfacial Tension with Protective Colloid Concentration

Log Concentration/Log Interfacial Tension/Data

Polyacrylamide Concentration % wt/wt	Log of Concentration	σ Interfacial Tension Dynes/cm	Log of Interfacial Tension σ	Monomer Composition	ϕ Monomer Volume Fraction	Temp. ^{o}C
0.25	-0.6021	6.94	0.8414	St/BMA 1:1	0.20	75
0.50	-0.3010	6.23	0.7945	St/BMA 1:1	0.20	75
1.00	0	5.65	0.7520	St/BMA 1:1	0.20	75
1.50	0.1761	5.42	0.7339	St/BMA 1:1	0.20	75
2.00	0.3010	5.20	0.7160	St/BMA 1:1	0.20	75

Key to Monomers used: St = Styrene
BMA = n-Butyl Methacrylate

TABLE 24

Effect of an Inorganic Salt (Na_2HPO_4) on Interfacial Tension between Polyacrylamide Solution and Styrene Monomer

Polyacryl-Amide Level % wt/wt	% Salt Level (Na_2HPO_4)	$\frac{h^2}{r^2}$	Density Aqueous Phase PA	Density Monomer Phase DM	ΔP Diff.	Interfacial Tension Dynes/Cm 6	Temp °C	Monomer Composition
0.50	0.0	0.3446	0.9983	0.9100	0.0870	12.70	20	St
0.50	0.5	0.3776	0.9997	0.9100	0.0900	12.59	20	St
0.50	1.0	0.2973	1.0050	0.9100	0.0950	9.89	20	St
0.50	1.5	0.2789	1.0100	0.9100	0.1000	8.30	20	St
0.50	2,0	0.3253	1.0153	0.9100	0.1053	12.37	20	St
0.50	4.0	0.2528	1.0343	0.9100	0.1243	12.13	20	St

TABLE 25

The effect of Agitator Speed Upon Final Particle Size

Exp. No	Monomer Volume Fraction ∅	Stirrer Speed N (RPM)	Log N	Stirrer Diameter L (cm)	Polyacryl-amide Concentration % wt/wt	Monomer	Reaction Temp °C	Saulter Mean Particle size d (microns)	Log d
10	0.20	300	2.48	10.0	0.5	St	75	523	2.719
42	0.20	350	2.54	10.0	0.5	St	75	520	2.715
28	0.20	400	2.60	10.0	0.5	St	75	520	2.715
32	0.20	500	2.69	10.0	0.5	St	75	510	2.707
43	0.20	550	2.74	10.0	0.5	St	75	505	2.703
40	0.20	600	2.78	10.0	0.5	St	75	500	2.698
35	0.30	300	2.48	10.0	0.5	St	75	328	2.516
36	0.30	400	2.60	10.0	0.5	St	75	320	2.505
37	0.30	500	2.69	10.0	0.5	St	75	320	2.505
14	0.30	600	2.78	10.0	0.5	St	75	316	2.499

Monomer used: St = Styrene
Benzoyl peroxide employed as initiator.

TABLE 26

The Effect of Monomer Volume Fraction Upon Final Particle Size

Exp No	Monomer Volume Fraction θ	Stirrer Speed N (RPM)	Stirrer Diameter L Cm	Polyacryl-amide Concentration % wt/wt	Monomer	Reaction Temp ^{o}C	Saulter Mean Particle Size d (Microns)
11	0.10	300	10.0	0.50	St	75	540
23	0.15	300	10.0	0.50	St	75	530
10	0.20	300	10.0	0.50	St	75	523
24	0.25	300	10.0	0.50	St	75	430
12	0.30	300	10.0	0.50	St	75	330
41	0.10	600	10.0	0.5	St	75	Unstable
60	0.20	600	10.0	0.5	St	75	500
25	0.25	600	10.0	0.5	St	75	410
14	0.30	600	10.0	0.5	St	75	316
26	0.35	600	10.0	0.5	St	75	310
13	0.40	600	10.0	0.5	St	75	259

Monomer Used: St = Styrene

TABLE 27

The Effect of Protective Colloid Concentration Upon Final Particle Size

Exp No	Monomer Volume Fraction θ	Stirrer Speed N (RPM)	Stirrer Diameter L Cm	Polyacryl-amide Concentration % wt/wt	Monomer	Reaction Temp °C	Saulter Mean Particle Size d (Microns)
20	0.20	600	10.0	0.50	St/BMA 1:1	75°C	580
22	0.20	600	10.0	0.75	St/BMA 1:1	75°	285
15	0.20	600	10.0	1.00	St/BMA 1:1	75°	235
17	0.20	600	10.0	1.50	St/BMA 1:1	75°	176
19	0.20	600	10.0	2.00	St/BMA 1:1	75°	153

.Key to Monomers Used: St = Styrene
BMA = n-Butyl Methacrylate

TABLE 28

The Effect of Interfacial Tension Upon the Final Particle Size

Exp. No.	Poly Acrylamide Concentration % wt/wt	Temp °C	Interfacial Tension σ dynes/cm	Log σ	Saulter Mean Particle Size d (Microns)	Log d	Monomer Composition	Stirrer Speed N RPM
20	0.5	75	6.23	0.7945	580	2.7596	St/BMA 1:1	600
22	0.75	"	5.70	0.7560	285	2.4548	St/BMA 1:1	600
15	1.00	"	5.65	0.7520	235	2.3710	St/BMA 1:1	600
17	1.50	"	5.42	0.7340	176	2.2450	St/BMA 1:1	600
19	2.0	"	5.20	0.7160	153	2.1840	St/BMA 1:1	600
60	0.5	"	6.35	0.8027	600	2.7780	St	600
61	1.0	"	5.80	0.7634	320	2.5050	St	600
58	0.5	"	5.00	0.6989	100	2.000	MMA	600
59	1.0	"	4.80	0.6812	88	1.94	MMA	600
68	0.5	"	5.68	0.7482	280	2.447	MM/St 3:1 1:1	600

Key to Monomers Used: St = Styrene
BMA = Butyl Methacrylate
MMA = Methyl Methacrylate

Fixed Physical System Parameters
Stirrer diameter L = 10.5 cm
Monomer Volume fraction = 0.20

TABLE 29

Effect of an Inorganic Salt (Na_2HPO_4) on the final particle size

Exp No	Poly-Acrylamide Conc(C) % wt/wt	Stirrer Speed N (RPM)	Stirrer Diameter L (cm)	Salt Conc(C') % wt/wt	Monomer	Monomer Volume Fraction ϕ	Reaction Temperature °C	Saulter Mean Particle Size d
15	1.0	600	10.0	0	St/BMA 1:1	0.20	75°	235
29	1.0	600	10.0	0.5	St/BMA 1:1	0.20	75	300
30	1.0	600	10.0	1.0	St/BMA 1:1	0.20	75	350
31	1.0	600	10.0	1.5	St/BMA 1:1	0.20	75	550
33	1.0	600	10.0	2.0	St/BMA 1:1	0.20	75	Aggiometeration unstable

Key to Monomer used: St/BMA = Styrene/n Butyl Methacrylate

TABLE 30

Calculation of Reynolds Number Cone and Plate Viscometer Data For Polyacrylamide Solutions at 75°C

Stirrer Speed N RPS	Stirrer Diameter L Cm	Graph Intercept (Fig 14)	Constant K	Slope of Line	Exponent n	Density P	Re	Solution Code
5	10.5	-1.34	.0457	-0.3	0.70	.9372	31,687	Soln. 1
10	10.5	-1.34	.0457	-0.3	0.70	.9372	78,016	"
5	10.5	-0.40	.3981	- .441	.556	.9400	6,050.8	Soln. 2
10	10.5	-0.4	.3981	- .441	.556	.9400	16,459	"
5	10.5	+0.38	2.398	- .7785	.2215	.9400	3,339	Soln. 3
10	10.5	+0.38	2.398	- .7785	.2215	.9400	11,456	"
5	10.5	+0.48	3.0199	- .8143	0.1857	.9450	3,030.7	Soln. 4
10	10.5	+0.48	3.0199	- .8143	.1857	.9450	10,657.5	"

Key: Soln. 1 = 0.5% polyacrylamide wt/wt
2 = 1.0 " "
3 = 1.5 " "
4 = 2.0% " "

TABLE 31

Calculation of Reynolds Number Coaxial Cylinder Viscometer Data For Polyacrylamide Solutions at 75°C

Stirrer Speed N RPS	Stirrer Diameter L Cm	Graph Intercept (Fig 17-20)	Constant K	Slope of Line	Exponent n	Density P	Re	Solution Code
10	10.5	-0.5	.3162	-0.5	0.5	.937	26137	Soln. 1.
10	10.5	+0.4	2.51	-0.68	0.32	.937	5894	Soln. 2.
10	10.5	+0.7	5.012	-0.6538	0.346	.9425	3182	Soln. 3.

Solution 1 = 0.5% Polyacrylamide wt/wt
2 = 1.0% " "
3 = 1.5% " "

TABLE 32

Correlation of Particle size with Reynolds Number

Cone and Plate Viscometer

Exp No	Poly Acrylamide Conc(C) % wt/wt	Stirrer Speed N RPM	Re	Log Re	Saulter Mean Particle Size d (Microns)	Log d	Monomer Volume Fraction ϕ	Monomer
20	0.5	600	78016	4.8922	580	2.7634	0.20	St/BMA 1:1
15	1.0	600	16459	4.2164	235	2.3617	0.20	St/BMA 1:1
17	1.5	600	11456	4.0590	176	2.2455	0.20	St/BMA 1:1
19	2.0	600	10658	4.0276	153	2.1847	0.20	St/BMA 1:1

Key to Monomers Used: St = Styrene
BMA = n-Butyl Methacrylate

TABLE 33

Correlation of Particle Size with Reynolds Number

Coaxial Cylinder Viscometer

Exp No	Poly-Acrylamide Concentration % wt/wt	Stirrer Speed N (RPM)	Re	Log Re	Saulter Mean Particle size d microns	Log d	Monomer Volume Fraction ϕ	Monomer
20	0.5	600	26137	4.417	580	2.7634	0.20	St/BMA 1:1
15	1.0	600	5893	3.7704	230	2.3617	0.20	St/BMA 1:1
17	1.5	600	3182	3.5027	176	2.2455	0.20	St/BMA 1:1

Key to Monomers Used:

St = Styrene
BMA = n-Butyl Methacrylate

TABLE 34

Correlation of Particle Size with Reynolds Number

Cone and Plate Viscosity Data

Exp No.	Poly Acrylamide Conc(C) % wt/wt	Log(C)	Stirrer Speed N (RPM)	Stirrer Diam L (cm)	Re	Log Re	Saulter Mean Particle Size d Microns	Log d	Monomer Volume Fraction ϕ	Monomers	Reaction Temp °C
18	0.5	-0.30	300	10.0	31687	4.5000	610	2.7780	0.20	St	75
20	0.5	-0.30	600	10.0	78016	4.8900	580	2.7634	0.20	St/BMA 1:1	75
15	1.0	0	600	10.0	16459	4.216	235	2.3617	0.20	St/BMA 1:1	75
17	1.5	0.1761	600	10.0	11456	4.059	176	2.2455	0.20	St/BMA 1:1	75
19	2.0	0.3010	600	10.0	10658	4.027	153	2.1847	0.20	St/BMA 1:1	75
58	0.5	-0.30	600	10.0	78016	4.890	100	2.000	0.20	MMA	75
59	1.0	0	600	10.0	16459	4.2160	88	1.9440	0.20	MMA/St 3:1	75
60	0.5	-0.30	600	10.0	78016	4.890	600	2.7780	0.20	St	75
61	1.0	0	600	10.0	16459	4.2160	320	2.5050	0.20	St	75
68	0.5	-0.30	600	10.0	78016	4.892	280	2.4470	0.20	St/MMA 1:1	75
70	0.5	-0.30	600	10.0	78016	4.890	160	2.204	0.20	St/MMA 1:3	75
72	0.5	-0.30	600	10.0	78016	4.890	330	2.519	0.20	St/MMA 3:1	75
74	1.0	0	600	10.0	16459	4.216	110	2.04	0.20	St/MMA 1:1	75

Kay to Monomers used:

St = Styrene
BMA = n-Butyl Methacrylate
MMA = Methyl Methacrylate

TABLE 35

Polymer-Water Interfacial Tension and Polarity of Various Polymers at 20°C

Polymer	γ_2 (Surface Tension)	γ_{12} Interfacial Tension	γ_2^d Dispersion Contribution	γ_2^P Polar Contribution	$x^P = \gamma^P_2 / \gamma_2$ Polarity
Polystyrene	40.7	32.7	32.5	8.2	0.20
Poly (Butylmeth-acrylate	31.2	36.7	25.7	5.5	0.18
Poly (Methyl-methacrylate	41.1	26.0	29.7	11.4	0.28
Poly (Vinyl Acetate)	36.5	23.5	24.2	12.3	0.34
Poly (Vinyl Chloride)	41.9	37.8	35.6	6.3	0.15

Ref: B.R. Vizayerdran. J.A.P.S. Vol. 23 733-742 (1979)
S.Wu. J. Macromol Sci-Rev Macromol Chem. C_{10},1 (1974)

TABLE 36

Interfacial Tension and Polarity Data for various monomers

(0.5% Polyacrylamide as the Aqueous phase)

Poly-Acrylamide Conc (C) % wt/wt	Monomer	Interfacial Tension δ Dynes/cm 75°C	20°C	Polarity $X^P = \gamma^P_2 / \gamma^2$
0.5	St	6.44	12.70	0.20
	Comonomers			
0.5	St/BMA 1:1	6.23	12.03	0.19
0.5	MMA	5.0	8.9	0.28
0.5	VA	-	7.8	0.34
	Comonomers St/MMA			
	1:1	-	11.0	0.24
	3:1	-	11.5	0.22
	1:3	-	10.0	0.26

Key to Monomers used: St = Styrene; BMA = n-Butyl methacrylate; VA = Vinyl Acetate; MMA = Methyl Methacrylate

TABLE 37

Correlation between Polarity and the final Particle Size

Exp No	Poly-Acrylamide Conc(C) % wt/wt	Stirrer Speed N (RPM)	Stirer Diameter L (cm)	Monomer	Monomer Vol Fraction ϕ	Interfacial Tension Dynes/cm ($20^{o}C$) σ	Polarity X_{20}^{P}	Log X_{20}^{P}	Saulter Mean Particle Size d microns	Log d
60	0.5	600	10.0	St	0.20	12.70	0.20	-0.6989	600	2.778
20	0.5	600	10.0	St/BMA 1:1	0.20	12.03	0.19	-0.7212	580	2.763
68	0.5	600	10.0	St/MMA 1:1	0.20	11.00	0.24	-0.6197	280	2.447
58	0.5	600	10.0	MMA	0.20	8.90	0.28	-0.5500	100	2.000
70	0.5	600	10.0	St/MMA 1:3	0.20	10.00	0.26	-0.5850	160	2.204
72	0.5	600	10.0	St/MMA 3:1	0.20	11.50	0.22	-0.6575	330	2.519

Key to Monomers used:

St = Styrene
BMA = n-Butyl Methacrylate
MMA = Methyl Methacrylate

TABLE 38

Protective Colloid Properties of Polyvinyl Alcohol

	Saponification Solvent			Residual Acetyl Content	Protective Colloid Prop.(Gold Number)
	Methanol	Benzene	H_2O		
A	80.7	0	3.2	10.28	1.4
B	64.6	16.1	3.2	10.15	2.5
C	48.5	32.2	3.2	9.23	3.3
D	32.5	48.3	3.2	10.45	3.3

TABLE 39

Interfacial Tension between a 0.25% wt/wt Aqueous polyvinyl alcohol Solution and Styrene Monomer

Materials Used:

(1) Grade of Polyvinyl Alcohol = 52.22

where 52 = degree of hydrolysis
22 = Solution viscosity

(11) Styrene Monomer (commercial grade)

Measurements Method	Interfacial tension 0
Drop Volume method	3.5 dynes /cm (20°C)
Sessile drop method	3.0 dynes/ cm (20°C)

TABLE 40

Opacity and Time Data for

Different Initiator Levels

Standard Emulsion Latex taken as Zero, Solution

1, 2, 3, 4, 5 made by 100% Dilution of Each:

Time (Since Start) (Minutes)	Opacity Number		
	A	B	C
5	4.5	4.5	4.5
10	4.5	4.5	4.5
15	3.5	4.0	4.0
20	2.5	3.5	3.5
25	2.0	2.5	3.0
30	1.5	2.0	3.0
35	1.0	1.5	2.5
40	0.5	1.5	2.5
45	0.5	1.5	2.5
50	0.5	1.0	2.5
55	0	1.0	2.5
60		1.0	2.0
65		0.5	1.5
70		0.5	
75		1	
80			

A = Initiator Doubled
B = Standard Level
C = Initiator Halved

TABLE 41

The Polymerisation System
Spherical Agglomeration

Water	800.0
Poly Vinyl Alcohol (1)	4.0
Monomer (2)	188.0
Benzoyl Peroxide	2.8
	994.8

(1) Various Grades (DuPont Elvanol Grades)

(2) Styrene/Methyl Methacrylate

TABLE 42

The Effect of Stirrer Speed on
The Primary Particle Size (d) and Agglomerate Size (D)

Exp No	Stirrer Speed N RPM	Stirrer Diameter L (cm)	Monomer	Reaction Temp ^{o}C	Primary Particle Size d (microns)	Agglomerate Size D (microns)	Notes
C1	400	10.0	St	80	0.15	80	
C2	200	10.0	St	80	0.25	20) 150)	primary particle size very polydisperse Agglomerat shows Bimodal size distribution
C3	600	10.0	St	80	0.25	60	
C4	400	4.0	St	80	0.15	20) 100)	Agglomerate shows Bimodal size distribution
C5	400	10.0	MMA	80	0.10	None	No evidence of Agglomeration

Kay to Monomers used: St = Styrene
MMA = Methyl Methacrylate

Primary Particle Size (d) from SEM Data
Agglomerate Particle Size (D) from Coulter Counter Data

TABLE 43
Rheological Data Sample 83
Cone and Plate Viscometer

Speed (RPM)	Reading	Cone Constant	Viscosity U (Poise)	$\sqrt{U}$	$\sqrt{U}$ X10	$\frac{1}{\sqrt{F}}$ ($X10^{-2}$)
100	6.5	6.73	.4370	.6600	6.6	2.38
200	7.0	"	.2350	.4800	4.8	1.68
300	6.5	"	.1458	.3818	3.8	1.37
400	6.8	"	.1144	.3382	3.3	1.19
500	6.7	"	.0902	.3003	3.0	1.06
600	7.2	"	.0690	.2630	2.6	.97
700	7.3	"	.0702	.2650	2.65	.89
800	6.5	"	.0546	.2340	2.34	.84
900	6.2	"	.0463	.2150	2.15	.79
1000	5.9	"	.0397	.1990	1.99	.75

TABLE 44
Rheological Data Sample 84
Cone and Plate Viscometer

Speed (RPM)	Reading	Cone Constant	Viscosity U (Poise)	$\sqrt{U}$	$\sqrt{U}$ X10	$\frac{1_1}{r^2}$ ($X10^{-2}$)
100	4.5	6.73	.3029	.5503	5.50	2.38
200	4.0	"	.1346	.3669	3.67	1.68
300	3.0	"	.0673	.2594	2.59	1.37
400	2.8	"	.0471	.2170	2.17	1.19
500	3.0	"	.0404	.2009	2.01	1.06
600	3.5	"	.0392	.1979	1.98	.97
700	2.0	"	.0192	.1386	1.39	.89
800	1.5	"	.0126	.1122	1.12	.84
900	1.5	"	.0105	.1024	1.02	.79
1000	1.5	"	.0100	.1000	1.00	.75

TABLE 45
Rheological Data Sample 85
Cone and Plate Viscometer

Speed (RPM)	Reading	Cone Constant	Viscosity U (Poise)	$\sqrt{U}$	$\sqrt{U}$ X10	$\frac{1_1}{\dot{\gamma}^2}$ ($X10^{-2}$)
100	7.0	6.73	.4711	.6864	6.86	2.38
200	10.0	"	.3365	.5801	5.80	1.68
300	11.0	"	.2467	.4967	4.97	1.37
400	13.5	"	.2271	.4766	4.77	1.19
500	17.0	"	.2288	.4783	4.78	1.06
600	19.0	"	.2131	.4616	4.62	.97
700	21.0	"	.2019	.4493	4.49	.89
800	22.5	"	.1893	.4350	4.35	.84
900	24.0	"	.1795	.4237	4.24	.79
1000	28.0	"	.1884	.4340	4.34	.75

TABLE 46

Rheological Data Sample 86
Cone and Plate Viscometer

Speed (RPM)	Reading	Cone Constant	Viscosity U (Poise)	$\sqrt{U}$	$\sqrt{U}$ X10	$\frac{1}{\sqrt{r^2}}$ ($X10^{-2}$)
100	5.3	6.73	.3567	.600	6.0	2.38
200	5.0	"	.1683	.410	4.1	1.68
300	4.0	"	.0897	.300	3.0	1.37
400	4.7	"	.0790	.2812	2.8	1.19
500	4.5	"	.0606	.2461	2.46	1.06
600	4.9	"	.0549	.2345	2.35	.97
700	5.0	"	.0481	.2193	2.19	.89
800	4.8	"	.0404	.2009	2.0	.84
900	3.6	"	.0269	.1640	1.64	.79
1000	2.7	"	.0182	.1348	1.348	.75

TABLE 47
Rheological Data
0.5% wt/wt PVA Solution
Cone and Plate Viscometer

Speed (RPM)	Reading	Cone Constant	Viscosity U (Poise)	$\sqrt{U}$	$\sqrt{U}$ X10	$\frac{1}{\dot{\gamma}^2}$ ($X10^{-2}$)
100	0	6.73	-	-	-	2.35
200	0	"	-	-	-	1.68
300	.1	"	.0022	.0473	.473	1.37
400	.2	"	.0034	.0580	.58	1.19
500	.45	"	.0061	.0778	.78	1.06
600	.60	"	.0067	.0818	.82	.97
700	.75	"	.0072	.0849	.849	.89
800	.85	"	.0071	.0846	.846	.84
900	1.00	"	.0075	.0864	.864	.79
1000	1.35	"	.00875	.0935	.935	.75

TABLE 48
Rheological Data
1.0% wt/wt PVA Solution
Cone and Plate Viscometer

Speed (RPM)	Reading	Cone Constant	Viscosity U (Poise)	$\sqrt{U}$	$\sqrt{U}$ X10	$\frac{1_1}{r^2}$ ($X10^{-2}$)
100	-	6.73	-	-	-	2.38
200	0.1	"	.0034	.0580	.58	1.68
300	0.25	"	.0056	.0748	.748	1.37
400	0.50	"	.0084	.0917	.917	1.19
500	0.75	"	.0100	.1004	1.004	1.06
600	1.00	"	.0112	.1059	1.060	.97
700	1.30	"	.0124	.1117	1.110	.89
800	1.70	"	.0143	.1196	1.190	.84
900	2.0	"	.0149	.1222	1.220	.79
1000	2.3	"	.0155	0.1244	1.244	.75

TABLE 49
Rheological Data
2.0% wt/wt PVA Solution
Cone and Plate Viscometer

Speed (RPM)	Reading	Cone Constant	Viscosity U (Poise)	$\sqrt{U}$	$\sqrt{U}$ X10	$\frac{1}{\dot{\gamma}^2}$ ($X10^{-2}$)
100	0.25	6.73	.0168	.1296	1.296	2.38
200	0.50	"	.0168	.1296	1.296	1.68
300	0.75	"	.0168	.1296	1.296	1.37
400	1.50	"	.0337	.1835	1.835	1.19
500	2.00	"	.0269	.1640	1.640	1.06
600	2.75	"	.0308	.1755	1.755	.97
700	3.50	"	.0336	.1833	1.833	.89
800	4.00	"	.0336	.1833	1.833	.84
900	4.75	"	.0355	.1884	1.884	.79
1000	5.50	"	.037015	0.19239	1.924	.75

TABLE 50

Rheological Data
4.0% wt/wt PVA Solution
Cone and Plate Viscometer

Speed (RPM)	Reading	Cone Constant	Viscosity U (Poise)	$\sqrt{U}$	$\sqrt{U}$ X10	$\frac{1}{\dot{\gamma}^2}$ ($X10^{-2}$)
100	1.0	6.73	.0673	.2594	2.59	2.38
200	4.0	"	.1346	.3668	3.67	1.68
300	7.0	"	.1570	.3962	3.96	1.37
400	9.5	"	.1598	.3990	3.99	1.19
500	12.0	"	.1615	.4019	4.02	1.06
600	14.5	"	.1626	.4032	4.03	.97
700	17.0	"	.1634	.4043	4.04	.89
800	19.5	"	.1640	.4050	4.05	.84
900	22.0	"	.1645	.4056	4.06	.79
1000	22.5	"	0.1514	0.3891	3.891	.75

TABLE 51
Rheological Data (Sample 83)
Measurement of $n_A^{\frac{1}{2}}$
Cone and Plate Viscometer

Speed RPM	Reading	r_A Shear Stress dynes/cm^2	$r_A^{\frac{1}{2}}$	Shear Rate $\dot{\gamma}$ (Sec^{-1})	$\dot{\gamma}^{\frac{1}{2}}$	$\frac{1}{\dot{\gamma}^{\frac{1}{2}}}$ X10^{-2}	$\frac{r_A^{\frac{1}{2}}}{\dot{\gamma}^{\frac{1}{2}}} = n_A^{\frac{1}{2}}$
100	6.5	779.74	27.92	1765	42.02	2.38	0.6644
200	7.0	839.72	28.98	3530	59.42	1.68	0.4877
300	6.5	779.74	27.92	5295	72.77	1.37	0.3837
400	6.8	815.73	28.56	7060	84.04	1.19	0.3398
500	6.7	803.73	28.35	8825	93.95	1.06	0.3018
600	7.2	863.71	29.39	10590	102.92	0.97	0.2855
700	7.3	875.71	29.59	12355	111.17	0.89	0.2662
800	6.5	779.74	27.92	14120	118.84	0.84	0.2349
900	6.2	743.75	27.27	15885	126.05	0.79	0.2163
1000	5.9	707.76	26.60	17650	132.87	0.75	0.2002

TABLE 52
Rheological Data (Sample 84)
Measurement of $nA^{\frac{1}{2}}$
Cone and Plate Viscometer

Speed RPM	Reading	rA Shear Stress dynes/cm^2	$rA^{\frac{1}{2}}$	Shear Rate $\dot{\gamma}$ (Sec^{-1})	$\dot{\gamma}^{\frac{1}{2}}$	$\frac{1}{\dot{\gamma}^{\frac{1}{2}}}$ X10^{-2}	$\frac{rA^{\frac{1}{2}}}{\dot{\gamma}^{\frac{1}{2}}} = nA^{\frac{1}{2}}$
100	4.5	539.8	23.2	1765	42.02	2.38	0.552
200	4.0	479.8	21.9	3530	59.42	1.68	0.368
300	3.0	359.9	19.0	5295	72.77	1.37	0.261
400	2.8	335.9	18.3	7060	84.04	1.19	0.218
500	3.0	359.9	19.0	8825	93.95	1.06	0.202
600	3.5	419.9	20.5	10590	102.92	0.97	0.199
700	2.0	239.9	15.5	12355	111.17	0.89	0.139
800	1.5	179.9	13.4	14120	118.84	0.84	0.113
900	1.5	179.9	13.4	15885	126.05	0.79	0.106
1000	1.5	179.9	13.4	17650	132.87	0.75	0.101

TABLE 53
Rheological Data (Sample 85)
Measurement of $n_A^{\frac{1}{2}}$
Cone and Plate Viscometer

Speed RPM	Reading	rA Shear Stress dynes/cm^2	$rA^{\frac{1}{2}}$	Shear Rate $\dot{\gamma}$ (Sec^{-1})	$\dot{\gamma}^{\frac{1}{2}}$	$\frac{1}{\dot{\gamma}^{\frac{1}{2}}}$ X10^{-2}	$\frac{rA^{\frac{1}{2}}}{\dot{\gamma}^{\frac{1}{2}}} = nA^{\frac{1}{2}}$
100	7.0	839.7	28.97	1765	42.02	2.38	0.690
200	10.0	1199.6	34.64	3530	59.42	1.68	0.580
300	11.0	1319.6	36.33	5295	72.77	1.37	0.500
400	13.5	1619.5	40.24	7060	84.04	1.19	0.478
500	17.0	2039.3	45.16	8825	93.95	1.06	0.481
600	19.0	2279.2	47.74	10590	102.92	0.97	0.464
700	21.0	2519.1	50.19	12355	111.17	0.89	0.451
800	22.5	2699.1	51.95	14120	118.84	0.84	0.437
900	24.0	2879.0	53.66	15885	126.05	0.79	0.425
1000	28.0	3358.9	57.95	17650	132.87	0.75	0.4361

TABLE 54
Rheological Data (Sample 86)
Measurement of $n_A^{\frac{1}{2}}$
Cone and Plate Viscometer

Speed RPM	Reading	r_A Shear Stress dynes/cm^2	$r_A^{\frac{1}{2}}$	Shear Rate $\dot{\gamma}$ (Sec^{-1})	$\dot{\gamma}^{\frac{1}{2}}$	$\frac{1}{\dot{\gamma}^{\frac{1}{2}}}$ X10^{-2}	$\frac{r_A^{\frac{1}{2}}}{\dot{\gamma}^{\frac{1}{2}}} = n_A^{\frac{1}{2}}$
100	5.3	635.79	25.21	1765	42.02	2.38	0.600
200	5.0	599.8	24.49	3530	59.42	1.68	0.412
300	4.0	479.84	21.91	5295	72.77	1.37	0.301
400	4.7	563.81	23.74	7060	84.04	1.19	0.283
500	4.5	539.82	23.23	8825	93.95	1.06	0.247
600	4.9	587.80	24.24	10590	102.92	0.97	0.236
700	5.0	599.80	24.49	12355	111.17	0.89	0.220
800	4.8	575.81	23.99	14120	118.84	0.84	0.202
900	3.6	431.85	20.78	15885	126.05	0.79	0.165
1000	2.7	323.89	17.99	17650	132.87	0.75	0.1354

TABLE 55

Rheological Data (0.5% PVA Solution)

Measurement of $n_A^{\frac{1}{2}}$

Cone and Plate Viscometer

Speed RPM	Reading	r_A Shear Stress dynes/cm^2	$r_A^{\frac{1}{2}}$	Shear Rate $\dot{\gamma}$ (Sec^{-1})	$\dot{\gamma}^{\frac{1}{2}}$	$\frac{1}{\dot{\gamma}^{\frac{1}{2}}}$ X10^{-2}	$\frac{r_A^{\frac{1}{2}}}{\dot{\gamma}^{\frac{1}{2}}} = n_A^{\frac{1}{2}}$
100	0	-	-	1765	42.02	2.38	
200	0	-	-	3530	59.42	1.68	
300	0.1	11.99	3.463	5295	72.77	1.37	.0476
400	0.2	23.99	4.898	7060	84.04	1.19	.0583
500	0.45	53.98	7.347	8825	93.95	1.06	.0782
600	0.60	71.98	8.484	10590	102.92	0.97	.0824
700	0.75	89.97	9.485	12355	111.17	0.89	.0853
800	0.85	101.97	10.098	14120	118.84	0.84	.0850
900	1.00	119.96	10.953	15885	126.05	0.79	.0869
1000	1.35	161.95	12.726	17650	132.87	0.75	.0957

TABLE 56

Rheological Data (1.0% PVA Solution)
Measurement of $n_A^{\frac{1}{2}}$
Cone and Plate Viscometer

Speed RPM	Reading	r_A Shear Stress dynes/cm^2	$r_A^{\frac{1}{2}}$	Shear Rate $\dot{\gamma}$ (Sec^{-1})	$\dot{\gamma}^{\frac{1}{2}}$	$\frac{1}{\dot{\gamma}^{\frac{1}{2}}}$ X10^{-2}	$\frac{r_A^{\frac{1}{2}}}{\dot{\gamma}^{\frac{1}{2}}} = n_A^{\frac{1}{2}}$
100	0			1765	42.02	2.38	
200	0.1	11.99	3.462	3530	59.42	1.68	.0583
300	0.25	29.99	5.476	5295	72.77	1.37	.0753
400	0.50	59.98	7.745	7060	84.04	1.19	.0922
500	0.75	89.97	9.485	8825	93.95	1.06	0.1009
600	1.00	119.96	10.953	10590	102.92	0.97	0.1064
700	1.30	155.94	12.488	12355	111.17	0.89	0.1123
800	1.70	203.93	14.280	14120	118.84	0.84	0.1202
900	2.00	239.92	15.489	15885	126.05	0.79	0.1229
1000	2.30	275.91	16.610	17650	132.87	0.75	0.1250

TABLE 57
Rheological Data (2.0% PVA Solution)
Measurement of $n_A^{\frac{1}{2}}$
Cone and Plate Viscometer

Speed RPM	Reading	τ_A Shear Stress dynes/cm^2	$\tau_A^{\frac{1}{2}}$	Shear Rate $\dot{\gamma}$ (Sec^{-1})	$\dot{\gamma}^{\frac{1}{2}}$	$\frac{1}{\dot{\gamma}^{\frac{1}{2}}}$ X10^{-2}	$\frac{\tau_A^{\frac{1}{2}}}{\dot{\gamma}^{\frac{1}{2}}} = n_A^{\frac{1}{2}}$
100	0.25	29.99	5.476	1765	42.02	2.38	0.1303
200	0.50	59.98	7.745	3530	59.42	1.68	0.1303
300	0.75	89.97	9.485	5295	72.77	1.37	0.1303
400	1.50	179.94	13.414	7060	84.04	1.19	0.1596
500	2.00	239.92	15.489	8825	93.95	1.06	0.1649
600	2.75	329.89	18.163	10590	102.92	0.97	0.1765
700	3.50	419.86	20.490	12355	111.17	0.89	0.1843
800	4.00	479.84	21.905	14120	118.84	0.84	0.1843
900	4.75	569.81	23.871	15885	126.05	0.79	0.1894
1000	5.50	659.78	25.686	17650	132.87	0.75	0.1933

TABLE 58

Rheological Data (4.0% PVA Solution)

Measurement of $n_A^{\frac{1}{2}}$

Cone and Plate Viscometer

Speed RPM	Reading	rA Shear Stress dynes/cm^2	$rA^{\frac{1}{2}}$	Shear Rate $\dot{\gamma}$ (Sec^{-1})	$\dot{\gamma}^{\frac{1}{2}}$	$\frac{1}{\dot{\gamma}^{\frac{1}{2}}}$ X10^{-2}	$\frac{rA^{\frac{1}{2}}}{\dot{\gamma}^{\frac{1}{2}}} = nA^{\frac{1}{2}}$
100	1.0	119.96	10.950	1765	42.02	2.38	0.2606
200	4.0	479.84	21.905	3530	59.42	1.68	0.3686
300	7.0	839.72	28.978	5295	72.77	1.37	0.3982
400	9.5	1139.62	33.758	7060	84.04	1.19	0.4017
500	12.0	1439.52	37.941	8825	93.95	1.06	0.4038
600	14.5	1739.42	41.706	10590	102.92	0.97	0.4052
700	17.0	2039.32	45.159	12355	111.17	0.89	0.4062
800	19.5	2339.22	48.365	14120	118.84	0.84	0.4070
900	22.0	2639.12	51.372	15885	126.05	0.79	0.4076
1000	24.5	2939.02	54.212	17650	132.87	0.75	0.4080

TABLE 59

Calculation of Bonding Energy in a Spherical Agglomerate of Polystyrene Protective Colloid Concentration Varied Between 0.5% and 4.0%

Exp.No.	Plot $n_A^{\frac{1}{2}} - \frac{1}{\dot{\gamma}^{\frac{1}{2}}}$ Slope	$n_8^{\frac{1}{2}}$	$n_0^{\frac{1}{2}}$	$OC^{\frac{1}{2}}$	$\frac{D}{d} - 1$	$F_A^{\frac{1}{2}}$	FA Dynes/cm^2	$fa=fad^2$ Dynes Per Pair
84 (0.5% PVA)	28.02	0.1010	0.0957	.0554	1265	0.3998	0.1598	0.36×10^{-10}
				D = 190 microns d = 0.15 "				
86 (1.0% PVA)	29.37	0.1354	0.1250	.0832	999	.3536	0.1249	0.12×10^{-10}
				D = 100 microns d = 0.10 "				
83 (2.0% PVA)	28.74	0.2002	0.1933	.0357	943	.8537	0.7288	0.59×10^{-10}
				D = 85 microns d = 0.09 "				
85 (4.0% PVA)	17.20	0.4361	0.4080	.0688	599	0.4174	0.1742	0.17×10^{-10}
				D = 60 microns d = 0.10 "				
							Average Bonding Force	0.31×10^{-10} Dynes Per Pair

TABLE 60

Effect of Protective Colloid Level on Agglomerate Size

% Poly Vinyl Alcohol & Agglomerate Size Ratios

Exp No	% (52.22 Grade PVA)	d (u) Microns	D (u) Microns	$\frac{d}{D}$	$\frac{D}{d}$	Monomer
84	0.5	.15	190.0	0.78×10^{-3}	1266	St
86	1.0	.10	100.0	1×10^{-3}	1000	St
83	2.0	.09	85.0	1.06×10^{-3}	944	St
85	4.0	0.10	60.0	1.66×10^{-2}	600	St

Fixed Stirrer Geometry and Stirrer Speed (N = 300 RPM)
D = Agglomerate Diameter (Coulter Counter Data)
d = Primary Particle Diameter (SEM)

Key to Monomer Used:

St = Styrene

TABLE 61

The Polymerisation System
Fibre Agglomeration

Water	800.0
Poly Vinyl Alcohol (1)	2.0
Difunctional Monomer (2)	4.4
Monomer (3)	188.0
Methacrylic Acid	3.0
Benzoyl Peroxide (70%)	2.6
	1000.0

(1) Various grades (DuPont Elvanol Grades)

(2) Neopentyl glycol diacrylate

(3) Styrene/Methlmethacrylate

TABLE 62
Rheological Data
Fibre Agglomerate
Cone and Plate Viscometer

Speed (RPM)	Reading	Cone Constant	Viscosity (Poise)	$\sqrt{u}$	$\sqrt{u}$ X 10	$\dot{\gamma}$ (sec^{-1})	$\frac{l_1}{\dot{\gamma}_2}$ X10
100	7.5	6.73	0.5047	0.7104	7.100	1765	2.38
200	6.5	"	0.2187	0.4676	4.680	3530	1.68
300	5.0	"	0.1122	0.3349	3.350	5295	1.37
400	4.5	"	0.0757	0.2751	2.750	7060	1.19
500	4.0	"	0.0538	0.2319	2.320	8825	1.06
600	3.5	"	0.0392	0.1980	1.980	10590	0.97
700	3.5	"	0.0336	0.1833	1.830	12355	0.89
800	3.0	"	0.0252	0.1587	1.587	14120	0.84
900	3.0	"	0.0224	0.1496	1.496	15885	0.79
1000	3.5	"	0.0235	0.1535	1.525	17650	0.75

TABLE 63

Rheological Data - Measurement of $n_A^{\frac{1}{2}}$ (Fibre Agglomerate)

Cone and Plate Viscometer

Speed RPM	Reading	r_A Shear Stress dynes/cm^2	$r_A^{\frac{1}{2}}$	Shear Rate $\dot{\gamma}$ (Sec^{-1})	$\dot{\gamma}^{\frac{1}{2}}$	$\frac{1}{\dot{\gamma}^{\frac{1}{2}}}$ X10^{-2}	$\frac{r_A^{\frac{1}{2}}}{\dot{\gamma}^{\frac{1}{2}}} = n_A^{\frac{1}{2}}$
100	7.5	99.60	29.99	1765	42.02	2.38	0.7137
200	6.5	779.74	27.92	3530	59.42	1.68	0.4698
300	5.0	599.80	24.49	5295	72.77	1.37	0.3365
400	4.5	539.82	23.23	7060	84.04	1.19	0.2764
500	4.0	479.84	21.91	8825	93.95	1.06	0.2332
600	3.5	419.86	20.49	10590	102.92	0.97	0.1991
700	3.5	419.86	20.49	12355	111.17	0.89	0.1843
800	3.0	359.90	18.97	14120	118.84	0.84	0.1596
900	3.0	359.90	18.97	15885	126.05	0.79	0.1504
1000	3.5	419.86	20.49	17650	132.87	0.75	0.1542

TABLE 64

Calculation of Bonding Energy in a Fibre Agglomerate
Protective Colloid Concentration 0.5% PVA

Exp.No.	Plot $N_A^{\frac{1}{2}}$ $\frac{1}{\dot{\gamma}^{\frac{1}{2}}}$ Slope	$N_\infty^{\frac{1}{2}}$	$No^{\frac{1}{2}}$	$0\ C^{\frac{1}{2}}$	$\frac{D}{d}-1$	$FA^{\frac{1}{2}}$	FA Dynes/cm^2	fa = FAd^2 Dynes Per Pair of particles
(C8) Fibre Agglomgrate	30.36	0.1542	0.0957	0.6112	1049	0.0473	0.00224	0.22×10^{-12}
				D = 105 microns d = 0.10 "				

TABLE 65

Effect of Formulation Changes on the Agglomeration Process

Exp. No.	Poly Vinyl Alcohol (Grade)	wt/wt Concentration	Monomer Type	Difunctional Monomer	Concentration (C) % Monomer	Agglomeration Observed	Type of Agglomeration	
C1	52.22	0.5	St	None	0.0	Yes (Level)	Spherical	
C2	52.22	0.5	MMA	"	0.0	None	-	
C3	51.05	0.5	St	"	0.0	None	-	
C4	52.22	2.0	St	"	0.0	Yes (Reduced)	Spherical	PVA
C5	52.22	0.2	St	"	0.0	Yes (Increased)	Spherical	Level
C6	52.22	2.5	St		0.5	None	-	PVA
C7	52.22	1.0	St	NPD	0.5	Yes (Reduced)	Fibre	Concentration
C8	52.22	0.5	St	NPD	0.5	Yes (Normal)	Fibre	Change
C9	52.22	0.2	St	NPD	0.5	Yes (Increased)	Fibre	
C10	52.22	0.5	St	NPD	0.5	Yes	Fibre	PVA
C11	51.05	0.5	St	NPD	0.5	None	Fibre	Grade
C12	50.42	0.5	St	NPD	0.5	Yes (Much reduced)	Fibre	Change
C13	52.22	0.5	St	None	None	Yes	Spherical	Cross
C14	52.22	0.5	St	NPD	0.5	Yes	Fibre	linking level
C15	52.22	0.5	St	NPD	30.0	None	-	
C16	52.22	0.5	MMA	NPD	0.5	Yes	Fibre	Different
C17	52.22	0.5	MMA	NPD	0.2	Yes (Increased)	Fibre	Monomer
C18	52.22	0.5	St	NPD	0.5	Yes	Fibre	Different
C19	52.22	0.5	St	TPGD	0.5	Yes	Fibre	Cross linking
C20	52.22	0.5	St	DVB	0.5	Yes	Fibre	Monomer
C21	52.22	0.5	MMA	NPD	0.5	Yes	Fibre	Different
C22	52.22	0.5	MMA	TPGD	0.5	Yes	Fibre	Cross linking
C23	52.22	0.5	MMA	DVB	0.5	Yes	Fibre	Monomer

Key to Monomers used:

St = Styrene
MMA = Methyl Methacrylate
NPD = Neopentyldiacrylate
TPGD = Tripropyleneglycoldiacrylate.
DVB = Divinylbenzene

PVA Grade

51.05 (Reduced mol.wt)
50.42 (Increased mol. wt)

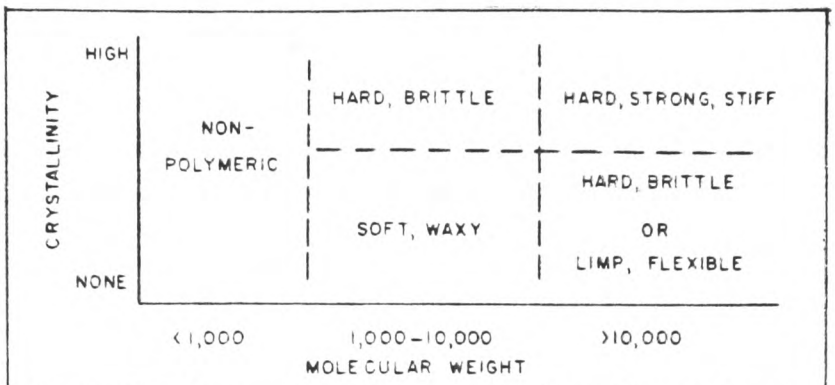

Fig. 1 Classification of the expected properties of materials on the basis of molecular weight and crystallinity.

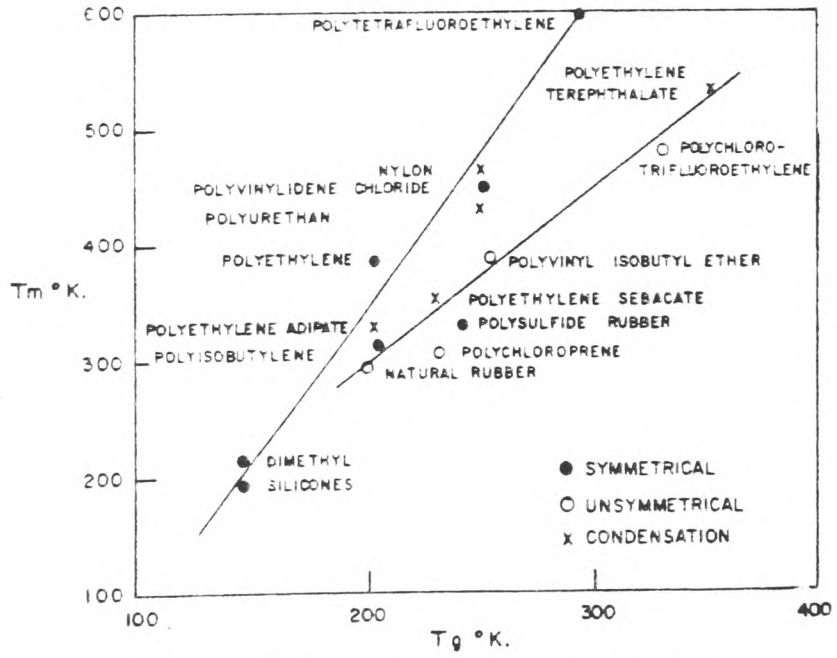

Fig. 2 Relation between T_m and T_g for various polymers

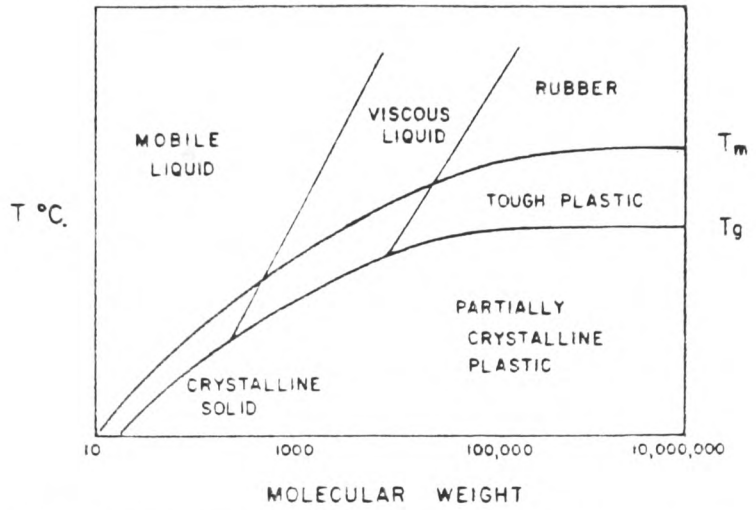

Fig 3 Relations among molecular weight, T_g, T_m, and polymer properties.

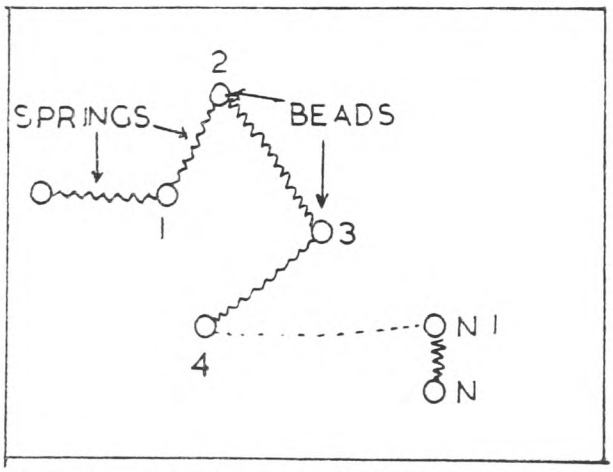

FIG 4 SPRING AND BEAD MODEL

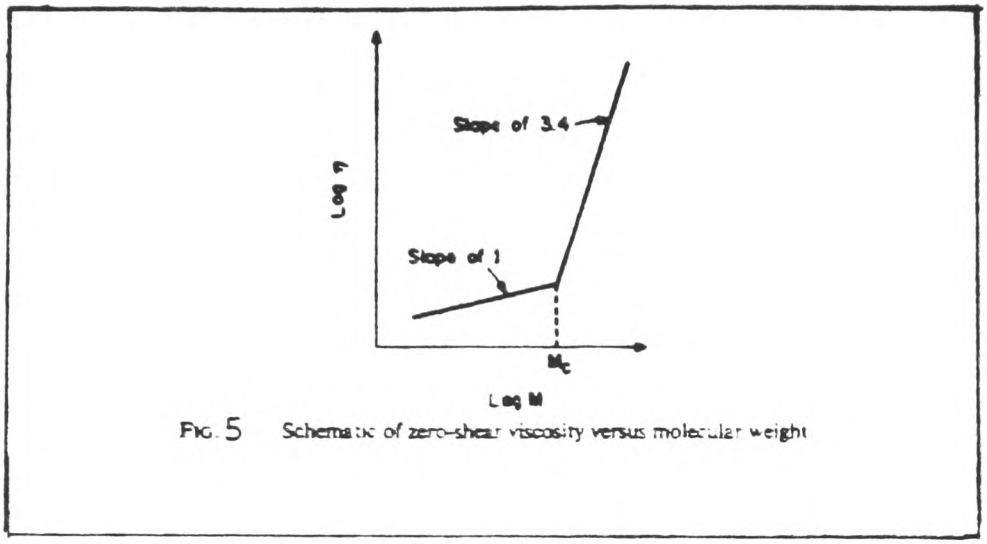

Fig. 5 Schematic of zero-shear viscosity versus molecular weight

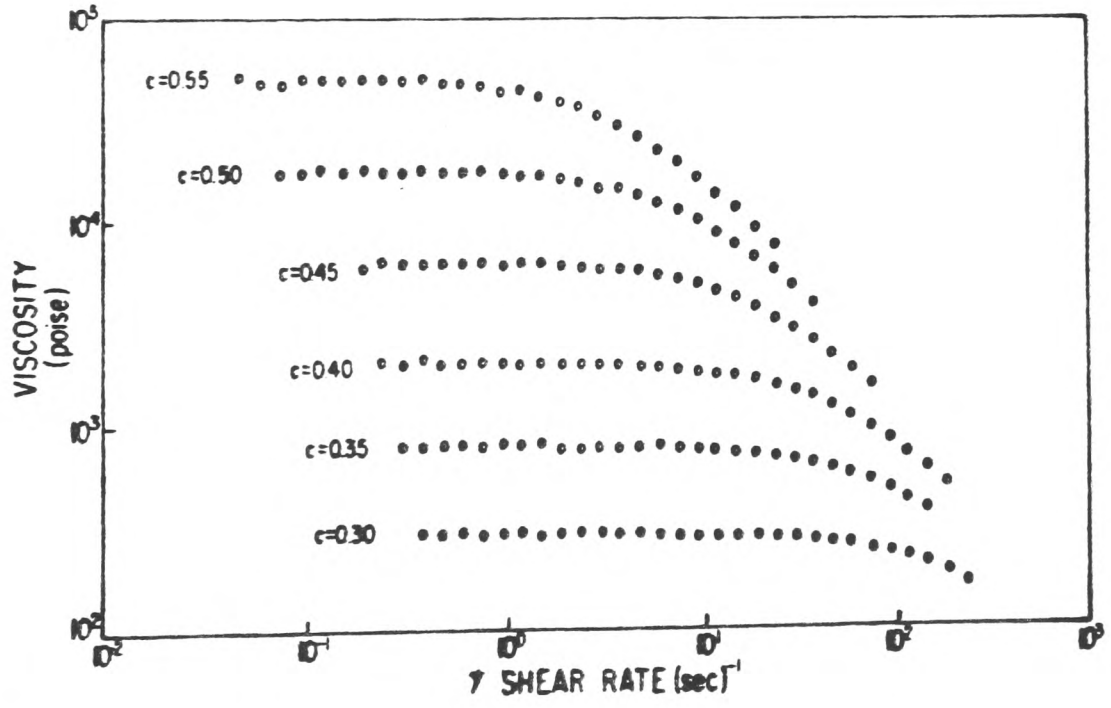

Fig. 6 Shear rate dependence of polystyrene solutions in n-butyl benzene at different concentrations (g/cc) at 30°C. Molecular weight = 411,000. [Reprinted from Trans. Soc. Rheol., 11, 267 (1967)].

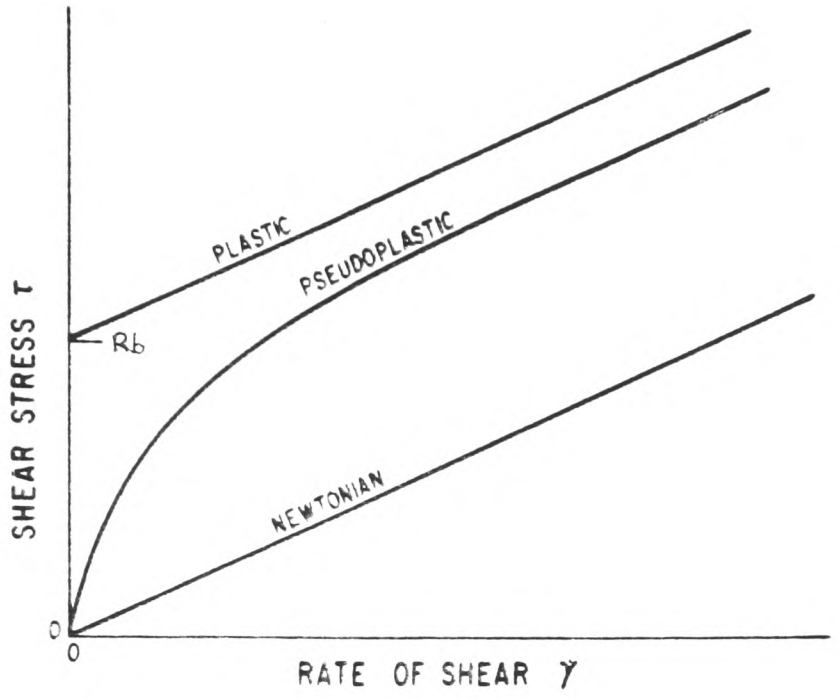

Figure 6a Typical flow curves for Newtonian, pseudoplastic, and plastic materials.

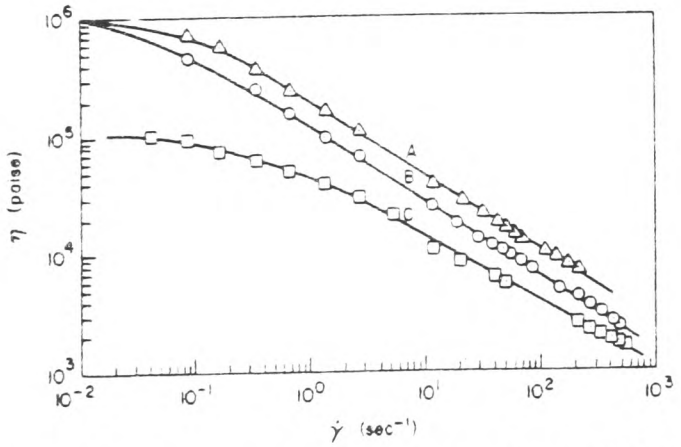

FIG. 7 Melt viscosity versus shear rate. (A) high-density polyethylene, $\bar{M}_w/\bar{M}_n = 16$; (B) high-density polyethylene, $\bar{M}_w/\bar{M}_n = 84$; (C) low-density polyethylene, $\bar{M}_w/\bar{M}_n = 20$

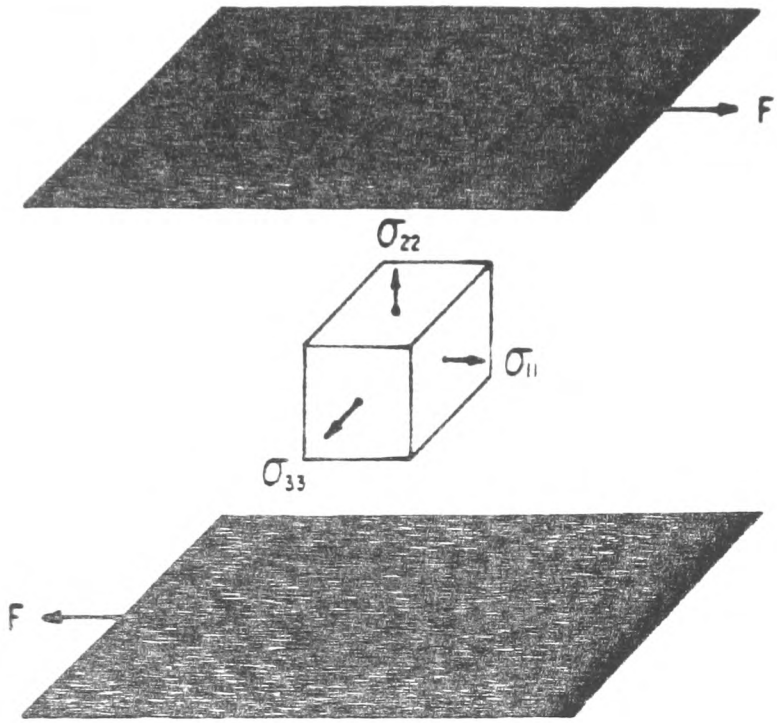

Fig. 8 Schematic diagram showing the notation for normal stresses in a shear field.

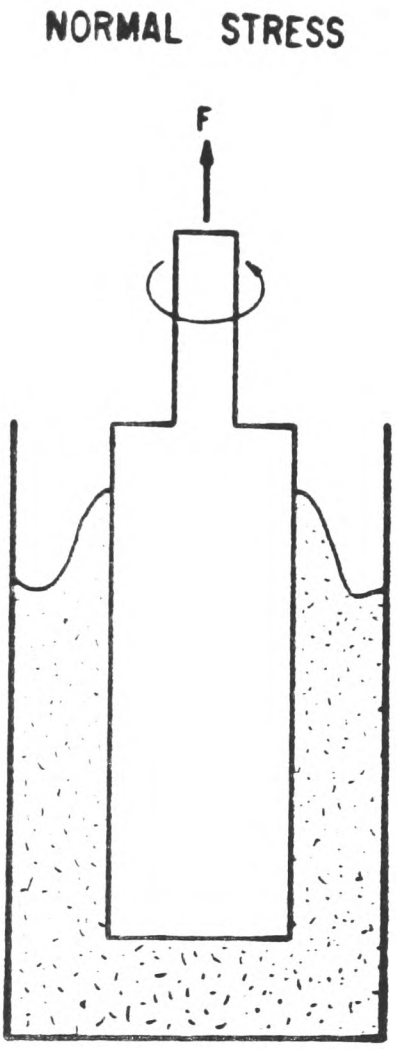

Figure 9 Creep of a polymeric liquid up the rotating inner cylinder of a coaxial cylinder rheometer.

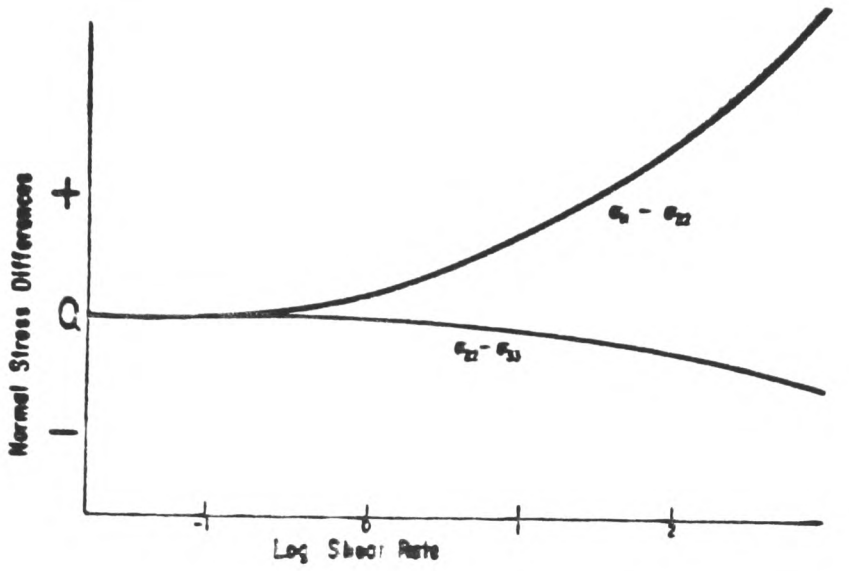

Figure 10 General behavior of the first and second normal stress differences in polymer melts and solutions as a function of rate of shear.

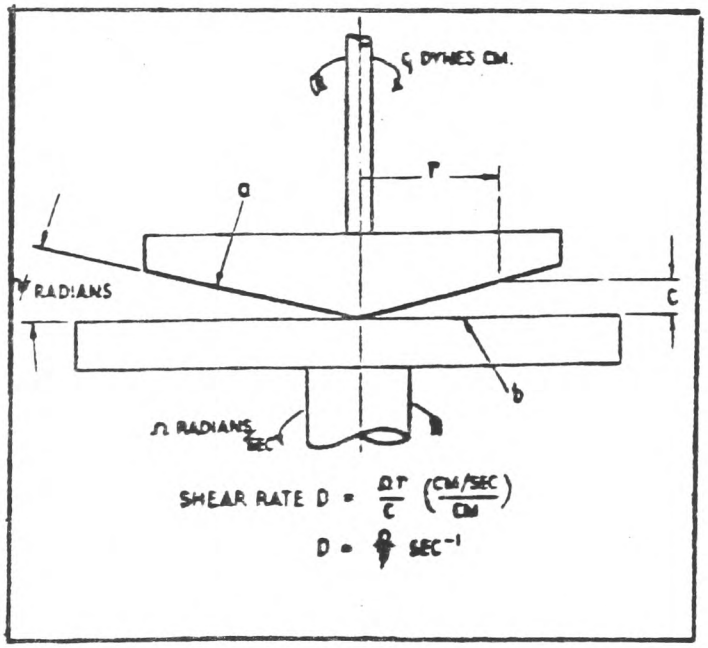

FIG 11 THE CONE AND PLATE VISCOMETER

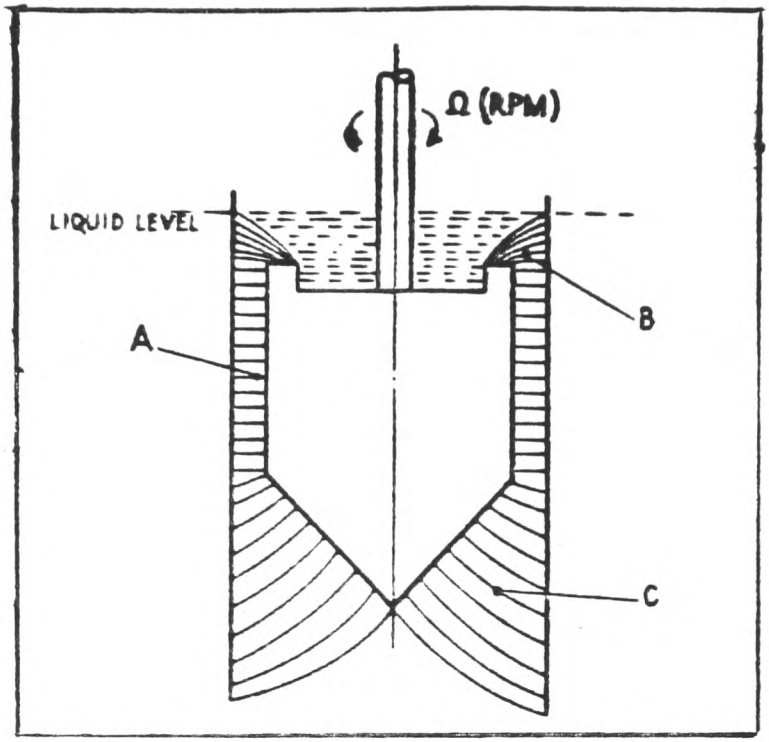

FIG 12 THE COAXIAL CYLINDER VISCOMETER

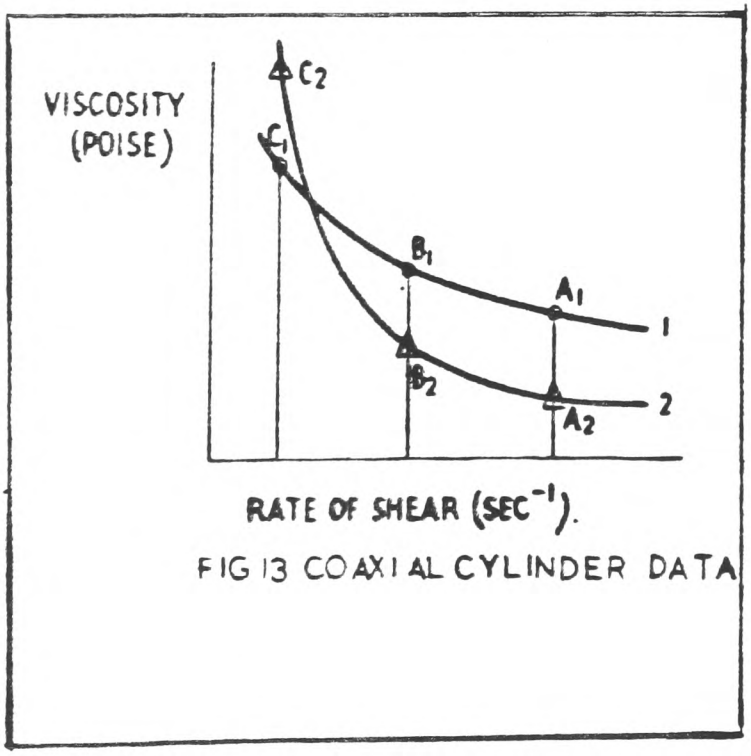

FIG 13 COAXIAL CYLINDER DATA

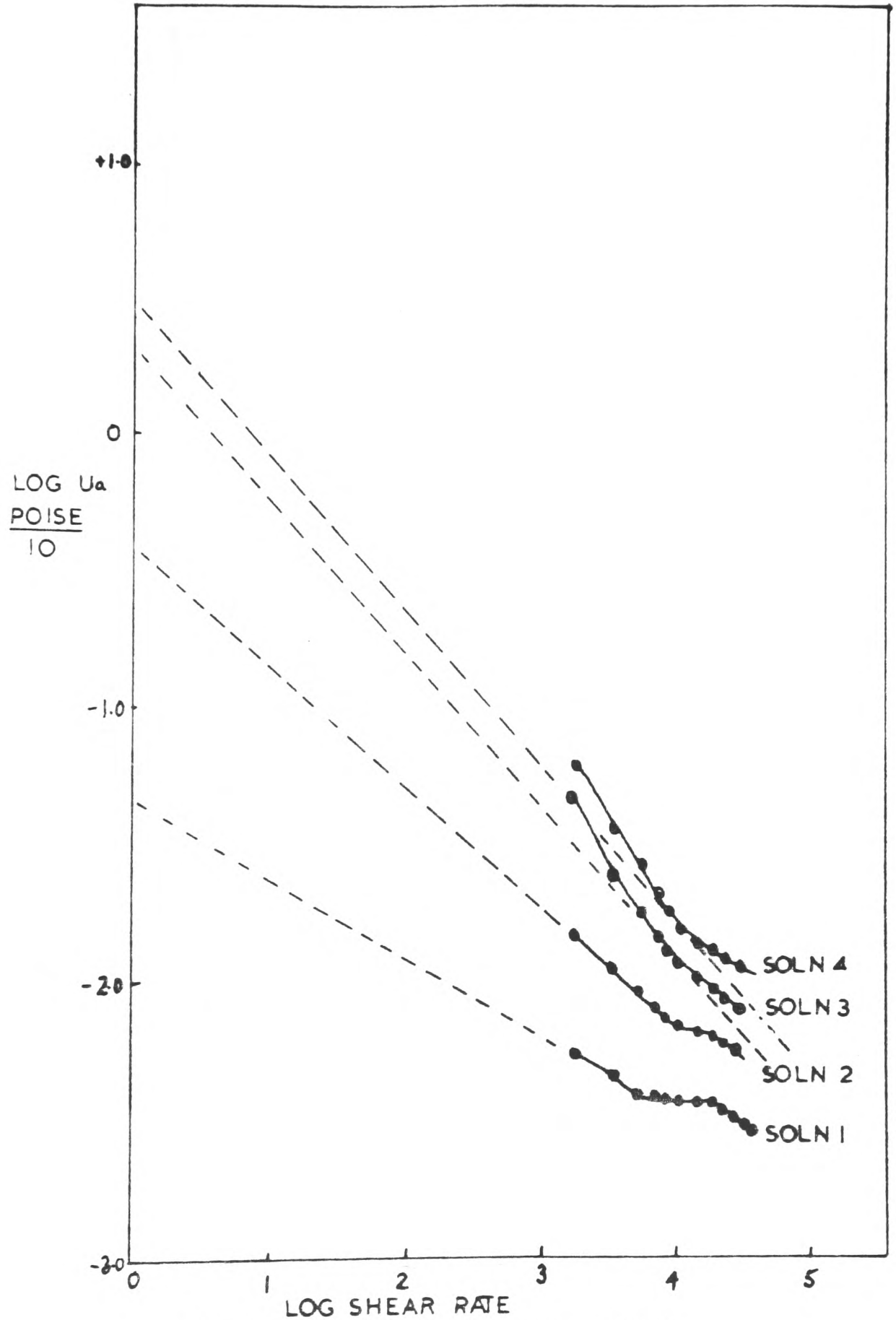

FIG 14 PLOT OF LOG U_a AGAINST LOG $\dot{Y}$
CONE AND PLATE DATA

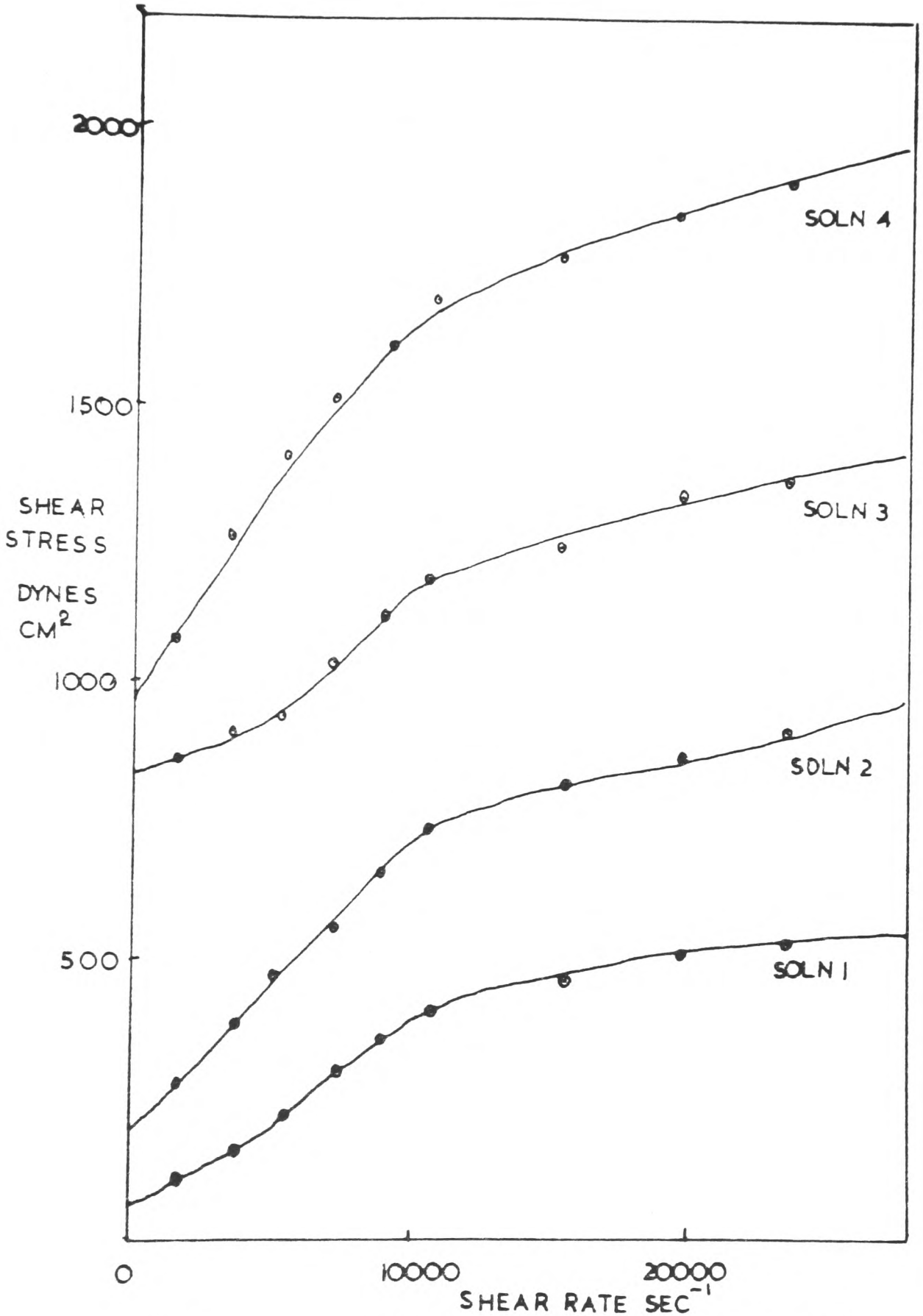

FIG 15 SHEAR STRESS AGAINST SHEAR RATE (CONE AND PLATE DATA)

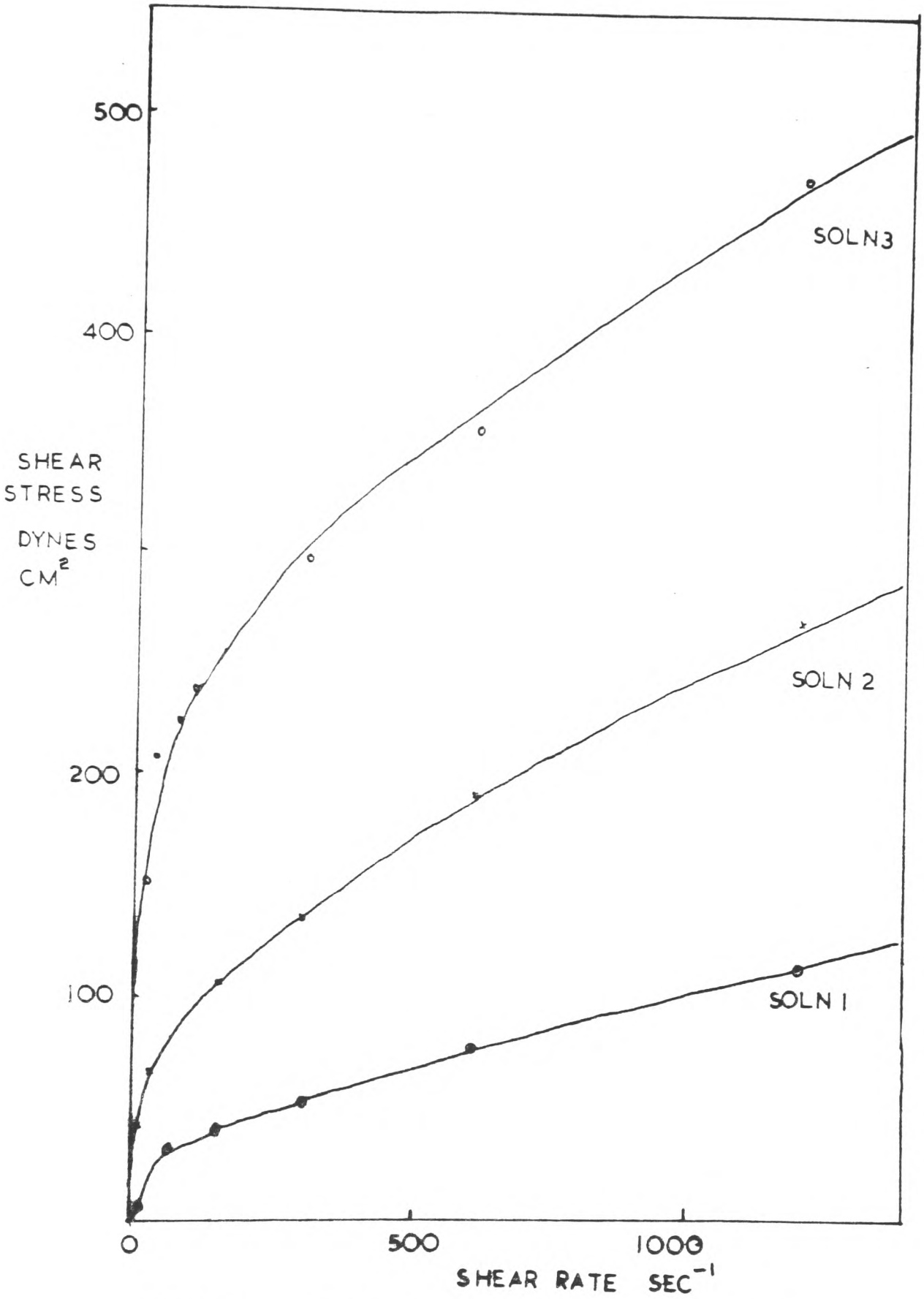

FIG 16 SHEAR STRESS AGAINST SHEAR RATE
(COAXIAL CYLINDER DATA)

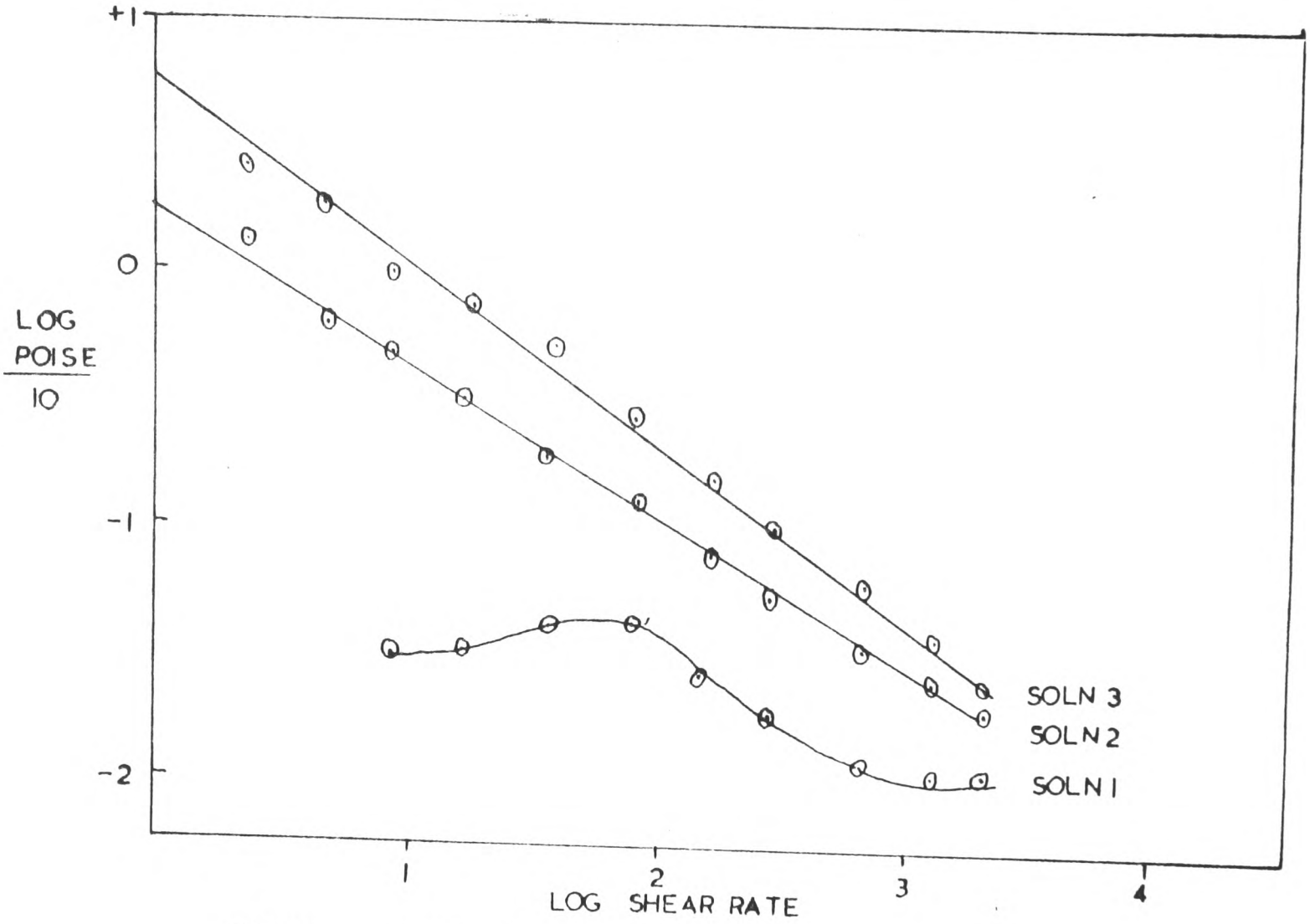

FIG 17 LOG POISE/10 AGAINST LOG SHEAR RATE
(COAXIAL CYLINDER DATA)

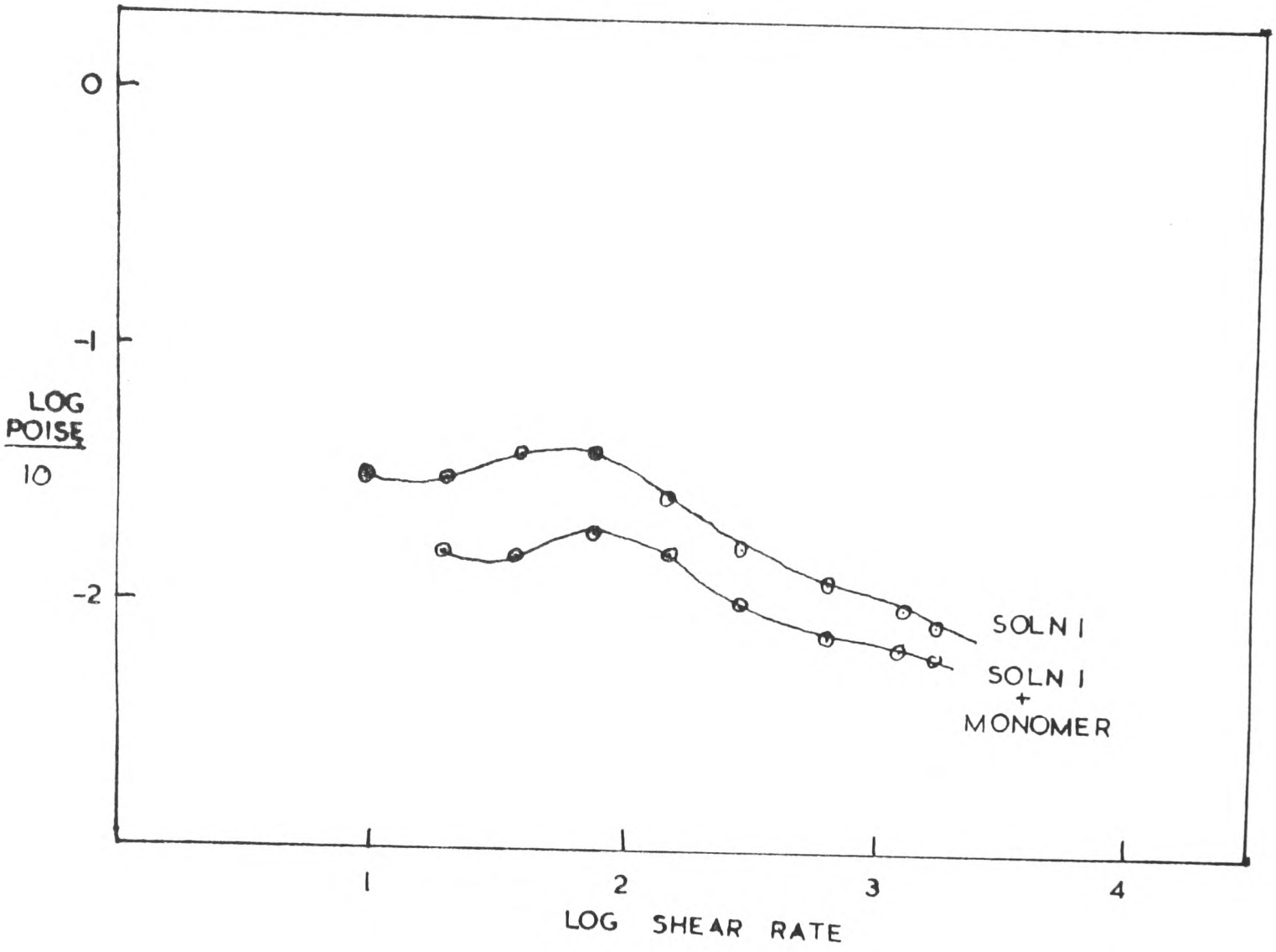

FIG 18 LOG POISE / 10 AGAINST LOG SHEAR RATE
(COAXIAL CYLINDER DATA)

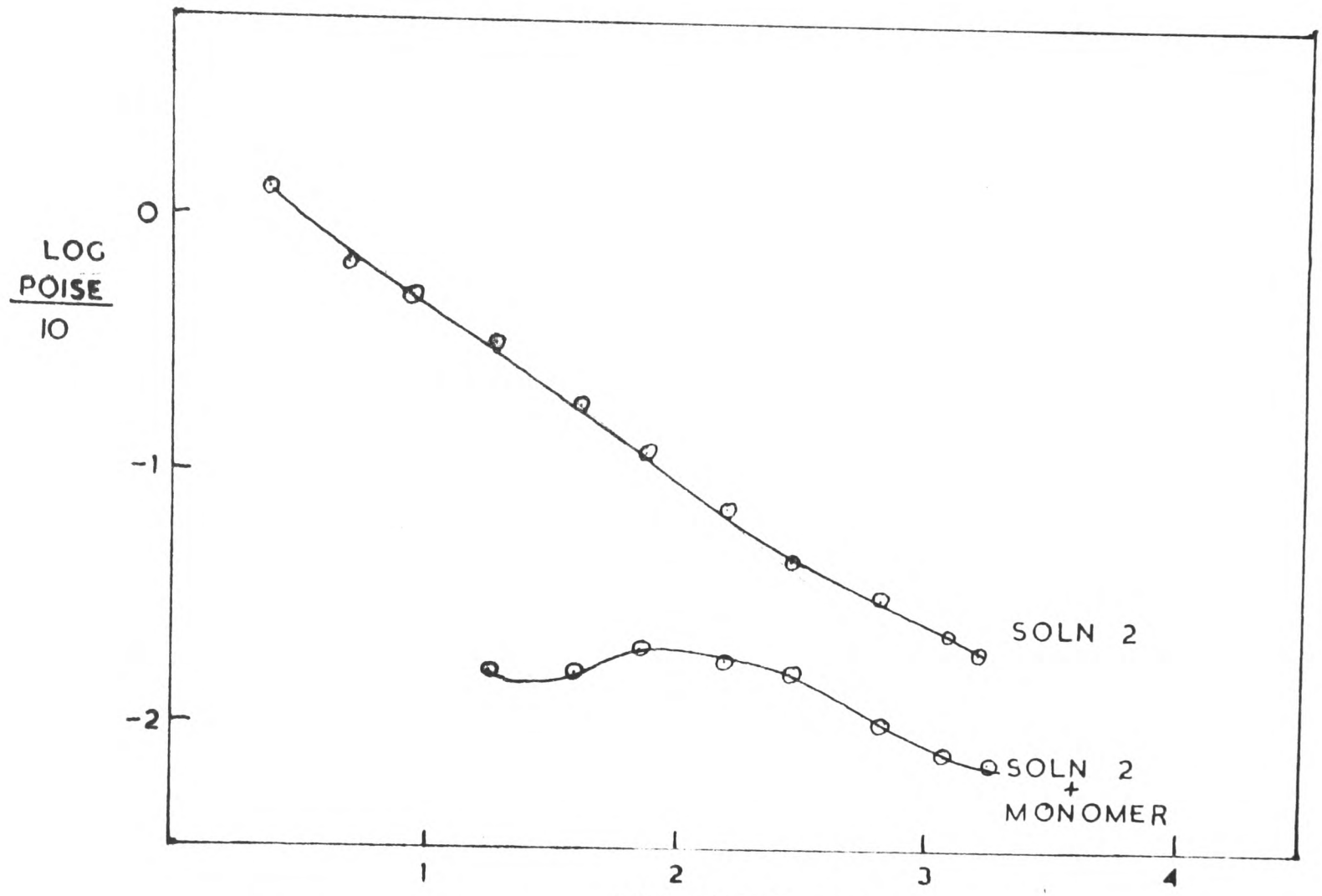

FIG 19 LOG POISE/10 AGAINST LOG SHEAR RATE
(COAXIAL CYLINDER DATA)

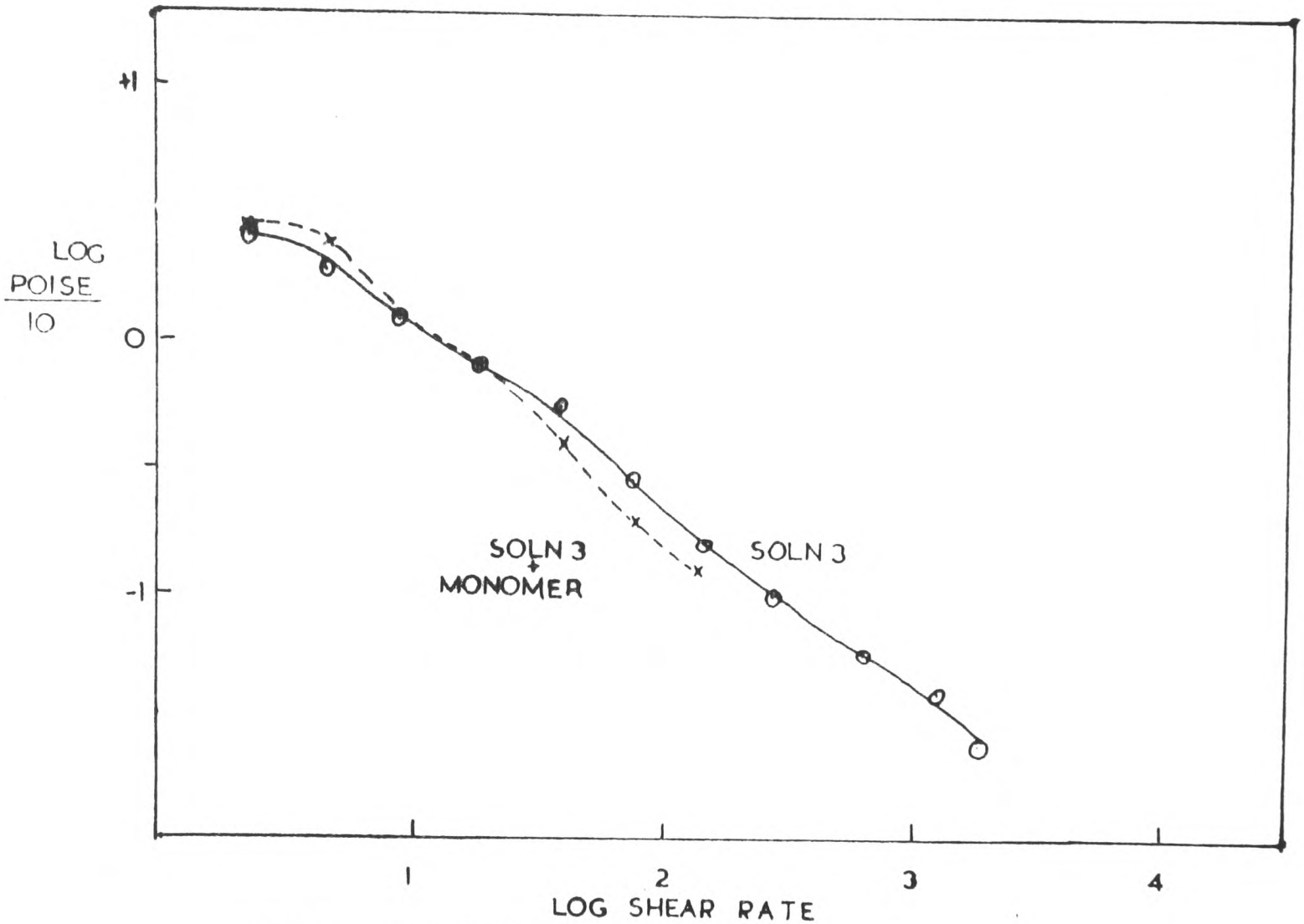

FIG 20 LOG POISE / 10 AGAINST LOG SHEAR RATE
(COAXIAL CYLINDER DATA)

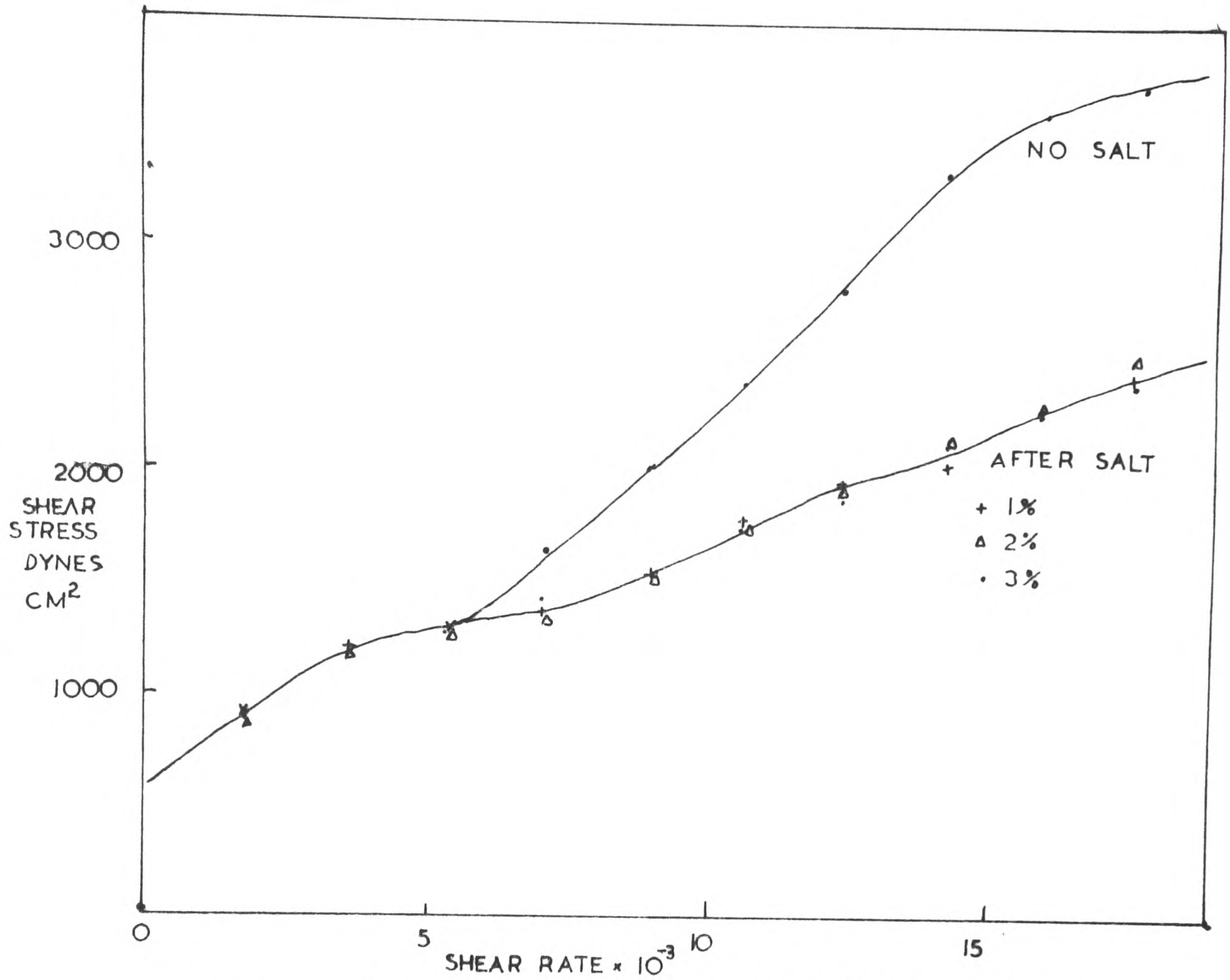

FIG 21 SHEAR STRESS AGAINST SHEAR RATE (SALT ADDITION)

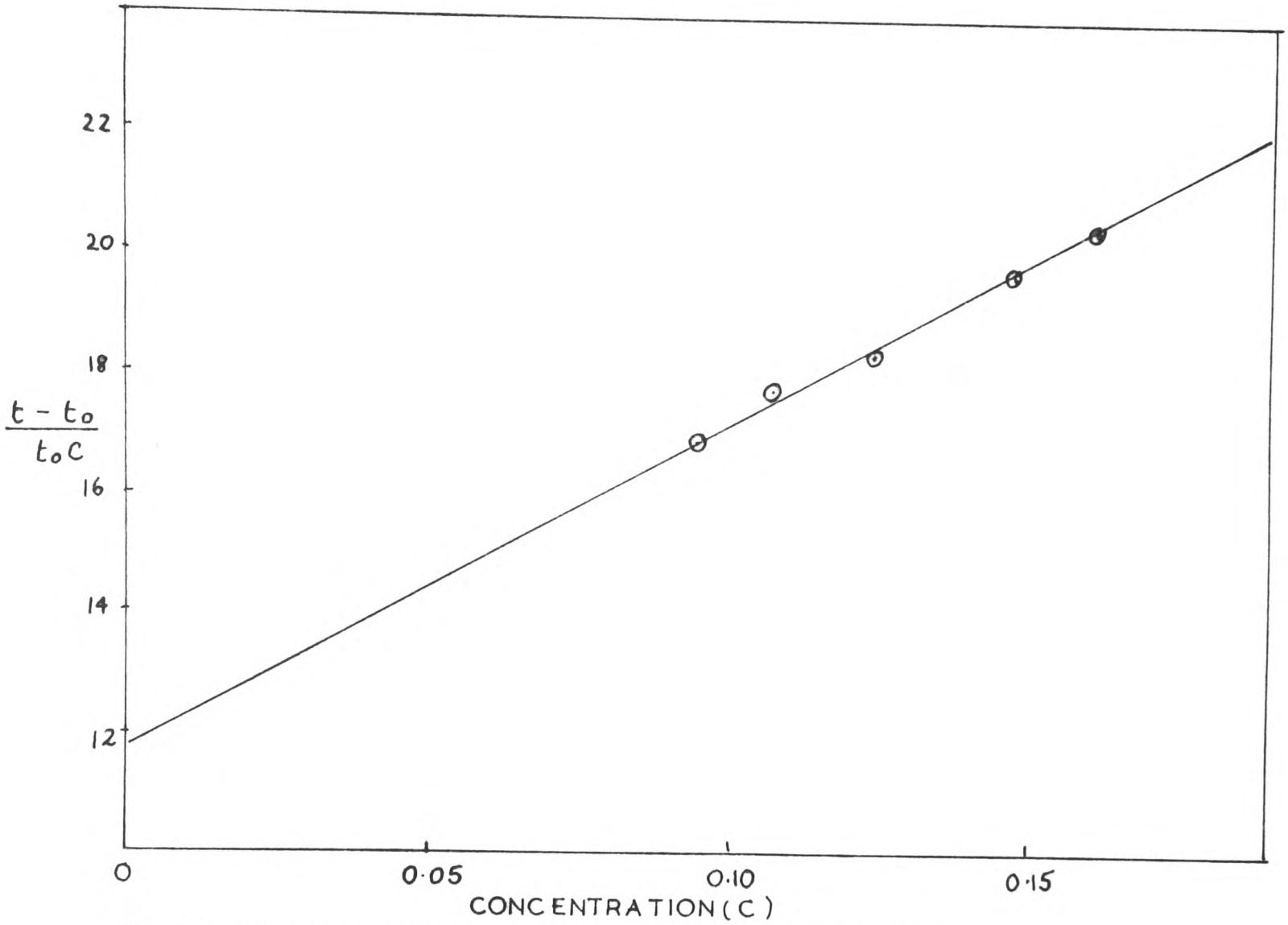

FIG 22 PLOT OF $\frac{t - t_o}{t_o C}$ AGAINST CONCENTRATION (C)

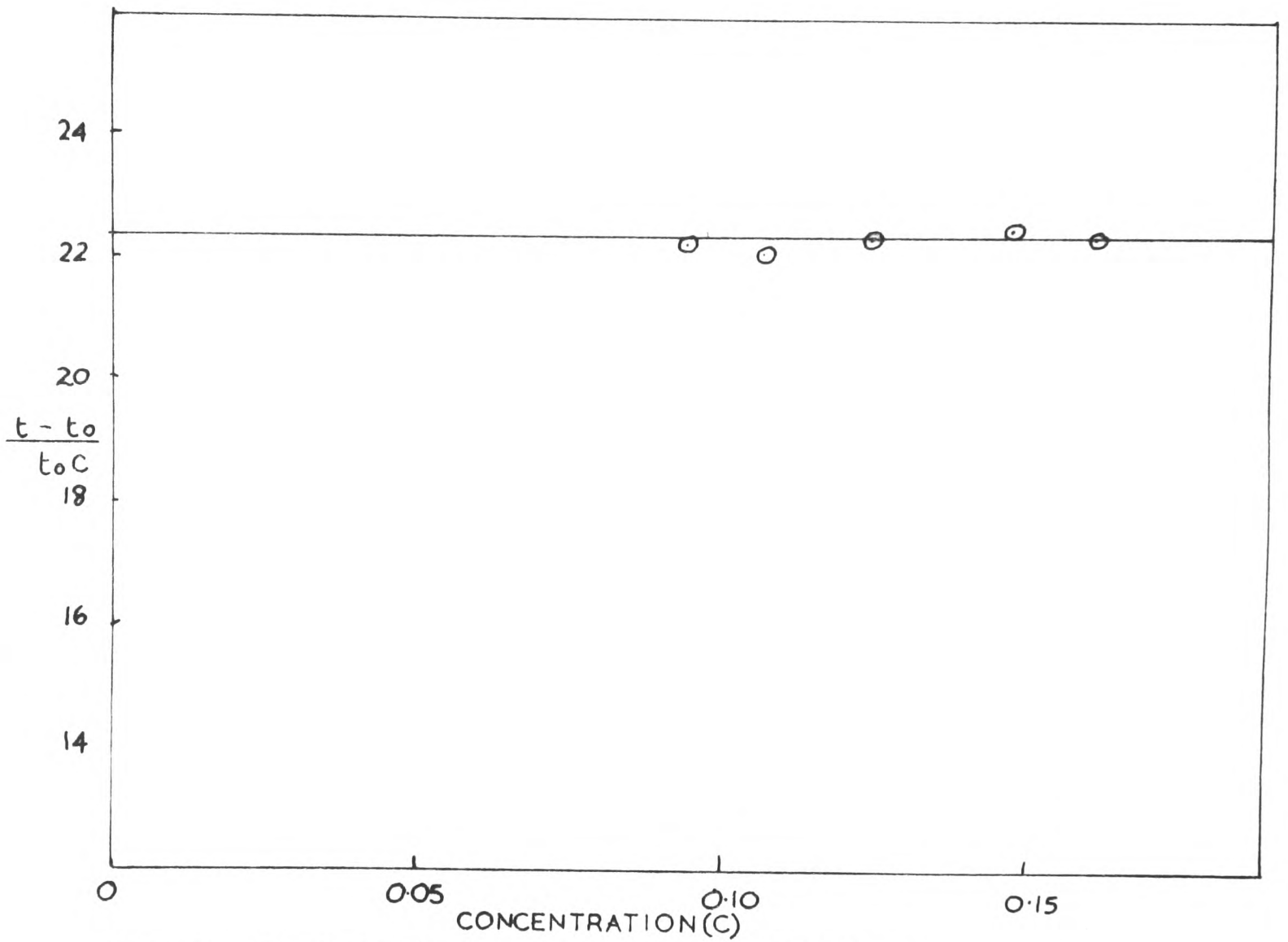

FIG 23 PLOT OF $\frac{t - to}{toC}$ AGAINST CONCENTRATION C

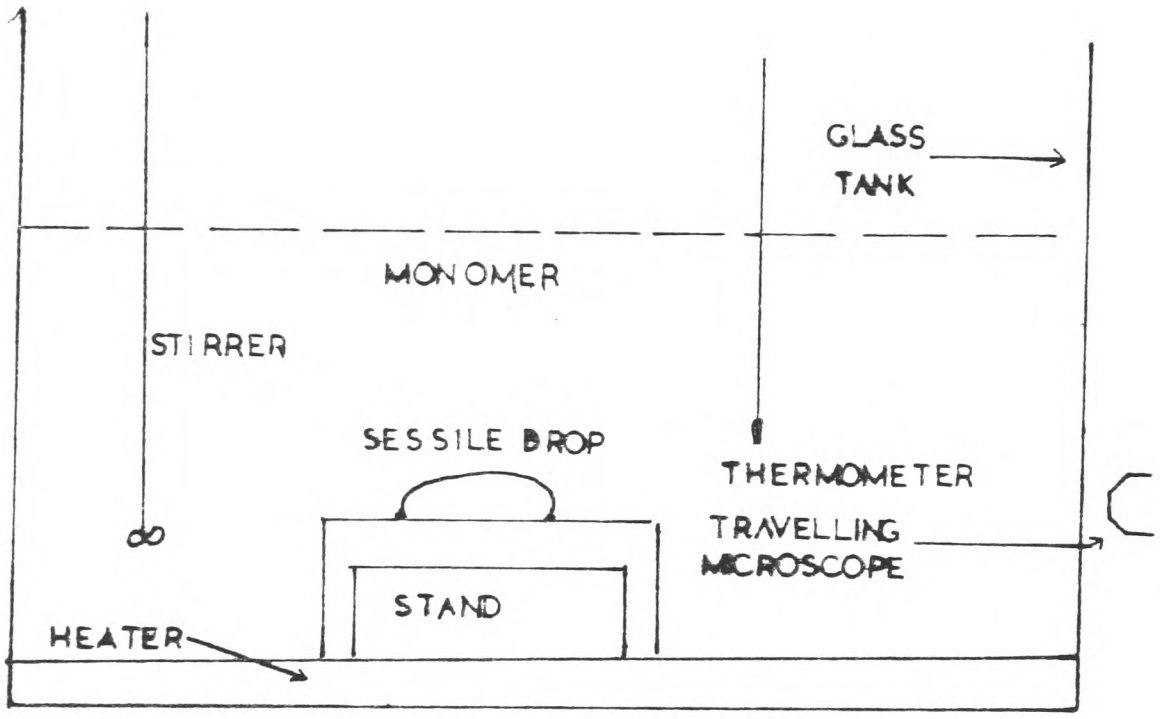

FIG 24 APPARATUS FOR SESSILE DROP MEASUREMENT

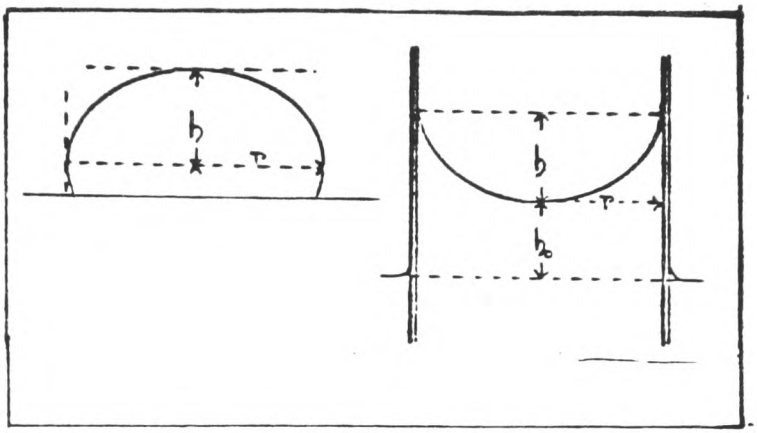

FIG 25 THE SESSILE DROP METHOD

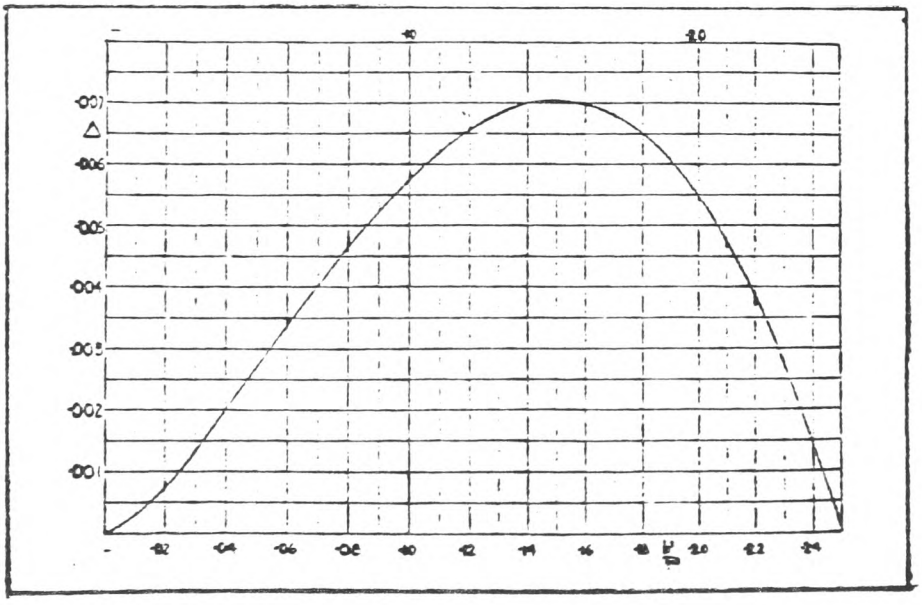

FIG 26 CORRECTION CURVE $\Delta/\frac{h^2}{r^2}$

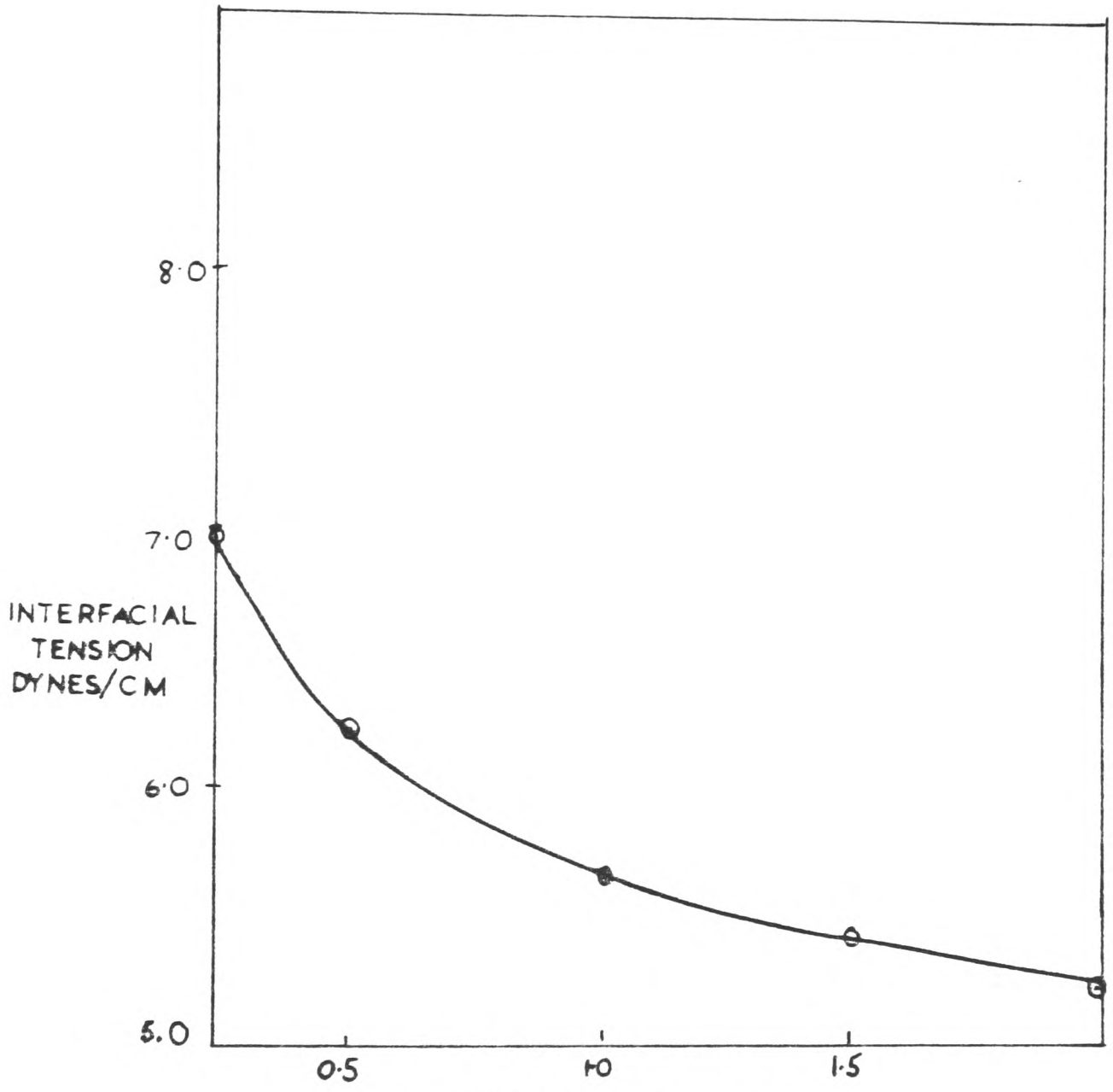

FIG 27 PLOT OF INTERFACIAL TENSION AGAINST COLLOID CONCENTRATION

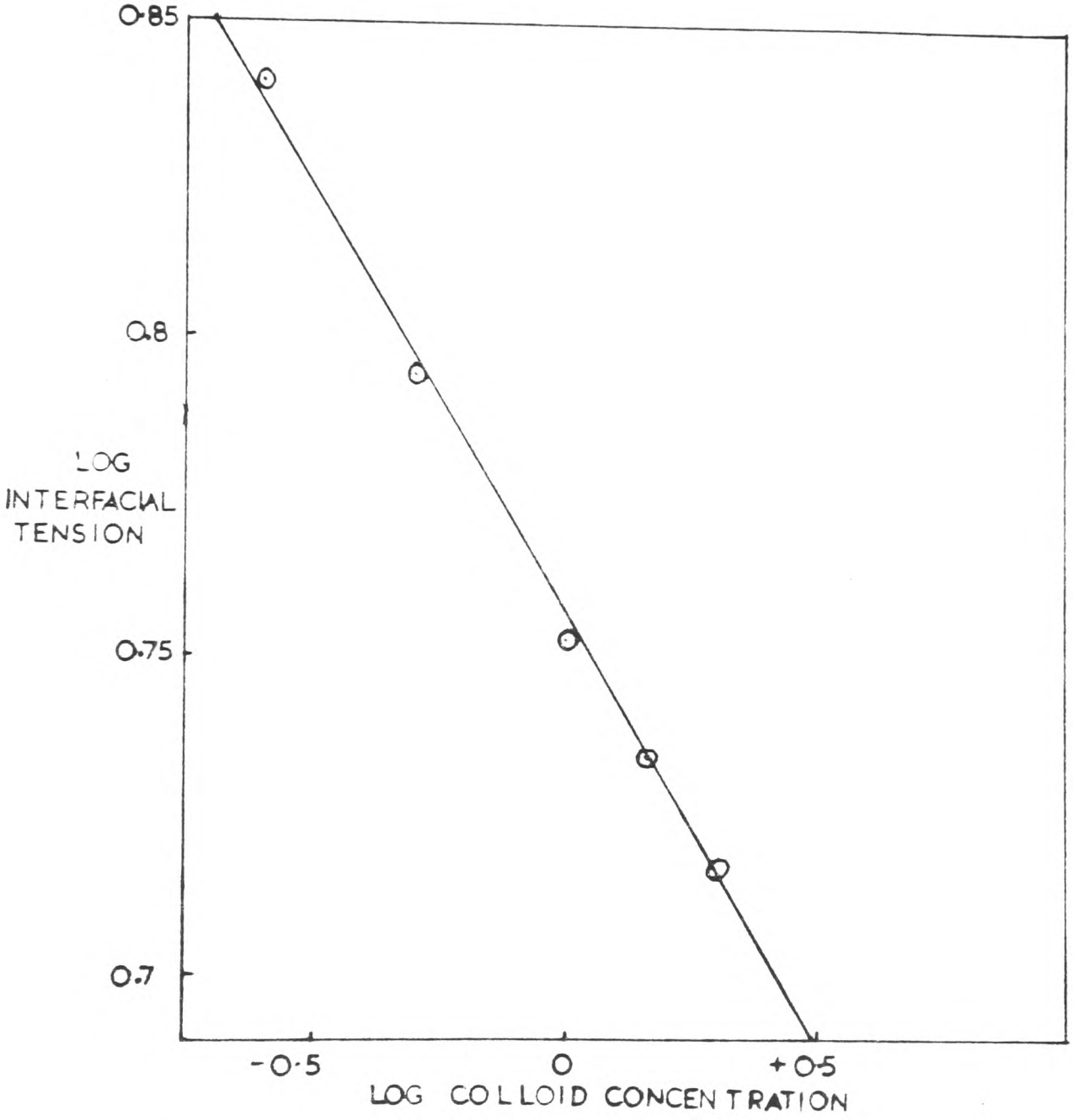

FIG 28 PLOT OF LOG INTERFACIAL TENSION AGAINST LOG COLLOID CONCENTRATION

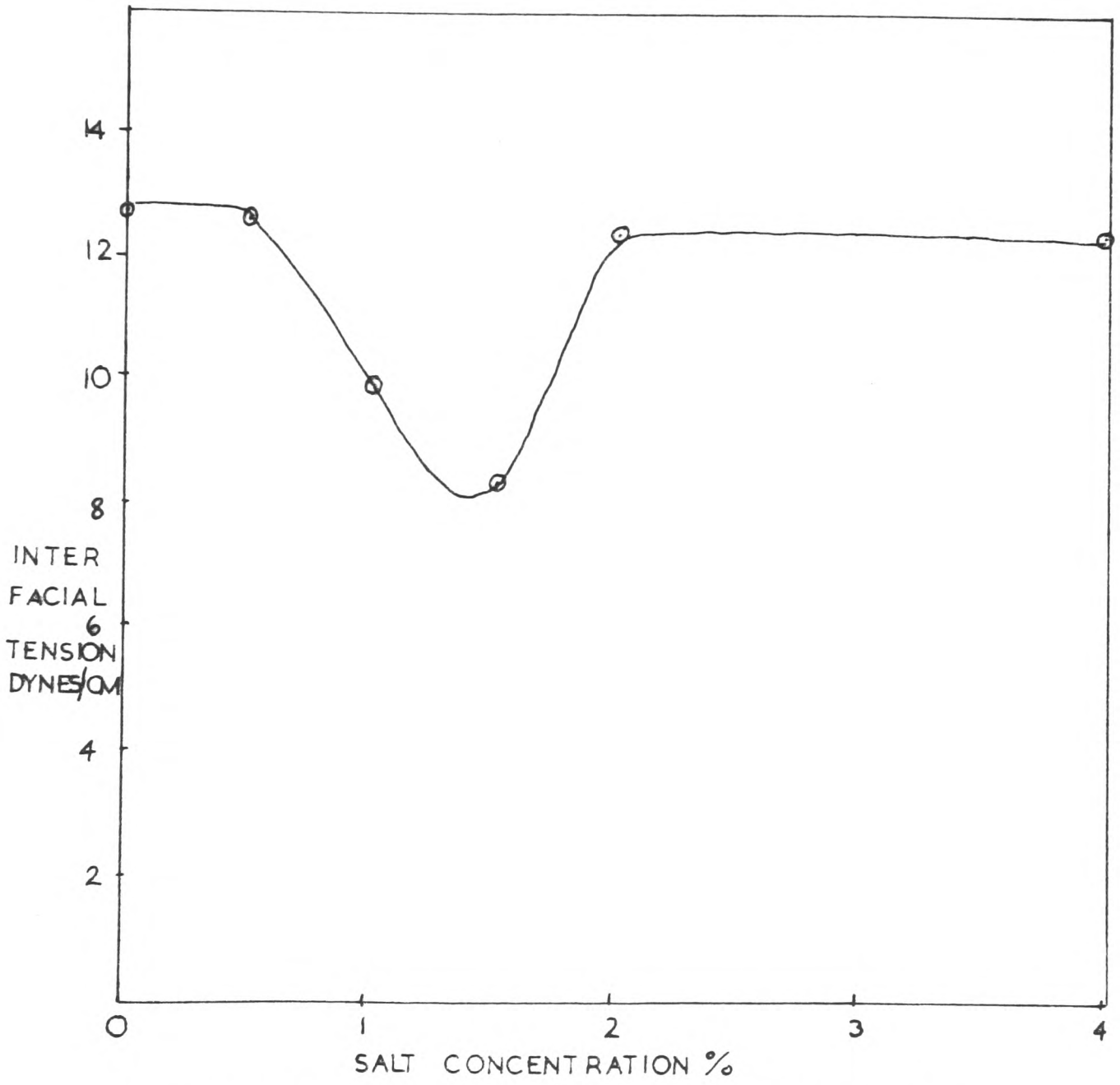

FIG 29 PLOT OF INTERFACIAL TENSION AGAINST SALT CONCENTRATION

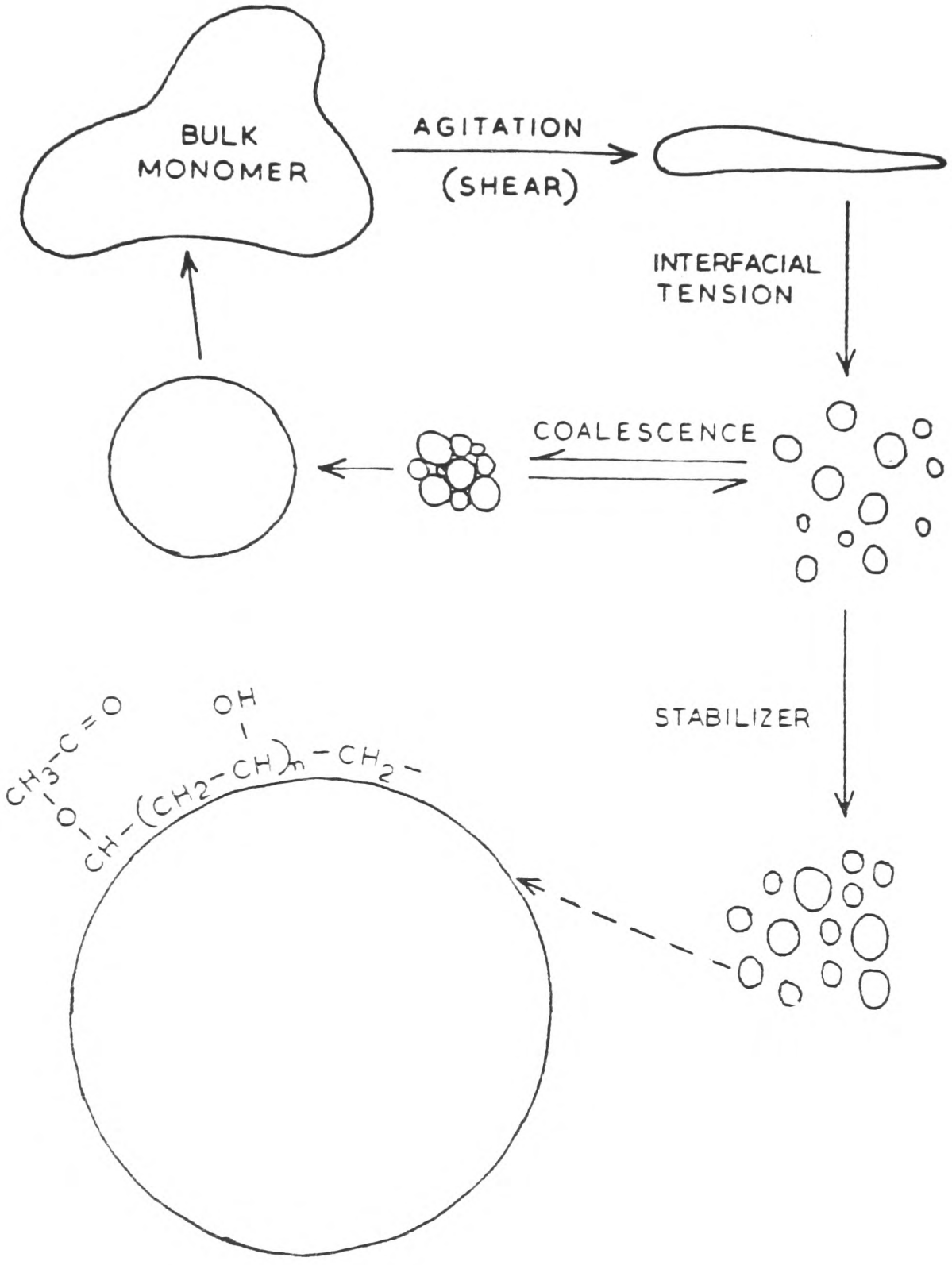

FIG 30 SCHEMATIC DIAGRAM OF STATES OF DISPERSION IN SUSPENSION POLYMERISATION

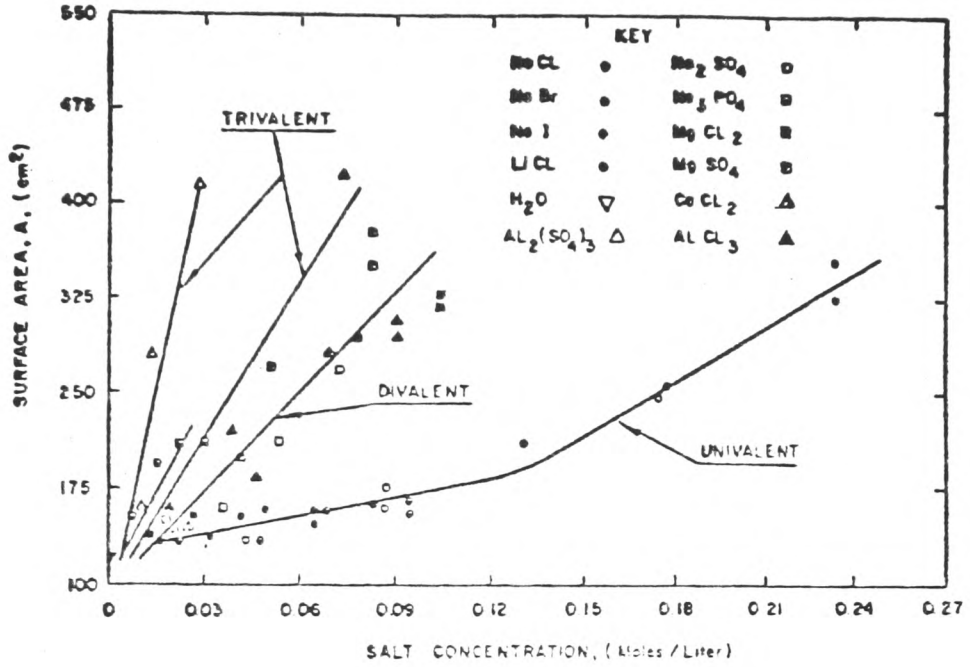

FIG 31 THE EFFECT OF INORGANIC SALTS UPON BUBBLE SURFACE AREA

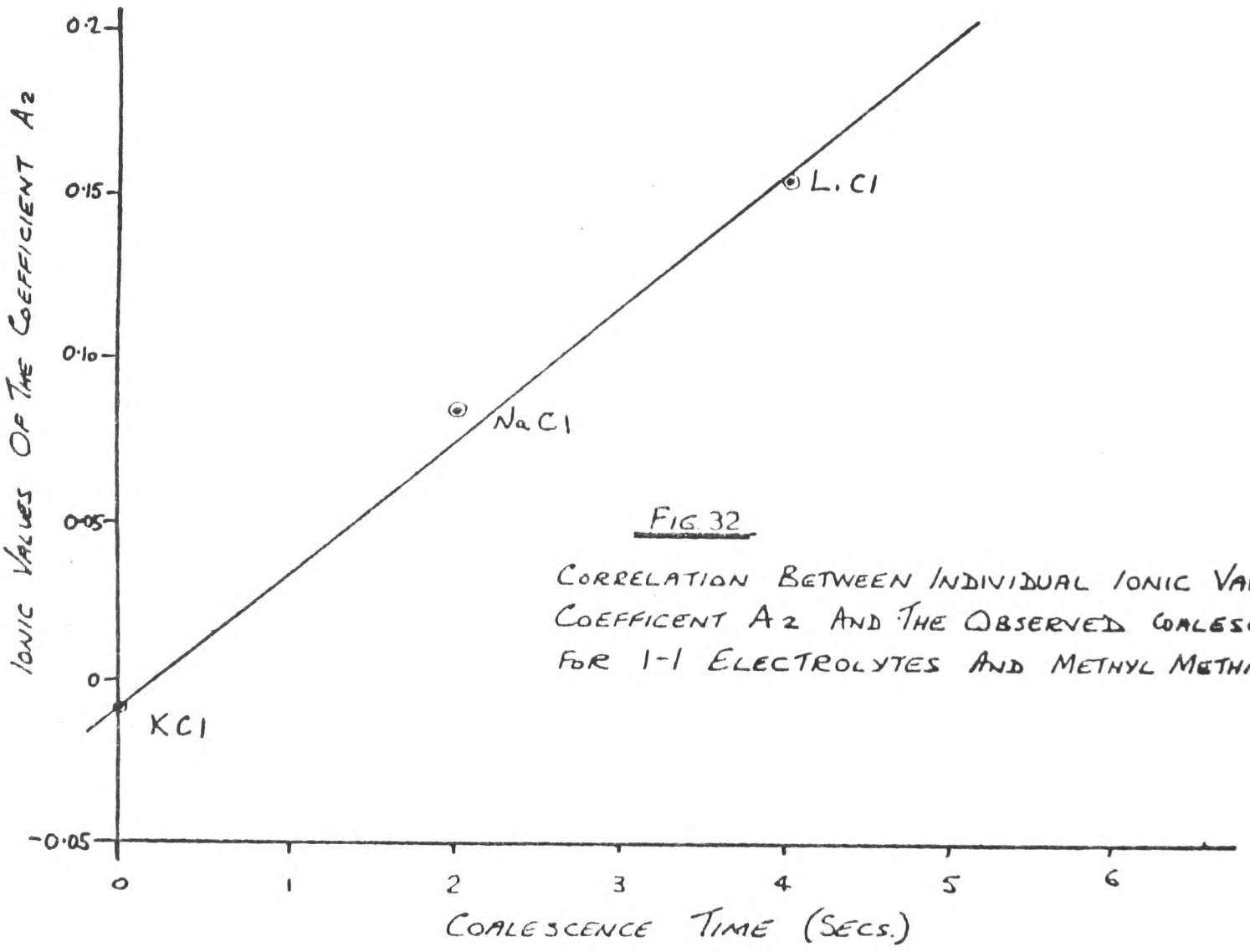

FIG 32

CORRELATION BETWEEN INDIVIDUAL IONIC VALUES OF THE COEFFICENT A2 AND THE OBSERVED COALESCENCE TIME FOR 1-1 ELECTROLYTES AND METHYL METHACRYLATE MONOMER.

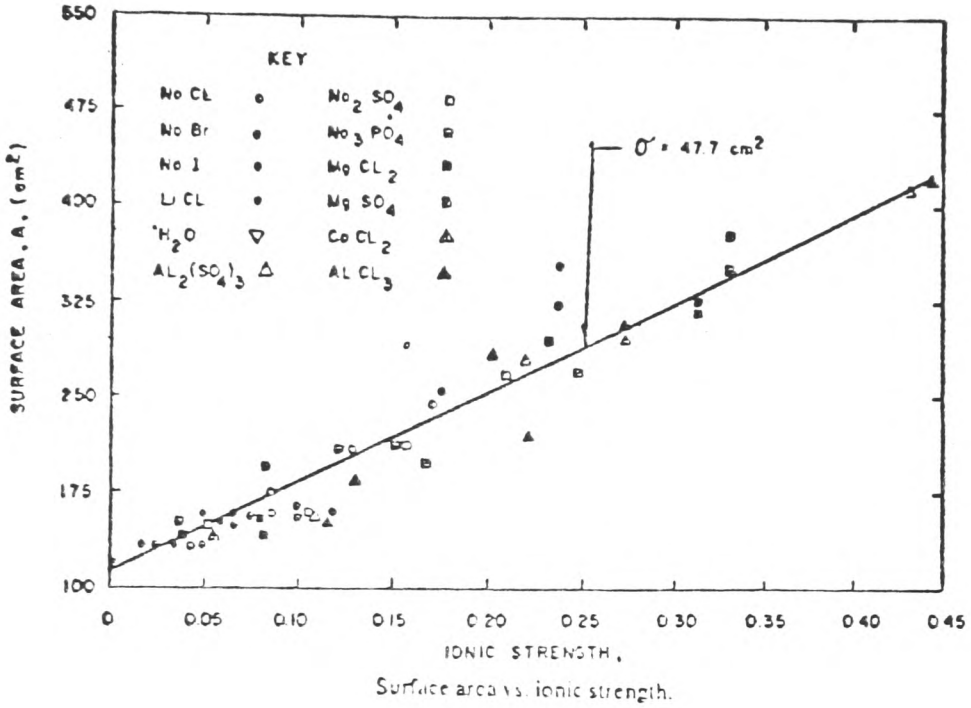

Surface area vs. ionic strength.

FIG 33 SURFACE AREA AGAINST IONIC STRENGTH (GAS BUBBLES)

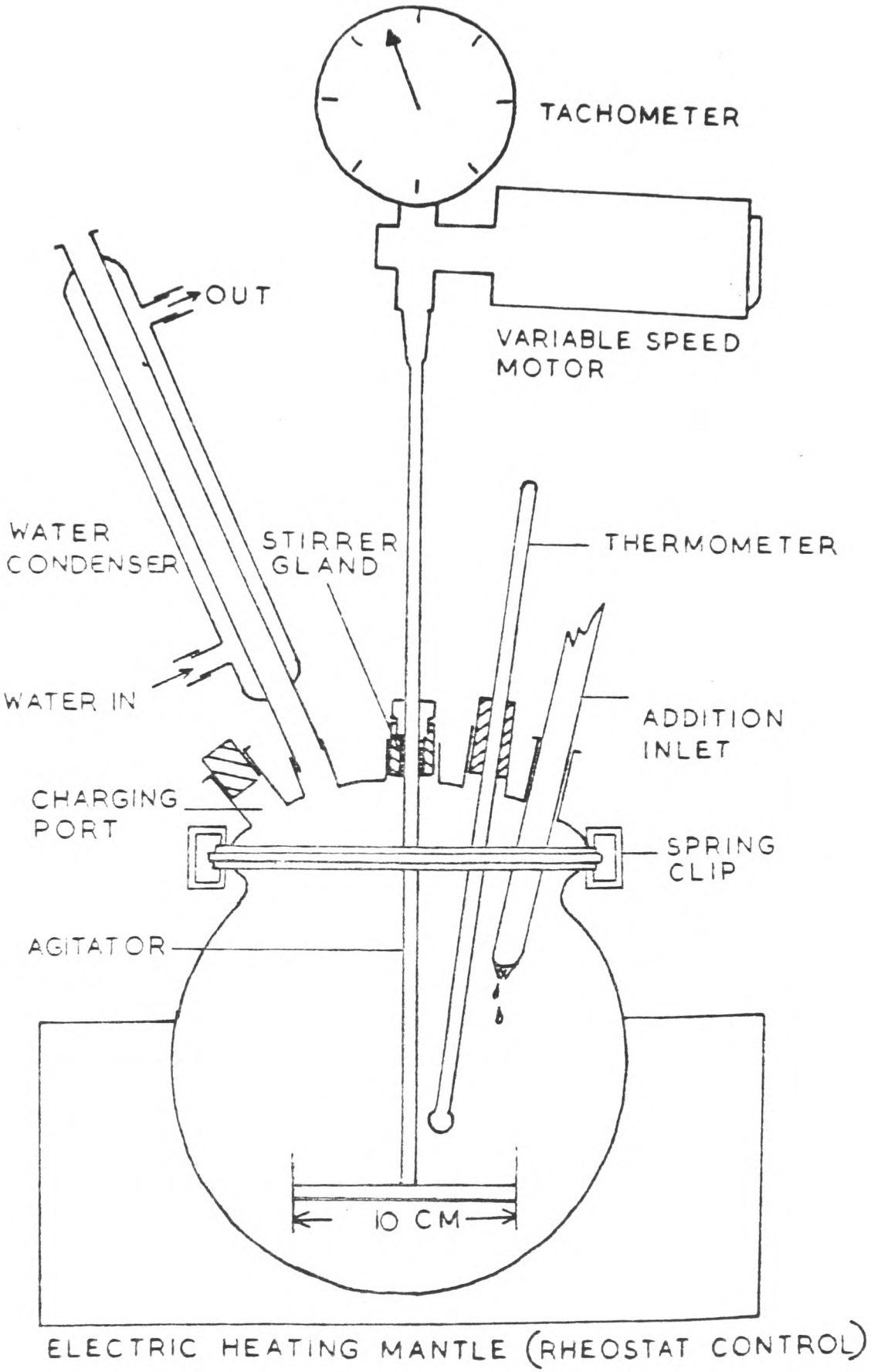

FIG 3.4 APPARATUS FOR THE PRODUCTION OF SUSPENSION POLYMERS

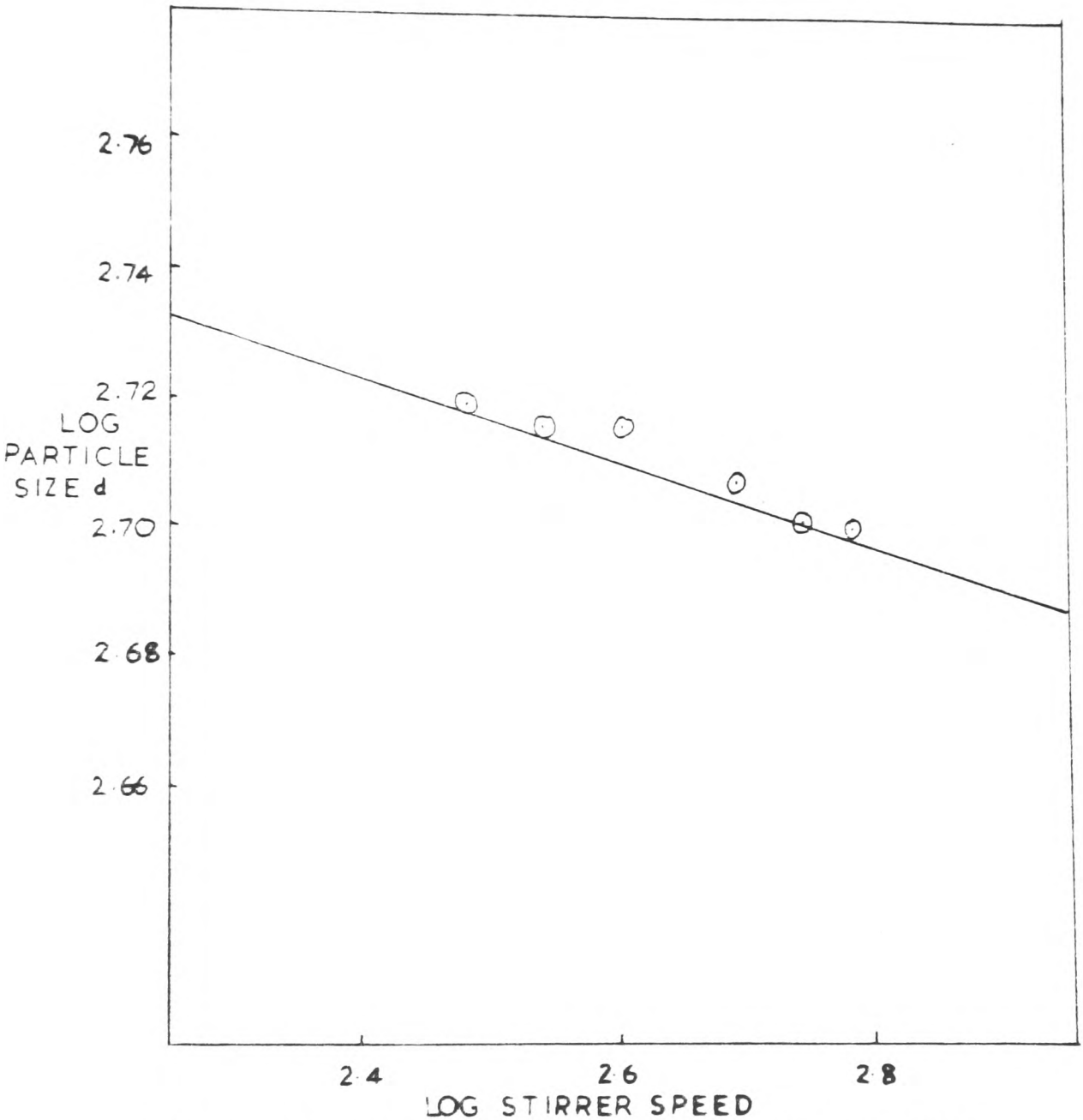

FIG 35 PLOT OF LOG PARTICLE SIZE AGAINST LOG SPEED (VOLUME FRACTION Ø·2)

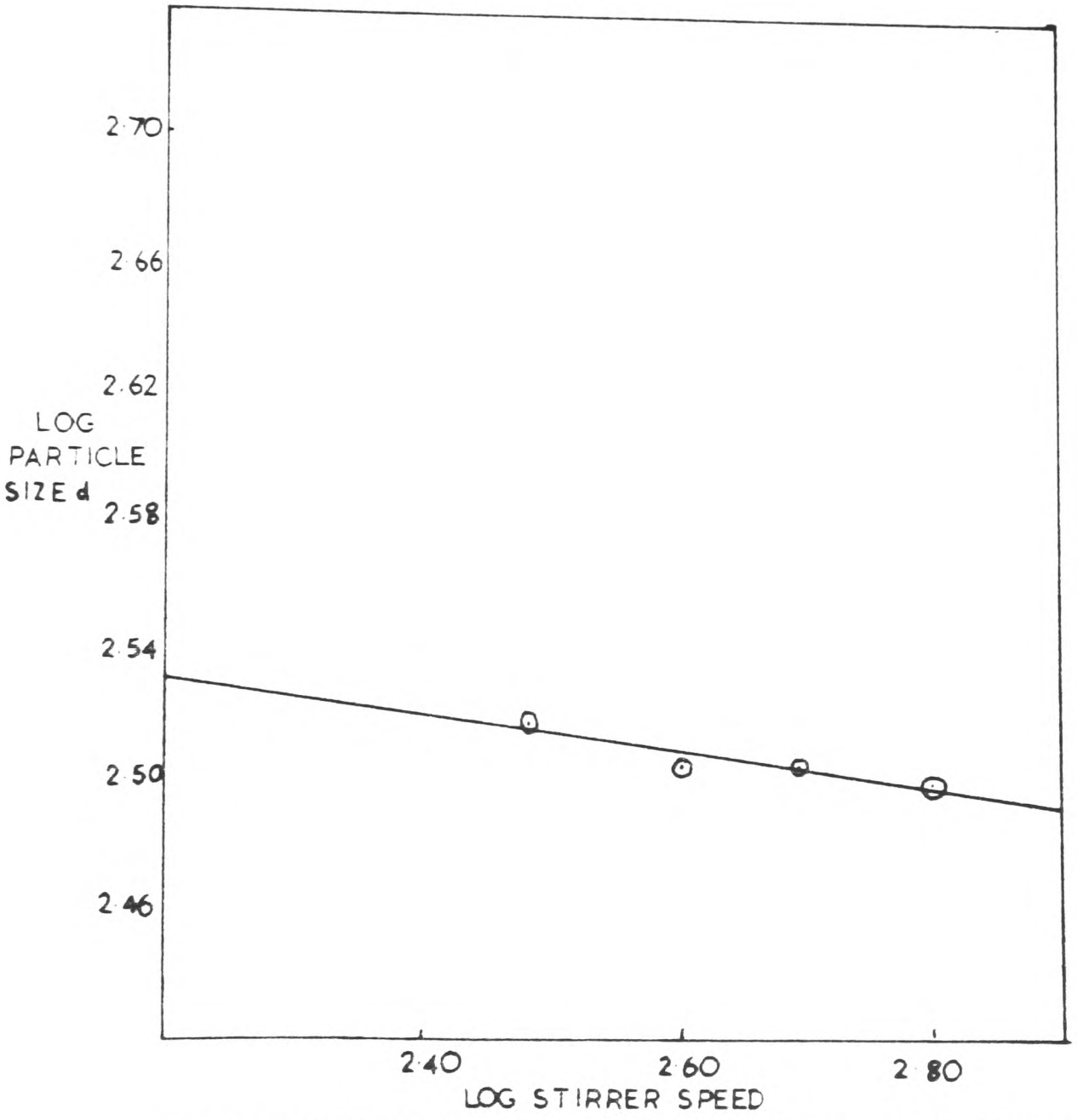

FIG 36 PLOT OF LOG PARTICLE SIZE AGAINST LOG STIRRER SPEED(VOLUME FRACTION ϕ·3)

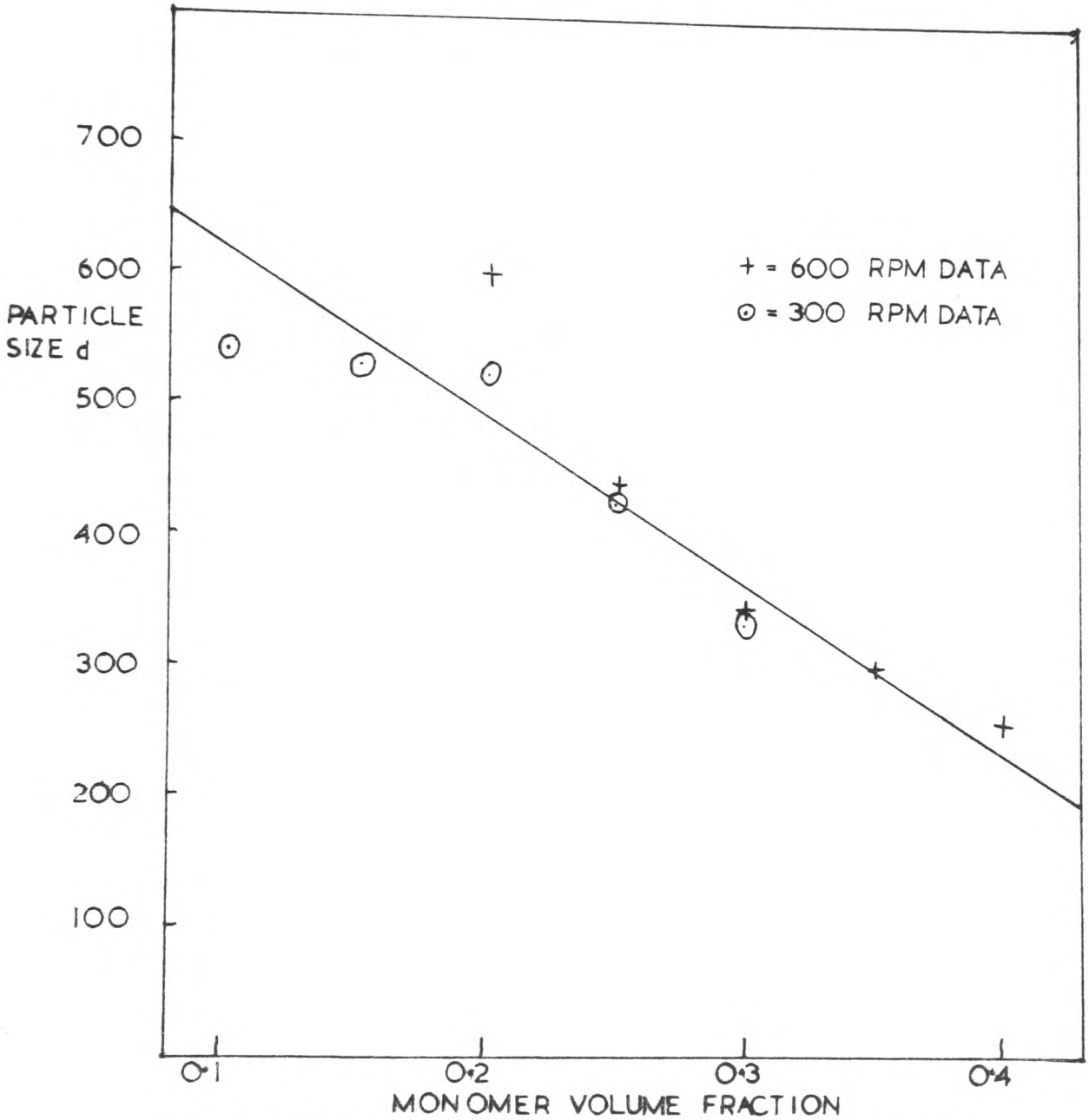

FIG 37 PLOT OF PARTICLE SIZE AGAINST MONOMER VOLUME FRACTION

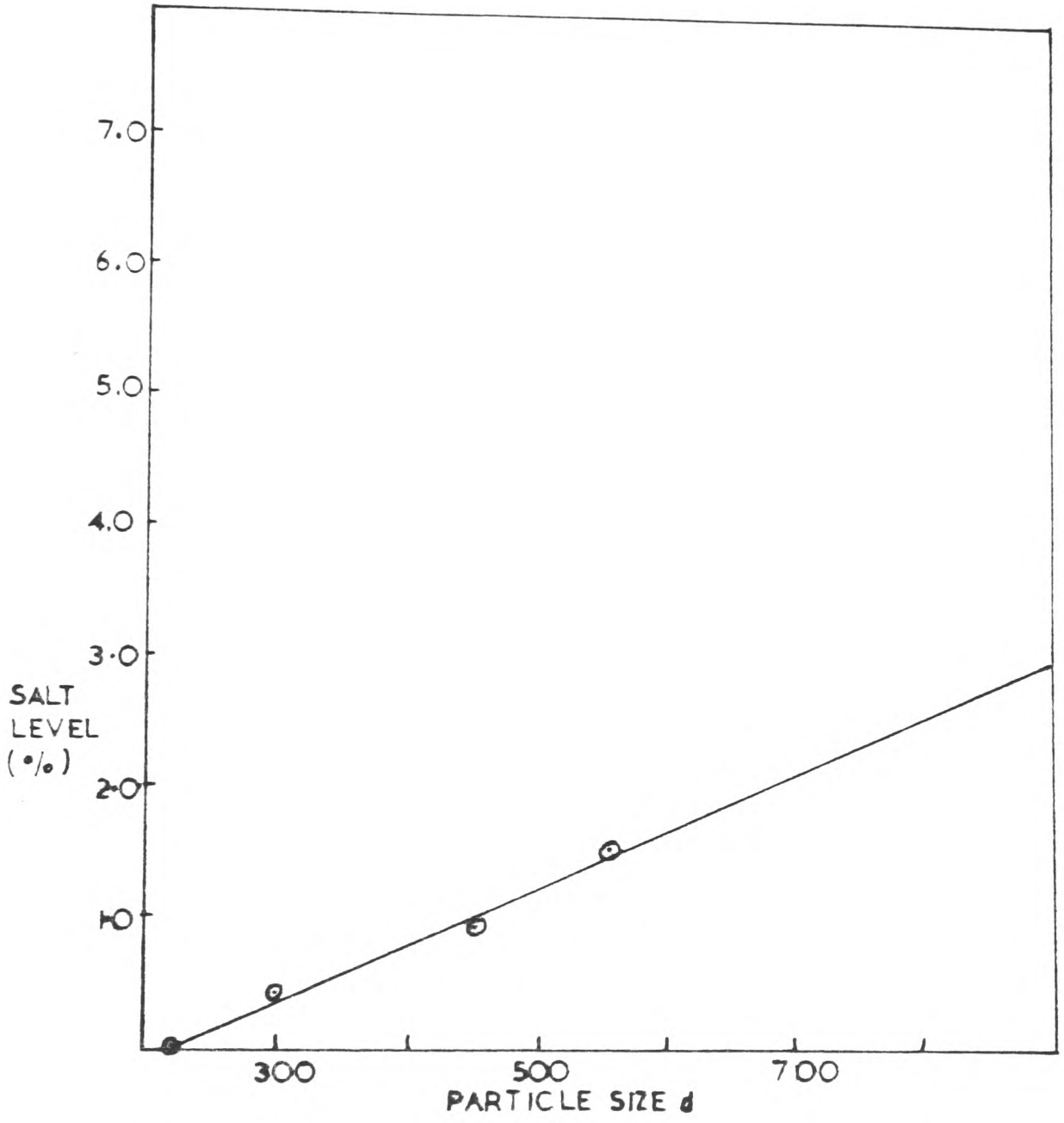

FIG 38 PLOT OF SALT LEVEL AGAINST PARTICLE SIZE d

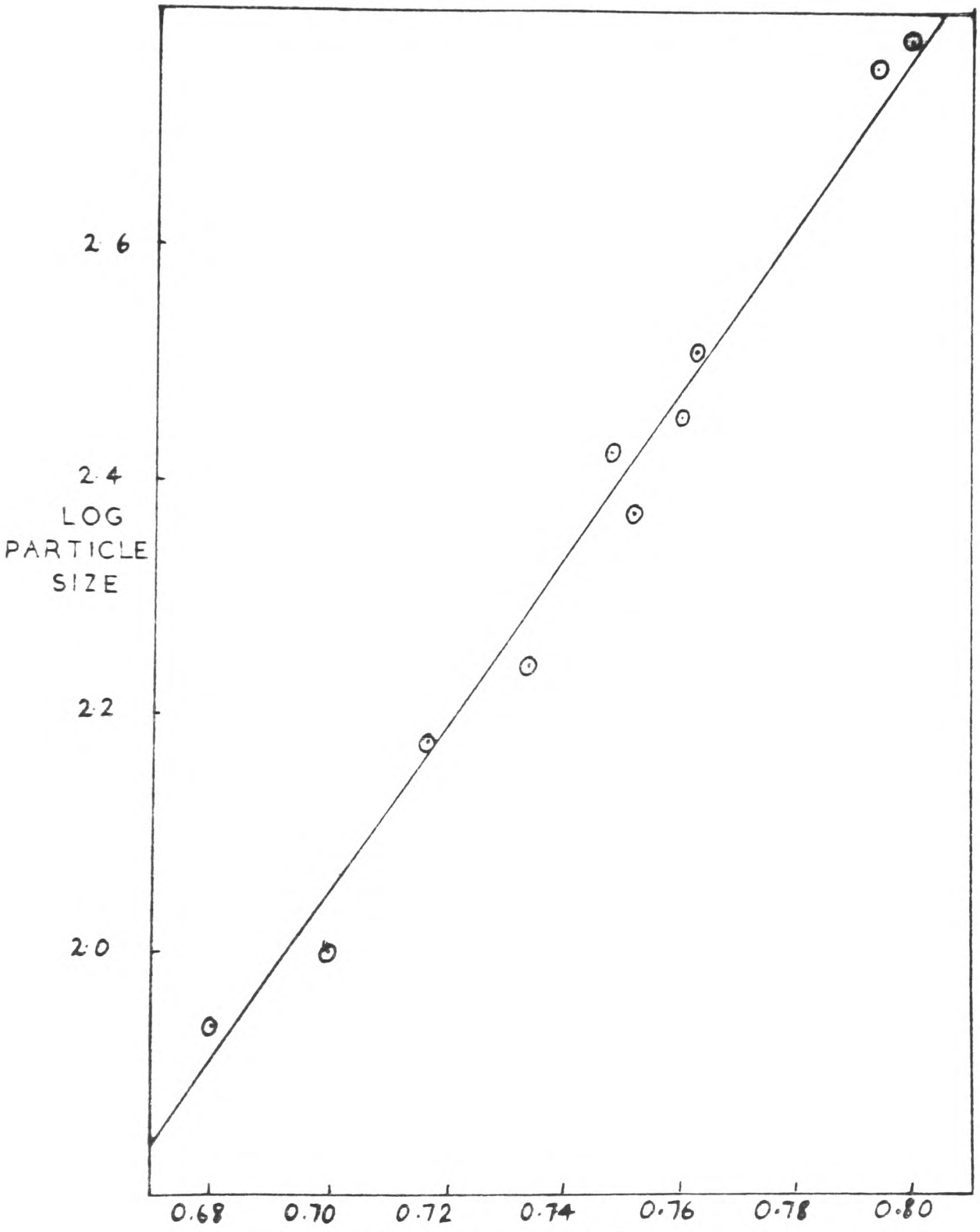

FIG 39 PLOT OF LOG PARTICLE SIZE AGAINST LOG INTERFACIAL TENSION

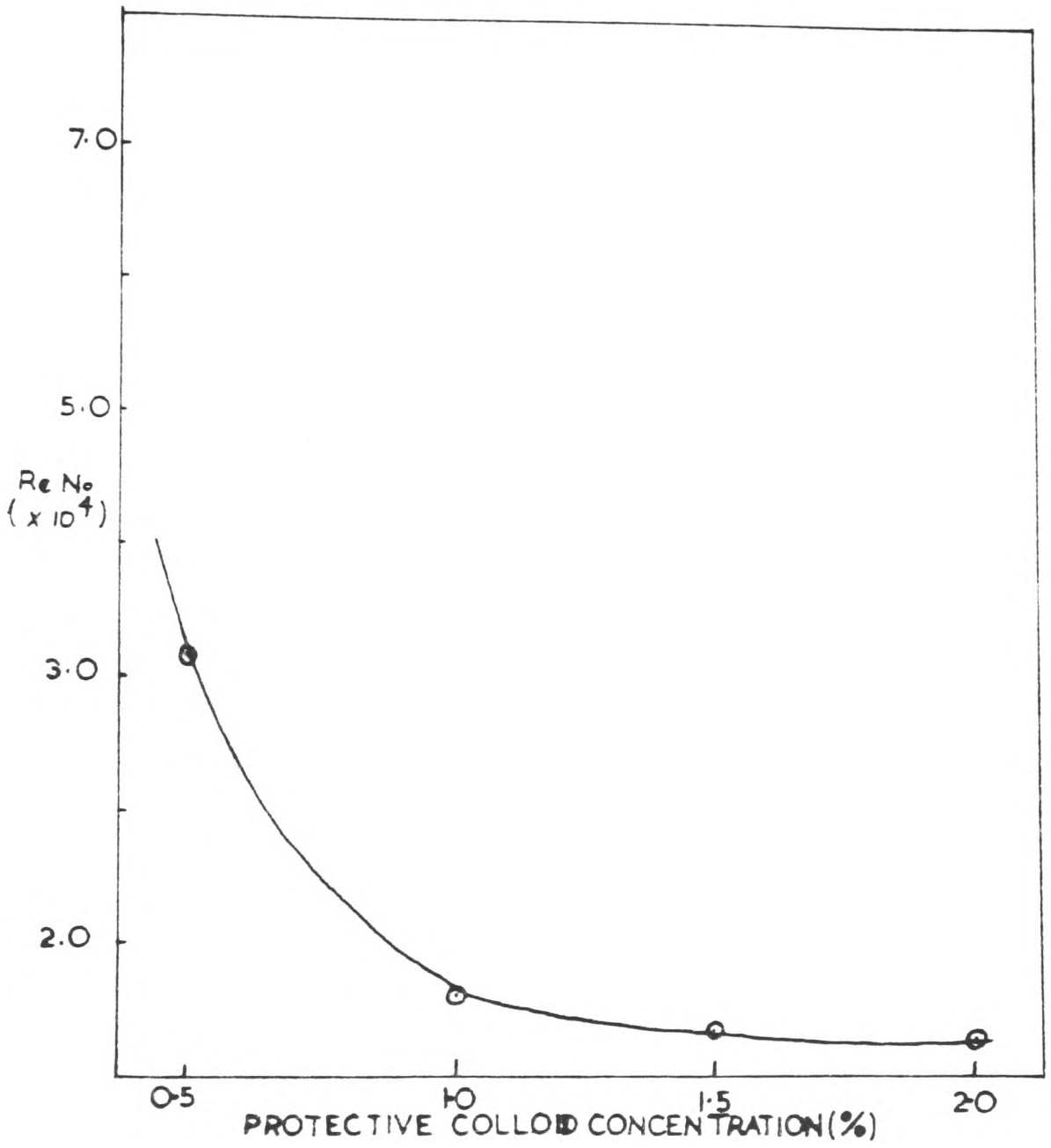

FIG 40 PLOT OF REYNOLDS NUMBER AGAINST PROTECTIVE COLLOID CONCENTRATION

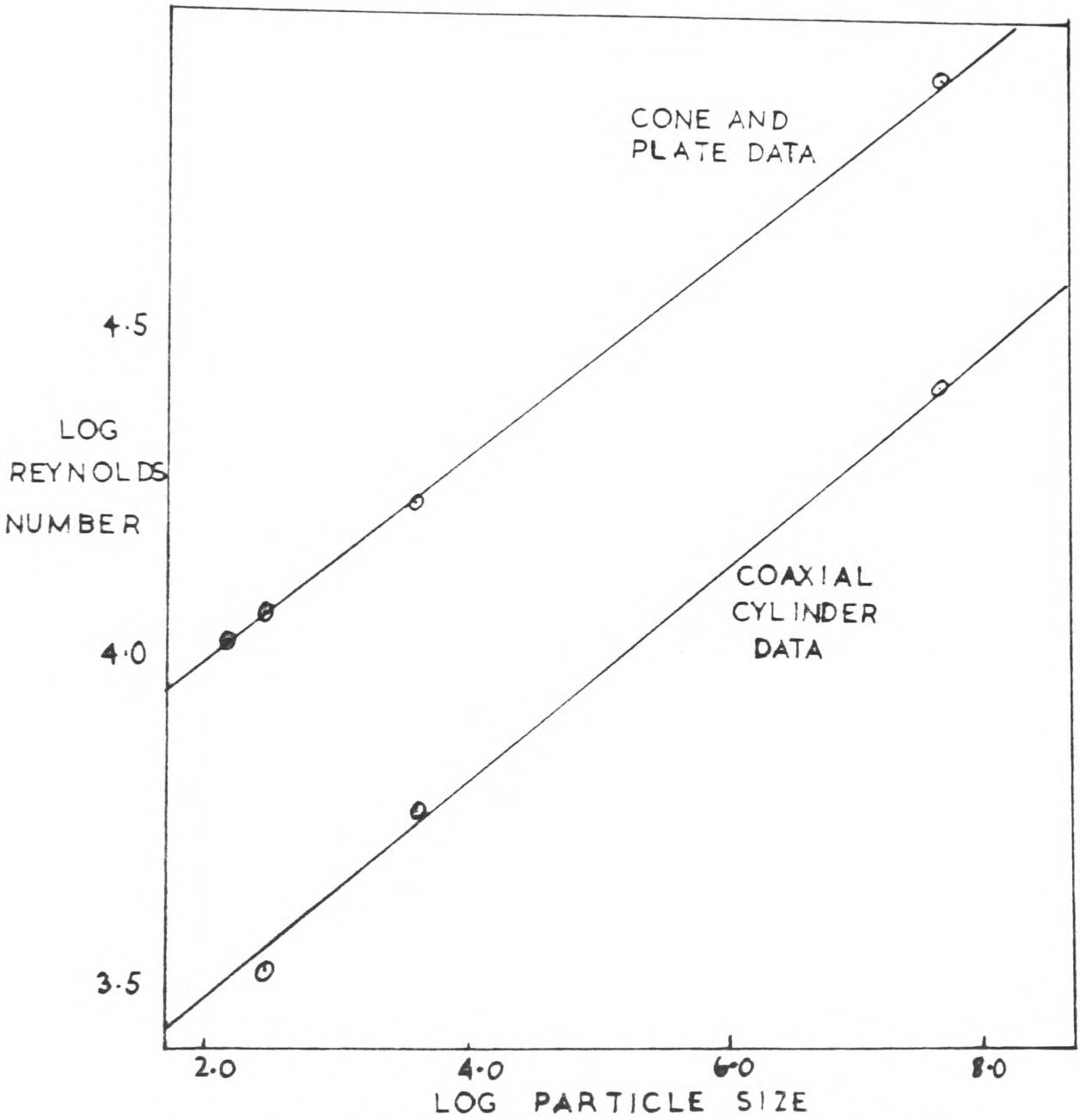

FIG 41 PLOT OF LOG REYNOLDS NUMBER AGAINST LOG PARTICLE SIZE

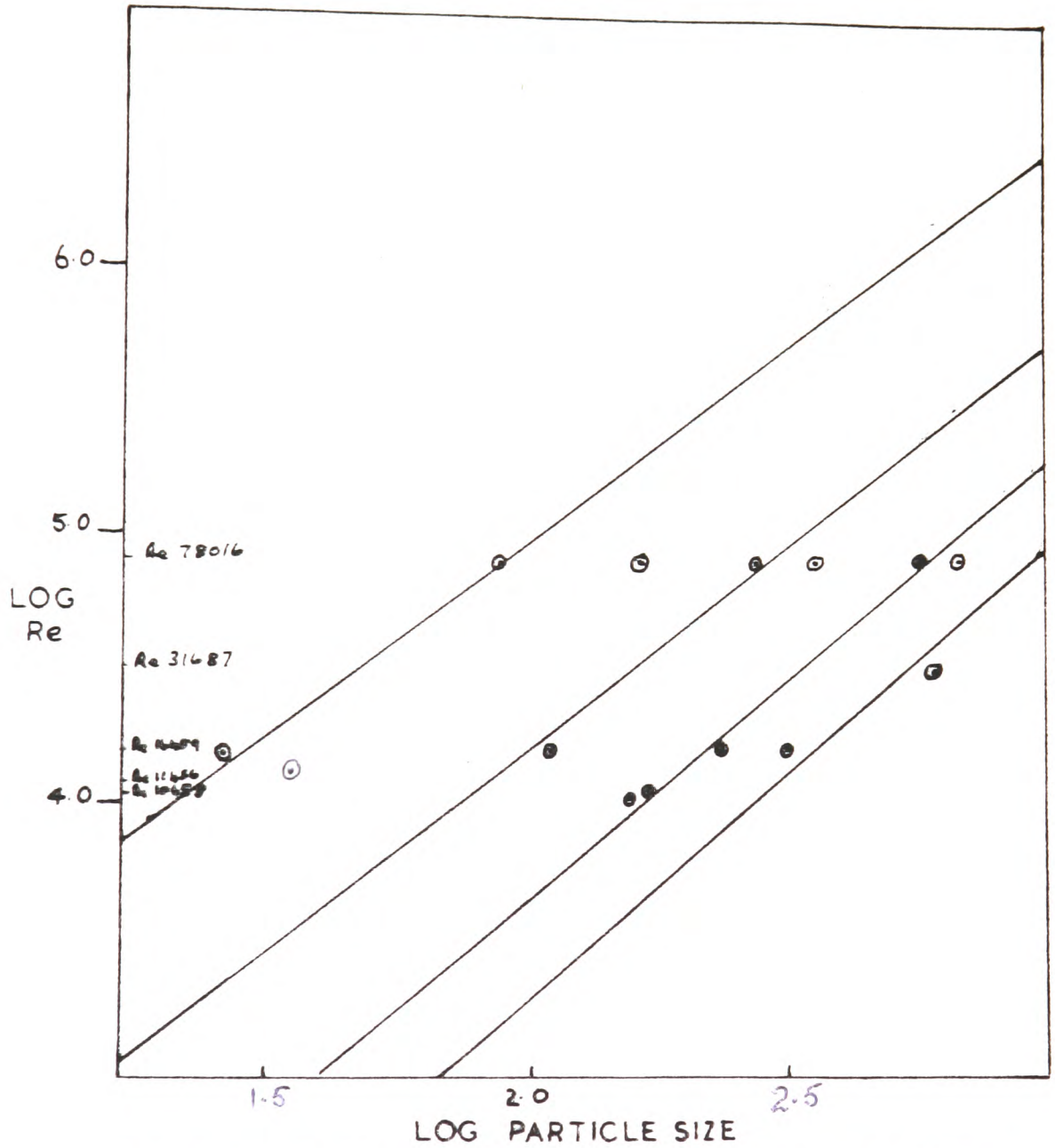

FIG 42 PLOT OF LOG REYNOLDS NUMBER AGAINST LOG PARTICLE SIZE

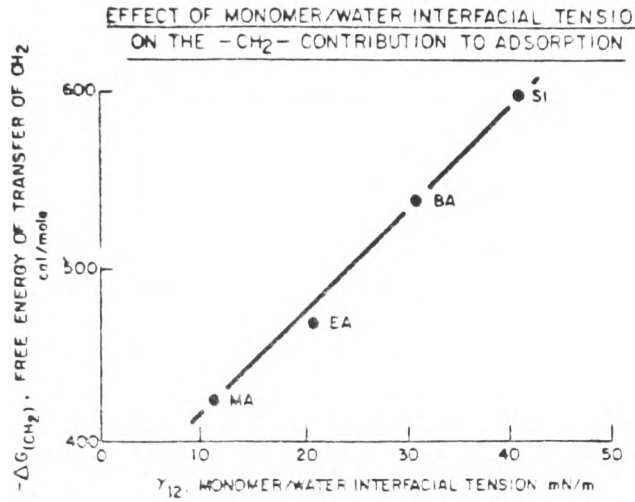

FIG 43 Plot of free energy of transfer ($-\Delta G_{CH_2}$) of a CH_2 group from water to monomer-water interface against monomer-water interfacial tension (γ_{12}).

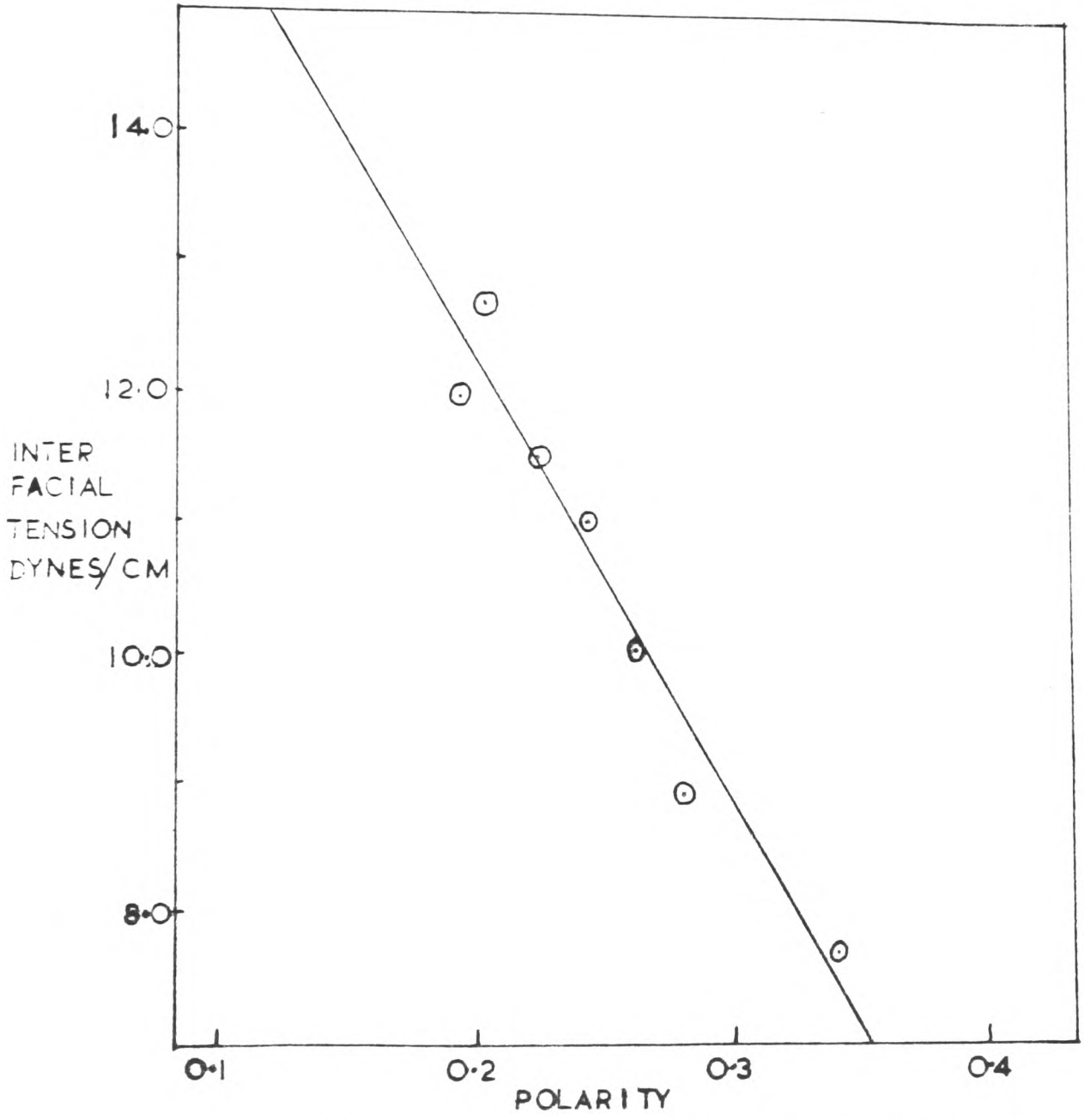

FIG 44 PLOT OF INTERFACIAL TENSION AGAINST POLARITY

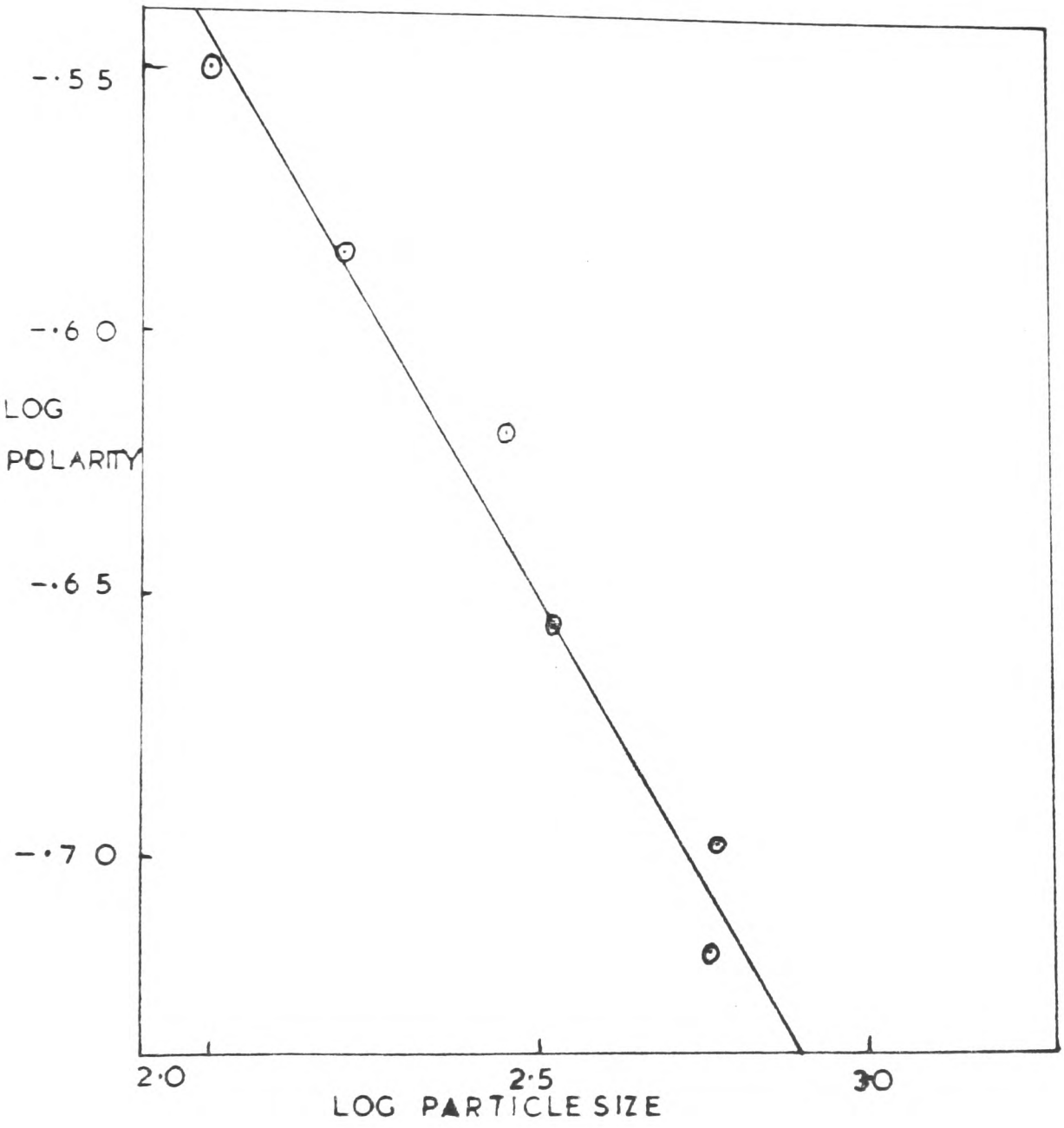

FIG 45 PLOT OF LOG POLARITY AGAINST LOG PARTICLE SIZE

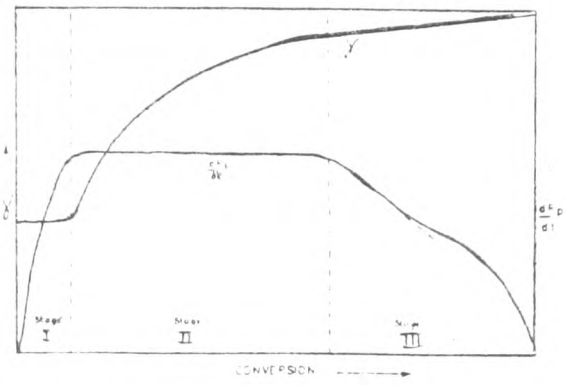

Variation of rate, dR_p/dt, and surface tension, γ, with conversion in emulsion polymerisation

FIG 46

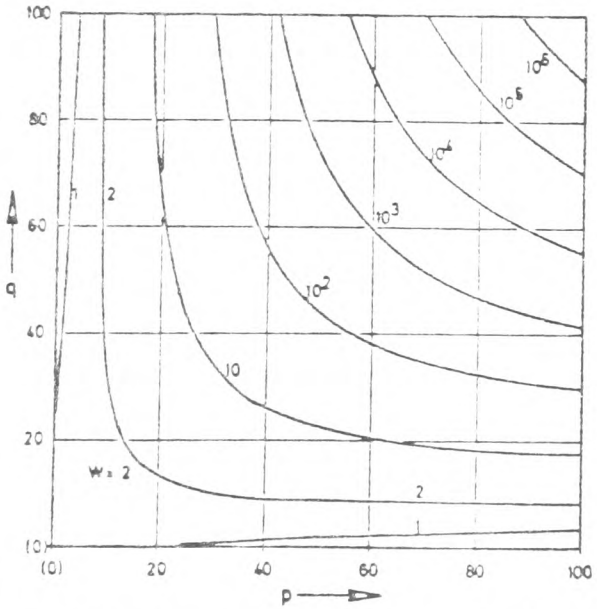

FIG 47

Contour map of Fuchs' stability ratio W_{pq} as a function of class indices p and q. $T = 60°C$, $C_0 = 6.44 \times 10^{-3}$ N, $r_1 = 2$ nm, $\varepsilon/\varepsilon_0 = 80$, $A = 5 \times 10^{-21}$ J, $\lambda = 100$ nm

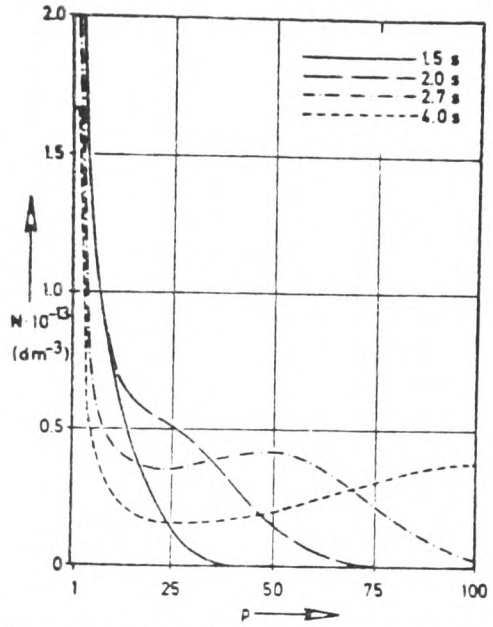

FIG 48

Particle class distribution after different reaction times calculated by numerical integration of particle nucleation and flocculation equations. W_{pq} as in Figure ., $D = 10^{-8}$ dm^2/sec, $W_j' = 1.0$, other constants as in Figure 1.

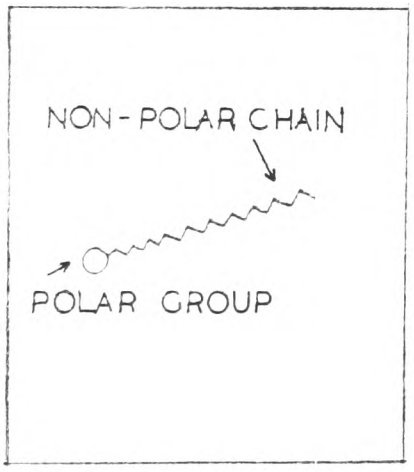

FIG 49

SURFACTANT MOLECULE

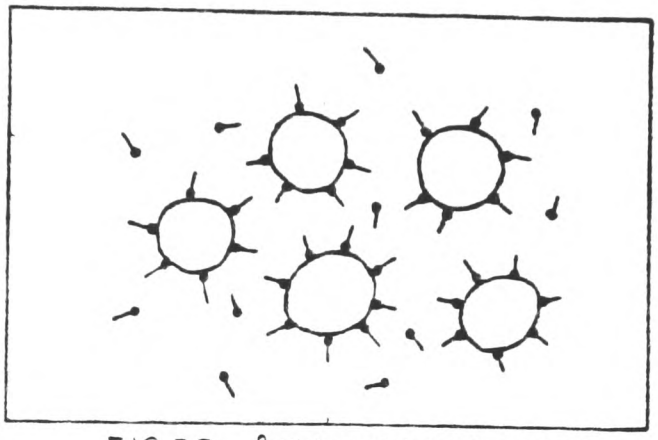

FIG 50 Particles and dispersing molecules

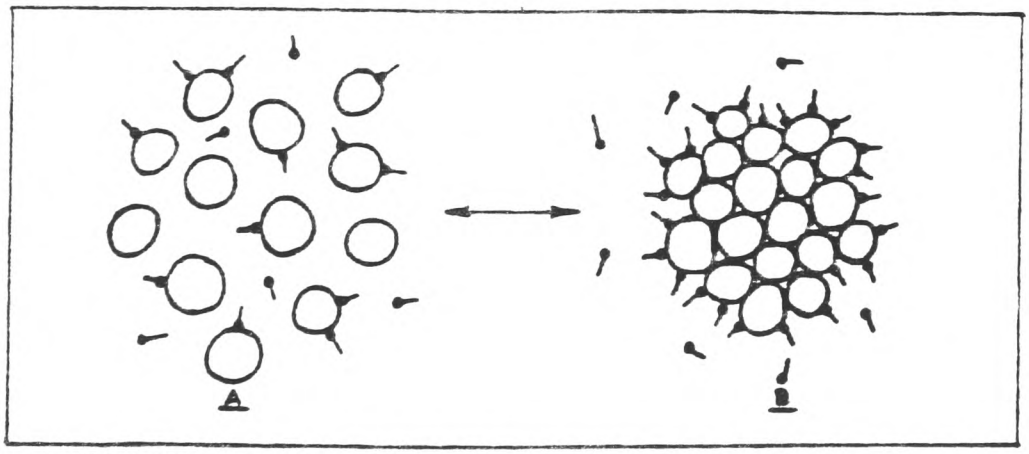

FIG 51 Particles with insufficient number of dispersing molecules

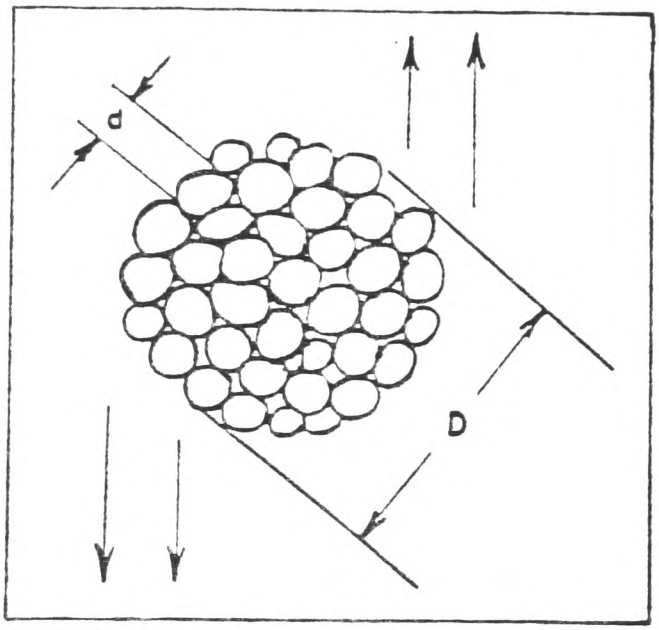

Figure 52 - Agglomerated particle suspended in unit shear field

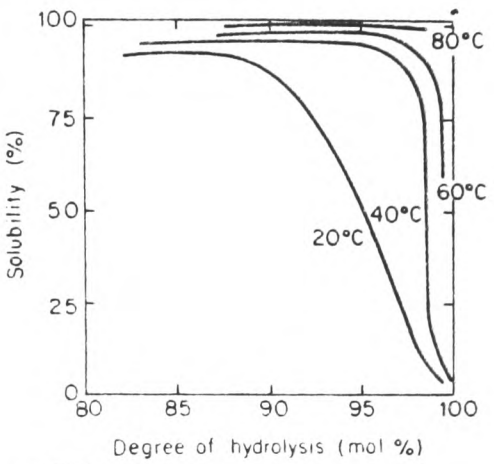

FIG 53 Water solubility against degree of hydrolysis for d.p. = 1750 polyvinyl alcohol

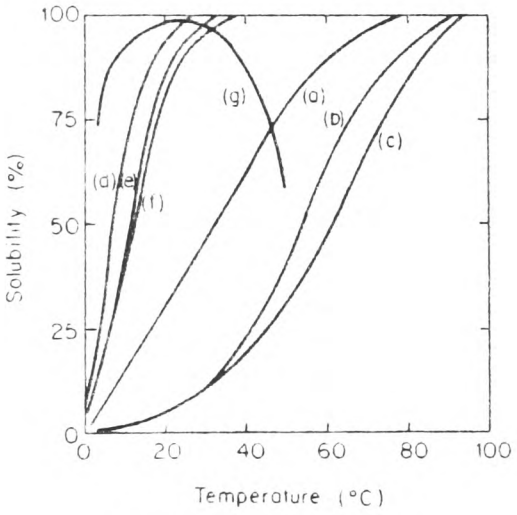

	Hydrolysis(mol %)	D.P.
(a)	98–99	500–600
(b)	98–99	1700–1800
(c)	98–99	2400–2500
(d)	87–89	500–600
(e)	87–89	1700–1800
(f)	87–89	2400–2500
(g)	78–81	2000–2100

FIG 54 WATER SOLUBILITY AGAINST TEMPERATURE FOR POLYVINYL ALCOHOL

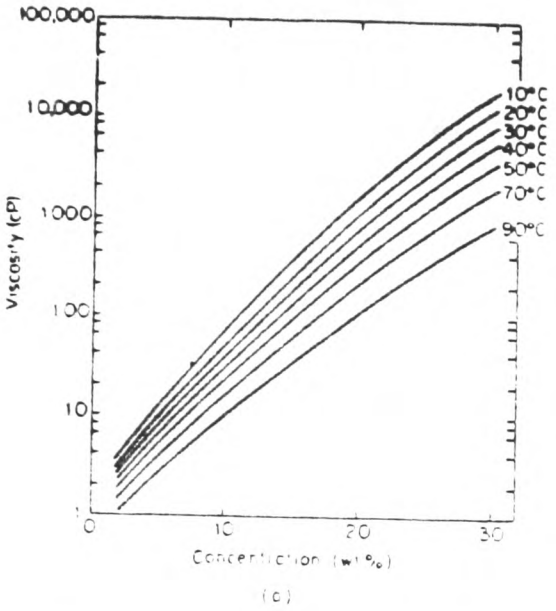

(a)

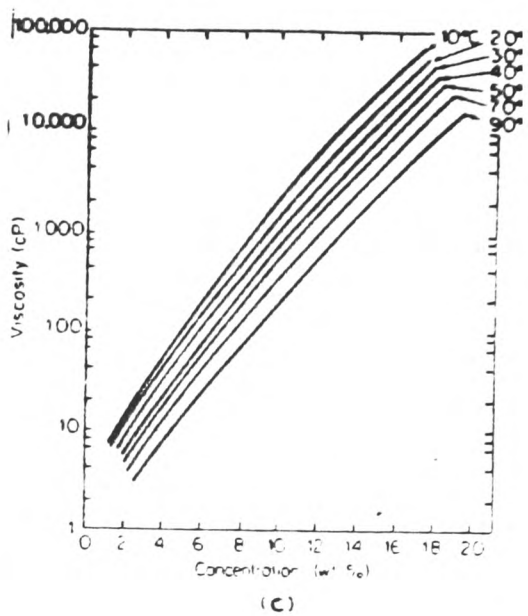

(c)

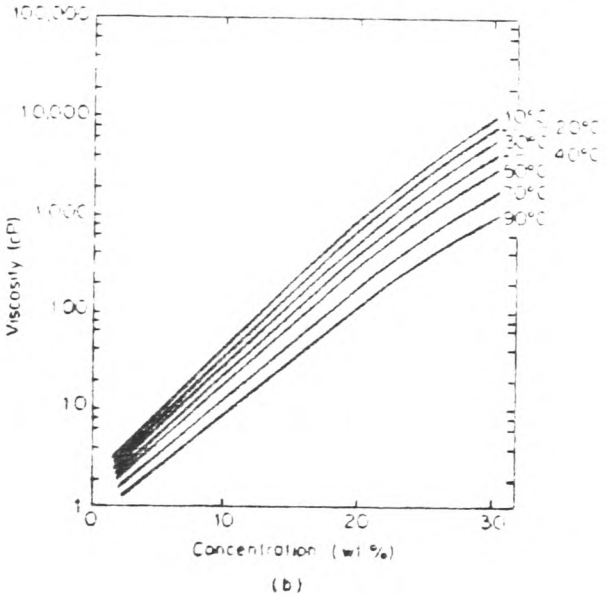

(b)

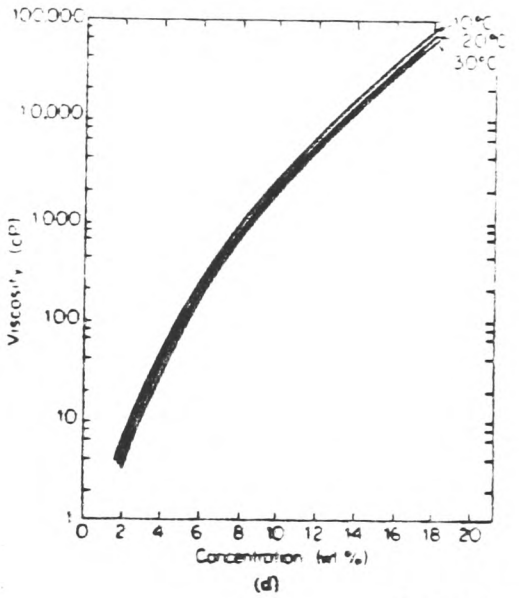

(d)

	D.P.	Degree of hydrolysis (%)
(a)	500	98.5
(b)	500	88

	D.P.	Degree of hydrolysis (%)
(c)	2000	88
(d)	2000	80

FIG 55 Viscosity against concentration (PVA)

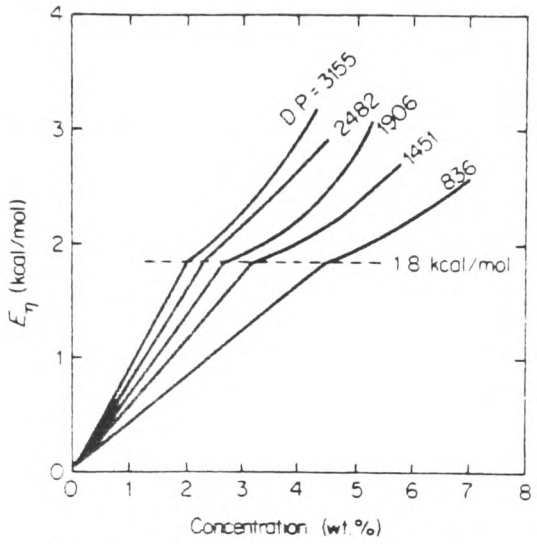

Figure 56 Apparent activation energy of flow E_η against concentration

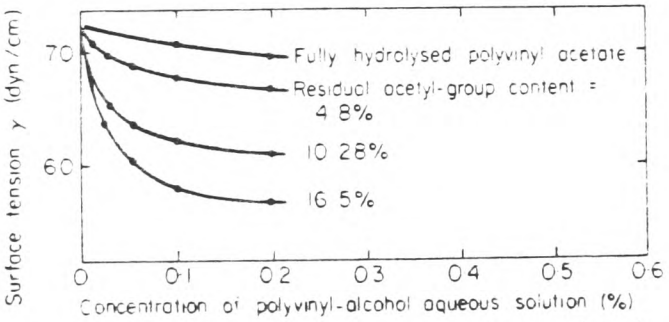

Figure 57 Surface tension of aqueous solutions of partly hydrolysed polyvinyl alcohol obtained by hydrolysis in methanol solvent

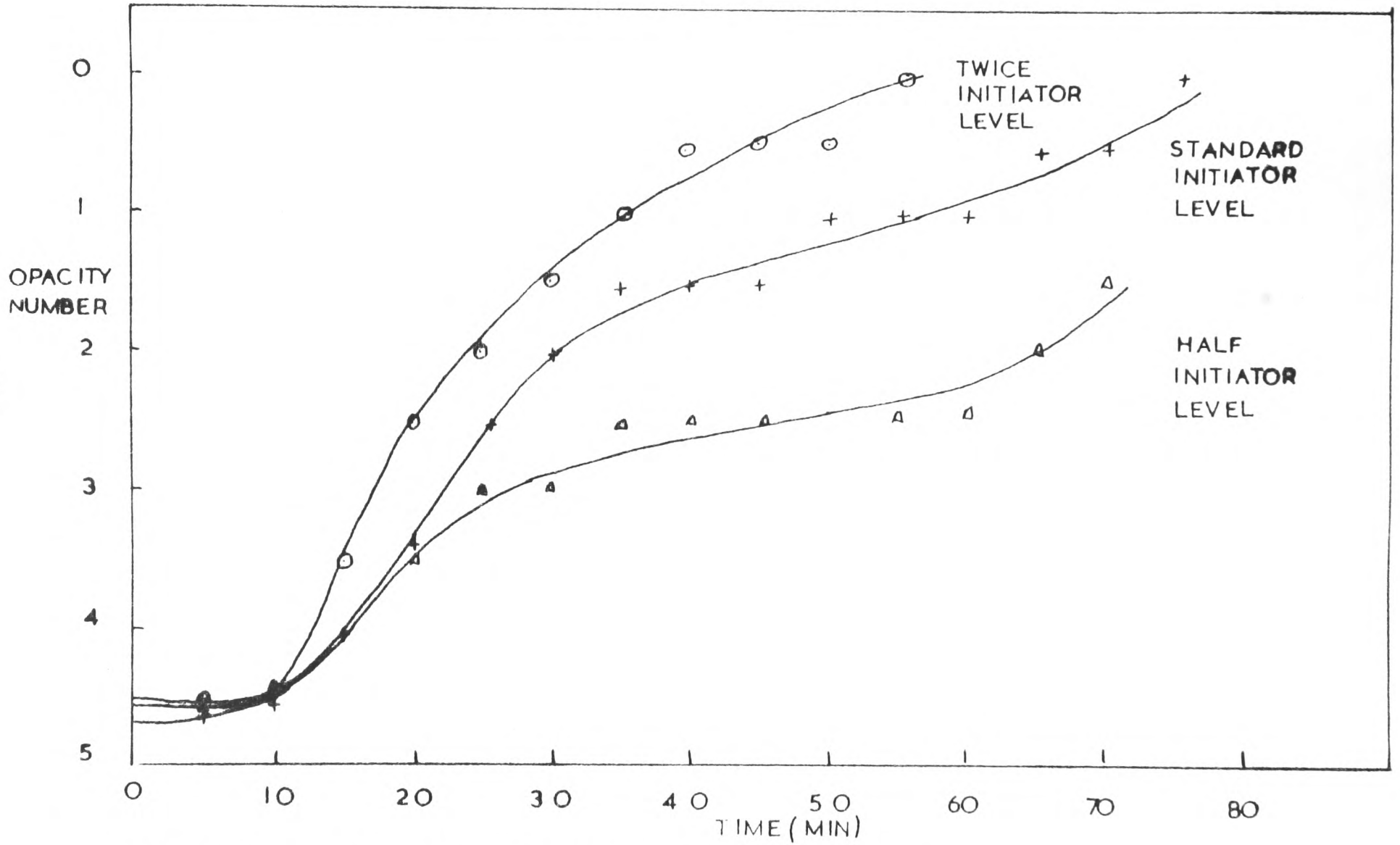

FIG 58 PLOT OF OPACITY NUMBER AGAINST TIME

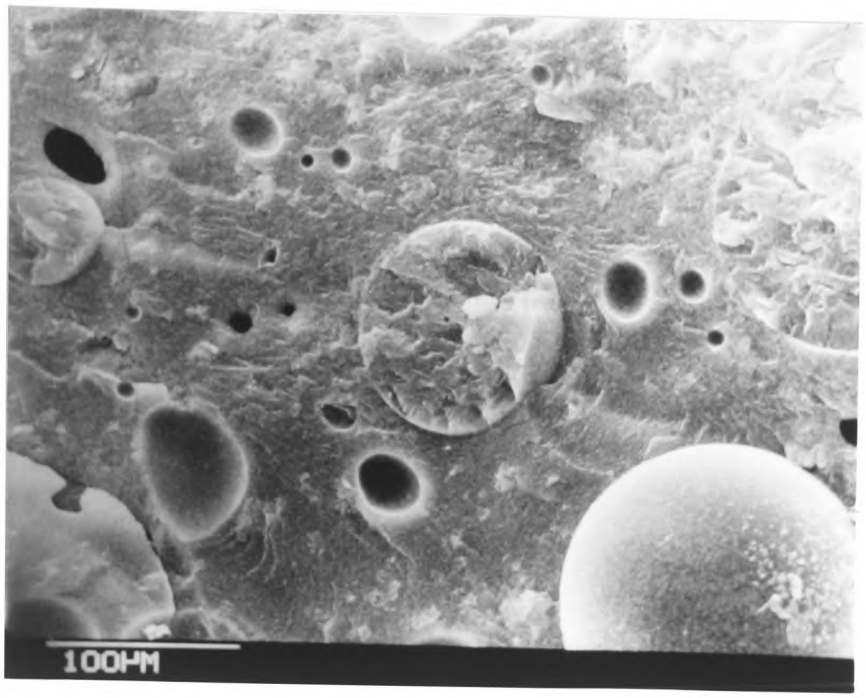

FIG 59 THE SPHERICAL AGGLOMERATE (S.E.M)

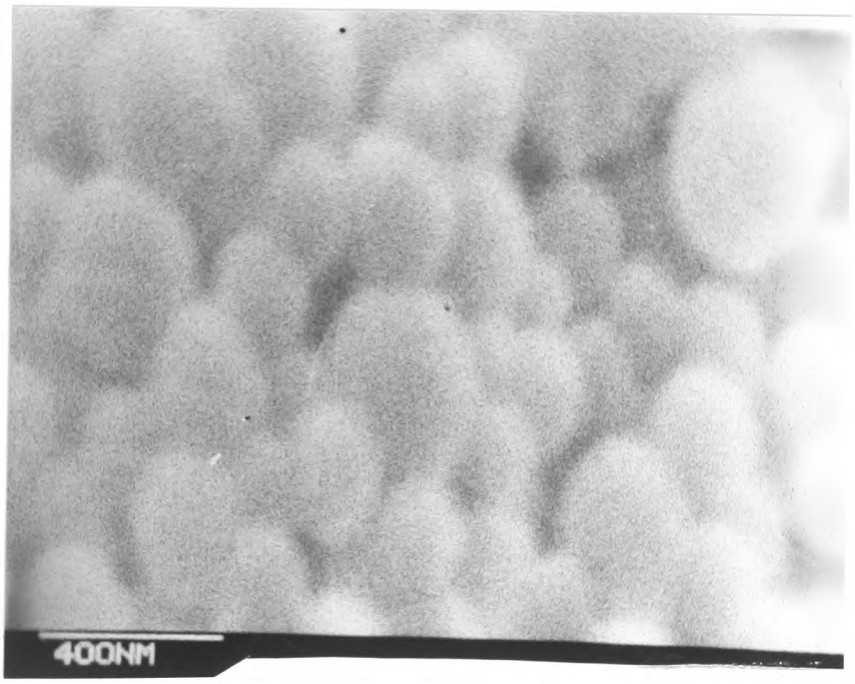

FIG 60 THE SURFACE OF A SPHERICAL AGGLOMERATE (S.E.M)

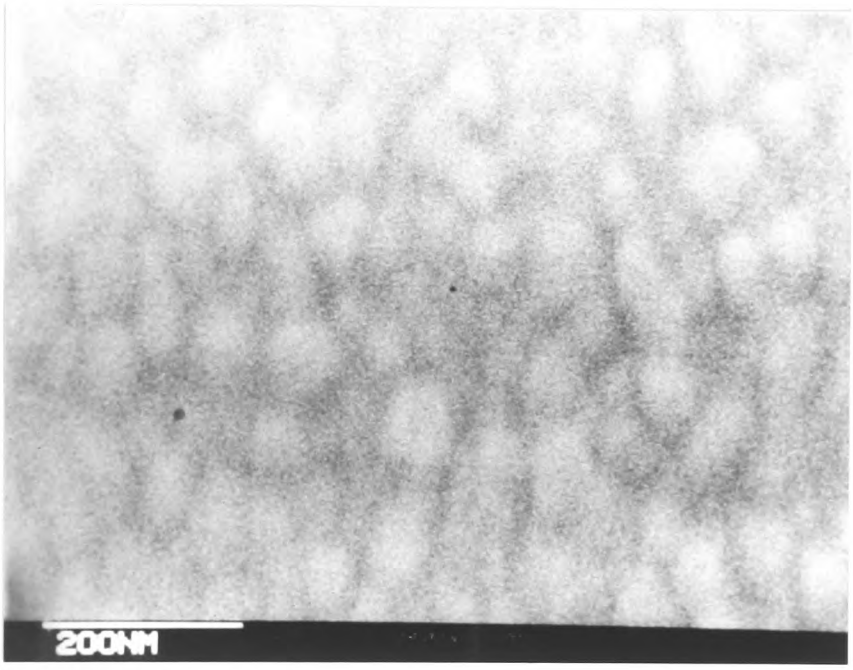

FIG 61 THE INTERIOR OF A SPHERICAL AGGLOMERATE (S.E.M.)

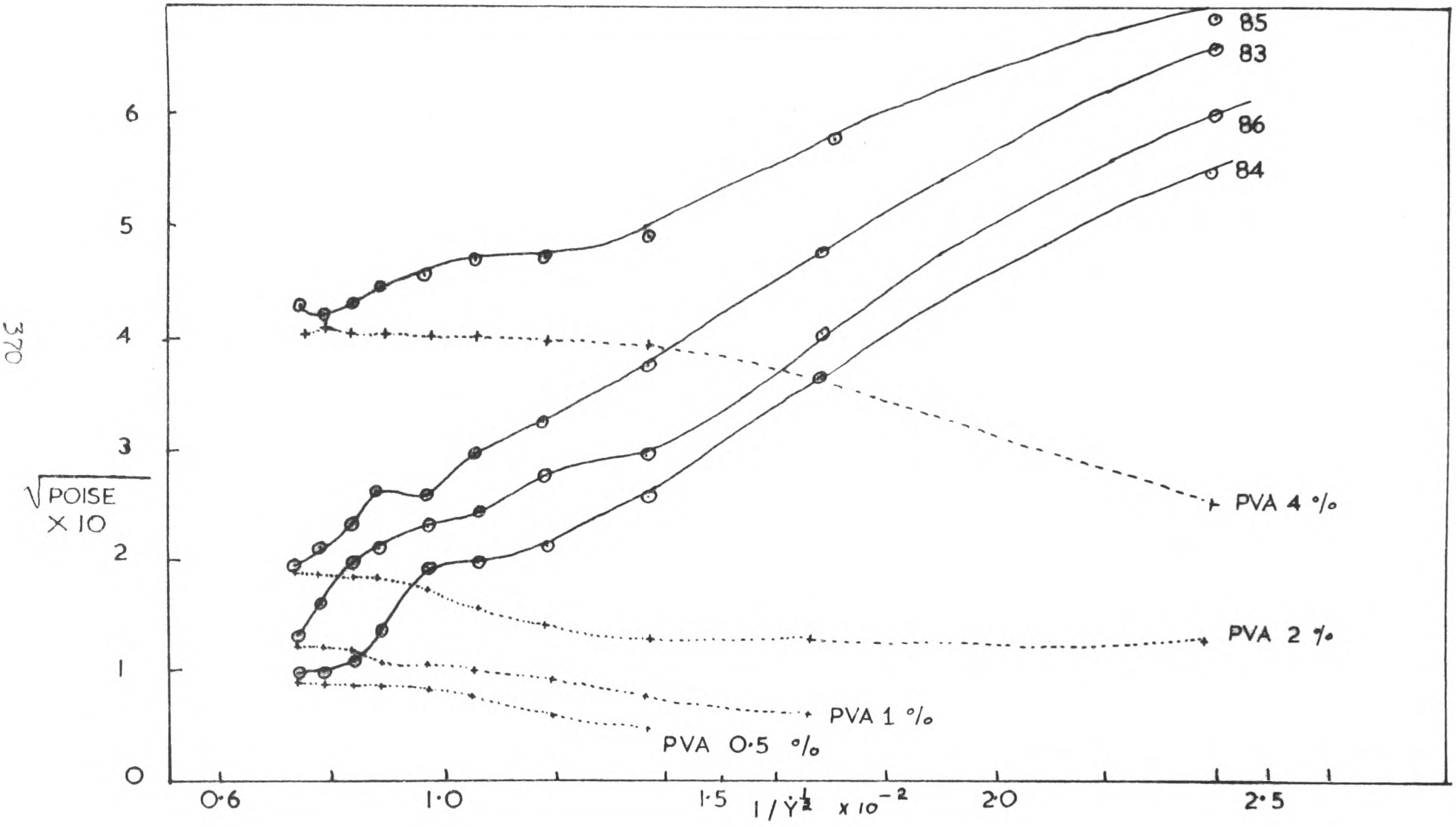

FIG 62 PLOT OF $\sqrt{\text{POISE}} \times 10$ AGAINST $1/\dot{Y} \times 10^{-2}$ FOR AGGLOMERATES AND PVA SOLUTIONS

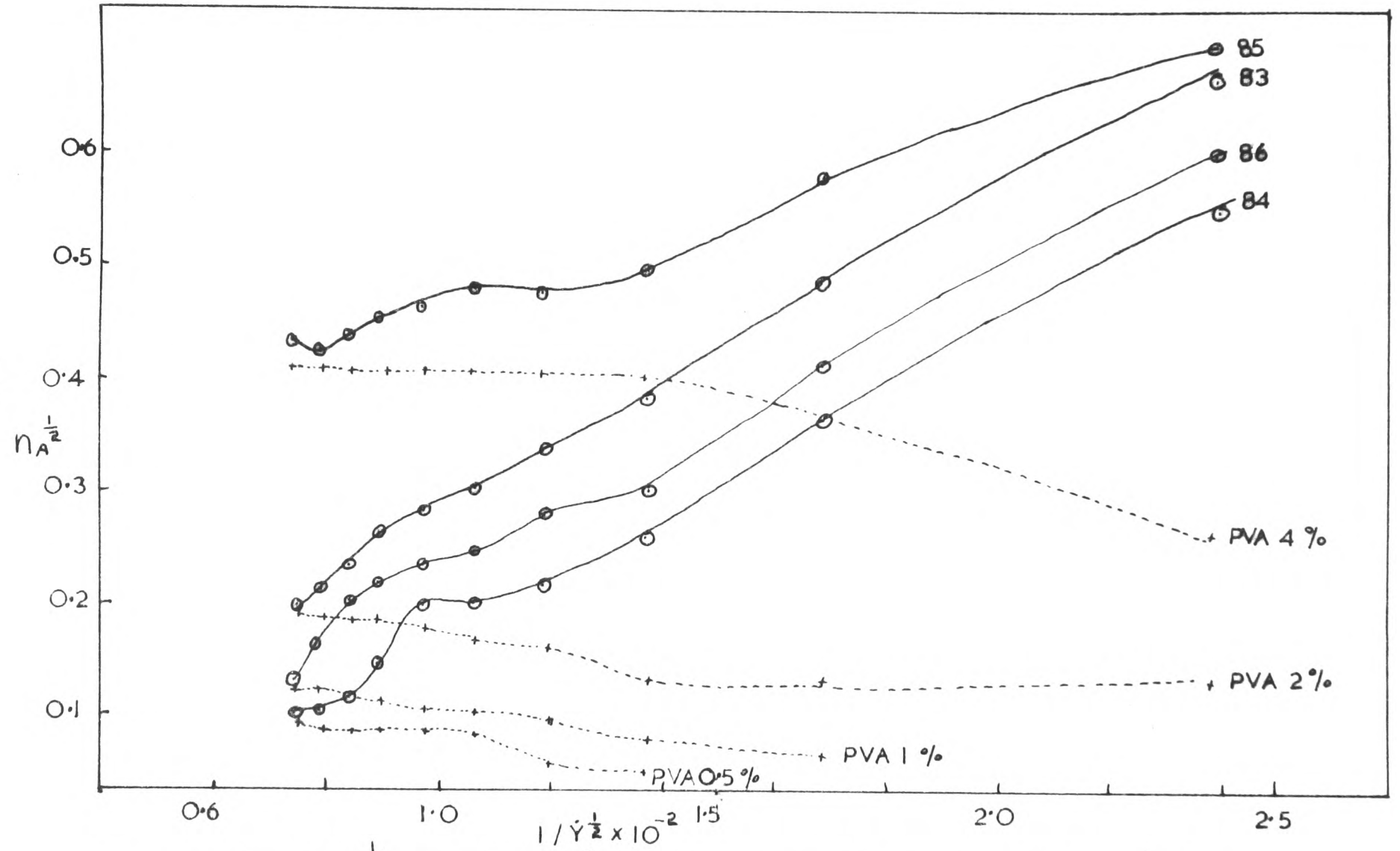

FIG 63 PLOT OF $n_A^{\frac{1}{2}}$ AGAINST $1/\dot{Y}^{\frac{1}{2}} \times 10$ FOR AGGLOMERATES AND PVA SOLUTIONS

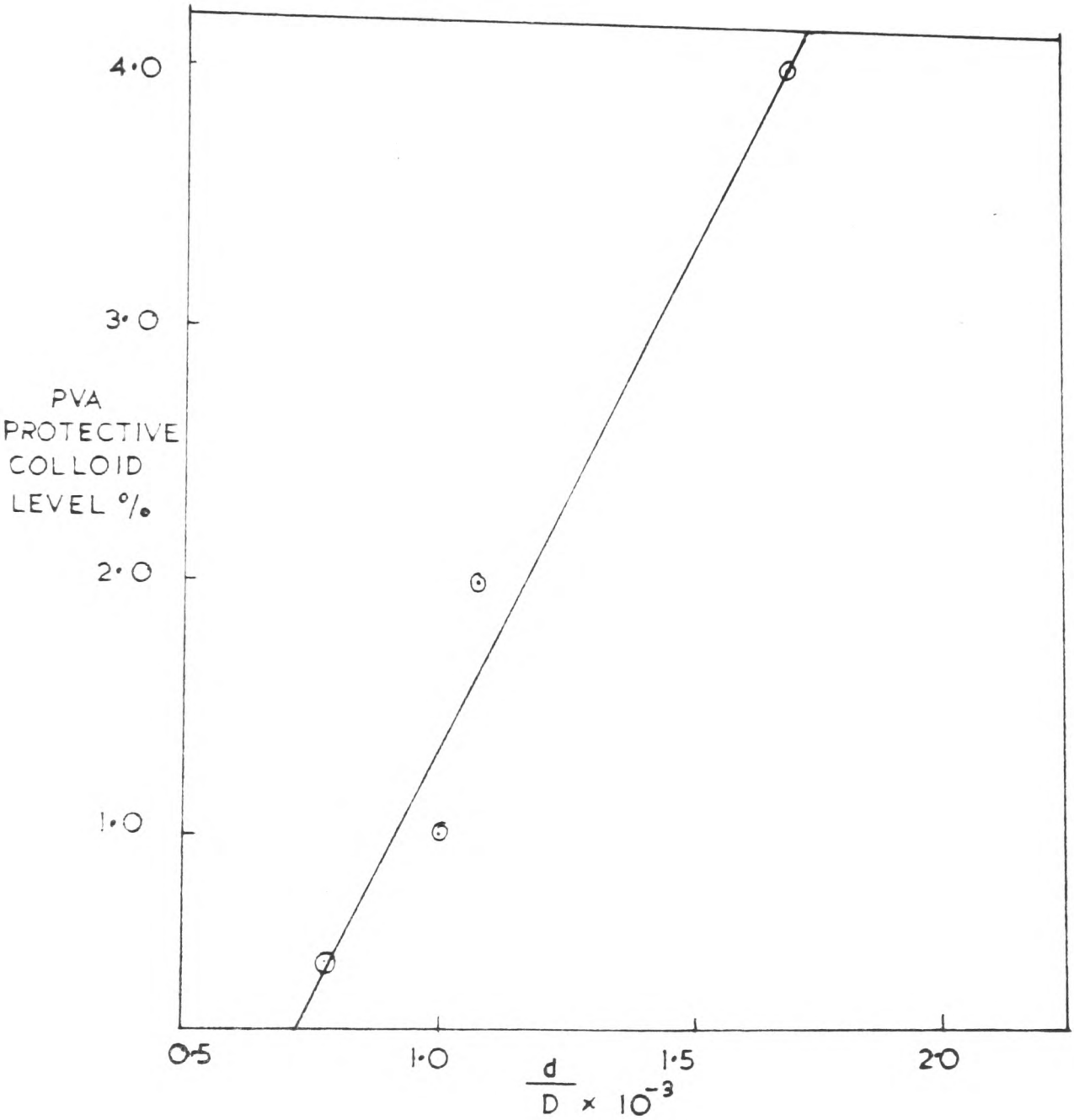

FIG 64 PLOT OF PROTECTIVE COLLOID LEVEL %
AGAINST $d/D \times 10^{-3}$

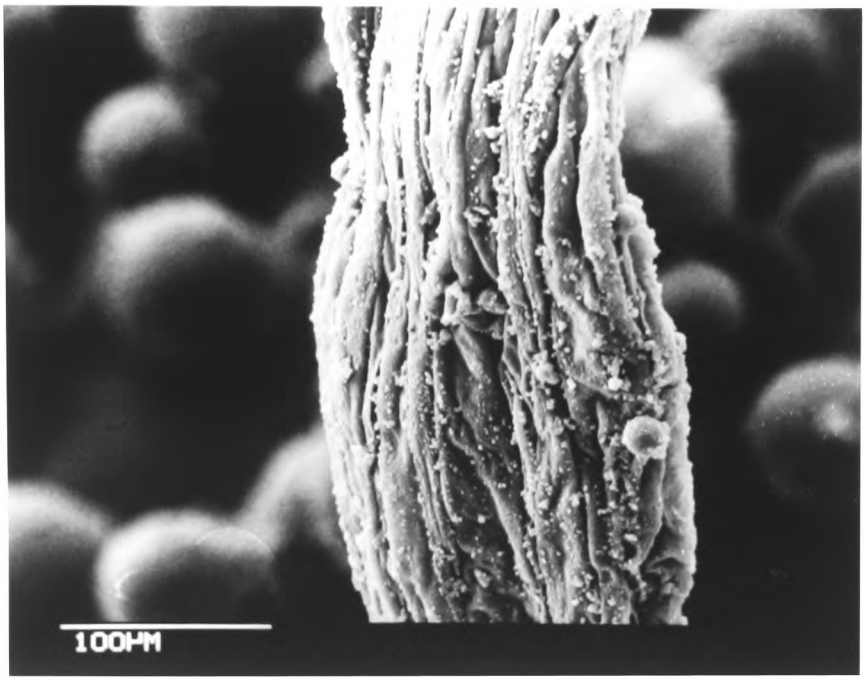

FIG 65 THE FIBRE AGGLOMERATE (S.E.M)

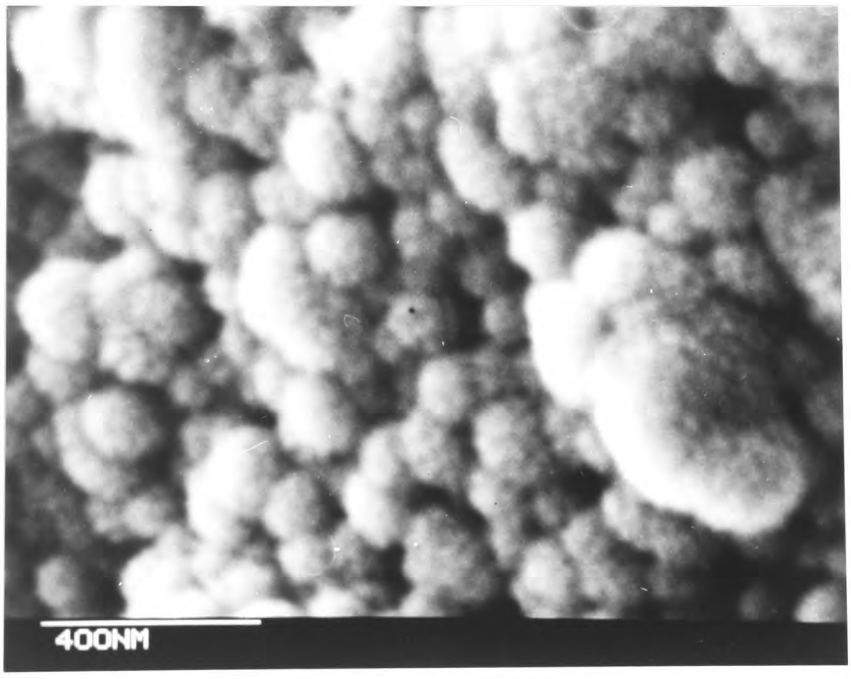

FIG 66 THE SURFACE OF A FIBRE AGGLOMERATE (S.E.M)

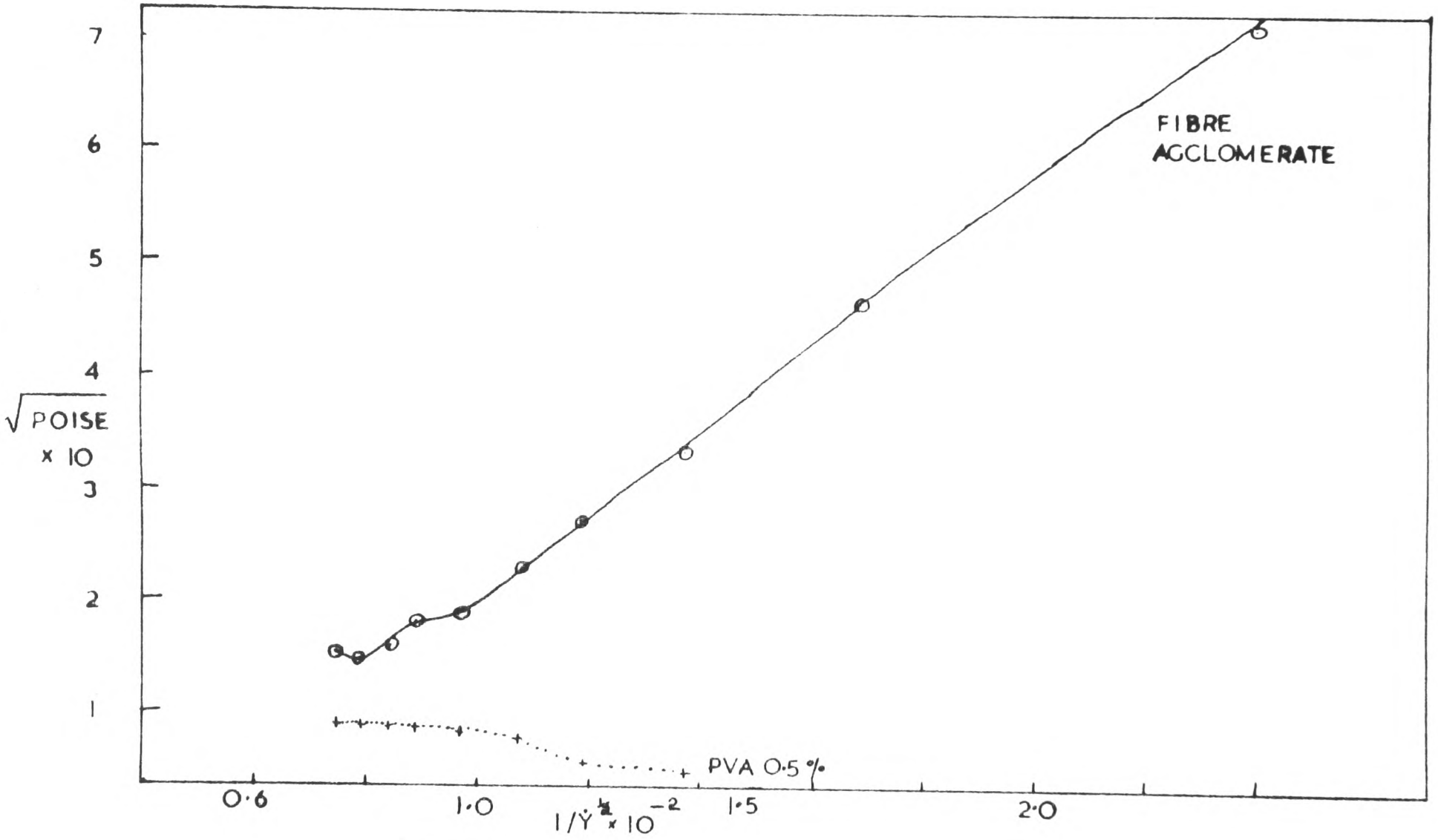

FIG 67 PLOT OF $\sqrt{\text{POISE}} \times 10$ AGAINST $1/\dot{\gamma} \times 10$ FOR A FIBRE AGGLOMERATE

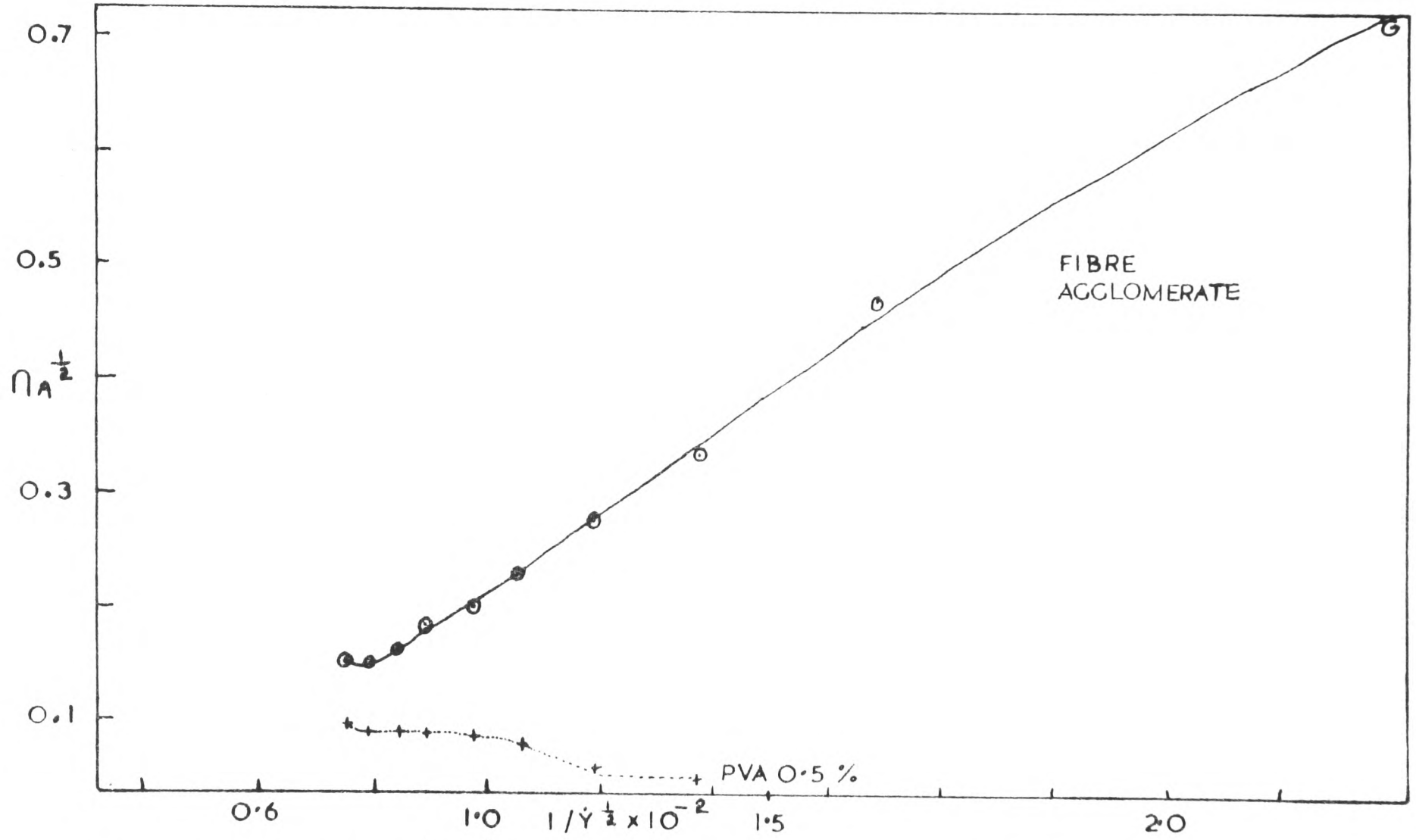

FIG 68 PLOT OF $\eta_A^{\frac{1}{2}}$ AGAINST $1/\dot{\gamma}^{\frac{1}{2}} \times 10^{-2}$ FOR A FIBRE AGGLOMERATE

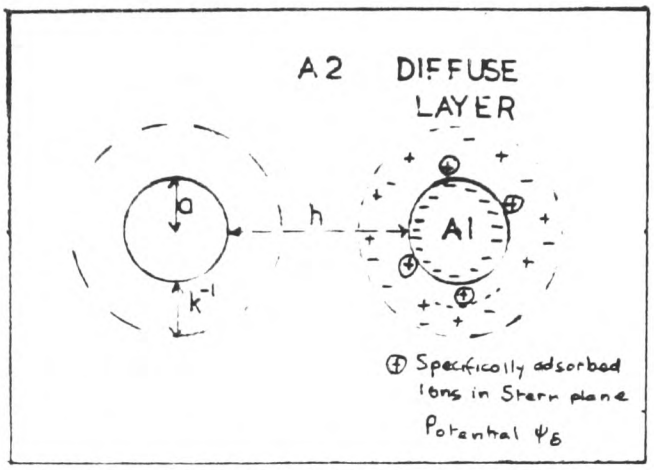

FIG 69 INTERACTIONS BETWEEN CHARGED PARTICLES

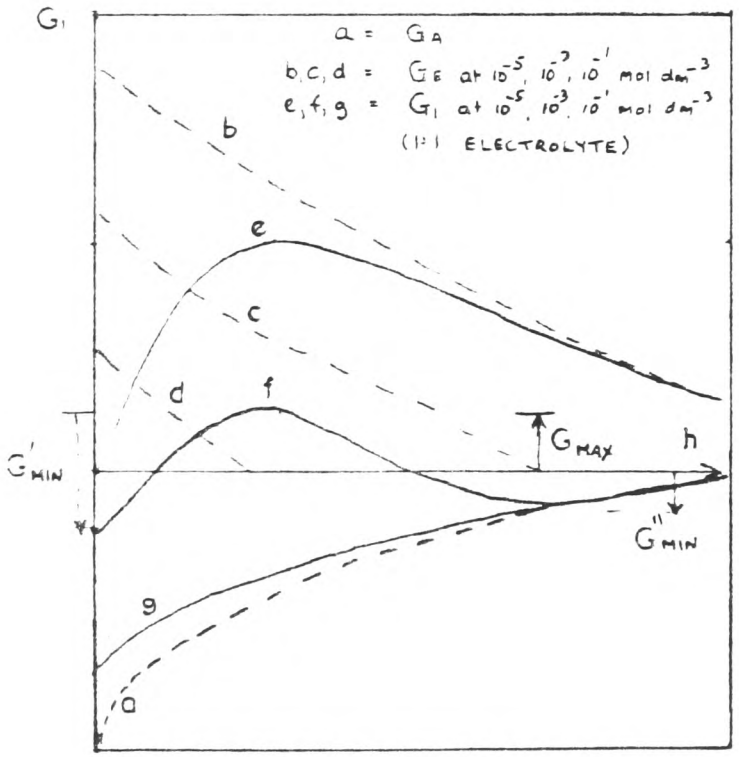

FIG 70 FUNCTIONAL FORM OF $G_1(h)$ FOR AQUEOUS SUSPENSION OF CHARGE STABILISED PARTICLES

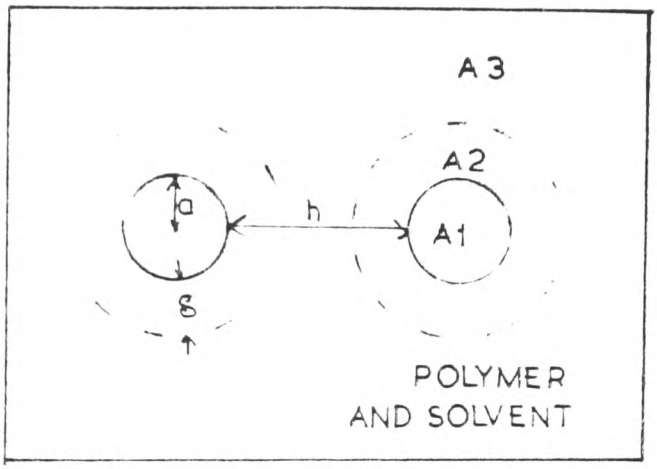

FIG 71 STERIC INTERACTIONS BETWEEN POLYMER COVERED PARTICLES

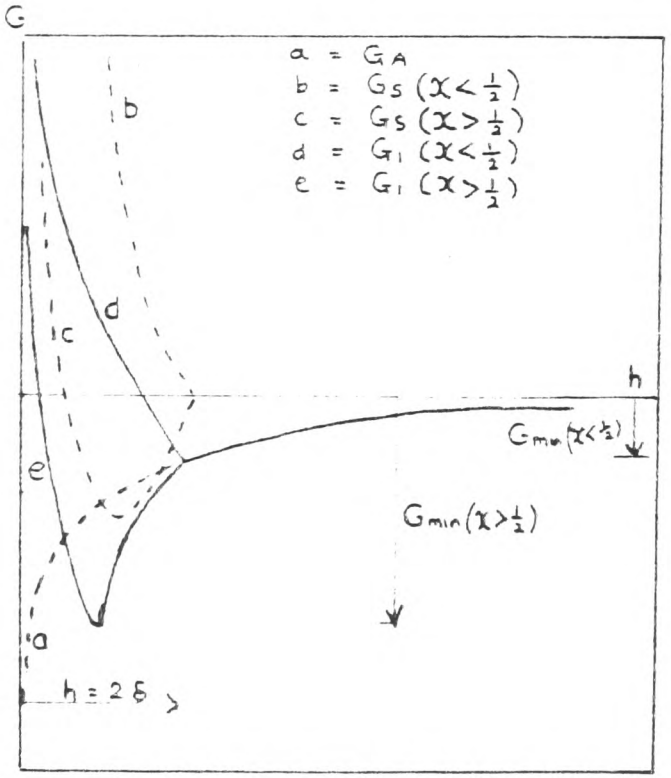

FIG 72 FUNCTIONAL FORM OF $G_1(h)$ FOR A STERICALLY STABILISED SUSPENSION

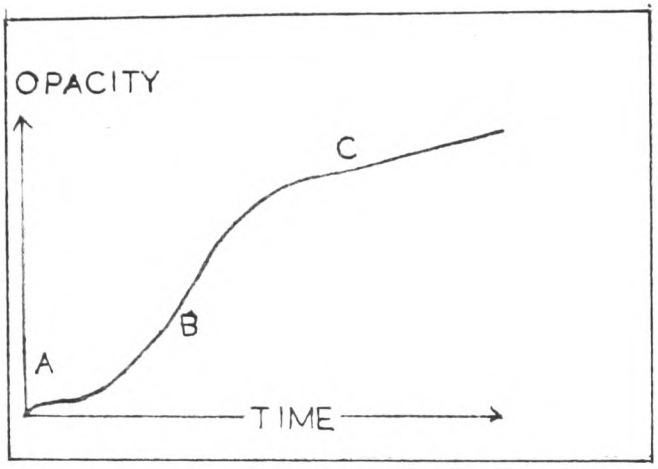

FIG 73 PLOT OF OPACITY AGAINST TIME

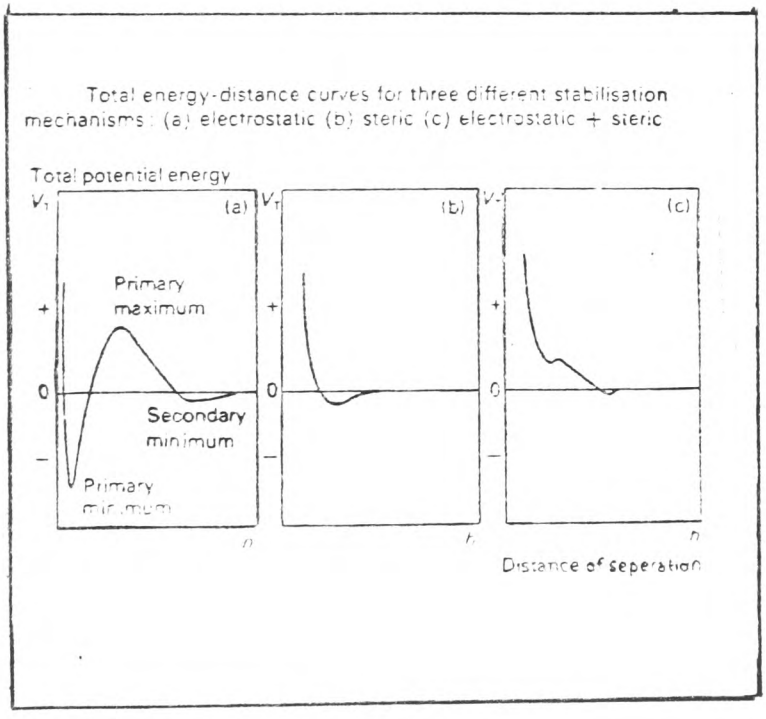

FIG 74

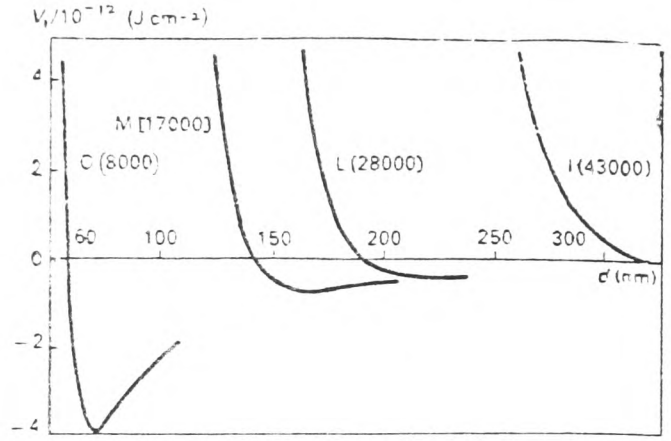

Total potential energy of interaction versus separation for polystyrene latex with adsorbed layers of PVA of various thicknesses*

FIG 75